Regulation and Developmental Expression of *Periaxin* in the Peripheral Nervous System

Diane Lynn Sherman

Ph.D.

University of Edinburgh

Preclinical Veterinary Sciences

1998

DECLARATION

I declare that I composed this thesis and the work in this thesis is my own except where indicated.

Diane L. Sherman
March 1998

CONTENTS

FIGURES

TABLES

ABBREVIATIONS

BDNF	brain-derived neurotrophic factor
BES	N,N-bis(2- hydroxyethyl)-2-aminoethanesufonic acid
bp	base pair
BSA	bovine serum albumin
cDNA	complementary DNA
CMT	Charcot-Marie-Tooth neuropathy
CMV	cytomegalovirus
CNPase	2',3'-cyclic nucleotide-3'phosphodiesterase
CNS	central nervous system
CNTF	ciliary neurotrophic factor
Cx32	connexin 32
DEPC	diethyl pyrocarbonate
DTT	Dithiothreitol
DMEM	Dulbecco's modified Eagle's medium
DMSO	dimethyl sulfoxide
DNA	deoxyribonucleic acid
DRG	dorsal root ganglia
DSS	Dejerine-Sottas syndrome
EDTA	ethylene diaminetetra-acetic acid
EM	electron microscopy
ER	endoplasmic reticulum
FCS	fetal calf serum
FITC	fluorescein isothiocyanate
GalC	galactocerebroside
GAP43	growth-associated protein 43
GCRE	glial cAMP response element
GDNF	glial-cell-line derived neurotrophic factor
GFP	green fluorescent protein
GGF	glial growth factor
HBSS	Hank's balanced salt solution
HGF	hepatocyte growth factor
HNPP	hereditary neuropathy with liability to pressure palsy
HRP	horseradish peroxidase
Ig	immunoglobulin
InaD	inactivation no-after potential

IPL	intraperiod line
ISH	*in-situ* hybridization
kb	kilobase
kD	kiloDalton
LB	Luria-Bertani medium
LIF	leukaemia inhibitory factor
MAG	myelin-associated glycoprotein
MBP	myelin basic protein
MDL	major dense line
MHC	myosin heavy chain
mRNA	messenger ribonucleic acid
NCAM	neural cell adhesion molecule
NF-M	neurofilament M
NGFR	nerve growth factor receptor
NLS	nuclear localization signal
nNOS	neuronal nitric oxide synthase
nt	nucleotide
NT-3	neurotrophin-3
PBS	phosphate-buffered saline
PCR	polymerase chain reaction
Pen/Strep	penicillin (100 IU/ml) and streptomycin (100 μg/ml)
PLP	proteolipid protein
PMP22	peripheral myelin protein 22
PMSF	p-methane-sulfonic acid
PNS	peripheral nervous system
P0	protein 0
Prx	periaxin
Prx	*periaxin* gene
PVDF	polyvinylidene difluoride
RNA	ribonucleic acid
RNase	ribonuclease
rpm	revolutions per minute
RT-PCR	reverse transcription - polymerase chain reaction
SAP97	synapse-associated protein 97
SCIP	supressed cAMP-inducible protein
SDS	sodium dodecyl sulfate
SDS-PAGE	sodium dodecyl sulfate-polyacrylamide gel electrophoresis

SV40	simian virus 40
TAE	10 mM TRIS, 1 mM EDTA, pH8
TdT	terminal deoxynucleotide transferase
TE	10mM Tris, 1mM EDTA, pH 8
TLCK	tosyl-L-lysyl-chloromethylketone
TRITC	tetramethylrhodamine isothiocyanate
UV	ultraviolet
ZO1	zonula occludens 1

ABSTRACT

The Schwann cell is the major glial cell of the vertebrate peripheral nervous system (PNS) where its prime function is to ensheathe and myelinate nerve fibers. Although axons promote the differentiation of Schwann cells, the identity of the signalling molecules responsible is unknown. It is likely that the cytoskeleton plays a vital role in regulating both the changes in cell shape and the expression of myelin protein genes that are required for myelination. Hence the discovery of L- and S-periaxin, putative cytoskeletal-associated proteins of myelinating Schwann cells, has prompted a detailed examination of their localization and developmental expression in differentiating Schwann cells. In this work, in a search for protein-binding domains which might help elucidate the function of the periaxin isoforms, a single modular PDZ protein-binding domain was identified at the extreme N-terminus. This strongly suggests that these proteins play a role in signalling axon-glial interactions.

The localization of L- and S-periaxin was studied in the developing axon-Schwann cell unit where both proteins were localized exclusively to myelin-forming cells. During initial axonal ensheathment L-periaxin was detected at the Schwann cell plasma membrane and in uncompacted myelin whorls. In early postnatal nerve it was concentrated in the adaxonal (apposing the axon) and abaxonal (apposing the basal lamina) membranes, but as the myelin sheath matures, L-periaxin became predominantly localized to the abaxonal Schwann cell membrane demonstrating a dynamic change in localization during development and ensheathment. This shift in localization of the protein after completion of the spiralization phase of myelination suggests that it participates in stabilizing the mature mmyelin sheath. In contrast, S-periaxin was not associated with membranes but appeared to be present throughout the Schwann cell cytoplasm. Both proteins were excluded from compact myelin.

During embryogenesis, Schwann cell precursor cells develop from migrating neural crest cells. At around E14.5 in the mouse sciatic nerve, the precursor cells differentiate to form embryonic Schwann cells which in turn become either myelin-forming or non-myelin-forming Schwann cells in the mature PNS. In contrast to the gene encoding the major myelin protein P0, which is expressed in neural crest cells, Schwann cell precursor cells and embryonic Schwann cells, L-periaxin mRNA and protein were first detected in embryonic Schwann cells. S-periaxin was detectable somewhat later at post-natal day 1.

L-periaxin was initially detected in the nuclei of embryonic Schwann cells; however it was predominantly localized to the plasma membrane by E17.5. To investigate the embryonic nuclear expression further, transfection experiments of full length and various deletion constructs of L-periaxin cDNA were undertaken which indicated that the basic domain in the N-terminus of L-periaxin was responsible for nuclear localization.

The regulation of the *periaxin* gene was investigated by transgenesis. It was shown that a region of 5.5 kb upstream from the transcription initiation site along with the first intron could direct expression to myelinating Schwann cells as well as cells in the central nervous system indicating the presence of a neuronal silencer in the *periaxin* gene.

ACKNOWLEDGMENTS

I would like to thank Peter for the continuous support and encouragement that he has given me over the course of this work. I should also like to thank the Medical Research Council for funding the project.

The members of the Brophy lab both past and present are due my gratitude for helpful discussions. I specifically want to thank Linda Ferguson for excellent technical assistance and the continuous supply of timed mated mice that she provided for these studies. Thanks also go to Dr. Rebecca Hardy for user friendly advice on operating an unuser friendly confocal microscope and for advice in general during the final stages of preparing this thesis. I want to acknowledge the help of Dr. Christine Thompson, University of Glasgow for demonstrating the sympathetic trunk dissection in embryos to me. I want to acknowledge all the technical staff of the Department of Preclinical Veterinary Sciences who have been extremely helpful particularly Colin Warwick and Gordon Goodall.

Introduction

1.1 INTRODUCTION

The vertebrate nervous system develops from a dorsal specialization of the embryonic ectoderm. During neurulation the ectoderm at the midline thickens to form the neural plate. This region of dorsal ectoderm invaginates to give rise to the neural tube which develops into the brain and spinal cord. At the end of neurulation a population of cells emerges bilaterally from the dorsal regions of the neural folds, emigrates from the neural tube and initiates a program of migration, proliferation and finally differentiation (Fig. 1). These cells are the neural crest cells and they give rise to diverse cell types in the developing embryo including the neurons and glia of the peripheral nervous system (PNS), melanocytes, endocrine cells, smooth muscle, and cells that contribute to cranio-facial structures. These crest derivatives were identified by LeDouarin and co-workers using quail-chick embryonic chimæras in which they could precisely map the fate of neural crest cells at every axial level (LeDouarin, 1982). By this means, sensory and autonomic neurons, neurons and glial cells of the enteric nervous system, Schwann cells in peripheral nerves, and ganglionic satellite cells were shown to originate from the neural crest (Dupin et al., 1998; LeDouarin, 1993; LeDouarin and Smith, 1988; Weston, 1991). However, not all glial cells in the PNS originate from the neural crest. Some Schwann cells in the spinal ventral roots may arise from the ventral neural tube (LeDouarin, 1982; Lunn et al., 1887) and some satellite cells of dorsal root ganglia originate from spinal cord neuroepithelia after crest migration has taken place (Sharma et al., 1995).

In the vertebrate PNS the major glial cell is the cell named after Theodor Schwann (Schwann, 1839) first noted surrounding nerve fibers by Virchow (Virchow, 1854). The Schwann cell is responsible for elaborating and maintaining the myelin sheath. Intercellular interactions between neurons and Schwann cells direct development of both the Schwann cell and the neuron and are responsible for

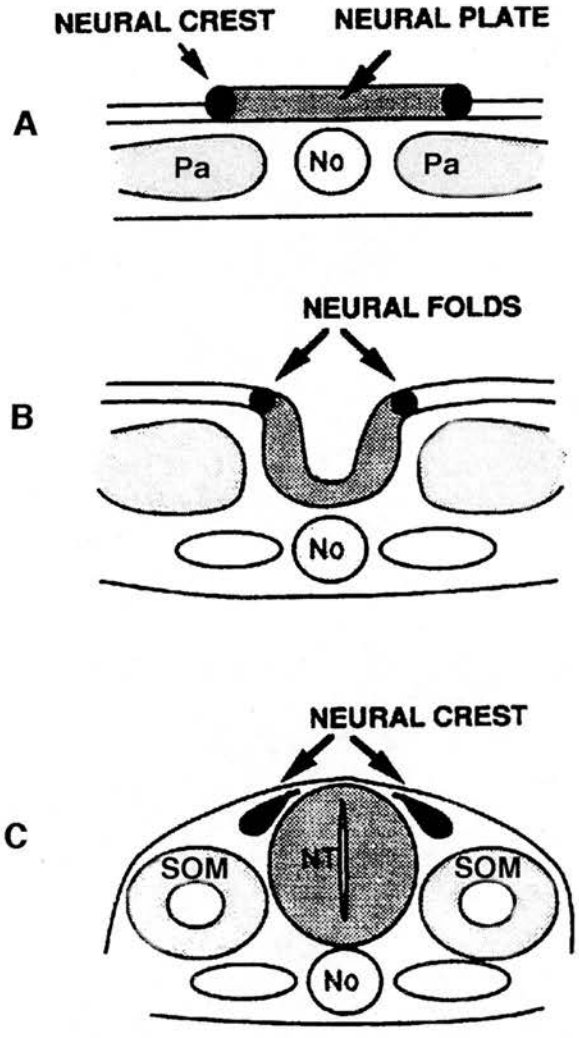

Figure 1. Diagrammatic representation of neurulation. (A) The ectoderm lying above the notochord (No) and paraxial mesoderm (Pa) thickens to form the neural plate. The cells which will become the neural crest originate from the lateral regions of the neural plate. (B) The neural plate invaginates to form the neural tube. (C) the neural tube (NT) fuses at the dorsal midline and separates from the overlying ectoderm which will form the epidermis. Neural crest cells then migrate ventrally and laterally. The paraxial mesoderm forms the somites, SOM.
From Selleck et al., 1993.

maintenance as well as repair of peripheral nerves. Axonal signals regulate the expression of myelin-specific genes (Jessen and Mirsky, 1992) and Schwann cells can in turn influence the phosphorylation state of neurofilaments and axonal calibre (DeWaegh et al., 1992), the segregation of Na^+ and K^+ channels, and the velocity of nerve conduction by the production of the myelin sheath (Joe and Angelides, 1992; Vabnick et al., 1997). In spite of the importance of these interactions between the Schwann cell and the axon that it ensheathes we still know little about the molecular basis of this signalling. It is therefore of great importance to identify the molecules that are involved in the process of myelination in order to shed light on the mechanisms that permit the glial cell and the neuron to communicate.

1.2 THE DEVELOPMENT OF THE SCHWANN CELL

1.2.1 Neural crest cells are multipotent

An important question in embryonic development is whether individual neural crest cells are precommitted to a specific lineage or whether they are multipotent (reviewed in, Selleck et al., 1993; Stemple and Anderson, 1993). To address this question, lineage tracing studies have been conducted *in vivo* by marking individual trunk neural crest cells with dye or recombinant retrovirus and by tracing their fates within the embryo. These experiments have shown that neural crest cells are multipotent and that they can give rise to multiple crest derivatives (Frank and Sanes, 1991; Fraser and Bronner-Fraser, 1991). Similar results have been obtained by growing avian neural crest cells in clonal cultures (Baroffio et al., 1988; Dupin et al., 1990; Sieber-Blum and Cohen, 1980). The *in vivo* studies showed some cells which exhibited multipotency but others generated a subset of the possible lineages indicating that there may be subpopulations of crest cells with a restricted potential or which do not encounter the environment necessary to

develop to their full potential. Transplantation of crest cells to different locations or exposure of these cells to different environments *in vitro* has indeed demonstrated that environmental cues can influence lineage fate (see section 1.2..4.1) (for review, LeDouarin et al., 1993).

1.2.2 The Schwann cell precursor

It has been shown by ablation experiments that neural crest cells and axons migrate to form nerves independently of each other (Loring and Erickson, 1987; Rickmann et al., 1985). In the rat embryo the period of nerve development in the limb begins at E13/14 and spans a week until birth (Jessen et al., 1994). Cells isolated from newly formed nerves have a different phenotype from neural crest cells (Stewart et al., 1996) and are distinct from neonatal Schwann cells (Jessen et al., 1994). These Schwann cell precursors represent an intermediate stage in Schwann cell differentiation from the neural crest. Precursor cells differ from Schwann cells in that they are flattened rather than bipolar *in vitro* and they do not express S100 protein. They also undergo programmed cell death when removed from axonal contact and placed in high density cultures whereas Schwann cells do not, and they are not induced to synthesize DNA by Schwann cell mitogens (Gavrilovic et al., 1995; Jessen et al., 1994). In the rat hindlimb, the switch from precursor phenotype to embryonic Schwann cell phenotype occurs at E16 (Jessen et al., 1994).

The embryonic Schwann cell displays some of the same molecular markers as the precursor cell, growth-associated protein-43 (GAP-43), the neural cell adhesion molecules (N-CAM) and L1 but they can be distinguished from precursors by cell shape and by the presence of S100 protein (Jessen et al., 1994) (Fig. 2).

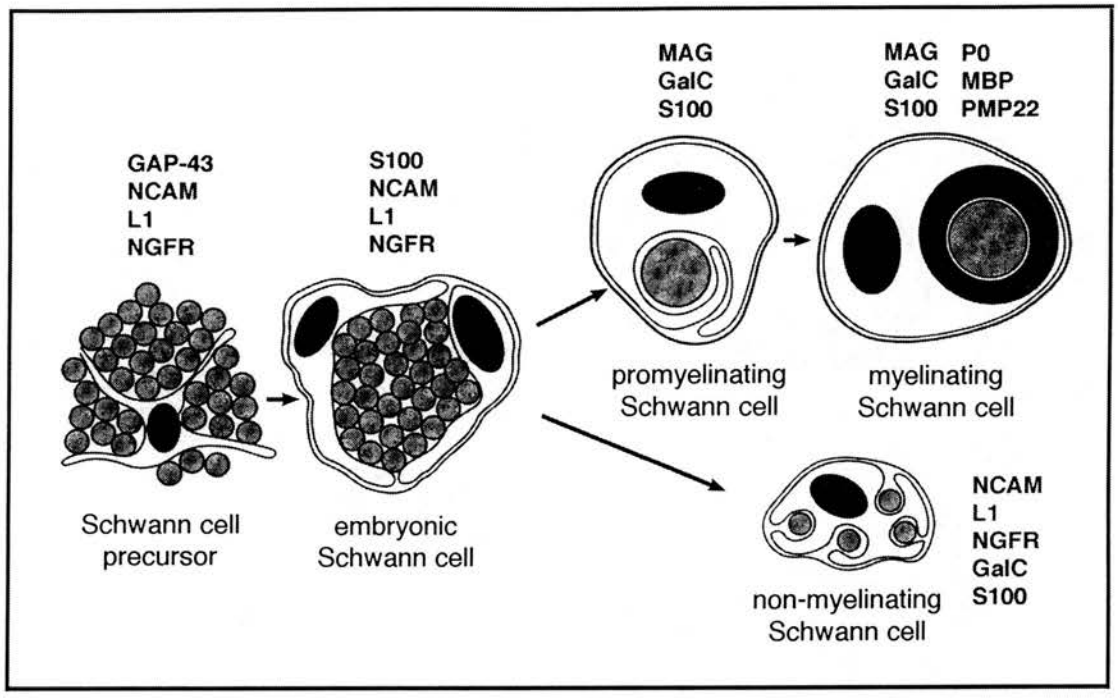

Figure 2. Diagrammatic representation of murine Schwann cell development with stage specific molecular markers. Schwann cell precursors differentiate to embryonic Schwann cells. Embryonic Schwann cells will become either promyelinating or non-myelinating. The promyelinating Schwann cell becomes a myelinating cell and forms a myelin sheath. GAP-43, growth associated protein 43; NCAM, neural cell adhesion molecule; NGFR, nerve growth factor receptor; MAG, myelin-associated glycoprotein; GalC, galactocerebroside; MBP, myelin basic protein; PMP22, peripheral myelin protein 22.
Modified from Scherer, 1997.

1.2.3 Two forms of Schwann cells arise from embryonic Schwann cells

There are of two types of Schwann cells in normal peripheral nerves, a cell which forms a myelin sheath and ensheathes a single axon and a non-myelin-forming cell that ensheathes multiple smaller calibre axons (Fig. 3) (Ochoa, 1976; Webster and Favilla, 1984). They both arise from the same pool of embryonic cells. Non-myelin-forming cells retain many of the characteristics of embryonic Schwann cells in that they associate with multiple axons and express some of the same phenotypic markers. Myelin-forming and non-myelin-forming Schwann cells each display a distinct complement of genes. Non-myelin-forming Schwann cells express the cell adhesion molecules L1 and neural cell adhesion molecule (NCAM), nerve growth factor receptor (NGFR), growth-associated protein 43 (GAP-43) and glial fibrillary acidic protein (GFAP) while myelin-forming cells express protein 0 (P0), myelin basic protein (MBP), myelin-associated protein (MAG), and peripheral myelin protein 22 (PMP22), some of which are structural components of the myelin sheath (Scherer and Salzer, 1996). Schwann cells can exhibit a third phenotype when deprived of axonal contact, either following nerve injury or when cultured alone i*n vitro* (Curtis et al., 1992; Daniloff et al., 1986; Lemke and Chao, 1988; Martini and Schachner, 1988; Scherer et al., 1994; Taniuchi et al., 1986; Taniuchi et al., 1988). Both myelin-forming and non-myelin-forming Schwann cells can become denervated or dedifferentiated. The myelin-forming cell reverts to the L1, NCAM, NGFR, GAP-43 expressing cell and down-regulates the synthesis of myelin proteins and the glycolipids. After the loss of axonal contact the mature non-myelin-forming Schwann cell also down-regulates the glycolipids galactocerebroside and sulfatide (Jessen et al., 1987). The dedifferentiated Schwann cell can also express proteins which are unique to its phenotype such as the neurofilament proteins NF-M and NF-L which are not normally expressed (Fabrizi et al., 1997). Although certain aspects of dedifferentiation may represent the reversal of differentiation and the loss of proteins they no longer require, it is likely that the denervated Schwann cell

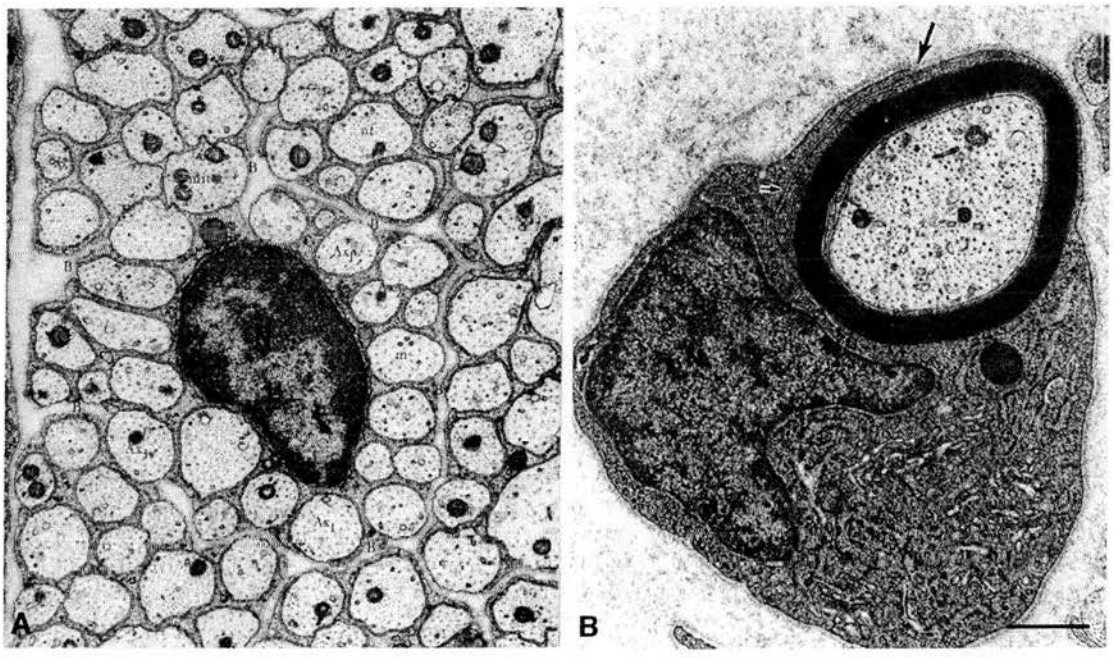

Figure 3. Two types of Schwann cell are found in the peripheral nervous system. (A) Electron micrograph of a non-myelin-forming Schwann cell with cytoplasmic processes surrounding multiple small diameter axons. (B) An electron micrograph of a myelin-forming Schwann cell which has formed a compact myelin sheath. The inner mesaxon and outer mesaxon (large arrow) are visible with an electron dense plaque along the outer mesaxon (small arrow). N, nucleus. Bar in B, 0.5 μm.

From (A) Peters et al., 1991; (B) Raine, 1994.

expresses proteins which relate to promoting axonal regeneration and hence constitutes a third phenotype (Scherer and Salzer, 1996).

The striking changes that Schwann cells undergo when removed from axons indicates that axonal signals are required to maintain the Schwann cell phenotype. This was first shown (Langley and Anderson, 1903) in experiments where axons from a myelinated nerve were forced to regenerate into the distal stump of an unmyelinated nerve. This induced Schwann cells from the unmyelinated nerve to myelinate indicating that axons destined to be myelinated induced Schwann cells to form a myelin sheath. The potential for Schwann cells from unmyelinated nerves to produce myelin was confirmed by other studies (Aguayo et al., 1976; Weinberg and Spencer, 1976). Thus, Schwann cells are adaptable and depend on signals from axons to exhibit the phenotype required for myelination. The nature of the axonal signal or signals which induce myelination remain elusive. They may include axonal calibre as shown in experiments where postganglionic sympathetic non-myelinated axons were induced to myelinate as a result of increased target size (Voyvodic, 1989).

1.2.4 Regulation of Schwann cell development by neuregulins

Neuregulins are a group of structurally related proteins that are alternatively spliced products of a single gene, neuregulin 1 (Burden and Yarden, 1997). These proteins are known to regulate cell survival, proliferation and differentiation in different tissues. Neuregulin is the consensus name for the isoforms (Marchionni et al., 1993) although they were independently identified as glial growth factor (GGF), Neu differentiation factor (NDF), heregulin, acetylcholine receptor inducing activity (ARIA), and sensory and motor neuron-derived factor (SMDF) (for reviews Lemke, 1996; Gassmann and Lemke, 1997). The neuregulin isoforms have been recently classified into three types (Fig. 4): type I isoforms (originally identified as NDF, ARIA, heregulin) contain an EGF-like domain (α- and β- varient), an Ig-like domain

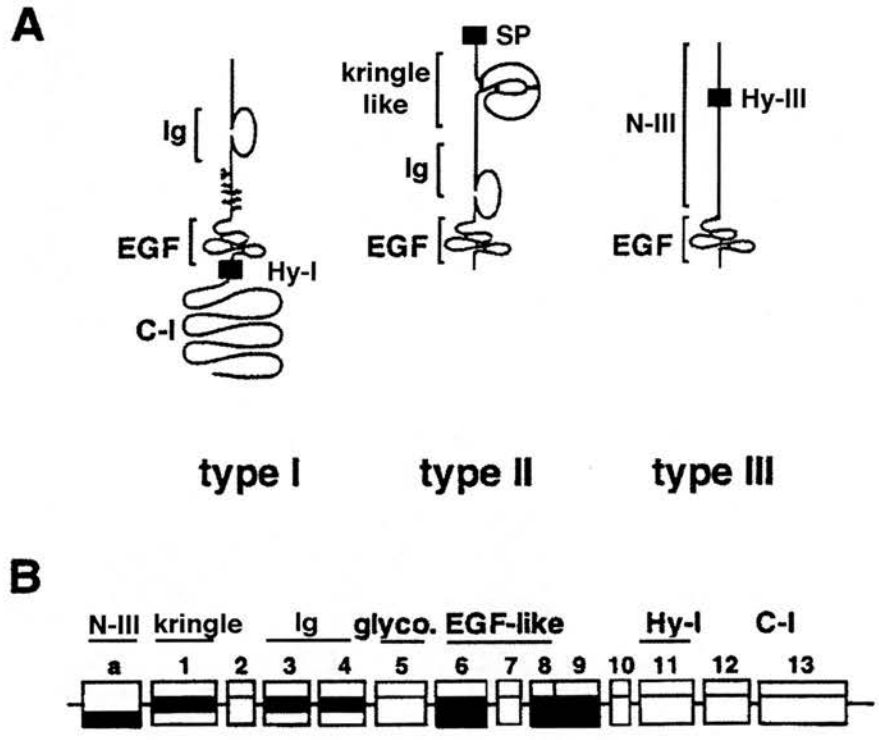

Figure 4. Schematic representation of the three types of neuregulin and the *neuregulin* gene. (A) The structure of type I neuregulins (NDF/heregulin and ARIA), type II (GGF), and type III (SMDF). The EGF-like domain is present in all isoforms; the Ig-like domain is present in type I and II isoforms; a signal peptide (SP) is present in type II neuregulin; kringle-like domain is present in type II neuregulin; Hy-I and Hy-III are internal hydrophobic stretches in type I and type III isoforms; N-III is the unique cysteine-rich N-terminal domain in type III; C-1 is the unique C-terminal domain of type I. (B) Hypothetical structure of the *neuregulin* gene. Domains encoded by different exons are indicated.
Modified from Meyer et al., 1997.

and a glycosylation domain; type II isoforms (originally identified as GGF) contain an EGF-like domain (β-variant), an Ig-like domain but no glycosylation domain; type III isoforms (originally identified as SMDF) contain an EGF-like domain (β-variant) and a cysteine-rich domain (Burden and Yarden, 1997; Meyer et al., 1997).

1.2.4.1 Glial growth factor can influence fate determination of neural crest cells towards a glial lineage.

GGF was originally identified and purified as a Schwann cell mitogen (Brockes et al., 1980; Lemke and Brockes, 1984) because it stimulates their proliferation and survival *in vitro*. GGF was the first extrinsic signal shown to alter choice towards a glial lineage in neural crest cells. GGF was used in clonal cultures of multipotent rat neural crest cells to determine its effect on lineage determination. In standard media, the majority of the clones contained neurons and glia while 10% of the clones contained only glia. After the addition of GGF, 95% of the clones contained only glia indicating that GGF had a dramatic effect on crest cells to suppress neuronal differentiation and promote or allow glial differentiation (Shah et al., 1994).

1.2.4.2 Neuregulin receptors

Neuregulin-induced cellular responses are mediated by tyrosine kinase receptors of the ErbB family which are structurally related to the EGF receptor (ErbB1) (Carraway and Burden, 1995). These receptors include three closely related proteins ErbB2, ErbB3, and ErbB4 (Fig. 5). Neuregulin isoforms bind directly to ErbB3 and ErbB4 with high affinity but recruit ErbB1 and ErbB2 as co-receptors (Burden and Yarden, 1997; Peles and Yarden, 1993). A functional neuregulin receptor complex with the highest affinity for neuregulins is the result of ligand-induced heterodimerization of ErbB2 with ErbB3 or ErbB4 and subsequent receptor tyrosine phosphorylation (Carraway and Cantley, 1994). Ligand-induced

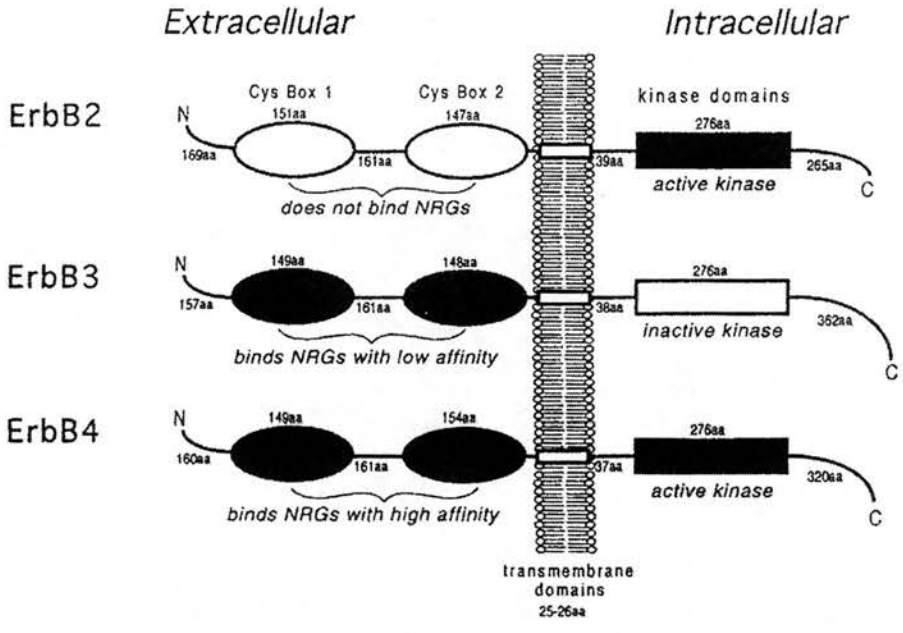

Figure 5. The structure and sequence identity of ErbB2, ErbB3 and ErbB4 receptors. The extracellular domains of the ErbB receptors contain two cysteine-rich boxes (ovals, Cys Box 1 and 2) which exhibit 40 to 50% sequence identity. The receptors exhibit 60 to 80% sequence identity in their intracellular kinase domains. The cytoplasmic tails of the three receptors are divergent with very little identity. From Lemke, 1996.

formation of homo- and heterodimers can produce 10 possible receptor combinations and most, but not all, become tyrosine phosphorylated upon ligand-binding and initiate signaling cascades. The mechanism for the promotion of different receptor combinations by ligand-binding is still unclear (Burden and Yarden, 1997).

1.2.4.3 Expression and activities of neuregulin and the ErbB receptors

Recent studies have shown that in addition to their role in neural crest cell differentiation (see section 1.2.4.1), ErbB receptors and their ligands have a crucial role in Schwann cell development. The activity of neuregulin has been shown to regulate DNA synthesis of Schwann cell precursors and support lineage progression *in vitro* in a time course which parallels *in vivo* progression (Dong et al., 1995). No other known growth factor is capable of this activity.

Axonal contact has been shown to induce proliferation of Schwann cells *in vitro* (Wood and Bunge, 1975) and it has more recently been shown that neuregulin and its receptor ErbB2 are components of the Schwann cell mitogenic activity provided by axonal contact (Morrissey et al., 1995). Neuregulins synthesized by PNS neurons are axonally transported and biologically active (Marchionni et al., 1993; Sandrock et al., 1995; Vartanian et al., 1997).

In addition to the activity of neuregulins in Schwann cell proliferation and development they can regulate survival. Neuregulins can rescue Schwann cell precursors from the dramatic programmed cell death they undergo *in vitro* (Dong et al., 1995; Murphy et al., 1996). The survival activity of neuregulins is not restricted to precursor cells since they has been shown to regulate programmed cell death in Schwann cells *in vitro* induced by serum withdrawal in cultured cells (Syroid et al., 1995), *in vivo* after nerve transection in early postnatal sciatic nerve (Grinspan et al., 1996; Syroid et al., 1995) and at the neuromuscular junction (Trachtenberg and Thompson, 1996).

Numerous studies have defined the embryonic expression pattern of neuregulins (reviewed in Gassmann and Lemke, 1997) which are expressed widely but most recently using isoform specific probes for *in situ* hybridization studies it was shown that the isoforms have distinct expression patterns: type I neuregulins are the only isoforms detected in the early embryo and are predominantly expressed in cephalic mesenchyme, neural crest-derived neurons in cranial ganglia and endocardium; type II neuregulins are the major isoforms expressed in embryonic muscle; type III neuregulin is expressed in sympathetic, sensory and motor neurons whereas all isoforms are expressed in the ventricular zone of the telencephalon (Burden and Yarden, 1997; Meyer et al., 1997).

ErbB2 and ErbB3 mRNA and protein are expressed by neonatal Schwann cells and phosphorylated *in vivo* indicating that they are active (Grinspan et al., 1996; Jin et al., 1993; Levi et al., 1995; Meyer and Birchmeier, 1995; Morrissey et al., 1995). *In vitro* studies showed that the heterodimerization of ErbB2 and ErbB3 in Schwann cells was ligand-induced with subsequent tyrosine phosphorylation of both subunits (Vartanian et al., 1997). The fact that neuregulins are expressed by neurons in the right place combined with the presence of the appropriate receptors on Schwann cells indicates that this ligand-receptor system is responsible for the regulation of Schwann cell development..

1.2.4.4 Targeted mutation of neuregulin and the ErbB receptors

Targeted deletion in mice of *neuregulin* (Meyer and Birchmeier, 1995), *ErbB2* (Lee et al., 1995), *ErbB3* (Riethmacher et al., 1997), and *ErbB4* genes (Gassmann et al., 1995) have indicated that neuregulins and their receptors have multiple independent and essential functions in embryonic development particularly in the nervous system and heart. Analysis of E10.5 mouse embryos with the *neuregulin* null mutation show that ErbB3-expressing cranial ganglia and Schwann cell precursors fail to develop normally and are reduced in number while sensory

neurons of the dorsal root ganglia are normal. These results demonstrate that neuregulins are essential for the neurogenic lineage in cranial neural crest whereas in trunk neural crest they only affect early Schwann cell development consistent with earlier studies on Schwann cell precursor survival (Meyer and Birchmeier, 1995). The *neuregulin* and *ErbB2* mutant mice display similar defects in cranial neural crest derived sensory ganglia development. Most neural crest derived portions of these ganglia are missing (Lee et al., 1995). Analysis of the phenotype of mice with a targeted mutation in the *neuregulin* Ig-like domain (*neuregulin*^{Ig}) which causes premature translational termination of neuregulin isoforms containing the Ig domain (types I and II), demonstates that Schwann cell precursors develop normally, indicating that Schwann cells do not depend on the Ig-like isoforms of neuregulins for their development (Meyer et al., 1997).

Most recently Birchmeier and co-workers generated mice lacking the ErbB3 receptor (Riethmacher et al., 1997). Most homozygous null embryos died before E13.5. The most striking feature of the E12.5 mutant embryos was the complete absence of Schwann cell precursors in sensory and motor peripheral nerves and a complete absence of Schwann cells in older embryos of E18.5. These results demonstrate that ErbB3 is essential for the development of Schwann cells. Enteric glial cells were also absent but satellite cells in dorsal root ganglia and CNS glia were normal. The appearence of normal glial cells in the CNS is consistent with the fact that oligodendrocytes have been shown to express the neuregulin receptors ErbB2 and ErbB4 but not ErbB3 (Vartanian et al., 1997). On the other hand it is surprising that the supporting cells in the dorsal root ganglia are not affected in the mutant embryos because their phenotype is very like Schwann cell precursors.

Another very interesting finding by Birchmeier and co-workers was that sensory and motor neurons are formed in the mutant embryos but subsequently degenerate by programmed cell death. The dorsal root ganglion neurons were of a similar number to wild type on E12.5 but by E14.5 and E18.5 they were reduced by

70% and 82% respectively. The loss of motor neurons takes place 2 days later in mutant embryos, the number was normal at E16.5 but drastically reduced by E18.5. To distinguish whether this neuronal loss in mutant embryos was a consequence of the role of ErbB3 in mediating trophic signals directly to neurons or indirectly through the loss of Schwann cells, chimæric embryos were generated by injection of *ErbB3* $^{-/-}$ embryonic stem cells into wild-type blastocysts (Riethmacher et al., 1997). While the contribution of mutant and wild type cells from chimæric pups was similar in dorsal root ganglia, spinal cord and other tissues, there was no contribution of mutant cells to Schwann cell precursors. This important experiment demonstrates that ErbB3 functions in a cell autonomous fashion in Schwann cell development but acts indirectly in the survival of sensory and motor neurons.

The loss of motor and sensory neurons in the *ErbB3* mutant embryos is most likely due to the complete loss of trophic support provided by Schwann cells and their precursor cells. Schwann cells have been reported to produce many neurotrophic factors such as CNTF, GDNF, BDNF, LIF, NT-3, and HGF which are all capable of promoting sensory and motor neuron survival *in vitro* (Davies, 1998). The fact that more neurons die in the *ErbB3* mutant embryos than in any single neurotrophic factor-null mouse, suggests that Schwann cells and their precursors provide multiple survival factors for early sensory and motor neurons which probably include as yet uncharacterized neurotrophic factors (Davies, 1998).

1.2.5 Transcriptional regulation during Schwann cell development

Schwann cells have been shown to express many transcription factors (reviewed in Stewart et al., 1996) but so far only two, Krox-20 and Oct-6, have been shown to be important for the development of the myelinating Schwann cell lineage.

The Jun family of leucine zipper transcription factors, c-Jun, Jun B, and Jun D, are expressed in Schwann cells *in vitro* and at low levels *in vivo*. Expression of

c-Jun is associated with the non-myelin-forming phenotype and is regulated by axonal contact in that it is increased in the distal stump after nerve crush and rapidly decreases when axons re-grow (Shy et al., 1996; Stewart, 1995). Another leucine zipper transcription factor, cAMP response element binding protein (CREB), which mediates the actions of cAMP, is expressed during all stages of Schwann cell development (Stewart, 1995). It was thought that CREB may be important in regulating myelin-forming cells since up-regulation of cAMP *in vitro* can reproduce the myelinating Schwann cell phenotype induced by axonal contact (Lemke and Chao, 1988; Morgan et al., 1991), but cAMP response element (CRE) sites have not been found in any of the Schwann cell myelin genes (Lemke and Chao, 1988; Stewart et al., 1996). The zinc finger transcription factor Krox-24 is expressed by immature and non-myelin-forming Schwann cells but not by myelin-forming cells (Nikam et al., 1995). Several basic helix-loop-helix (bHLH) transcription factors are found in the Schwann cell lineage but their mRNAs are not strongly regulated during development (Stewart et al., 1997).

1.2.5.1 Pax3

Pax3 is a paired box gene expressed in craniofacial neural crest cells derivatives and in the spinal ganglia (Goulding et al., 1991). Expression is maintained in Schwann cell precursors but is down-regulated in embryonic Schwann cells (Kioussi and Gruss, 1996). Homozygous *Splotch* mutant mice which have a mutation resulting in a truncated Pax3 protein die at E13.5 and lack Schwann cell precursors. In contrast, a point mutation in the paired domain of *Pax3, splotch delayed*, causes a decrease in the number of Schwann cells in the sciatic nerve (Kioussi et al., 1995). A second wave of high level Pax3 expression occurs at E18.5 to postnatal-day 5. Pax3 levels remain high in the non-myelin-forming Schwann cells but Pax3 expression is down-regulated as Schwann cells begin to myelinate. Myelin-specific genes may be negatively related targets of Pax3. *In vitro*

experiments have shown that Pax3 expression in Schwann cells results in repression of *Mbp* promoter activity and activation of *GFAP, NCAM, L1 and NGFR* promoters (Kioussi et al., 1995). Therefore Pax3 expression may be involved in maintaining gene expression in non-myelin-forming cells.

1.2.5.2 SCIP/Tst-1/Oct-6

SCIP (suppressed-cyclic AMP-inducible protein) is a member of the POU-homeo-domain family of proteins which are expressed in the nervous system and other tissues (He et al., 1989; Meijer et al., 1989; Monuki et al., 1989; Suzuki et al., 1990). SCIP is strongly induced by elevating cAMP in Schwann cells *in vitro* (Monuki et al., 1990; Monuki et al., 1989) and can also act as a repressor of P0 and MBP expression in transfection studies (He et al., 1991; Monuki et al., 1993). SCIP protein is present in the sciatic nerve in Schwann cell precursors, embryonic Schwann cells, and myelin-forming Schwann cells until postnatal-day 12, and in many non-myelin-forming Schwann cells in the adult (Blanchard et al., 1996; Scherer et al., 1994) and demonstrates a transient expression pattern in the myelin-forming lineage (Zorick et al., 1996). Targeted deletion of the *SCIP* gene in mice delays the appearance of myelin-forming Schwann cells by 1 to 2 weeks so that they are arrested at the stage when there is a 1:1 relationship between Schwann cell and axon prior to myelin sheath formation (Bermingham et al., 1996; Jaegle et al., 1996). The levels of P0 and MBP mRNAs in *SCIP* null mice were not reduced (Bermingham et al., 1996) indicating that SCIP does not regulate these genes. Therefore SCIP acts to regulate genes in embryonic Schwann cells that are involved in the transition to a myelin-forming phenotype.

1.2.5.3 Krox-20

The expression pattern of the zinc-finger transcription factor Krox-20 has been described by 2 groups using different methods of analysis. Topilko and co-

workers used β-galactosidase histochemistry in mice carrying a *lacZ pgk-neo* gene inserted into the *Krox-20* locus (Topilko et al., 1994) whereas Zorick and co-workers used Northern analysis to examine mRNA expression and immunohistochemistry with an antibody to Krox-20 to localize protein in rats (Zorick et al., 1996). Rats are delayed in the maturation of the PNS by 1 to 2 days when compared to mice. The difference in the sensitivity of the detection methods used could account for the different results. Topilko and co-workers first detected *Krox-20* at E11.5 in the dorsal and ventral spinal roots but the gene is not expressed in distal peripheral nerves until E16.5. Zorick and co-workers showed that Krox-20 appears in the dorsal root Schwann cells at P1 in the rat 24 to 36 h after they become $SCIP^+$. A third group demonstrated Krox-20 mRNA by RT-PCR in mice after the transition from precursor cell to embryonic Schwann cell while SCIP is expressed in precursor cells (Blanchard et al., 1996). Therefore SCIP expression precedes Krox-20 expression during Schwann cell development. *Krox*-20 is never expressed in non-myelin-forming cells but its expression is maintained in myelin-forming Schwann cells in the adult (Zorick et al., 1996) where it requires axonal contact *in vitro* and *in vivo* (Murphy et al., 1996; Zorick et al., 1996).

Mutant mice homozygous for a null allele in the *Krox*-20 gene are never able to myelinate axons. The Schwann cells spiral just one and a half turns around an axon and the only myelin protein they express is MAG (Topilko et al., 1994) an early marker of myelination. The phenotype observed in *Krox*-20 null mice, the absence of myelination and of myelin gene products, suggests that Krox-20 may be involved in controlling genes required for the completion of the myelination programme.

1.3 MYELINATION

1.3.1 The myelination process

Embryonic Schwann cells migrate along axons in developing peripheral nerves and loosely ensheath bundles of axons. Over time their processes extend into the bundles and gradually segregate smaller bundles of axons until only one axon is surrounded by Schwann cell cytoplasm (Webster, 1971; Webster and Favilla, 1984). The process of spiralization of the Schwann cell plasma membrane around the axon begins with the inner mesaxon spiraling under the outer mesaxon when axonal diameter reaches approximately 1 to 1.6 μm (Fraher, 1978; Peters and Vaughn, 1970; Voyvodic, 1989; Webster, 1971). The spiralization process continues and the cytoplasm within the spirals is extruded after 3 to 4 complete turns thus forming the compact myelin sheath (Fig. 6). Even after sheath formation there remains some uncompacted membranes containing cytoplasm on the external mesaxon side which eventually decrease in size and disappear as the turns increase. This process of spiralization to produce a myelin sheath was first described by Geren (Geren, 1954).

Like other epithelial cells Schwann cells synthesize a basal lamina which is composed of laminin, nidogen, type IV collagen, heparin sulfate proteoglycan, and fibronectin and is characteristic of the axon-Schwann cell unit. The basal lamina is formed when Schwann cells first associate with axons (Billings-Gagliardi et al., 1974). Studies using an *in vitro* co-culture system of dorsal root ganglion neurons with Schwann cells has provided evidence that in addition to axonal contact, the deposition of a basal lamina is necessary for myelination (Bunge, 1993; Bunge et al., 1990).

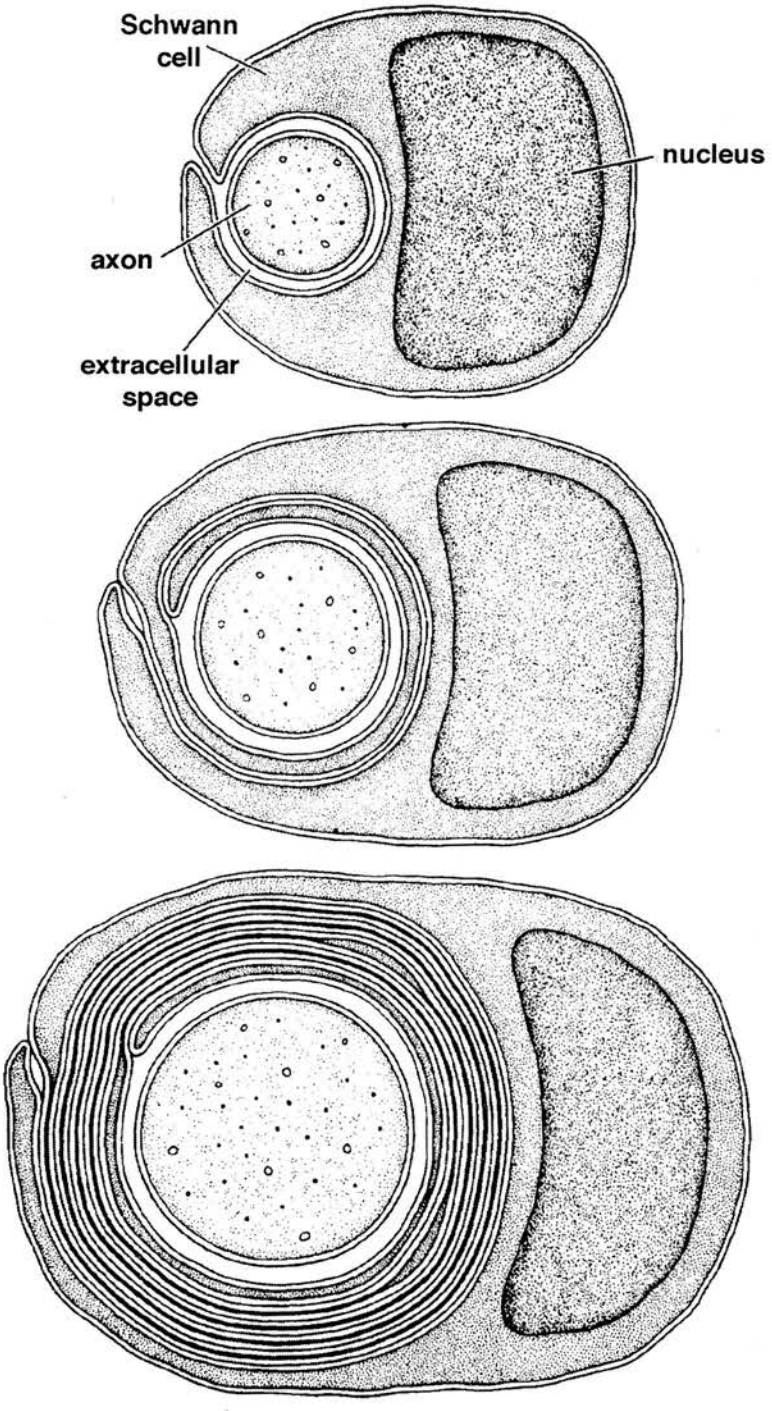

Figure 6. Schematic representation of myelination in the peripheral nervous system. The process of ensheathment and spiralization is depicted with the inner mesaxon wrapping around the axon. Compaction of the lamellae forms the multilamellar myelin sheath composed of the major dense lines and the thinner intraperiod lines. From Raine, 1984.

1.3.2 The domain structure of a myelinated fiber

The myelinated peripheral nerve fiber has a distinctive morphology with the myelin sheath appearing as a segmented tube surrounding the axon. As first described by Ranvier, (Ranvier, 1871), the interruptions in the sheath causing the segmental appearance are the nodes of Ranvier and the segments of myelin between nodes are the internodes formed by the acquisition of a length of axon by a single Schwann cell with its spindle-shaped nucleus located in the approximate center of the internode. The length of an internode increases proportionally to axon diameter and internodal segments can range from 200 to 2000 μm (Hiscoe, 1947; Schlaepfer and Myers, 1973; Vizoso and Young, 1948).

Schwann cells like other epithelial cells polarize their surfaces thereby creating distinct domains: compact myelin, uncompacted regions or cytoplasmic channels, and plasma membrane (Trapp et al., 1995).

1.3.2.1 Cytoplasmic channels within the internode

All myelin-forming Schwann cells have a network of cytoplasmic channels that are precisely organized in the internode. After myelin sheath formation, Schwann cell cytoplasm is retained on the inside of the sheath (the periaxonal region), the outside of the sheath where the bulk of the cell body is located, channels within the sheath, and at the paranodes (Fig. 7). The thin cytoplasmic periaxonal domain, enclosed by periaxonal membrane on one side and sheath on the other, is separated by a 12 to 14 nm gap or periaxonal space from the axolemma (Trapp and Quarles, 1982).

Within the internode are the cytoplasmic channels that traverse the myelin sheath known as Schmidt-Lanterman incisures (Fig. 7). They were described over a century ago as a series of funnel-shaped clefts in the myelin sheath (Boll, 1877; Lanterman, 1877; Schmidt, 1874; Zawerthal, 1874). These channels provide a direct connection from the perinuclear to the periaxonal cytoplasm apposing the

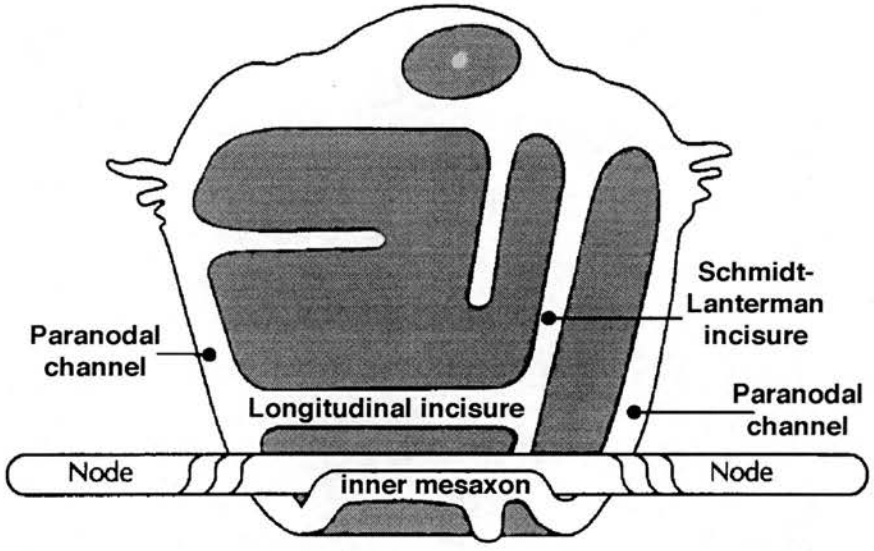

Figure 7. Diagram of an "unrolled" Schwann cell. When the Schwann is viewed "unrolled" the cytoplasmic network is more clearly visible. The Schmidt-Lanterman channels which traverse the sheath are distinguished from the outer boundaries of the cell which include the lateral paranodal channel or loops and the inner and outer mesaxons.

From Doyle and Colman, 1993

axon. The Schmidt-Lanterman incisures have been implicated in the metabolic maintenance of the myelin sheath (Ghabriel and Allt, 1981) but their function remains unclear. The cytoplasm of the incisure usually contains a single microtubule, microfilaments, mitochondria and smooth endoplasmic reticulum but no Golgi vesicles, rough ER or free polysomes thereby unable to participate in protein synthesis and processing (Gould and Mattingly, 1990; Hall and Williams, 1970; Rosenbluth, 1980). Electron densities within the incisures have been described (Hall and Williams, 1970) and it is now known that these densities are components of adherens-like junctions (Fannon et al., 1995).

The paranode is the region of the internode where the myelin sheath terminates close to the node of Ranvier. When viewed in a longitudinal section by electron microscopy it is clear that the major dense line of the compacted sheath opens in these regions and the resulting loops, which abut each side of the axon, are filled with cytoplasmic components (Fig, 8A). The loop from the outer most myelin lamellae is closest to the node. Within the cytoplasm of paranodes there are abundant microtubules which are suggested to be involved in myelin protein transport (Kidd et al., 1994; Peters et al., 1991; Trapp et al., 1995). Covering the node, in close contact with the axolemma are interdigitating microvilli extending from each Schwann cell plasma membrane at each end of the internode. If the myelin sheath was unrolled as seen in Fig 7, the paranodal loops would be seen to form a continuous channel at the lateral boundary of the cell.

1.3.2.2 Molecular and structural organization of the node of Ranvier and paranode

Originally described as desmosomes (Harkin, 1964), a series of helically arranged densities are seen that traverse the cytoplasm between the paranodal loops. It is now clear that these electron densities are components of an adherens-type junction which contains the adhesion molecule E-cadherin (epithelial cadherin)

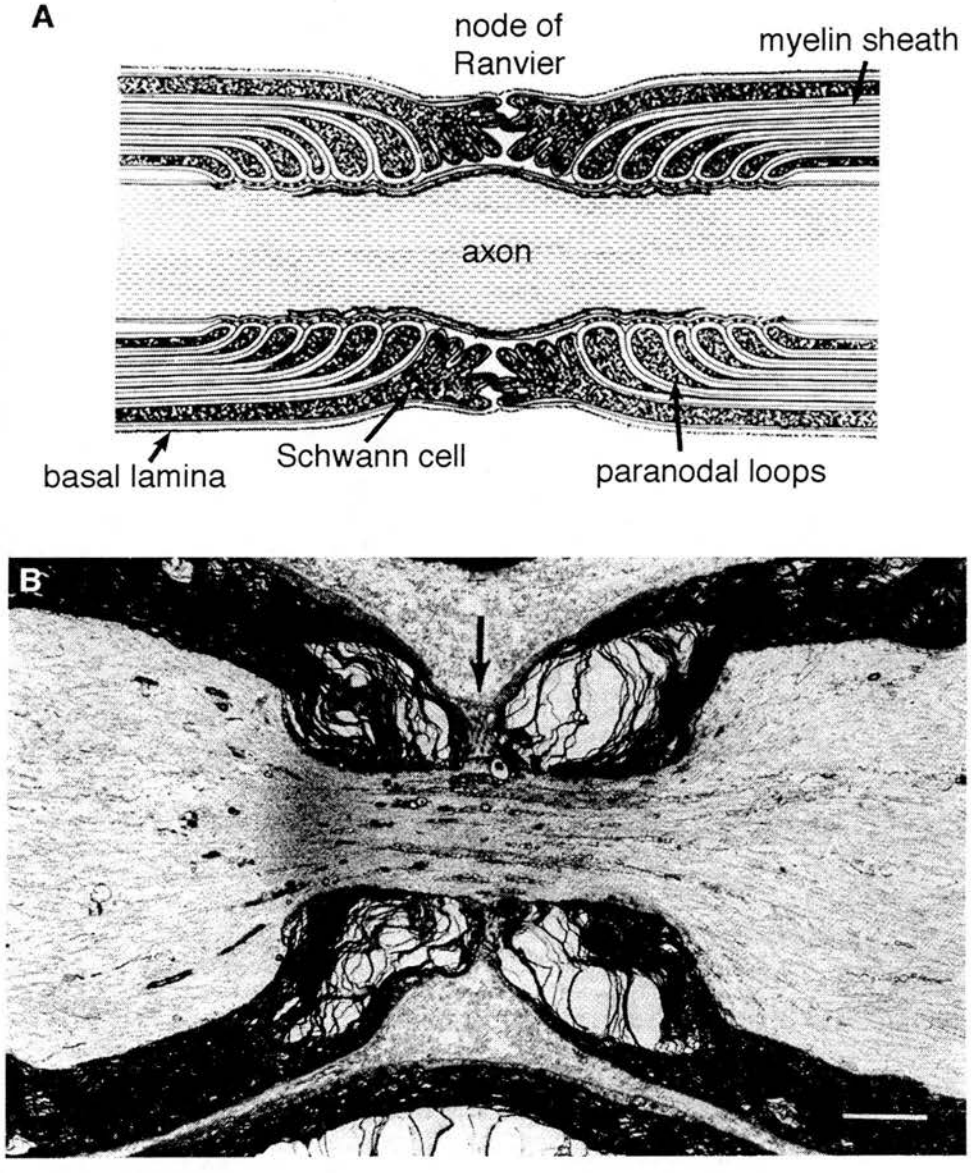

Figure 8. Diagram of a node of Ranvier (A) and an electron micrograph of a node of Ranvier from a large diameter axon (B). The ends of the cytoplasmic-filled paranodal loops directly appose the axon. Interdigitating Schwann cell microvilli are visible at the node (B, arrow) and a basal lamina can be seen. In (B) the axonal narrowing at the node is evident as well as the condensation of axonal organelles and neurofilaments. Bar, 2 μm.
From Raine, 1984.

and its associated protein β-catenin (Fannon et al., 1995) and which serves to anchor adjacent membranes. E-cadherin adhesion plaques are restricted to the uncompacted channel networks in the Schwann cell: paranodes, Schmidt-Lanterman incisures, and mesaxons. In other epithelial cells E-cadherin mediates intercellular adhesion. Thus the Schwann cell provides a novel role for E-cadherin in mediating adhesion within the membrane system of a single cell.

The gap junction protein connexin32 (Cx32) has been localized to the same Schwann cell regions as E-cadherin; paranodes, Schmidt-Lanterman incisures and mesaxons (Scherer et al., 1995). Mutations affecting the *CX32* gene are associated with the X-linked form of the hereditary peripheral neuropathy Charcot-Marie-Tooth disease (CMTX) in humans (Bergoffen et al., 1993; Ionasescu et al., 1994). Some *Cx32* mutations lack the ability to form functional gap junctions when tested by transfection *in vitro* (Bruzzone et al., 1994; Omori et al., 1996) which may restrict diffusion within the cytoplasmic channels in the myelin sheath leading to pathology. A null mutation of the *Cx32* gene has been generated in mice resulting in a late-onset progressive neuropathy with morphological abnormalities comparable to CMTX (Anzini et al., 1997; Nelles et al., 1996). The striking difference between the null mutant and CMTX is the absence of a behavioral phenotype in the mutant mice which have normal nerve conduction compared to CMTX patients with impaired nerve conduction.

The organization of the paranodal and nodal regions contain many cellular specializations to aid nerve conduction. At the internode the axolemma and Schwann cell periaxonal membrane are separated by a gap of approximately 12 nm which narrows at the node to 2.5 to 3.0 nm (Peters et al., 1991). The axonal diameter is also reduced at the node compared with the internode and has a higher density of neurofilaments (DeWaegh et al., 1992) (Fig. 8B).

The specialization of a myelin sheath allows for the propagation of faster nerve impulses which travel down the fiber from node to node by a process called

saltatory conduction. For a given conduction velocity myelination reduces the size of the axon required by a factor of ten (Ritchie, 1984). Hence the acquisition of a myelin sheath has played a key role in the evolution of complex nervous systems. The nerve impulse or action potential in a peripheral myelinated fiber is generated by the activation of voltage-gated sodium channels (Ritchie, 1984). At the node there is a vast increase in clusters of voltage-dependent sodium channels by comparison with the internode, ~1500/mm^2 compared with <25 mm^2 (Salzer, 1997). The Schwann cell has been shown to be essential for the clustering of sodium channels at the node and the clustering only takes place with the concurrent commitment of Schwann cells to a myelin-forming phenotype (Dugandzija-Novakovic et al., 1995; Joe and Angelides, 1992; Vabnick et al., 1997; Vabnick et al., 1996). Oligodendrocytes, the myelin-forming cell in the CNS, have also been shown to induce Na^+ channel clustering *in vitro* and *in vivo* (Kaplan et al., 1997). Other molecules which may have a function in channel clustering include two components of the actin cytoskeleton, spectrin and ankyrin, which are concentrated at the nodal subaxolemma (Kordeli et al., 1995). Ankyrin$_G$ colocalizes with Na^+ channels at the node as well as with the cell adhesion molecules (CAMs) neurofascin and NrCAM, members of the L1 family of CAMS (Davis et al., 1996). The function of these molecules in sodium channel clustering is as yet unknown.

Interestingly, voltage-gated K^+ channels are absent at the node and electrophysiological studies have suggested that K^+ channels are present in paranodal and internodal regions and that they do not contribute to the action potential but play a role in stabilizing action potential discharge at the node (Chiu and Richie, 1980). Recent immunolocalization studies of three K^+ channel subunits, Kv1.1, Kv1.2 (members of the Shaker gene subfamily) and Kvβ2, demonstrate that the channels are located in the juxtaparanodal regions (Mi et al., 1995; Rasband et al., 1998; Wang et al., 1993). Therefore there is a channel-free gap between the precise localization of Na^+ channels at the node and the K^+ channels on the other

side of the paranode leaving the paranodal region where the Schwann cell paranodal loops are in close apposition to the axolemma free of channels perhaps for a specialized axon-glial interaction. Rasband and co-workers have shown by using a demyelination and remyelination paradigm that Schwann cells are important for K^+ channel clustering and redistribution (Rasband et al., 1998).

The axolemma and Schwann cell plasma membrane are tightly apposed at the paranode where electron microscopic studies have shown rows of regularly spaced particles in the membranes of both the axon and Schwann cell (Ichimura and Ellisman, 1991; Wiley and Ellisman, 1980). This close association between the membranes of both cells in the paranodal region may be functionally very significant since it is found to be a site for disruption in peripheral neuropathy (Griffin et al., 1996). This junctional specialization of intermittent densities has been described as being similar to septate junctions. Recently a component of the paranodal septate-like junction has been identified by two groups. Paranodin (Menegoz et al., 1997) also called Caspr (Peles et al., 1997) is a transmembrane protein expressed by neurons in the PNS and CNS and is developmentally regulated distributing to the paranodes of mature myelinated axons (Einheber et al., 1997). Paranodin/Caspr appears to interact with the cytoskeleton through a region in its intracellular domain which is capable of binding the erythrocyte protein 4.1 which links the erythrocyte plasma membrane to cortical actin and spectrin. Thus Caspr has been implicated as a potential candidate to mediate axon-glial interactions at the paranodes.

In spite of the functional importance the node of Ranvier and paranodal regions have in impulse conduction, the molecules which play important roles in axon-Schwann cell interactions remain largely unknown.

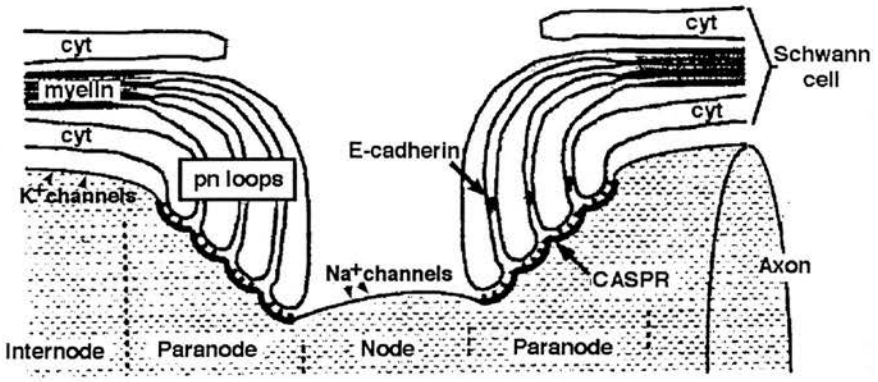

Diagrammatic representation of a node of Ranvier and paranode indicating the locations of E-cadherin, CASPR, Na^+ and K^+ channels. Modified from Einheber et al., 1997.

1.4 THE MOLECULAR ORGANIZATION OF COMPACT MYELIN

After spiralization the compact myelin sheath is formed by the simultaneous loss of cytoplasm within the spirals bringing the cytoplasmic faces of the plasma membrane together to fuse forming the major dense line and the closing of the 12-14 nm gap in the outer faces of the plasma membrane of the mesaxon to 2.0-2.5 nm thereby forming the intraperiod line (Peters et al., 1991) (Fig. 9A). It appears that myelin sheath thickness is directly related to axonal calibre with larger diameter axons possessing thicker sheaths (Fraher, 1978; Friede and Samorajski, 1967; Hahn et al., 1987). Therefore axonal calibre regulates whether a Schwann cell will myelinate or not as well as how much myelin it will produce which again implicates neuronal regulatory influences on Schwann cells.

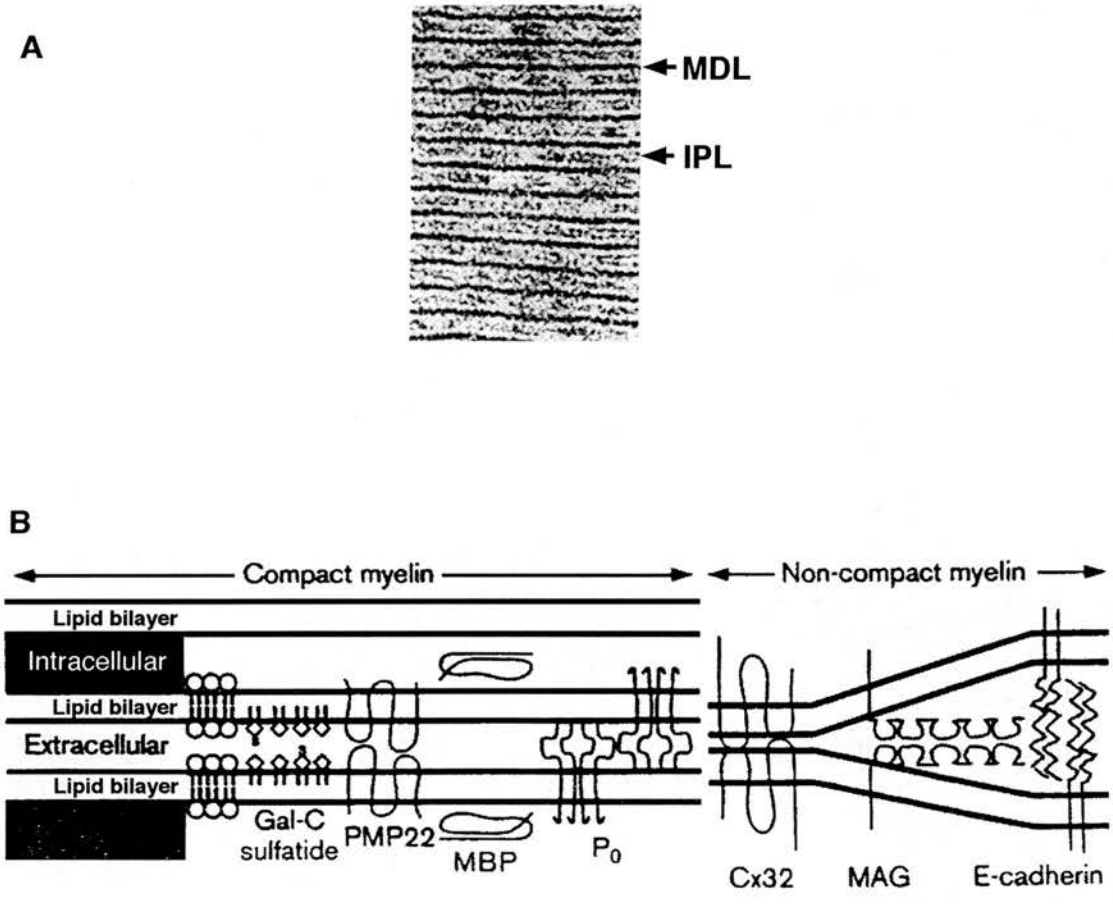

Figure 9. Multilamellar structure of the compact myelin sheath (A) and topology of myelin components in the compact and non-compact myelin sheath (B). (A) A high magnification electron micrograph of the myelin sheath demonstrates the fused cytoplasmic membranes which form the major dense line (MDL) and the intraperiod line (IPL) formed by the close apposition of the outer faces of the plasma membrane. (B) The myelin proteins P0, PMP22, and MBP are present in compact myelin and MAG, Cx32, and E-cadherin are in uncompacted regions of the Schwann cell cytoplasmic channel network.

From (A) Raine, 1984; (B) Scherer, 1997.

1.4.1 The lipid composition of the myelin membrane

The elaboration of a myelin sheath requires an enormous increase in the biosynthesis of lipids and membrane-associated proteins which compose the bilayer and which play a role in generating this crystalline multilammelar structure (Fig. 9B). It is not surprising that the myelin membrane has a high lipid content due to its specialized function as an insulator of nerve fibers essential for saltatory conduction (Ritchie, 1984). Myelin has an extremely high ratio of lipid to protein, 80% to 20% respectively, in comparison with equal amounts of lipid and protein in most plasma membranes. As in all plasma membranes the lipid content in myelin membranes consists of cholesterol, glycolipids and phospholipids differing only in that it has a higher cholesterol content (Stoffel and Bosio, 1997) than other membranes, less phosphatidylcholine, and an abundance of the glycolipids galactocerebroside and galactosulfatide (Kirschner et al., 1984). Cholesterol is the most abundant single lipid comprising 25% of the dry weight of PNS myelin, whereas the phospholipids as a group comprise 50% of the dry weight of myelin (Norton and Cammer, 1984). Of the phospholipid species, there is about twice as much by weight of phosphatidylethanolamine as the other species (phosphatidylcholine, phosphatidylserine, phosphatidylinositol, and sphingomyelin). The phospholipids and glycolipids are asymmetrically arranged in the bilayer. Phosphatidylethanolamine, phosphatidylcholine, phosphatidylserine and phosphatidylinositol are predominantly found in the inner leaflet whereas the outer extracellular leaflet contains sphingomyelin and the glycolipids (Kirschner and Ganser, 1982; Stoffel and Bosio, 1997). The unique lipid composition of myelin is predominantly due to its enrichment of galactocerebroside (GalC) and galactosulfatide (sulfatide).

The expression of GalC and sulfatide are have been shown to be developmentally regulated in both the oligodendrocyte lineage and the Schwann cell lineage (Jessen et al., 1985; Mirsky et al., 1990; Mirsky et al., 1980; Raff et al., 1978;

Ranscht et al., 1982) and in Schwann cells expression of both glycolipids is up-regulated by axonal contact (Mirsky et al., 1990; Mirsky et al., 1980). Using the monoclonal antibodies O1 for GalC and O4 for sulfatide (amongst other species) the developmental stage of expression of each lipid antigen was determined demonstrating that in the Schwann cell lineage O4 is expressed in embryonic Schwann cells and GalC expression parallels the expression of myelin proteins (Mirsky et al., 1990; Schachner et al., 1981; Sommer and Schachner, 1981). GalC is also expressed by non-myelin-forming Schwann cells showing that the plasma membranes of myelin-forming and non-myelin-forming Schwann cells differ less in lipid than protein composition (Jessen et al., 1985).

Studies using dorsal root ganglion neuron and Schwann cell co-cultures grown in the presence of saturating levels of the Ranscht anti-GalC monoclonal antibody to deplete surface GalC indicated that GalC was essential for the formation of myelin even though these Schwann cells did form 1:1 relationships with axons (Owens and Bunge, 1990; Ranscht et al., 1987). This suggests that GalC depletion may alter the physical properties of the membrane resulting in the inhibition of myelination. It should be noted that the Ranscht monoclonal antibody is not specific for GalC and also recognizes monogalactosyldiglyceride, sulfatide, seminolipid and psychosine whereas the O1 antibody recognizes GalC, monogalactosyldiglyceride, and psychosine, and the O4 antibody recognizes sulfatide and seminolipid (Bansal et al., 1990).

Two groups have generated a null mutant in which the UDP-galactose-ceramide galactosyltransferase gene (*cgt*), the key enzyme in glycolipid synthesis, has been ablated by gene targeting (Bosio et al., 1996; Coetzee et al., 1996). GalC, sulfatide and galactodiglyceride were completely absent in the CNS and PNS of the mutant mice resulting in dysmyelinosis at around postnatal-day 10 to death after 3 weeks. Nerve conduction velocity was drastically reduced. Interestingly, in spite of the severe phenotype of the mutant mice expression of the genes for the myelin

proteins *Mbp, Plp, Mag* and *P0* were normal and the ultrastructure of myelin appeared normal in the PNS but in the CNS the periaxonal space was enlarged and the paranodal loops and nodes were disorganized and lost contact with the axolemma (Stoffel and Bosio, 1997). The lipid bilayers of the mutants have an altered lipid composition which leads to increased fluidity, permeability, and impaired packing (Bosio et al., 1998). It appears that the main function of GalC and sulfatide is in their contribution to an ion-permeable bilayer necessary for impulse propagation.

1.4.2 PNS myelin proteins

As lipids play a necessary role in myelination the less abundant protein constituents of myelin also play an important role in the architecture of the myelin sheath. The proteins are largely specific to myelin-forming cells in the PNS and CNS. Early studies at the protein level has shown that many of the myelin proteins have a role in myelin sheath structure but cloning of the major myelin genes has led to functional studies *in vivo* by targeted deletion of each gene through homologous recombination.

1.4.2.1 P0

P0 is the most abundant protein of PNS myelin and accounts for over 50% of the total protein in compact myelin (Greenfield et al., 1973; Ishaque et al., 1980). It is a glycoprotein with a molecular weight of 28,500 originally identified by lectin binding studies (Brostoff et al., 1975; Everly et al., 1973; Kitamura et al., 1976; Wood and Dawson, 1973). The nucleotide sequence of P0 as deduced from the cDNA sequence and by the direct protein sequence depicts an integral membrane protein with a single transmembrane domain, an N-terminal extracellular domain and a C-terminal cytoplasmic domain (Barbu, 1990; Hayasaka et al., 1991; Lemke and Axel, 1985; Sakamoto et al., 1987). X-ray crystallography of the extracellular

domain of P0 has revealed that P0 forms tetramers in the plane of the membrane which interact with tetramers in the apposing membrane forming a lattice that holds myelin together (Shapiro et al., 1996).

The primary structure of P0 reveals a signal sequence comprising the first 28 amino acids of the open reading frame which is necessary for protein translocation and membrane insertion. The extracellular domain contains one site for N-linked glycosylation. P0 has previously been shown to be N-glycosylated at a single position with an extracellularly positioned oligosaccharide chain (Ishaque et al., 1980; Peterson and Grevner, 1978; Wood and McLaughlin, 1975). Two carbohydrate epitopes, L2/HNK-1 and L3, which are found in neural cell adhesion molecules (CAMs) are present on the chain (Bollensen and Schachner, 1987; Edelman, 1983). The carbohydrates may be important for P0 by influencing the conformation of the extracellular domain, but they are unlikely to participate in the homophilic adhesion of the extracellular myelin membranes (Filbin and Tennekoon, 1993; Filbin and Tennekoon, 1991). The homophilic adhesive properties of P0 are more likely due to the presence of a single immunoglobulin-like (Ig-like) domain in its extracellular region (Filbin et al., 1990). Thus P0 is a member of the immunoglobulin gene superfamily (Lai et al., 1987; Salzer and Colman, 1989) a large family of proteins known to mediate cell-cell interactions in the nervous and immune systems but unlike most members of this family which possess multiple Ig-like domains (Williams and Barclay, 1988). Transfection studies have provided direct evidence that P0 functions homotypically to adhere plasma membranes of adjacent cells (D'Urso et al., 1990; Filbin and Tennekoon, 1990; Schneider-Schaulies et al., 1990). Zones of cell-cell contact in transfected cells expressing P0 were shown to contain high concentrations of the protein. Transfection studies also show that formation of a disulfide bond in the Ig domain is essential for its homophilic adhesion (Zhang and Filbin, 1994) and site-directed mutagenesis studies demonstrated that both molecules of P0 in the homophilic pair must be

glycosylated for adhesion to occur (Filbin and Tennekoon, 1993). Although one adhesive domain in the protein has been mapped to amino acids 91-95 there is an indication that there is more than one domain responsible for cell adhesion (Zhang et al., 1996). Transfection studies have shown that the adhesive properties of the extracellular domain depends on the intact cytoplasmic domain (Wong and Filbin, 1994) and the interaction of P0 with microtubules was important for this adhesion (Wong and Filbin, 1996).

Myelin basic proteins (MBPs) have been postulated to be involved in myelin compaction based on studies of the *shiverer* mouse mutant. In the *shiverer* mutant there is a deletion of a large part of the *Mbp* gene resulting in a severe CNS phenotype (Kirschner and Ganser, 1980). In the fibres where myelin has formed, the major dense line is missing which implies that MBPs function in compaction of the apposed cytoplasmic faces of myelin to form the major dense line (Privat et al., 1979). Although MBP is normally expressed in the CNS and the PNS, the mutant mice have functionally normal myelin with little structural abnormality in peripheral nerves (Kirschner and Ganser, 1980; Rosenbluth, 1980). Since P0, which is specific to PNS myelin, has a basic C-terminal tail, it has been suggested that P0 takes the place of MBP in the PNS since P0 is expressed exclusively in the PNS (Lemke and Axel, 1985).

The cytoplasmic domain of P0 has been postulated to interact electrostatically with acidic lipids present in the cytoplasmic face of the bilayer to form the major dense line of the myelin sheath. When P0 is purified from myelin it is complexed with tightly bound acidic lipids of which the most abundant is phosphatidylserine (Ishaque et al., 1980). Phosphorylation by protein kinase C regulates the strength of the electrostatic interaction between P0 and negatively charged phospholipids and alters myelin compaction. Dephosphorylation of P0 is known to occur during compaction when the major dense line forms (Eichberg and Iyer, 1996; Hilmi et al., 1995; Rowe-Rendleman and Eichberg, 1994; Suzuki et al.,

1990). A peptide fragment containing the cytoplasmic region of P0 was found to bind and aggregate phospholipid vesicles by ionic interactions providing further evidence that the cytoplasmic domain of P0 may be responsible for the formation and maintenance of the major dense line (Ding and Brunden, 1994).

Earlier studies have shown that P0 is expressed exclusively in the PNS in myelin-forming Schwann cells and localized to compact myelin (Brockes et al., 1980; Trapp et al., 1981). P0 mRNA levels rise dramatically from birth and peak in actively myelinating Schwann cells (Stahl et al., 1990; Trapp et al., 1988). Axonal contact regulates P0 expression since levels fall sharply in transected nerve or when Schwann cells are removed from axonal contact and placed in culture (Lemke et al., 1988; Mirsky et al., 1980; Politis et al., 1982). Some studies have shown that even after permanent nerve transection a basal level of P0 mRNA and protein remain (LeBlanc and Poduslo, 1990; Poduslo et al., 1984; Poduslo et al., 1985; Poduslo and Windebank, 1985). In addition Po mRNA and protein is expressed long before myelination during embryogenesis in the neural crest, Schwann cell precursors and embryonic Schwann cells indicating an early role for P0 in Schwann cell development (Bhattacharyya et al., 1991; Lee et al., 1997; Zhang et al., 1995). When Schwann cells myelinate, there is a dramatic up-regulation of P0 basal level expression and the basal expression down-regulates in Schwann cells that do not myelinate indicating that there is both positive and negative regulation of P0 gene expression.

The *P0* gene has been isolated and consists of 6 exons distributed over 7 kb and is located on mouse chromosome 1 (Lemke et al., 1988; You et al., 1991). Evidence that P0 expression is important for myelination came from experiments using a retrovirus-mediated antisense mRNA strategy which suppressed P0 protein synthesis and thereby inhibited spiralization and compaction (Owens and Boyd, 1991).

Mice with a null mutation of the *P0* gene have been generated by homologous recombination (Giese et al., 1992). Homozygous null mice exhibit a behavioral phenotype first evident at 2 to 4 weeks of age with progressive disturbances in motor coordination, tremors, and eventually occasional convulsions but not death. At the cellular level, peripheral nerves were severely hypomyelinated with a majority of fibers containing fewer spirals around axons, non-compacted regions, and fewer compacted regions with widened intraperiod lines in support of the role of P0 as a mediator of intracellular and extracellular membrane adhesion. The loss of P0 did not prevent the segregation of axons in a 1:1 relationship or ensheathment. Interestingly, there was some axonal degeneration and an up-regulation of several proteins, L1, NCAM, NGFR, MAG, PLP, and tenascin. Some sheaths were observed with normal periodicity and a normal major dense line suggesting that other proteins may compensate for the lack of P0 or membrane adhesion can be mediated by other proteins. Double mutants generated by crossing the *P0* null mutant with the *shiverer* mutant have peripheral nerve myelin devoid of both the major dense line and the intraperiod line implicating MBP as the mediator of intracellular adhesion in the *P0* null mutants (Martini et al., 1995). Therefore both P0 and MBP contribute to the formation of the major dense line. The phenotype of the double mutant mice also revealed that not only are MBP and P0 involved in compaction but also regulate myelin thickness (Martini et al., 1995).

The *P0* gene does not show linkage with any spontaneous mutations in the mouse. Point mutations in the human *P0* gene have been linked to the peripheral neuropathy Charcot-Marie Tooth neuropathy type 1B (CMT1B), Dejerine-Sottas syndrome, and congenital hypomyelination (Hayasaka et al., 1993; Kulkens et al., 1993; Warner et al., 1996). These mutations are dominant because individuals with CMT1B are heterozygous for the normal and mutant alleles whereas heterozygous mice for the *P0* null allele have a normal phenotype.

Transgenic mouse studies have indicated that the transcriptional regulation of the *P0* gene is controlled by a 1.1 kb region flanking the transcription start site. When linked to reporter genes this fragment drives developmental stage and Schwann cell specific expression in transgenic mice (Hayasaka et al., 1993; Kulkens et al., 1993; Messing et al., 1992; Messing et al., 1994; Warner et al., 1996). Further dissection of the regulatory elements in the core *P0* promoter has identified two regulatory elements, a G/C-rich element that binds nuclear factor Sp1 and a CAAT box that binds NF-Y. These elements were shown to be essential for transcription in transfected Schwann cells (Brown and Lemke, 1997).

1.4.2.2 Myelin Basic Proteins

The myelin basic proteins (MBPs) are a group of small, peripheral membrane proteins synthesized on free polysomes, whose mRNAs originate from a single gene by alternative splicing of the primary transcript (Aruga et al., 1991; de Ferra et al., 1985; Kitamura et al., 1990; Newman et al., 1987; Takahashi et al., 1985). Although the MBPs are quite abundant proteins in CNS myelin, in PNS myelin they comprise less than 15% of the total protein (Greenfield et al., 1973). They are thought to bring about the apposition of the cytoplasmic membrane leaflets that form the major dense line of the myelin sheath. The MBPs are positively charged molecules which exhibit a high affinity for acidic lipids in the bilayer (Maggio and Yu, 1992; Mendz, 1992; Ong and Yu, 1984). It has been suggested that this affinity for membranes is non-specific and a mechanism for MBP mRNA transport has evolved which targets these proteins to regions where myelin compaction occurs (Brophy et al., 1993; Colman et al., 1982; Gould and G., 1990; Griffiths et al., 1989; Trapp et al., 1987; Verity and Campagnoni, 1988). The transport of MBP mRNA requires microtubules and kinesin as demonstrated in culture studies using anti-sense oligonucleotides to suppress kinesin expression and agents to depolymerize microtubules (Carson et al., 1997).

The mouse *Mbp* gene is 32 kb in size comprising seven exons and maps to chromosome 18 (Roach et al., 1985; Takahashi et al., 1985). The MBP isoforms which range in size from 14 kDa to 21.5 kDa differ by the presence or absence of sequences encoded by exons 2, 5, and 6 (de Ferra et al., 1985; Newman et al., 1987; Roach et al., 1985; Takahashi et al., 1985). Although functional differences between the isoforms are not apparent, when MBP isoforms are expressed in heterologous cells and *shiverer* oligodendrocytes, the exon 2 containing isoforms, 17 kDa and 21.5 kDa, have a diffuse cytoplasmic and nuclear distribution whereas the 14 kDa and 18.5 kDa isoforms are membrane-associated (Allinquant et al., 1991; Pedraza et al., 1997; Staugaitis et al., 1990). The isoforms are developmentally regulated with exon 2 containing isoforms appearing earlier (Barbarese et al., 1978; Carson et al., 1983).

Recently the 32 kb *Mbp* gene has been found to part of a larger gene called *golli-mbp* (gene in the oligodendrocyte lineage) which spans over 100 kb in length (Campagnoni et al., 1993; Pribyl et al., 1993). The *golli-mbp* gene includes 5 additional exons with an additional transcription initiation site far upstream of the myelin-specific site and encodes at least three alternatively spliced golli mRNAs. The *golli-mbp* gene is expressed early during development in CNS neurons as well as other tissues (Landry et al., 1996).

As mentioned in the previous section, the *shiverer* mutant has a deletion in the *Mbp* gene which encompasses exon 3 to 7 resulting in the complete absence of all the MBP isoforms (Molineaux et al., 1986; Roach et al., 1985). Homozygotes for the mutation display a tremor or "shivering" phenotype, convulsions and early death. The PNS of *shiverer* mice is functionally normal and few structural abnormalities are found. These include reduction in axon calibre and myelin sheath thickness and an increase in the number of Schmidt-Lanterman incisures to more than double (Gould et al., 1995; Peterson and Bray, 1984). The wild type *Mbp* gene introduced by transgenesis can rescue the shiverer phenotype both behaviorally and

structurally (Readhead et al., 1987). Interestingly, when transgenic *shiverer* mice were generated using a construct which encoded the 14 kDa isoform only, the mutant phenotype was also rescued indicating that just one MBP isoform is sufficient for normal myelin compaction (Kimura et al., 1989).

The *Mbp* gene contains separate enhancers for CNS and PNS expression (Gow et al., 1992). The regulatory elements for Schwann cell specific expression are still unknown but a 1.9 kb sequence upstream of the myelin transcription initiation site of the *Mbp* gene can direct transcription in oligodendrocytes at the correct developmental stage but not in Schwann cells.

1.4.2.3 Peripheral Myelin Protein 22

The glycoprotein peripheral myelin protein 22 (PMP22) accounts for 2 to 5% of total protein from rat PNS myelin (Suter and Snipes, 1995b). Although PMP22 is most abundant in peripheral nerve its expression is not restricted to the PNS; there are low levels of mRNA expression in lung, intestine, heart, brain, skeletal muscle, testis, and liver (Baechner et al., 1995; Manfioletti et al., 1990; Spreyer et al., 1991; Suter and Snipes, 1995b; Welcher et al., 1991). PMP22 is identical to the growth arrest-specific mRNA gas-3, periodic acid Schiff protein (PASII), crushed denervated cDNA 25 (CD25) and sciatic nerve regeneration clone 13 (SR13) but was finally called PMP22 (Kitamura et al., 1976; Manfioletti et al., 1990; Snipes et al., 1992; Spreyer et al., 1991; Welcher et al., 1991). The identification of gas-3 was based on its upregulation in growth-arrested NIH 3T3 fibroblasts indicating that PMP22 may be involved in cell cycle regulation in non-neural tissue (Suter and Snipes, 1995b).

The deduced amino acid sequence of PMP22 predicts a protein of 17 kDa which has one N-linked glycosylation site hence the M_r on SDS-PAGE is 22 kDa (Manfioletti et al., 1990; Snipes et al., 1992; Spreyer et al., 1991; Welcher et al., 1991). PMP22 is an extremely hydrophobic protein with four transmembrane

domains (Spreyer et al., 1991), two extracellular domains and amino- and carboxy-terminal domains residing in the cytosol (D'Urso and Müller, 1997). An N-linked carbohydrate chain carries the L2/HNK-1 adhesion epitope (Snipes et al., 1993) and is located in the first putative extracellular loop (Pareek et al., 1993). The protein has a signal sequence at its amino terminus which is not cleaved in the mature protein (Manfioletti et al., 1990).

PMP22 has been localized to myelin-forming Schwann cells in peripheral nerve and more specifically to the compact myelin sheath (Haney et al., 1996; Snipes et al., 1992). In addition, at the ultrastructural level PMP22 was localized to the membranes of non-myelin-forming Schwann cells in human peripheral nerve (Haney et al., 1996). In the CNS PMP22 mRNA has been detected in motoneurons by *in situ* hybridization (Parmantier et al., 1995). Like other myelin proteins, *Pmp22* gene expression is regulated by axonal contact as shown by sciatic nerve transection (Snipes et al., 1992; Spreyer et al., 1991) and is also upregulated in cultured Schwann cells by exposure to agents which elevate intracellular cAMP (Pareek et al., 1993). Interestingly, PMP22 mRNA in other cell types is not upregulated by raising intracellular cAMP (Spreyer et al., 1991). This suggests that cAMP may induce the expression of a Schwann cell specific transcription factor which influences differentiation specific genes.

The human *PMP22* gene spans 40 kb and contains 4 coding exons and two alternatively spliced 5'-non-coding exons (exon 1A and 1B) (Suter et al., 1994). The gene is regulated by the use of two alternative promoters, one located upstream of exon 1A and the other upstream of exon 1B. The proteins produced from each mRNA are identical but transcripts containing exon 1A are preferentially expressed in peripheral nerve while transcripts containing exon 1B are preferentially expressed in other tissues (Suter et al., 1994). It is likely that there may be Schwann cell specific regulatory elements controlling Schwann cell *PMP22* expression.

Point mutations in the *PMP22* gene are responsible for autosomal dominant peripheral neuropathies in humans and mice. The most common type in humans is Charcot-Marie-Tooth disease 1A (CMT1A) affecting 1 in 2,500 people (for reviews, (Suter and Snipes, 1995a; Suter and Snipes, 1995b). The human *PMP22* gene was mapped within a 1.5 Mb duplication on human chromosome 17 associated with the most common form of CMT1A disease (Lupski et al., 1991; Matsunami et al., 1992; Timmerman et al., 1992; Valentijn et al., 1992). A smaller number of patients with CMT1A have a point mutation in the gene but have a similar phenotype as the increased gene dosage form (Suter and Snipes, 1995a). A more severe peripheral neuropathy called Dejerine-Sottas syndrome (DSS) is also the result of point mutations in the *PMP22* gene (Roa et al., 1993). Mutations in the *PMP22* gene also result in a disease with a mild phenotype called hereditary neuropathy with liability to pressure palsies (HNPP) also referred to as tomaculous neuropathy which is associated with a deletion of the same region of chromosome 17 that is duplicated in CMT1A (Chance et al., 1993; Nicholson et al., 1994). Thus gene dosage and mutations in the *PMP22* gene give rise to distinct neuropathies indicating that the correct regulation of the gene is critical for normal function.

The *Trembler* (*Tr*) mutation in the mouse is characterized by a severe peripheral neuropathy with hypomyelination and Schwann cell proliferation into adulthood (Henry et al., 1983; Henry and Sidman, 1988). Heterozygous mutants have some axons with thin myelin sheaths but the majority of axons are unsheathed. The abnormal Schwann cell proliferation is characterized by onion bulb formation which is indicative of demyelination-induced Schwann cell hypertrophy (Dyck et al., 1993). Homozygous mutants have almost no myelin. The *Tr^j* allele has a more severe phenotype and the homozygous mutants are lethal. It has been shown that both *Tr* and *Tr^j* have point mutations in the *Pmp22* gene in putative transmembrane domains (Suter et al., 1992). In *Tr* there is a substitution of an aspartic acid residue for a glycine residue within the fourth transmembrane

domain of *Pmp22* whereas in the *Trj* there is a leucine to proline substitution in the first putative transmembrane domain (Suter et al., 1992). The same mutation in *PMP22* as in *Trj* mutant mice has been found in a family with a severe form of CMT1A (Valentijn et al., 1992). There is evidence from transfection studies that the *Tr* and *Trj* mutant proteins are not inserted into the plasma membrane and accumulate in the ER and Golgi compartments suggesting that impaired trafficking may contribute to the defect (D'Urso et al., 1998; Naef et al., 1997). One paper suggests than in *Trj* the PMP22 may be in the lysosomal/endosomal compartments (Notterpek et al., 1997).

Transgenic mice and rats have been generated which overexpress the *Pmp22* gene (Magyar et al., 1996; Sereda et al., 1996). Transgenic rats display a phenotype similar to CMT1A characterized by hypomyelination and Schwann cell hypertrophy (Sereda et al., 1996). Transgenic mice with a high copy number of *Pmp22* transgenes displayed a severe phenotype with almost a complete lack of myelin (Magyar et al., 1996). *Pmp22* null mutant mice have been generated by homologous recombination and display a progressive hind limb paralysis (Adlkofer et al., 1995). At the cellular level there was evidence of demyelination, tomacula, onion bulb formation and axonal loss. Heterozygous mice $Pmp^{+/-}$ display a neuropathy with a late onset and a mild degree of demyelination similar to HNPP (Adlkofer et al., 1997). Taken together the spontaneous mutations and engineered mutations and have shown that PMP22 is necessary for normal myelination and may have a role in cell growth, the regulation of myelin thickness, and maintenance of myelin.

1.4.2.4 Myelin Associated Glycoprotein

Myelin-associated glycoprotein (MAG) is a minor component of PNS and CNS myelin comprising about 0.1% (Figlewicz et al., 1981; Quarles, 1984). Its presence was first demonstrated biochemically in CNS myelin (Everly et al., 1973)

and it was later demonstrated by immunocytochemistry in the PNS where it specifically localized to the uncompacted regions in Schwann cells which include periaxonal membranes, Schmidt-Lanterman incisure, paranodal loops, and the outer mesaxon but was absent from compact myelin (Schober et al., 1981; Sternberger et al., 1979; Trapp et al., 1982; Trapp et al., 1984a). Based on its localization it was suggested that MAG had a role in forming and stabilizing the 12 to 14 nm periaxonal space and cytoplasmic collar (Trapp et al., 1984a; Trapp et al., 1984b). MAG was shown to be expressed early in development when Schwann cells first ensheathe axons and form a 1:1 relationship (Martini and Schachner, 1986; Owens and Bunge, 1989). MAG co-localizes with the microfilament components F-actin and spectrin suggesting that MAG may interact with the cytoskeleton (Trapp et al., 1989b).

The M_r of MAG by SDS-PAGE is 100 kDa but when deglycosylated, two isoforms of 72 kDa (L-MAG) and 67 kDa (S-MAG) are apparent (Frail and Braun, 1984). Both isoforms are present in the CNS where L-MAG is more abundant than the smaller isoform (Salzer et al., 1990). In the PNS S-MAG is predominant and peaks during the most active phase of myelination but, in contrast to the CNS ,the level of L-MAG is very low (Frail et al., 1985; Tropak et al., 1988). Two MAG mRNAs as deduced from cDNA clones arise by alternative splicing and differ in the presence or absence of an insert near the 3' end (Arquint et al., 1987; Lai et al., 1987; Salzer et al., 1987; Tropak et al., 1988). Both isoforms share an N-terminal signal sequence, a large extracellular N-terminal domain, a single transmembrane domain but have different C-terminal cytoplasmic domains (Pedraza et al., 1990). Analysis of the extracellular domain of MAG revealed five repeats with homology to each other and with the Ig domain of members of the immunoglobulin gene superfamily known to mediate cell adhesion which includes the neural cell adhesion molecules L1, NCAM, P0 (Arquint et al., 1987; Lai et al., 1987; Salzer et al., 1987). The extracellular region of MAG also has the L2/HNK-1 carbohydrate structure

which has been shown to be involved in cell-cell interactions (Kruse et al., 1984; Künemund et al., 1988; MacGarry et al., 1983). Based on MAGs structural similarilty to adhesion molecules with Ig domains and its localization to the periaxonal collar it was thought to have a role in axon-glial interactions through recognition and adhesion during initial envelopment. In fact when MAG was overexpressed *in vitro* it was shown to promote initial investment of axons by Schwann cells (Owens et al., 1990). Further support that MAG functions in cell adhesion came from the demonstration that MAG-containing liposomes specifically bind to axons (Johnson et al., 1989; Poltorak et al., 1987; Sadoul et al., 1990). MAG has been shown to promote (Johnson et al., 1989) or inhibit neurite outgrowth from certain neuronal populations (McKerracher et al., 1994; Mukhopadhyay et al., 1994) and the inhibitory interaction is through a sialoglycoprotein (Debellard et al., 1996). It has been suggested that MAG is a potent inhibitor of axonal regeneration in the CNS and could contribute to the absence of regeneration after injury (Tang et al., 1997).

The *Mag* gene consists of 13 exons spanning about 16 kb (Lai et al., 1987; Nakano et al., 1991) and maps to mouse chromosome 7 (D'Eustachio et al., 1988) and human chromosome 19 (Barton et al., 1987). The transcript which encodes L-MAG contains all of the exons except exon 12 which is present in S-MAG and introduces an in frame termination codon. S-MAG lacks the non-coding exon 2. A third MAG transcript has been identified which lacks exon 2 and 12 (Fujita et al., 1989).

Further support that MAG was essential for myelination came from *in vitro* experiments in which MAG antisense transcripts were constitutively expressed by retroviral transfection of Schwann cells with antisense oligonucleotides thereby inhibiting myelin formation (Owens and Bunge, 1991). Therefore it was surprising when two groups independently generated *Mag* null mice by homologous recombination and found that myelin formed normally in the PNS and CNS in the

absence of MAG (Li et al., 1994; Montag et al., 1994). The behavior of the mutant mice was normal except for a reduction in fine motor coordination (Li et al., 1994). On the cellular level there were no significant abnormalities in young animals but after 8 months of age, peripheral nerves showed signs of axon and myelin degeneration in about 30% of the fibers (Fruttiger et al., 1995). The phenotype of the *Mag* null mutant indicates that MAG is not required for initial ensheathment or spirialization in the PNS but has a role in maintenance. To test whether N-CAM may be compensating for MAG in the mutant, double mutants were generated by crossing *N-CAM* null mice with *Mag* null mice. The double mutants had a phenotype with a slightly earlier onset when compared to the *Mag* mutant demonstrating that N-CAM does not compensate for MAG but may have a partial effect on axon-Schwann cell integrity (Carenini et al., 1997).

1.4.2.5 Proteolipid Protein

Proteolipid protein (PLP) is the major integral membrane protein in CNS myelin comprising about 50% of total protein (Lees and Brostoff, 1984). Alternative splicing of the *Plp* gene results in two isoforms, PLP and the smaller isoform DM-20 (Nave et al., 1987). The isoforms are developmentally regulated in the CNS where PLP is a major structural component of myelin in the adult with a possible role in maintaining the intraperiod line (Duncan et al., 1987). DM-20 is expressed at lower levels in the adult but predominates during early myelination and is the only isoform expressed in oligodendrocyte precursors during embryogenesis suggesting an additional role for PLP (Ikenaka et al., 1992; Timsit et al., 1992; Timsit et al., 1995). Although PLP is the major component of myelin in the CNS it accounts for <1% of the total myelin protein in the PNS where DM-20 is the predominant isoform expressed during development and in the adult (Griffiths et al., 1995; Lemke, 1992; Pham-Dinh et al., 1991). PLP mRNA and protein have been detected in both myelin-forming and non-myelin-forming Schwann cells

(Agrawal and Agrawal, 1991; Griffiths et al., 1995; Griffiths et al., 1989; Puckett et al., 1987). DM-20 is the isoform which is present in the cytoplasmic regions of the internode, non-myelin-forming Schwann cells, the satellite cells of spinal, cranial and autonomic ganglia, and ensheathing cells of the olfactory bulb whereas PLP is present in the perinuclear region of myelin-forming Schwann cells (Griffiths et al., 1995). Neither isoform was found in compact myelin. Increasing the level of PLP and DM-20 expression in transgenic mice leads to the incorporation of PLP but not DM-20 into compact myelin indicating that each isoform is targeted differently in the Schwann cell (Anderson et al., 1997). The *Plp* gene is expressed early during Schwann cell development demonstrated by analysis of transgenic mice carrying a transgene composed of the *Plp* promoter and first intron fused to the *LacZ* gene (Wight et al., 1993) and at E12.5 by *in situ* hybridization using a DM-20 riboprobe (Peyron et al., 1997).

Although missense mutations in *PLP* can cause dysmyelination in the CNS which results in the severe Pelizaeus Merzbacher disease (PMD) and the milder X-linked spastic paraplegia type 2 in humans, the PNS of these patients remains normal. In addition the PNS is not affected in the *jimpy* mouse mutant which exhibits a severe CNS dysmyelination and death at 3 to 4 weeks of age (Griffiths et al., 1995; Nave, 1996). Recently, a kindred was described in which a novel single base-pair deletion resulted in the complete absence of PLP/DM-20 expression causing a less severe form of PMD with widespread CNS demyelination and progressive demyelinating peripheral neuropathy (Garbern et al., 1997). Because peripheral myelin is formed in this kindred and subsequently breaks down it suggests that PLP is necessary for the maintenance of PNS myelin sheaths in humans (Garbern et al., 1997). In contrast mice carrying a null allele for *Plp* as a result of targeted gene inactivation by homologous recombination do not exhibit dysmyelination and have normal motor function (Klugmann et al., 1997) but it remains to be seen if they will exhibit a similar phenotype to the human null

mutation at an older age; alternatively PLP may be more important for myelin stability in humans than in mice.

1.4.2.6 Minor components of the PNS myelin proteins

The protein P2 is a minor constituent of rodent PNS myelin protein comprising less than 1% of total myelin protein whereas in humans it comprises 14% of total myelin protein (Greenfield et al., 1973). P2 is a member of a large family of fatty acid binding proteins (FABPs) based on sequence homology with other family members and is thought to be involved with the transport of intracellular fatty acids (Martenson and Uyemura, 1992; Narayanan et al., 1988).

Another minor component of PNS myelin proteins is the enzyme 2',3'-cyclic nucleotide-3'-phosphodiesterase (CNPase) which comprises 0.5 to 1% of PNS myelin proteins. CNPase levels are much higher in oligodendrocytes compared to Schwann cells with even lower abundance in non-neural cells. CNPase was the first enzyme to be characterized as a component of the myelin membrane (Adams et al., 1963). Developmental studies have shown that CNPase is an early appearing myelin-associated protein in the developing nervous system (Braun et al., 1988). In myelin-forming cells, CNPase is concentrated at the cytoplasmic side of all membranes except those of compact myelin. The function of this protein in the myelin-forming cell is still unclear but studies in transgenic mice in which the protein was overexpressed revealed that CNPase may have a role in membrane expansion during myelination and may help target MBP to compact myelin (Yin et al., 1997).

1.5 BACKGROUND TO THE PROJECT

Myelination requires dramatic changes in cell shape which must involve the cytoskeleton to regulate the extension of myelin processes during axonal ensheathment. The cytoskeleton of oligodendrocytes has been shown to be intimately involved in the extension of myelin processes in the rat CNS (Wilson and Brophy, 1989). The Schwann cell cytoskeleton must also play a major role in the process of myelination because the Schwann cell undergoes dramatic changes in cell shape during process elongation along axons, in segregation of an individual axon, and in spiralization around the axon. In fact depolymerization of actin microfilaments in Schwann cell/neuron co-cultures disrupts myelination and results in the failure of Schwann cells to form a 1:1 relationship with axons (Fernandez-Valle et al., 1997).

It is well established that axonal signals are crucial for Schwann cell differentiation but the precise intracellular events following that interaction remain elusive. In an attempt to identify molecules that may be involved in the intracellular mechanism that drives axonal ensheathment and regulates changes in cell shape, a cytoskeleton-associated protein called periaxin was isolated from the Triton X-100 insoluble fraction of rat PNS myelin (Gillespie et al., 1994). An antibody raised against the protein (p170) recognized a relatively abundant protein of M_r 170 kDa in sciatic nerve homogenate on SDS-polyacrylamide gel electrophoresis. Immunofluorescence analysis of cultured cells from rat sciatic nerve demonstrated that periaxin was expressed by Schwann cells.

A full length cDNA was cloned and sequenced and the deduced amino acid sequence predicted a protein of 147 kDa with no sequence similarity to any other protein sequence in the database. Periaxin is not an integral membrane protein based on the absence of transmembrane domains by hydrophobicity plot analysis and it does not have N-glycosylation sites. The protein has a highly basic domain

Domain structure of L-periaxin

near the N-terminus from amino acid 118 to 196 and an acidic domain between amino acids 1036 to 1163 near the C-terminus. A unique region of pentamer repeats was identified which stretches over approximately 300 amino acids from amino acids 432 to 725 (Fig. 10). This repeat region comprised a consensus pentapeptide:

aliphatic nonpolar - pro - glu or asp - aliphatic nonpolar - variable

and the tripeptide spacer: leu pro lys.

It was suggested that the repeat region is more inflexible than the rest of the protein and may serve as an extender between the N and C-terminal domains.

Two other proteins with identical M_r had been isolated from PNS myelin, P_{170K} and Schwann cell associated glycoprotein (SAG) (Dieperink et al., 1992; Shuman et al., 1988). Both proteins had been characterized as glycoproteins but based on relative abundance (~5% of total myelin protein), localization by immunocytochemistry, Triton X-100 insolubility and upregulation by cAMP analogues (Shuman et al., 1988), they are probably periaxin (Gillespie et al., 1994).

The structure of the murine *Prx* gene was determined (Dytrych et al., 1998) and localized to mouse chromosome 7 (Gillespie et al., 1997) which is syntenic with human chromosome 19. The *Prx* gene comprises 7 exons and spans approximately 20.6 kb and encodes two mRNAs of 5.2 kb and 4.6 kb (Fig. 11). The two mRNAs are of approximately equal abundance and are produced by alternative splicing by

432	GPEVK	APK	531	VPEMK		627	IPDMA	
440	GPEVK	LPK	536	LPDMK	LPK	632	VPDVR	
448	VPEIK	LPK	544	VPEMA		637	LPEVQ	LPK
456	APEAA		549	VPDVH		645	VSELK	LPK
461	IPDVQ		554	LPDIQ	LPK	653	VPEMT	
466	LPEVQ	LPK	562	VPEMK		658	MPDIR	
474	MSDMK	LPK	567	LPDMK	LPK	663	LPEVQ	LPK
482	IPEMA		575	VPEMA		671	VPDIK	
487	VPDVH		580	VPDVR		676	LPEIK	LPK
492	LPEVK	LPK	585	IPEVQ	LPK	684	VPEMA	
500	VPEMK		593	VSEVK	LPK	689	VPDVP	
505	VPEMK	LPK	601	IPDMA		694	LPELQ	LPK
513	IPEMA		606	VPDVR		702		VPQ
518	VPDVH		611	LPELQ	LPK	705	VPDVH	LPK
523	LPDIQ	LPK	619	MSEVK	LPK	713	VPEMK	LPK
						721	VPEAQ	

Figure 10. Alignment of the deduced amino acid sequence comprising the repeat region of L-periaxin. The repeated pentapeptide motifs with the tripeptide spacers are shown. The underlined sequences contain a serine substitution for proline.

From Gillespie et al., 1994.

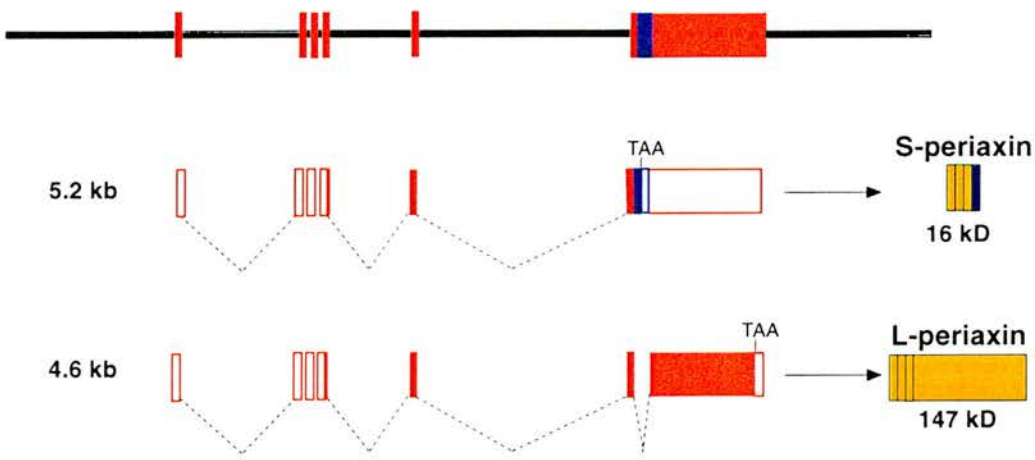

Figure 11. Schematic representation of the structure of the *periaxin* gene with the 5.2 and 4.6 kb mRNAs. The murine periaxin gene spans 20.6 kb and is comprised of 7 exons (red boxes). Alternative splicing of a retained intron generates two mRNAs, 5.2 and 4.6 kb. The 4.6 kb mRNA is translated into the 147 kDa protein, **L-periaxin**. Intron 6 (600 bp) is retained in the larger transcript which is translated into a 16 kDa protein, **S-periaxin**. Coding sequences are shown as filled boxes and non-coding sequences as empty boxes. Spliced sequences from the primary gene transcript are shown as dashed lines. Intron 6 is depicted as a purple box.

a rare retained intron mechanism (Dytrych et al., 1998). The 5.2 kb mRNA includes intron 6 located between exons 6 and 7. The retained intron introduces a stop codon and encodes a smaller isoform with an intron-encoded C-terminus of 21 amino acids. Therefore the *Prx* gene encodes two proteins, the larger 147 kDa protein now called L-periaxin and the truncated isoform of 16 kDa, S-periaxin (Dytrych et al., 1998).

The core promoter of the *Prx* gene (Fig. 12) lacks a TATA box but has a GC rich region between the transcription initiation site and a CAAT box (-86 to -76) which is common for TATA-less promoters (Dytrych et al., 1998). The presence of an octomer motif (-236 to -243) which is a potential binding site for POU family transcription factors may play an important role in cell-specific regulation but it is unlikely in this case since in the *SCIP* null mutants L-periaxin was expressed (Bermingham et al., 1996). A GCRE element (-317 to -306) has been identified in the promoters of several myelin genes and has been implicated in mediating the induction of these genes by forskolin (Li et al., 1994). The presence of this element in the *Prx* promoter and other myelin genes helps to explain the ability of cAMP to upregulate myelin gene expression in the absence of axonal contact (Lemke and Chao, 1988).

Figure 12. Sequence of the murine *periaxin* core promoter. The putative binding sites for SCIP and GCRE are underlined. The CAAT box is double underlined and the transcription initiation site is marked (+1).
From Dytrych et al., 1998.

1.6 AIMS OF THE PROJECT

In order to gain insight into the role of periaxin in Schwann cells, the first aim of the project was to investigate the localization of periaxin in peripheral nerve by immunofluorescence microscopy and immuno-electron microscopy. This was of particular importance since there was reason to believe that periaxin interacted with the cytoskeleton of Schwann cells. The second aim of the project was to determine the developmental stage in which periaxin mRNAs and protein isoforms are first expressed in developing Schwann cells since the gene encoding P0, the major protein on PNS myelin, is expressed very early in embryonic development prior to the appearance of phenotypically distinct Schwann cells (Lee et al., 1997).

Since it was believed that the gene was exclusively expressed in Schwann cells, the third aim of the project was to identify by trangenesis the regulatory elements in the *Prx* gene responsible for Schwann cell specific expression.

Materials and Methods

2.1 ELECTRON MICROSCOPY

2.1.1 Immunoelectron microscopy

Fixation

Fixation was either by immersion, for rat sciatic nerves up to postnatal-day 8, or by perfusion for older animals. Rats were anaesthetized with Sagatal (26 mg/kg) and perfused transcardially by inserting a needle into the left ventricle and clipping the right atrium. Heparinized (200 U heparin/100 ml) saline (0.89% NaCl) followed by freshly prepared formaldehyde-lysine-periodate fixative (Mclean and Nakane, 1974) was perfused through the animal. The sciatic and trigeminal nerves were removed and placed in fixative for 2-3 hours at room temperature.

Formaldehyde-lysine-periodate fixative

4% paraformaldehyde
0.01 M sodium periodate
0.075 M lysine hydrochloride
0.1 M sodium phosphate buffer, pH 7.4
3% sucrose

An 8% solution of paraformaldehyde (Sigma) in water was heated on a hot plate to 60°C and the solution was cleared by the dropwise addition of 1 M NaOH. An equal volume of 0.15 M lysine hydrochloride in 0.2 M sodium phosphate buffer (prepared by adding 0.2 M NaH_2PO_4 to 0.2 M Na_2HPO_4 to obtain pH 7.4) was added to the paraformaldehyde. Sodium periodate was added to the fixative to a final concentration of 0.01 M. The pH was adjusted to 7.4 and sucrose was added to a final concentration of 3%.

Tissue Processing

The tissue was processed according to the method of (Berryman et al., 1992).

1. The tissue was washed 3 times for 10 min each in 0.1 M phosphate buffer pH 7.4 containing 3.5% sucrose (buffer A).
2. Nerves were stained in 0.2% tannic acid (Mallincrodt) in buffer A for 1 h at 4°C. Subsequent steps were performed at 4°C.
3. The tissue was washed 3 times for 10 min each with buffer A.
4. Free aldehydes were quenched by incubating with 50 mM ammonium chloride in buffer A for 1 h.
5. Phosphate ions were removed by washing the tissue 4 times for 10 min each with 0.1 M maleate buffer pH 6.2 containing 4% sucrose (buffer B).
6. The tissue was stained en bloc with 1-2% uranyl acetate in buffer B for 1 h. Uranyl acetate was dissolved in buffer B and the pH was adjusted to 6.5 and then filtered through a 0.2 µm Millipore filter before use.
7. Dehydration through a series of ethanol solutions was performed according to the following schedule:

50% ethanol	2 times	5 min each	4°C
70% ethanol	1 time	30 min	-20°C
90% ethanol	1 time	30 min	-20°C
100% ethanol	3 times	5 min each	-20°C

8. Infiltration with LR Gold resin (Agar Scientific Ltd.) was performed by incubating the tissue with LR Gold and ethanol (1:1, v/v) for 1 h at -20°C followed by LR Gold and ethanol (7:3, v/v) for 1 h at -20°C. The tissue was infiltrated with LR Gold resin for 1-3 h, followed by overnight infiltration with fresh resin. Two changes of LR Gold containing 0.5% benzoin methyl ether (Sigma) was performed for 1-3 h and then overnight. The tissue was then embedded in fresh LR Gold containing 0.5% benzoin methyl ether in gelatin capsules, size 00 (Agar Scientific Ltd.). Polymerization was by UV irradiation at a wavelength of 365 nm for 24-48 h at -20°C.

Sectioning

Sections of approximately 70 nm were cut on either a LKB Ultratome III or a Reichert Ultracut E and collected on coated 200 mesh nickel grids (Agar Scientific Ltd.). The grids were first coated with formvar (0.5% in ethylene dichloride) followed by a very thin coat of carbon. The carbon was necessary to prevent the sections from floating off in buffers containing detergents. The grids were placed section side down on drops of all the solutions on dental wax in a humidified petri dish.

Immunostaining

Sections were blocked for 30 min at room temperature in a freshly prepared blocking buffer composed of 1% BSA, 0.5% fish skin gelatin (Sigma), 0.05% Triton X-100, 0.05% Tween-20 in a Tris buffer (10 mM Tris, 500 mM NaCl, pH 7.4). The blocking buffer was filtered (0.2 µm Millipore) before use. The grids were transferred to drops (~40 µl) of primary antibodies (see Table 1) diluted in blocking buffer and incubated overnight at 4°C. Controls were performed in which grids were incubated overnight in blocking buffer without primary antibodies. Grids were washed four times with the blocking buffer and incubated for 1 h with either goat anti-rabbit IgG conjugated to 10 nm colloidal gold (Amersham), 1:20 in blocking buffer or in combination with goat anti-mouse IgG conjugated to 5 nm colloidal gold (Amersham), 1:20 in blocking buffer. The gold solutions were centrifuged at 5000 rpm for 5 min to pellet any clumps and the supernatants recovered. The grids were washed by transfer through 6 drops of distilled water, fixed with 2.5 % aqueous glutaraldehyde for 5 min and rinsed in a stream of distilled water. Postfixation was performed with 2 % aqueous OsO_4 for 15 min. The grids were washed with distilled water and air dried. The sections were stained with lead citrate for 3 min and then rinsed with distilled water and examined at 80 kV with a JEOL 100CX or

TABLE 1

Primary antibodies used for immunolabelling

Antibody		Dilution	Source	
170pep1	polyclonal	1:3000/section 1:500 /cells 1:40 for EM	P. Brophy P. Brophy	affin. purified
p170	polyclonal	1:200	P. Brophy	
SPeri	polyclonal	1:2000	P. Brophy	affin. purified
NTerm	polyclonal	1:2000	P. Brophy	
CTerm	polyclonal	1:1000	P. Brophy	
MAG	polyclonal	1:100	D. Colman	
MAG	monoclonal	1:20	Boehringer	
NF-M	monoclonal	1:800	V. Lee	
MBP	monoclonal	1:100	N. Groome	
GAP-43	monoclonal	1:500	Boehringer	
myosin HC	monoclonal	1:400	Sigma	
O4	monoclonal	1:10	I. Sommer	
E-cadherin	polyclonal	25 µg/ml	D. Colman	EcadEC5
P0	polyclonal	1:100	D. Colman	
S100	monoclonal	1:200	Affiniti	
S100	polyclonal	1:1000	Dako	

Periaxin synthetic peptide sequences

170pep1	VPEMKLPKVPEAQRKSC
SPeri	AKLVRVLSPVPVQDSPSDRVAAAC
NTerm	EARSRSAEELRRAEC
CTERM	KARSGSRDREEGGFRVRLPSC

Anti-peptide antibodies were produced in New Zealand white rabbits after immunization with antigen comprising an emulsion of Freund's adjuvant and peptide (a kind gift of Prof. N. Groome, Oxford Brookes University) coupled to Keyhole Limpet Haemocyanin.

a Phillips 400 electron microscope. Photographs were taken using Kodak electron microscope film 4489.

Lead citrate stain

0.2% lead citrate in 0.1M NaOH (Venable and Coggeshall, 1965)

0.03 g lead citrate was placed in a 15 ml Falcon centrifuge tube containing 15 mls of distilled water that was previously boiled for 10 minutes. 150 µl of 10 M NaOH was added and the tube was mixed until the lead citrate was dissolved.

2.1.2 Electron microscopy of E16.5 and P1 sciatic nerves

For dating the embryos, the day of the vaginal plug was 0.5. E16.5 and P1 murine sciatic nerves were removed and placed in a 35 mm petri dish containing freshly prepared 4% paraformaldehyde, 2% glutaraldehyde in 0.1 M sodium cacodylate buffer, pH 7.4. After 1 h fixation the tissue was washed twice for 5 min with 0.1 M sodium cacodylate buffer and postfixed in reduced osmium tetroxide (1% OsO_4 in 0.1 M sodium cacodylate buffer containing 1% potassium ferrocyanide) for 1 h at 4°C. After one 5 min wash with 0.1 M sodium cacodylate buffer the nerves were dehydrated through an ascending series of ethanol for 5 min each (50%, 70%, 90%) and finally three changes of absolute ethanol for 10 min each. The tissue was infiltrated with Epon 812 (Taab) and ethanol (1:1, v/v) for 1 h followed by Epon 812 overnight at room temperature. The tissue was transferred to fresh Epon 812 for 2 h and embedded in Epon 812 in flat silicone moulds. The resin was polymerized at 60°C for 24-48 h. Silver sections were cut (~70 nm) and collected on 300 mesh copper grids (Agar Scientific Ltd.). The grids were stained with 2% uranyl acetate in 50% ethanol for 3 min, washed with distilled water, air dried and then stained with lead citrate for 3 min followed by washing in a stream

of distilled water. The grids were examined on a Phillips 400 electron microscope at 80 kV.

2.2 INDIRECT IMMUNOFLUORESCENCE

2.2.1 General fixation and tissue preparation

Immunofluorescence was performed on teased fibres of sciatic nerve, frozen sections, and cultured cells. In all cases the fixative was freshly prepared 4% paraformaldehyde in 0.1 M sodium phosphate buffer, pH 7.4. Paraformaldehyde (8%) in distilled water was heated to 60°C and cleared with 1 M NaOH added dropwise. An equal volume of 0.2 M sodium phosphate buffer was added and the pH adjusted to 7.4.

Cryo-sections

a. Sciatic nerves

Sciatic nerves from mice and rats were fixed by immersion for embryonic nerves and postnatal nerves from young animals and by perfusion at older ages. Fixation was at room temperature for 2 h. The nerves were washed in 3 changes of 0.1 M phosphate buffer for 10-15 min each and then cryo-protected by infiltrating the tissue with 5%, followed by 10% sucrose in 0.1 M phosphate buffer. After incubation in 20- 25% sucrose in 0.1 M phosphate buffer overnight at 4°C the nerves were frozen by placing them in OCT (Tissue-Tek, Miles Scientific) in a plastic mould (Polysciences) and the mould was frozen in isopentane cooled in liquid nitrogen. The blocks were stored at -70°C until needed.

b. Cervical sympathetic trunks

The rostral halves of E16.5 embryos or postnatal-day 1 mice were placed in fixative for 2 h at room temperature. The cervical sympathetic trunk was removed and placed in fixative in a 35 mm petri dish for 1 h. The tissues were washed in 3 changes of 0.1 M phosphate buffer for 10-15 min each and then cryo-protected by infiltration with 25% sucrose in 0.1 M phosphate buffer overnight at 4°C. The tissue was placed in OCT in a plastic mould and frozen in isopentane cooled in liquid nitrogen.

c. Embryos

Mouse embryos were dissected in cold HBSS and cut in half between the thoracic and lumbar vertebrae. The caudal and rostral halves were placed in fixative for 3-4 h at room temperature. The embryos were washed in 3 changes of 0.1 M phosphate buffer for 30 min each and then infiltrated with 5% sucrose in 0.1 M phosphate buffer for 30 min, 10% sucrose in 0.1 M phosphate buffer 30 min followed by 20-25% sucrose in 0.1 M phosphate buffer overnight at 4°C. The embryos were frozen in cooled isopentane.

Sectioning was performed on a cryostat (Bright OTF/AS) at -15 to -17°C. Approximately 7 µm sections were cut and collected on TESPA-coated (3-aminopropyltriethoxy-silane) slides. The sections were allowed to air dry for 1 h and then either used directly or stored at -40°C.

Preparation of TESPA-coated slides

TESPA-coated glass slides were prepared by dipping pre-cleaned glass slides in acetone for 1 min, 2% TESPA (Sigma) in acetone for 1 min, followed by two 30 s washes in acetone, and then air-dried. The slides were stored in a slide box containing silica gel.

2.2.2 Immunostaining controls

Controls in which the primary antibodies were omitted were performed for each experiment. The antibody raised against Speri has been previously characterized and preincubation of the antisera with 1 mg/ml of peptide abolished immunolabeling (Dytrych et al., 1998). The L-periaxin antibodies which were used in the experiments, anti-170pep1, anti-NTerm, and anti-CTerm have been described previously (Gillespie et al., 1994; Dytrych et al., 1998). Each antibody recognized one band with a M_r of 170 kDa by Western blotting and all showed the same staining pattern in rat peripheral nerve sections by immunofluorescence.

2.2.3 Immunostaining of cryo-sections

A ring of rubber cement was placed around the sections on the slides which produced a well for small volumes of antisera. The rubber cement was allowed to completely dry before the OCT was removed by rinsing twice with PBS. For all incubations the slides were placed in a humid chamber. The sections were blocked with 200 µl blocking buffer consisting of 10% goat serum, 0.2% gelatin, 0.3% Triton X-100 in PBS. Primary antibodies were diluted in 4% goat serum, 0.2% gelatin, 0.3% Triton X-100 in PBS and left on the sections overnight at room temperature or 4°C (see Table 1, p 58 for antibodies used and dilutions). The slides were washed in the same buffer 4 times for 5 min each. Secondary antibodies, goat anti-rabbit IgG coupled to fluorescein isothiocyanate (FITC; Cappel, 1:200) and biotinylated goat anti-mouse IgG (Kirkegaard and Perry, 1:500), were diluted in the same buffer and placed on the sections for 1 h at room temperature. The slides were washed with buffer 3 times for 5 min each and then incubated with streptavidin-Texas Red (Vector Laboratories, 1:1200). After 4 washes in PBS, coverslips were mounted on the slides with a drop of Vectashield non-fade mounting medium (Vector Laboratories). In some experiments propidium iodide binding was performed in

combination with L-periaxin immunolabelling. Sections were incubated with propidium iodide (100 μg/ml; Sigma) for 2 min after immunolabelling for L-periaxin was completed. The slides were viewed on a Olympus BX60 microscope equipped with a 460-490 excitation filter and 515-550 barrier filter for FITC and for Texas Red or tetramethylrhodamine isothiocyanate (TRITC) a 530-550 excitation filter and 590 barrier filter. The images were photographed on Fuji Provia color slide film. Alternatively, confocal microscopy was performed on a Leica TCS 4D scanning confocal microscope. A maximum projection was made from a series of optical scans through the z axis of the tissue. The digitized images were processed using Adobe Photoshop 3.0 software on a Power Macintosh 8600/200.

2.2.4 Tissue preparation and immunostaining of teased fibres

After fixation for 2 h, the sciatic nerves were washed in PBS several times. The nerves were placed in a 35 mm petri dish and the epineurium was removed. The tissue was cut into 3 mm segments and transferred to another petri dish containing 0.1% Triton X-100 in PBS. The fibres were teased using acupuncture needles and transferred to a dish containing Triton X-100 for 1 h (Kidd et al., 1994). The fibres were washed several times in PBS and then blocked with 10% goat serum, 0.2% gelatin, 0.3% Triton X-100 in PBS for 2 h. The fibres were then transferred to wells in a 24 well plate containing primary antibodies diluted in 4% goat serum, 0.2% gelatin, 0.3% Triton X-100 in PBS and incubated overnight at room temperature in a humid chamber. The rest of the procedure was the same as for cryosections except to change solutions the fibres were transferred from well to well with an acupuncture needle and finally placed in a drop of Vectashield mounting media on a glass slide, re-teased, and coversliped

2.2.5 Fixation and immunostaining of cultured cells

Monolayers grown on 13 mm glass coverslips (BDH) coated with poly-D-lysine (100 µg/ml, Sigma) were fixed with 4% paraformaldehyde in 0.1 M sodium phosphate buffer for 30 min at room temperature. O4 labelling was performed before fixation. Coverslips were rinsed with PBS and incubated with monoclonal anti-O4 (IgM) diluted with 2% goat serum in PBS for 30 min. For detection of L-periaxin on the cell surface, immunolabelling with anti-p170, anti-170pep1, anti-NTerm, and anti-CTerm was performed prior to fixation as for O4. After three rinses with PBS, the coverslips were fixed with 4% paraformaldehyde. For S-100 staining, the cells were fixed for 20 min with 4% paraformaldehyde followed by 10 min in cold methanol (-20°C). The cells were washed 4 times for 5 min each with PBS and blocked with 4% goat serum, 0.2% gelatin, 0.1% Triton X-100 in PBS for 30 min. The coverslips were placed on a piece of parafilm in a humid chamber and 40 µl of the diluted primary antibodies was placed on the coverslip. After 1 h the coverslips were washed 3 times with blocking buffer and the procedure repeated for the incubation with goat anti-rabbit FITC IgG (Cappel, 1:200) and goat anti-mouse TRITC IgG (Jackson Laboratories, 1:100) or donkey anti-mouse TRITC Ig (not type-specific) (Jackson Laboratories, 1:50) for O4. After 45 min the coverslips were washed with PBS and mounted on slides with Vectashield. The edges of the coverslips were sealed with nail varnish.

The numbers of O4 and L-periaxin positive cells were determined in three experiments, in each of which a minimum total of 400 cells per coverslip were scored in randomly selected fields. Cell numbers were calculated Mean ±SEM.

2.2.6 Terminal deoxynucleotide transferase mediated UTP nick end-labelling (TUNEL)

TUNEL combined with immunofluorescence for L-periaxin was performed on E15 sciatic nerve cryosections according to the method of Grinspan (Grinspan et

al., 1996).. Following immunostaining for L-periaxin, using 170pep1 followed by goat anti-rabbit FITC IgG, the sections were incubated in PBS containing 0.5% Triton X-100 for 15 min at room temperature followed by equilibration in TdT buffer (140 mM sodium cacodylate, 1 mM cobalt chloride, 30 mM Tris-HCl, pH 7.2) for 20 min. The sections were then incubated with 50 µl TdT buffer containing 17.9 U TdT (Gibco BRL) and 10 µM biotinyl-11-dUTP (Sigma) for 1 h at 37°C. Biotinyl-11-dUTP was omitted on a control slide. Room temperature incubation for 15 min with a buffer containing 300 mM NaCl and 30 mM sodium citrate terminated the reaction. Following a 10 min wash in 2% BSA in PBS, sections were incubated for 1 h with streptavidin- Texas Red (1:1200) in PBS. The slides were washed three times with PBS and mounted with Vectashield before examination on a Leica TCS 4D confocal microscope.

2.3 CELL CULTURE

2.3.1 General cell culture

Cell lines were maintained in complete medium (10% FCS, DMEM [ICN[containing penicillin (100 IU/ml) and streptomycin (100 µg/ml) (Sigma). When the cells were confluent they were passaged by washing once with HBSS (Gibco BRL) and incubating in trypsin-EDTA (Sigma) for 1-3 min. Complete medium was added and the cells were pelleted by centrifugation (1000 rpm for 3 min). The cells were resuspended in 1 ml of complete medium and plated in either 25 cm^2 flasks, coverslips or petri dishes at the appropriate densities. Cell were frozen for long-term storage in 20% FCS and 10% DMSO in DMEM by placing them at -70°C overnight and then transferring them to liquid nitrogen.

2.3.2 Schwann cell culture

Dissociation and cytosine arabinoside treatment

Sciatic nerves were removed from P5 rats and placed in a 35 mm petri dish containing pre-warmed L15 (Sigma). The epineurium was removed by dissection with fine forceps and the nerve fibres were cut into small pieces and placed in a bijou containing collagenase (0.24 mg/ml) in 1 ml of L15. The nerves were incubated for 45 min to 1 h in a 37°C incubator before the addition of trypsin (0.6 mg/ml) for 10 min. The trypsinization was terminated by the addition of 2 ml of complete medium (DMEM containing 10% FCS, Pen/Strep). The nerves were titurated using a 3 ml syringe with a 21 gauge needle 6 times, followed by 4 times with a 25 gauge needle. The cells were transferred to a 15 ml Falcon centrifuge tube and 5 ml of complete medium was added before centrifugation for 3 min at 1000 rpm. The pellet was resuspended in complete medium and cells were plated in 25 cm^2 flasks pre-coated with poly-D-lysine (0.1 mg/ml). The following day the medium was changed to fresh medium containing 10 µM cytosine arabinoside (Ara C, Sigma). The cells were cultured in medium containing Ara C for 7 d.

Complement-mediated lysis with anti-Thy1.1

The cells were trypsinized and centrifuged (1000 rpm for 3 min) after the addition of DMEM containing 10% FCS. The pellet was resuspended in 1.6 ml of DMEM and 0.4 ml Thy-1.1 monoclonal antibody diluted 1:10 (a gift of A. F. Williams, Oxford University) and incubated at 37°C. After 30 min, 0.4 ml baby rabbit complement (Cedarlane Laboratories Ltd, Canada) was added and incubated for a further 30 min at 37°C. DMEM containing 10% FCS (8 mls) was added and the cells were centrifuged at 1000 rpm for 3 min. The pellet was resuspended with DMEM containing 10% FCS, Pen/Strep, 2 µM forskolin (Sigma), and GGF (a gift of J. Brockes, Ludwig Institute, London) and seeded in 25 cm^2 flasks pre-coated with 0.1 mg/ml poly-D-lysine. After one week, the complement-

mediated lysis with anti-Thy1.1 was repeated. The pellets were resuspended with DMEM containing 10% FCS, Pen/Strep, and 2 μM forskolin and seeded in poly-D-lysine coated flasks. When the cells reached confluency they were passaged and plated on poly-D-lysine and laminin coated coverslips (see 2.4.2) for transfection. To coat coverslips with laminin, 50 μl of laminin (10 μg/ml, Sigma) in DMEM was placed on the coverslip and incubated in a 37°C CO_2 incubator for 2 h. The laminin was aspirated from the coverslips immediately before plating the cells.

2.3.2 Embryonic Schwann cell culture

Sciatic nerves were removed from E16.5 mouse embryos and placed in a dish containing L15 (Sigma). They were washed once with fresh L15 and cut into small segments. The nerves were incubated with collagenase (0.21 mg/ml) in L15 at 37°C for 40 min. Hyaluronidase (1 mg/ml, Sigma) was added to the nerve segments for 15 min after which an additional amount of collagenase was added (0.08 mg/ml). The nerve segments were triturated using a yellow Gilson pipette tip followed by glass micro-pipettes to completely dissociate the cells. The cells were transferred to a centrifuge tube and complete medium (5 mls) containing 10% FCS, Pen/Strep, 2 mM glutamine, DMEM was added followed by centrifugation at 1000 rpm for 3 min and resuspension in complete medium. Cells were plated on laminin-coated coverslips that had been pre-coated with poly-D-lysine. The cultures were incubated for 6.5 h before fixation.

2.4 TRANSFECTION

2.4.1 Production of 33B cells permanently expressing L-periaxin

DNA preparation

L-periaxin cDNA was directionally subcloned into pCB6 expression vector (a gift from Dr. David Russell, Southwestern Medical Center, Dallas, TX) at the MluI and XbaI sites and transformed into freshly prepared XL1-blue competent cells (Sambrook et al., 1989).. pCB6 contains the CMV promoter and a neomycin-resistance gene for selection. The insert was checked by restriction digest. To prepare DNA for transfection a maxiprep was performed on a 500 ml overnight culture in LB broth (Gibco BRL) containing ampicillin (0.1 mg/ml) using the Promega Wizard Maxiprep kit according to the manufacturer's instructions.

Dose response to G418

The Schwann cell line, 33B, was a generous gift from Dr. Eric Blair, Leeds University. First it was necessary to determine the dose-response of the cells to geneticin, (G418, Gibco BRL), the neomycin analog, before transfection to identify the optimum concentration for the cell line used. 33B cells were seeded in a 24 well plate at low density. A 5 mg/ml stock solution of G418 was prepared in complete medium (10% FCS, DMEM containing penicillin [100 IU/ml] and streptomycin [100 µg/ml]). Cells were grown in the presence of increasing concentrations (200 µg/ml, 400 µg/ml, 600 µg/ml and 800 µg/ml) of G418 or in the absence of G418. After approximately 10-12 days the wells were assessed for the lowest dose of G418 which produced cell death which for 33B cells was 600 µg/ml.

Cationic liposome-mediated transfection

33B cells were seeded in two 90 mm petri dishes and allowed to grow overnight to achieve 50 to 70% confluency. The medium was changed to fresh

medium for 3 h. DNA (24 μg) was added to 0.8 ml Optimem (Gibco BRL) and gently mixed and Lipofectamine (64 μg, Gibco BRL) was added to 0.8 ml Optimem in a polystyrene Falcon tube (Felgner et al., 1993). The DNA solution was then added to the Lipofectamine solution and mixed before incubating for 20 min at room temperature. The volume was brought to 8 ml with Optimem. The cells were rinsed three times with serum-free Optimem before 4 ml of DNA/Lipofectamine solution was added to each petri dish. The cells were transfected for 4 h at 37°C in a humidified CO_2 incubator. They were then washed and complete medium was added. After 48 hrs, 600 μg/ml G418 was added to the medium and the cultures were maintained until single G418 resistant colonies appeared. These colonies were isolated with cloning rings and seeded in a 24 well plate. Each clone was passaged and seeded on poly-D-lysine-coated (100 μg/ml, Sigma) glass coverslips and screened by indirect immunofluorescence for expression of L-periaxin. Clone 25 was selected for further studies.

Cytoskeleton Preparation

Cells cultures were washed briefly with extraction buffer, 10 mM Pipes, pH 6.9, 50 mM KCl, 2 mM EGTA, 1 mM $MgCl_2$, 2 M glycerol, 10 μg/ml leupeptin (Sigma) and 10 μg/ml antipain (Sigma), and extracted at room temperature for 3 min with the extraction buffer containing 0.5% Triton X-100 (Wilson and Brophy, 1989). The cytoskeletons were then washed in the same buffer without Triton X-100 prior to being fixed and processed for indirect immunofluorescence.

2.4.2 Methods for transient transfection

Transient transfection was carried out using either lipid-mediated transfection or by calcium-phosphate-DNA precipitation. Hela, 33B, NIH 3T3, or Cos7 cells were transiently transfected using both methods on each cell-line to obtain the most efficient transfection.

Liposome-mediated transfection

The same method was used for transient transfection as was used for permanent transfection except that cells were seeded on poly-D-lysine-coated coverslips in 35 mm dishes. For each dish 3 µg of plasmid DNA was diluted in 100 µl Optimem and 8 µg Lipofectamine was also diluted in 100 µl Optimem. The two solutions were mixed and incubated for 20 minutes in a polystyrene Falcon tube before 800 µl Optimem was added, mixed and then placed on cells that were rinsed 3 times in Optimem to remove the serum. After 4 h the cells were washed once with either serum-containing medium or HBSS and grown for 24 to 48 h in DMEM with 10% FCS. The cells were processed for immunofluorescence microscopy or for GFP they were viewed directly.

For Schwann cell cultures, the cells were plated on coverslips coated with poly-D-lysine and laminin. The cells were grown in the presence of 2 µM forskolin and when they reached 70-80% confluency they were transfected with Lipofectamine as above for 3 h. After washing, medium containing 2 µM forskolin was replaced. Higher concentrations of forskolin (50 µM) were used for Schwann cell cultures that were transfected with periaxin/LacZ constructs.

Calcium-phosphate-DNA precipitation

Cells were seeded on coverslips and grown for 17 h to 30-50% confluency. Fresh medium (2 ml) was added to each 35 mm dish for 1 h. The Stratagene Mammalian Transfection Kit was used to prepare the precipitate according to the manufacturer's instructions. Plasmid DNA (1.25 µg) was diluted in sterile distilled water to a volume of 45 µl. Solution 1 (5 µl: 2.5 M calcium chloride) was added to the DNA and an equal volume (50 µl) of solution 2 (50 mM BES, 280 mM NaCl, 1.5 mM Na_2HPO_4, pH 6.95) was added and gently mixed. One minute was allowed for precipitation (Jordan et al., 1996) before quickly adding the 100 µl to the cell culture. After 6 h the cells were washed with HBSS and changed to fresh medium.

2.4.3 Preparation of constructs for transfection

Diagrams of the constructs are illustrated in Fig. 13. All PCR reactions were performed with a proof-reading polymerase and the regions of each construct that were generated by PCR were sequenced using the Pharmacia T7 sequencing kit which employs the Sanger dideoxy-mediated chain-termination method (Sanger et al., 1977). The sequences were analyzed using MacVector sequence analysis software (Oxford Molecular Group) and the University of Wisconsin GCG package (Devereaux et al., 1984). Primers for PCR and sequencing were synthesized on an Applied Biosystems model 391 PCR-MATE and purified by butanol extraction (Sawadogo and Van Dyke, 1991). A list of all the primers used are listed in Table 2. The PCR reactions were performed on a Hybaid OmniGene Thermal Cycler. To prevent contamination the reaction was prepared in a hood equipped with UV illumination and before the template and enzyme were added, the reaction tubes were incubated for 10 minutes in a Amplirad UV illuminator (Genetic Research Instruments Ltd.). A typical 50 µl PCR reaction consisted of 10X reaction buffer (5 µl), 5 µM primer 1 (5 µl), 5 µM primer 2 (5 µl), 2 mM dNTPs (5 µl), template and enzyme. The reaction was overlayed with mineral oil. The cycle conditions were: 94°C for 1 min, 55°C for 1 min, 72°C extension (1 min/ 1 kb product) - 5 cycles; 94°C for 40 s, 55°C for 1 min, 72°C (1 min/ 1 kb product) -28 cycles; 94°C for 40 s, 55°C for 1 min, 72°C for 7 min - 1 cycle.

DNA Sequencing

Denaturation of double-strand DNA

Plasmid DNA (1 µg) was denatured with 2 M NaOH (2 µl) in a total volume of 10 µl for 10 min at room temperature. The DNA was precipitated by the addition of 0.9 M sodium acetate, pH 5.5 (10 µl) and ethanol (60 µl) and incubated at -70°C for 30 min. Following a 4°C centrifugation for 30 min at 13000 rpm, the pellet was washed with 70% cold ethanol and vacuum dried.

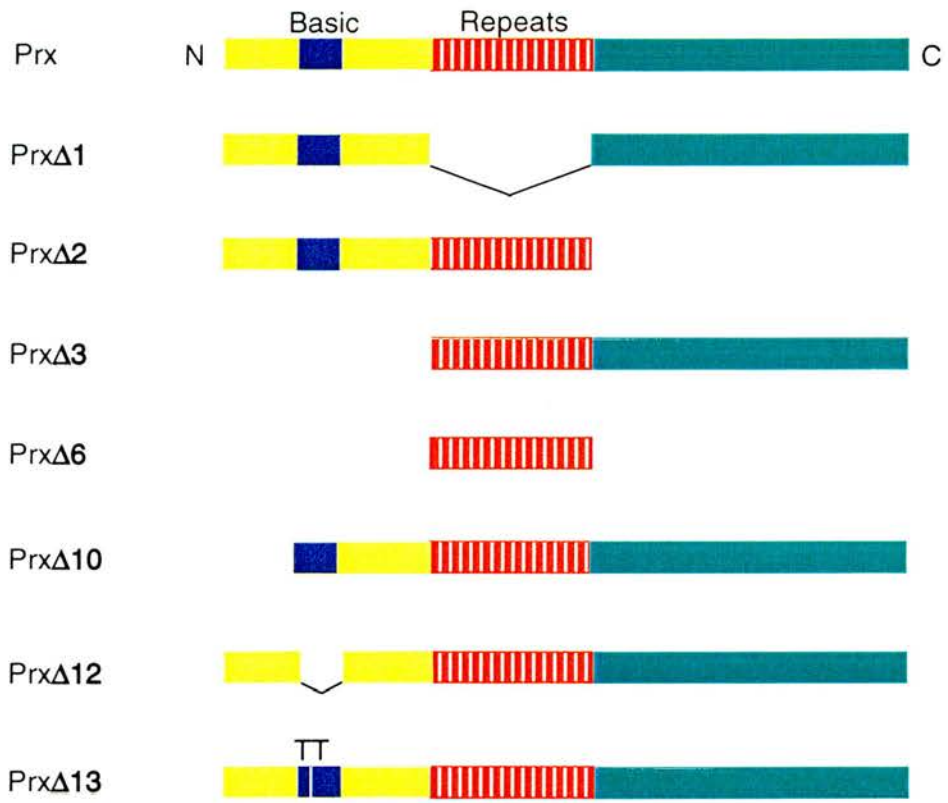

Figure 13. Schematic representations of L-periaxin deletion mutants. The repeat region of L-periaxin is depicted as a lined red box, the basic domain (blue box) is in the N-terminus which is represented by a yellow box, and the C-terminus is represented by a green box. The deleted regions are either missing or depicted as lines. PrxΔ13 has two mutated nts, TT.

TABLE 2

Oligonucleotide primer sequences

Primer	5' to 3'		Restrict. sites
DLS1	TGCTCTAGAGCATGCCATGGCATGAGGGTCACTTCCAGC	R	XbaI, NcoI
DLS8	CTTGACTACCTTGGCTTCAGT	R	
DLS9	GAGGTTCCAGACAAACTCCT	F	
DLS17	CATCTCGTATCCAGACACCGT	R	
DLS18	GAAGTAGCTGAAGAGGCCCA	F	
DLS19	CATGCCATGGTGGGCCTCCAGACACCTCCAGAGCT	R	NcoI
DLS21	GGAATTCCATGGTGGGCCTCCAGA	R	EcoRI, NcoI
DLS25	ACGCGTCGACACAACCTTCAAGAGGTAAGC	F	SalI
DLS26	CCCTGTGAAGACGACGAAGAT	F	
DLS27	GAATTCACCATGGAGATGAAGGGCCCGCGGGCCAA	F	EcoRI, Kozak seq
DLS28	CGGGATCCTCTCGGACACGTAGCCGAGGCA	R	BamHI
CSG1	GGAAGTTTCATGTCTGACAT	R	
LMD2	AAGTAGCTGGAACTGACCCTCA	F	
LMD6	CGAGCGGAGTTGGTGGAGATTATC	F	
LMD56	GACAGACTCTGG	R	
p300	CTGAAAATCCCACACT	R	
Lac1	GGCGTTTCATCTGTGGTGCA	F	
Lac2	AAACCGACATCGCAGGCTTC	R	

Labelling using the Pharmacia T7 sequencing kit

The primer was annealed to the template after resuspension with 5 µl distilled water and the addition of 1 µl annealing buffer and 1 µl sequencing primer (5 µM) to the DNA pellet and incubation for 20 min at 37°C followed by 10 min at room temperature. The labelling reaction consisted of a 4 min incubation of the annealed template (7 µl), labelling mix A (1.5 µl), [α-^{35}S] dATP (0.2 µl, ICN), distilled water (0.3 µl), and T7 DNA polymerase (1 µl of 1:4, v/v, enzyme with dilution buffer). The termination reaction followed the labelling by the addition of 2.25 µl of the labelling reaction to each of 4 pre-warmed tubes containing 1.25 µl of A, G, T, and C termination mixes and incubation for 5 min at 39°C. Stop solution (2.5 ml) was added to each of the 4 tubes.

Electrophoresis

The 4 tubes were incubated at 80°C for 3 min and a 2 µl aliquot of each was resolved on a sequencing gel in an IBI Base Runner. The pre-set gel consisted of 6% acrylamide/bisacrylamide (Ambion, 19:1), 42% urea, 0.005% TEMED, 0.025% ammonium persulfate in TBE (90 mM Tris-HCl, 90 mM boric acid, 2 mM EDTA, pH 8.0). The gel was fixed with 5% methanol and 5% acetic acid for 20 min and dried under vacuum for 1 h at 80°C. The gel was exposed to X-ray film (Agfa Curix RP-1 Plus) for 48 h at room temperature. The film was developed with Kodak LX24 X-ray developer and fixed with Kodak Industrex fixer.

PrxΔ1

The repeat region of L-periaxin cDNA was deleted from nt 1408 to nt 2556 using a PCR-ligation-PCR technique (Ali and Steinkasserer, 1995) as illustrated in Fig. 14. The template for the PCR was L-periaxin cDNA in pSPORT (Gibco BRL). It was important for the products to have blunt ends therefore pfu polymerase (Stratagene) was used. The first step was to perform PCR A using the T7

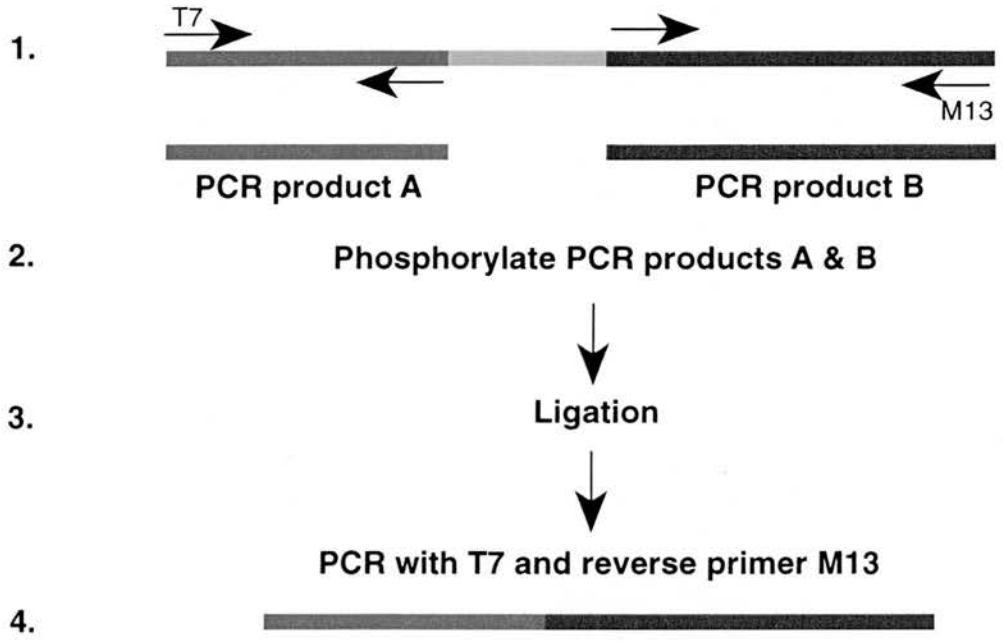

Figure 14. Diagrammatic representation of the PCR-ligation-PCR technique used to construct L-periaxin cDNA lacking the repeat region (yellow). (1) Two PCR reactions were performed; PCR A using T7 sequencing primer and a L-periaxin reverse primer which produced PCR product A (red), and PCR B using a L-periaxin forward primer and M13 reverse which produced PCR product B (blue). It was essential to use a polymerase which produced blunt ends. (2) An equal amount of PCR product from each PCR was phosphorylated with T4 kinase. (3) The phosphorylated PCR products were ligated with T4 DNA ligase. (4) A final PCR was performed with primers T7 and M13 reverse using 1/10 of the ligation as template which produced the final product containing the deletion.

sequencing primer and the periaxin reverse primer DLS 8 which produced a 1.4 kb product and PCR B using the periaxin forward primer DLS 9 and the primer M13 reverse which produced a 2.2 kb product. An equal amount of PCR product from each PCR was phosphorylated with T4 kinase (Gibco BRL). The reaction contained 10 µl 5X kinase buffer, 10 µl PCR product, 5 µl 10mM dATP, 1 µl T4 kinase (10 U) in a final volume of 50 µl. After incubation for 30 min at 37°C the enzyme was inactivated at 70°C for 5 min. After ethanol precipitation the two PCR products were ligated with T4 DNA ligase (3 U, Promega) for 1 h at room temperature. A final PCR was performed using 1/10th of the ligation as template with the forward primer T7 and the reverse primer p300. The PCR product was run on a 1% agarose gel, the bands were excised, the DNA was extracted from the gel using the Qiaex II gel extraction kit (Qiagen) according to the manufacturer's instructions, digested with EcoRI and XhoI, and subcloned into EcoRI/XhoI cut L-periaxin in pSV·SPORT by ligation with 1-2 U T4 DNA ligase (Fermentas) for 3 h at room temperature. Competent XL1-blue cells were transformed and plated on LB agar (Gibco BRL) containing 0.1 mg/ml ampicillin. Minipreps were performed by alkaline lysis (Sambrook et al., 1989) on 4 ml overnight cultures from individual colonies. Restriction digest followed by electrophoresis on 1% agarose gel revealed if the insert was present. The construct was checked by sequencing (Pharmacia). DNA for transfection was prepared using the Promega Maxi-prep kit on a 500 ml overnight culture.

PrxΔ2

The 3' end of L-periaxin cDNA was deleted from nt 2576 and a termination codon and XbaI site was introduced by PCR. The template was L-periaxin cDNA in pSPORT using the primers DLS 10 (reverse) and T7. The PCR reaction had an annealing temperature of 55°C and a 2.5 min extension at 72°C and used pfu polymerase. The PCR product was gel purified and restriction digested with EcoRI

and XbaI and cloned into pBlueScript KS (BS; Stratagene) which contained the first 2 kb of L-periaxin cDNA and the sequences generated by PCR were checked by DNA sequencing. The construct was released from the BS polylinker by digestion with SalI and NotI and cloned into pSV·SPORT. DNA for transfection was prepared from a 30 ml overnight culture using the Qiagen midi-prep kit.

PrxΔ3

The 5' end of L-periaxin cDNA was deleted up to nt 1562 and an initiation codon with a strong Kozak consensus sequence (Kozak, 1996) as well as a KpnI site was introduced by PCR. The template was L-periaxin cDNA in pSPORT using the primers DLS 11 (forward) and M13 forward sequencing primer. The PCR reaction had an annealing temperature of 60°C and a 3 min extension at 72°C and used pfu polymerase. The PCR product was gel purified and restriction digested with EcoRI and KpnI and cloned into EcoRI/KpnI digested L-periaxin in pSV·SPORT. The resulting construct was sequenced to check for fidelity of the PCR generated region. DNA for transfection was prepared from a 30 ml overnight culture using the Qiagen midi-prep kit.

PrxΔ12

A similar strategy was used to delete the basic domain (nt 622 to 859) as was used for PrxΔ1. The enzyme pfu polymerase (Stratagene) was used for all the PCRs. For PCR A the primers used were T7 and the periaxin reverse primer DLS 17. For PCR B the periaxin forward primer DLS 18 and the periaxin reverse primer CSG1 were used. The annealing temperature was 55°C with a 1 min extension at 72°C. The products were phosphorylated and ligated. The primers for the final PCR were T7 and CSG1 with an extension time of 1.5 min. The PCR product was Qiaex purified, digested with BstBI and SalI and subcloned into L-periaxin in

pSV·SPORT. DNA for transfection was prepared from 30 ml overnight cultures using the Qiagen midi-prep kit.

PrxΔ13

Two of the lysine residues (nt 137 and 138) in the basic domain of L-periaxin were mutated to threonine residues. K fi T

GAA fi GAC

Again the same strategy was used for the mutagenesis as for PrxΔ1 and PrxΔ12. PCR A used the forward primer DLS 26 5' CCCTGTGAA**GACGAC**GAAGAT 3'

K T T K

and the periaxin reverse primer CSG 1 5' GGAAGTTTCATGTCTGACAT 3' while the primers for PCR B were LMD 2 (forward) and LMD 56 (reverse). The products were phosphorylated and ligated. The primers for the final PCR were LMD 6 (forward) and CSG 1 (reverse). The PCR product was digested with BstBI and SfiI and subcloned into L-periaxin in pSV·SPORT. Plasmid DNA for transfection was prepared using the Qiagen midi-prep kit.

BD-GFP

The basic domain (244 bp) of L-periaxin which comprises nt 616 to 860 was generated by PCR. The forward primer DLS 27 was designed with an EcoRI site followed by an initiation codon with a strong Kozak consensus sequence. The reverse primer DLS 28 contained a BamHI site. The PCR product that was generated was digested with EcoRI and BamHI and cloned into pIBI30 in order to check the sequence. Several clones were sequenced with T3 and T7 sequencing primers. The basic domain was released from the pIBI30 polylinker by restriction digest with EcoRI and BamHI then cloned into the expression vector pEGFP-N1 (Clontech) in frame at the EcoRI and BamHI sites. pEGFP encodes a red-shifted variant of wild-type green fluorescent protein which has thirty times the

fluorescence intensity. The basic domain of L-periaxin will be expressed as an N-terminal fusion of EGFP. To obtain DNA for transfection Qiagen midi-preps were performed on 30 ml overnight cultures of BD-GFP and pEGFP.

2.4.4 Energy depletion

33B cells, Hela cells, and Schwann cells were transiently transfected with BD-GFP for 4 h using Lipofectamine. After 24 h, the cells were washed twice with glucose-free MEM (Gibco BRL) containing 10% dialysed FCS, penicillin (100 IU/ml) and streptomycin (100 µg/ml) and 2 mM glutamine. and then incubated with 6 mM 2-deoxyglucose (Sigma) and 10 mM sodium azide in glucose-free medium containing dialysed FCS for 1 h and 2 h. Some transfected cells were allowed to recover for 2 h in complete medium at 37°C. At the end of the incubation times the cells were fixed with 4% paraformaldehyde for 20 min, washed with PBS, mounted with Vectashield, and viewed on a fluorescence microscope and optical images were captured on a Leica TCS 4D scanning confocal microscope.

2.4.5 Cell surface biotinylation

Biotinylation of cell surface proteins was performed according to (Rosen et al., 1992). Permanently transfected 33B cells (clone 25) were grown in 35 mm petri dishes to confluency. The cells were washed twice with HBSS. For cell surface biotinylation, the cells were incubated with 0.5 mg/ml sulfo-NHS-biotin (Pierce Chemical Co.) in HBSS twice for 15 min at room temperature. Sulfo-NHS-biotin was diluted from a 200 mg/ml stock dissolved in DMSO. The cells were rinsed once with DMEM and twice with HBSS before the addition of 1 ml of solution A (2.5% (v/v) Triton X-100, 150 mM NaCl, 4 mM EDTA, 50 mM Tris HCl pH 7.4) containing the proteinase inhibitors, leupeptin (10 µg/ml), antipain (10 µg/ml), TLCK (1 mM), PMSF (200 µg/ml), chymostatin (660 µg/ml), and benzamidine (10µM). As a control, cells were permeabilized with 2% Triton X-100 in HBSS

containing proteinase inhibitors for 5 min prior to the addition of 0.5 mg/ml sulfo-NHS-biotin for 30 min. Glycine was added to a final concentration of 100 mM and Tris HCl pH 8 was added to a final concentration of 50 mM. The cells were removed by scraping, centrifuged and the supernatant was taken for immuneprecipitation.

2.5 METABOLIC LABELLING, IMMUNEPRECIPITATION, SDS PAGE AND WESTERN BLOTTING

2.5.1 Metabolic labelling with [^{35}S] methionine

Labelling was performed on 33B cells (clone 25) grown in 4 x 35 mm petri dishes. The cells were washed twice with HBSS and once with methionine and cysteine-free DMEM (ICN) containing 10% dialysed serum and 2 mM glutamine and incubated for 15 min. Fresh medium (1.2 ml) and 12 µl of Trans [^{35}S] label (ICN) were added to each dish and incubated for 3 h at 37°C with 95% CO_2. A 35 mm petri dish containing charcoal was placed with the dishes. The supernatant was removed and the cells were washed twice with complete medium and twice with HBSS. A solution of 2% SDS (200 µl) containing proteinase inhibitors, leupeptin (10 µg/ml), antipain (10 µg/ml), TLCK (1 mM), PMSF (200 µg/ml), chymostatin (660 µg/ml), and benzamidine (10µM), was added to each dish, the cells were scraped, centrifuged, and the supernatants were removed and placed in a microfuge tube for immuneprecipitation. Alternatively sciatic nerves were removed from postnatal-day 6 rats and placed in L15 medium in a 35 mm petri dish. The nerves were teased and placed into wells in a 24 well plate (6 nerves/well). The nerves were washed twice with methionine and cysteine-free DMEM containing 10% dialysed FCS and 2 mM glutamine and incubated in fresh medium. After 15 min, fresh medium (750 µl) and Trans [^{35}S] label (7.5 µl) were added to each well

and incubated for a further 3 h at 37°C. After washing twice with complete medium and twice with HBSS, the nerves were placed in a microfuge tube with 200 µl 2% SDS containing proteinase inhibitors and boiled for 2.5 min. Solution A containing 2.5% Triton X-100 and proteinase inhibitors was added to the tube, centrifuged, and the supernatant taken for immuneprecipitation.

2.5.2 Immuneprecipitation

Preparation of protein A agarose

Protein A agarose (Sigma) was swollen in an excess of distilled water for 1 hour at room temperature. The protein A agarose was washed twice with 2 volumes of solution A (as described in section 2.4.5) to 1 volume of agarose and resuspended in 2 volumes of solution A containing proteinase inhibitors and kept at 0°C until use.

Immuneprecipitation

Protein A agarose (60 µl) was added to the solublized pellet or supernatant and incubated for 1 hour at room temperature. All incubations were performed on a rotator. The sample was centrifuged and the supernatant was transferred to another microfuge tube. Rabbit polyclonal anti-170pep1 (10 µl) was added and incubated for 2 h at room temperature after which 60 µl of protein A agarose was added and incubated for 2 h. After centrifugation the pellet was washed three times with solution A containing proteinase inhibitors followed by one wash with solution A without Triton X-100. The pellet was resuspended in 80 µl SDS-PAGE sample buffer containing 62.5 mM dithiothreitol (DTT; Sigma) and boiled for 3 min. After centrifugation for 5 min, the supernatant was resolved by electrophoresis on a 4-20% gradient SDS-polyacrylamide gel. Gels were stained with 0.2% Coomassie blue (PAGE Blue 83, BDH), destained, and dried under vacuum. The dried gel was exposed to X-ray film (Agfa Curix RP-1 Plus) at room temperature and the

autoradiograph was developed using Kodak X-ray developer (LX24) and fixer (Industrex).

2.5.3 Western Blotting

Following SDS-PAGE electrophoresis, proteins were transferred to nitrocellulose (0.45 μm, Schleicher and Schuell) using a Hoefer Mighty Small Transphor Unit (Pharmacia Biotech) in a buffer containing 25 mM Tris HCL pH 8.3, 192 mM glycine, and 20% methanol (Towbin et al., 1979). The nitrocellulose was rinsed in PBS and blocked for 3 h with 0.2% gelatin, 0.1% Triton X-100 in PBS followed by a 1 hour incubation with primary antibody in blocking buffer. After 3 washes of 5 min each the membrane was incubated with donkey anti-rabbit IgG HRP conjugate (1:500, Scottish Antibody Production Unit) in blocking buffer for 1 hour. Following four washes in PBS (5 min each) the peroxidase was visualized by incubation first with 1 mg/ml 3,3'-diaminobenzidine tetrahydrochloride (DAB, Sigma) in 50 mM Tris HCl pH 7.4 and then initiating the reaction by the addition of H_2O_2 to a final concentration of 0.3%. When the color was sufficiently developed, the reaction was stopped by the addition of SDS.

For the surface biotinylation and biotinylation of total cellular proteins, the immuneprecipitated protein was probed with streptavidin-HRP (1:10,000). As a control, one lane was probed with anti-170pep (1:1000) followed by donkey anti-rabbit-IgG HRP conjugate (1:500).

2.5.4 SDS-PAGE of sciatic nerves

Sciatic nerves were removed from E15.5 mouse embryos and P3 mice, placed in 0.5 ml microfuge tubes and stored at -80°C. Boiling sample buffer containing 62.5 mM DTT was placed in the tube with the nerves and immediately boiled for 3 min. Following centrifugation the samples were loaded on a 10% SDS-polyacrylamide gel and resolved by electrophoresis using the Hoefer Mighty Small

Unit (Pharmacia Biotech). Following electrophoresis the proteins were transferred to PVDF (polyvinylidene difluoride) protein sequencing membrane (Bio-Rad). For the Western blot, the PVDF was blocked with 5% non-fat milk in PBS containing 0.1% Tween-20 overnight at 4°C. The membrane was incubated with anti-170pep1 (1:20,000) in 0.2% gelatin in PBS containing 0.1% Tween-20 for 1 h at room temperature. Following 6 washes in gelatin/PBS/Tween-20, the blot was incubated with donkey anti-rabbit IgG conjugated to HRP (1:500) for 1 h. After prolonged washing with PBS containing 0.1% Tween-20, enhanced chemiluminescence (ECL) was performed using the ECL Plus Kit (Amersham) according to the manufacturer's instructions. The excess buffer was drained from the PVDF membrane and the membrane was placed on Saran Wrap and overlayed with 2 mls of ECL detection reagent (2 mls of solution A + 40 µl solution B) for 5 minutes. Excess reagent was removed and the membrane was wrapped in Saran Wrap. The chemiluminescence was detected on X-ray film (Agfa Curix RP-1 Plus).

2.6 *IN SITU* HYBRIDIZATION

The method used for *in situ* hybridization (Griffiths et al., 1989; Wilkinson et al., 1987), was an adaptation of the original method of (Cox et al., 1984). The method of (Carrasco and Bravo, 1994) for frozen sections of mouse embryos was also useful.

2.6.1 [^{35}S]-labelled riboprobe preparation

Single-stranded riboprobes were prepared by *in vitro* transcription using insert cDNAs cloned into vectors containing RNA polymerase initiation sites.

L-periaxin riboprobes

The construct PrxΔ6, which consists of the repeat region of L-periaxin from nt 1500-2500 cloned into the expression vector pSV·SPORT (Gibco BRL), was used to prepare 1 kb antisense and sense riboprobes for L-periaxin. PrxΔ6 was prepared by PCR using primers DLS 10 and DLS 11, digestion with KpnI/XbaI, and ligation into pSV·SPORT. Plasmid DNA was prepared by using the Promega Wizard Maxiprep kit according to the manufacturer's directions on 500 mls of overnight culture. 5 µg plasmid DNA was linearized by restriction digest with KpnI in 50 µl total volume at 37°C overnight. For the antisense riboprobe, a KpnI restriction digest was used producing a 3' overhang. It has been reported that extraneous transcripts appear when templates contain 3´ overhangs. Hence it was necessary to convert the overhang to a blunt-end by incubation with 6 U Klenow DNA polymerase (Gibco BRL) and 20 µM dNTPs (Pharmacia) for 15 min at 30°C, followed by incubation at 75°C for 10 min to inactivate the enzyme. The plasmid DNA for the sense probe was linearized with MluI. The linearized plasmid DNA was electrophoresed on a 1% agarose gel containing ethidium bromide. The bands were excised and the DNA was extracted using the Qiaex II gel extraction kit according to the manufacturer's instructions. The DNA was eluted with 5 mM Tris HCl, pH 8 in DEPC water and the concentration of the linearized template was obtained by comparison with a DNA high mass ladder (Gibco BRL) on an agarose gel.

S-periaxin riboprobes

Restriction digest of the 5.2 kb cDNA in pSPORT with AccI followed by MluI yielded a 460 nt fragment which was excised from a 1% agarose gel. 200 ng of AccI- and MluI-cut pIBI30 was also excised from an agarose gel and the DNA was extracted from the gel slices using the Qiaex II gel extraction kit. The volume was reduced to 3 µl under vacuum and a ligation was performed with 1-2 U T4 DNA

ligase (Fermentas) for 3 h at room temperature. Competent XL1-blue cells were transformed and plated on LB agar (Gibco BRL) containing 0.1 mg/ml ampicillin, 300 µM IPTG and 80 µg/ml Xgal for blue/white selection. Minipreps were performed by alkaline lysis on 4 ml overnight cultures from individual white colonies. Restriction digest followed by electrophoresis on 1% agarose gel revealed if the insert was present. Four plasmids with the insert were sequenced (Pharmacia sequencing kit) with T7 sequencing primer to check that it was correct. Plasmid DNA was prepared for transcription by alkaline lysis midiprep and linearized with MluI for the antisense probe and BamHI for the sense probe.

P0 riboprobe

The 1 kb P0 cDNA in pSPORT cloned in at EcoRI and XbaI sites was used for riboprobe preparation. Plasmid was prepared by alkaline lysis midi-prep and linearized with EcoRI for an antisense probe.

***In-vitro* transcription**

Transcription was performed for 1 hour at 37°C. The reaction contained 4 µl transcription 5X buffer (Promega), 2 µl 100mM DTT, 20 U rRNasin ribonuclease inhibitor (Promega), 1 µl each of 10 mM rATP, rCTP, rGTP (Promega), 5 µl $\alpha[^{35}S]$ UTP (ICN), 1 µg linearized template DNA, DEPC water to 19 µl, 1 µl of either T7 (15 U, Promega), T3 (20 U, Boehringer Mannheim), or SP6 (20 U, Boehringer Mannheim) RNA polymerase. An additional 1 µl of the appropriate RNA polymerase was added after the first 30 min. Template DNA was removed by a 15 min incubation with 1 U RQ1 RNAse-free DNAse (Promega). The RNA was phenol chloroform extracted and ethanol precipitated with 0.5 volume 7.5 M ammonium acetate. In order to calculate the percent of isotope incorporation, 1 µl was removed before centrifugation and placed in 1 ml Optiphase 'Hisafe' (Fisons Chemicals). The pellet was taken up in 100 µl DEPC water. An aliquot of the

supernatant and an aliquot of the pellet were also added to 1 ml of Optiphase. Percent incorporation was calculated and the probe was resuspended at 1 ng/µl/kb in DEPC-treated water containing 10 mM DTT and stored at -40°C.

2.6.2 Tissue preparation for ISH

All glassware for the procedure was rinsed twice in 0.1% DEPC-treated water and either autoclaved or baked at 80°C until use. Slide preparation has been described in section 2.2.1. All solutions were made using DEPC-treated water and then autoclaved at 121°C whenever possible.

ISH was performed on unfixed tissue except for cervical sympathetic trunks which were fixed and then cryoprotected with 25% sucrose. Embryos and nerves were placed in OCT in plastic molds and quickly frozen in isopentane cooled in liquid nitrogen. The tissue was stored at -70°C until it was needed for sectioning. Sections (13 µm) were cut at -16°C on a cryostat and collected on TESPA-coated slides. The slides were kept at cryostat temperature during sectioning and then transferred to a -70°C freezer.

2.6.3 Fixation and preparation for hybridization

Slides were removed from the freezer and immediately fixed in freshly prepared 4% paraformaldehyde in PBS for 20 min at room temperature. They were rinsed in PBS and acetylated for 10 min by transferring them to a glass dish containing 200 ml of 100 mM triethanolamine. While stirring, 0.5 ml of acetic anhydride was added to a final concentration of 0.25% (v/v). The slides were washed in PBS twice for 5 min each and dehydrated by dipping for 2 min each in 70% ethanol, 90% ethanol, and twice in absolute ethanol. The slides were air-dried for ~1 h.

2.6.4 Hybridization

The probes were diluted 1:10 in hybridization buffer containing 10 mM DTT. Hybridization buffer consisted of 50% formamide, 10% dextran sulphate, 1X Denhardt's, 20 mM Tris HCl (pH 8), 0.3 M NaCl, 5 mM EDTA, 10 mM NaH_2PO_4 pH 8, and 0.5 mg/ml yeast tRNA. The diluted probes were denatured by heating at 80°C for 2 minutes, cooled on ice briefly and placed at room temperature. Diluted probe (25 µl) was placed on the slide over the sections and a 22 x 22 mm clean glass coverslip was placed over it. More probe was used for larger sections. The slides were placed horizontally in a slide box or alternatively in a plastic box. To provide a humid chamber, 3MM paper and a tissue soaked with 20 ml 50% formamide/5X SCC was placed in the box. The box was sealed with tape and placed in a zip-lock plastic bag in a humidified hybridization oven overnight at 52°C.

2.6.5 Post-hybridization washes

The slides were removed and placed in a glass rack in a glass staining dish containing the following solutions for the temperature and times indicated.

1. Solution A	5x SSC/10 mM DTT	52°C	30 min.
2. Solution B	2x SSC in 50% formamide/ 100 mM DTT	65°C	20 min.
3. Solution C	RNase buffer (0.5 M NaCl, 5 mM EDTA, 10 mM Tris-HCl (pH 7.5)	37°C	3x10 min.
4. RNase A	20 µg/ml (Sigma) in Solution C	37°C	30 min.
5. Solution C		37°C	10 min.
6. Solution B		65°C	20 min.
7. 2x SSC		22°C	15 min.
8. 0.1x SSC		22°C	15 min.

The sections were dehydrated by dipping the slides sequentially for 2 min in 30, 60, 80, 95% ethanol containing 300 mM ammonium acetate followed by absolute ethanol for 2 min. The slides were air-dried and exposed to Agfa Curix Xray film overnight in a film cassette as an indicator of exposure time for autoradiography.

2.6.6 Autoradiography, staining and photography

Ilford K5 nuclear emulsion was diluted 1:1 with distilled water containing 2% glycerol and was melted for 15 min at 42°C in a darkroom illuminated with a safelight (Ilford 902S filter). After gentle mixing the slides were dipped in the diluted emulsion and allowed to air-dry vertically. The slides were placed in light tight boxes containing a desiccant, sealed with tape and stored at 4°C. The slides were exposed for 2 to 4 weeks. The slides were developed in Kodak D19 for 4 minutes and fixed with 30% sodium thiosulfate. After washing in tap water the slides were stained with Ehrlich's hematoxylin for 20 s, dehydrated through ethanol and cleared in xylene before mounting with Cytoseal (Stevens Scientific). Darkfield photographs was taken using an Olympus SZH10 steromicroscope with Fuji Velvia film and scanned using a UMAX S12 scanner. Alternatively for higher magnification, epifluorescence microscopy was performed using an Olympus BX60 microscope and photographed with Fuji Provia film.

2.7 TRANSGENESIS

2.7.1 Construct preparation

Four promoter constructs containing *LacZ* as a reporter gene were prepared (Fig. 15). Different regions of the *periaxin* promoter were cloned into the plasmid pnlacF which contains the SV40 nuclear translocation signal (Lanford et al., 1988)

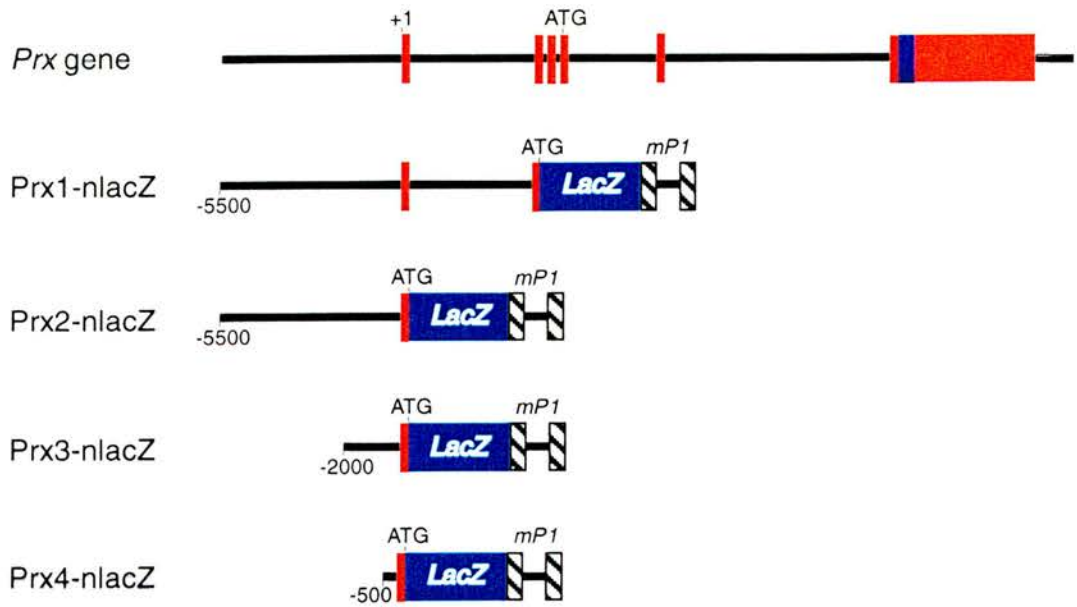

Figure 15. Schematic representation of Periaxin/LacZ transgenes. The *periaxin* (*prx*) gene is illustrated on the top with each transgene below. Prx1-nlacZ contains 5.5 kb of *prx* promoter, exon 1, intron 1, and most of exon 2, n*lacZ*, and murine protamine-1 (*mP1*) gene which provides an intron and polyadenylation signal; Prx2-nlacZ comprises 5.5 kb of *prx* promoter, exon 1, *lacZ* and *mP1*; Prx3-nlacZ comprises 2 kb of *prx* promoter, exon 1, *lacZ* and *mP1*; Prx4-nlacZ contains the 500 bp core promoter, exon 1, *lacZ* and *mP1*. The transcription initiation site is marked +1 and the translation start codon is marked ATG.

in frame with the lacZ coding sequence, to encode a nuclear targeted *E. coli* β-galactosidase. A segment of the mouse protamine-1 gene (mP1) (Peschon et al., 1987) from +95 relative to the transcription start site to +625, provides an intron and a polyadenylation site. The constructs were also cloned into the plasmid placF, lacking the nuclear localization signal.

The periaxin promoter constructs were tested by transient transfection in NIH 3T3 cells, and Schwann cells using either liposome-mediated transfection or calcium phosphate precipitation. Schwann cells were grown in the presence of 50 μM forskolin before and after Lipofectamine-mediated transfection. The transfected cells were identified by β-galactosidase histochemistry.

pPrx1-nlacZ

pPrx1-nlacZ consisted of 5.5 kb of the *periaxin* promoter, exon 1, intron 1, and 43 bp of exon 2 (5' untranslated region) linked to the *lacZ* reporter gene. PCR using a 5 kb fragment of genomic clone HH1 in pIBI30 as template introduced 2 restriction sites, XbaI and NcoI, into the 3' end of exon 2. The primers used for the PCR were T3 (forward primer) and DLS1 (reverse primer). The 3.5 kb PCR product was purified, digested with XbaI and EcoRI and ligated into pBlueScript KS (Stratagene), generating p3.5BS. A 7 kb fragment from the HH1 genomic clone was inserted in dephosphorylated (using the calf intestinal alkaline phosphatase kit, CIAP, Gibco BRL) EcoRI cut p3.5BS and the correct orientation was obtained by restriction digest. The 10.5 kb fragment was released from the BlueScript polylinker by digestion with NcoI and SalI and cloned into pnlacF to generate pPrx1-nlacZ. A Promega Wizard Maxiprep was performed and the vector sequence was removed by digestion with HindIII and SalI.

pPrx2-nlacZ

pPrx2-nLacZ consisted of 5.5 kb of the *periaxin* promoter and the reporter gene *LacZ*. Prx2-nLacZ was constructed by introducing NcoI and EcoRI sites into exon 1 by PCR. A PCR product of 2 kb of *periaxin* promoter including exon 1 was obtained using a pIBI30 subcloned 7 kb fragment of the HH1 genomic clone as template with the reverse primer DLS 21 and T3 (forward). Pfu polymerase (1 U, Stratagene) was used in a 50 µl PCR at an annealing temperature of 55°C with a 2 min extension. The bands of the expected size were excised from a 1% agarose gel, extracted using Qiaex II gel extraction kit (Qiagen), digested with KpnI and EcoRI, and ligated into KpnI and EcoRI cut pIBI30. A KpnI digest of HH7 released a 3.5 kb fragment which was then cloned into the 2 kb fragment in pIBI30 after KpnI digestion and dephosphorylation. The dephosphorylation was performed by incubation with CIAP (Gibco BRL) in CIP buffer for 30 min at 50°C. The orientation of the insert was determined by restriction digest. Finally the 5.5 kb fragment was released from the vector polylinker by digestion with NcoI and SalI and cloned into pnlacF at the NcoI and SalI sites to generate pPrx2-nlacZ. After plasmid preparation by Qiagen midi-prep, vector sequences were removed by digestion with HindIII and SalI.

pPrx3-nlacZ

This construct consisted of 2 kb of the *periaxin* promoter linked to the *lacZ* gene. pPrx3-nLacZ was constructed by introducing a NcoI site into exon 1 by PCR. A PCR product of 2 kb of the *periaxin* promoter including exon 1 was obtained using the 7 kb fragment in pIBI30 of genomic clone HH1 as template with the reverse primer DLS 19 and T3 (forward). 1 U of pfu polymerase (Stratagene) was used in a 50 µl PCR at an annealing temperature of 55°C with a 2 min extension. The bands of the expected size were excised from a 1% agarose gel, extracted using Qiaex II gel extraction kit (Qiagen), digested with KpnI and NcoI, and ligated into

pnlacF at the KpnI and NcoI sites. Following plasmid preparation by Qiagen midi-prep, vector sequences were removed by digestion with KpnI and HindIII.

pPrx4-nlacZ

The construct pPrx4-nlacZ contained the 500 bp of the *periaxin* core promoter linked to the *lacZ* gene. The restriction sites NcoI and SalI were introduced by PCR with the forward primer DLS 25 and the reverse primer DLS 21. A 50 µl PCR contained 1 U pfu polymerase, 0.5 µM primers, 200 µM dNTPs in pfu polymerase buffer. An annealing temperature of 55°C and an extension of 30 s was used for the PCR. After gel electrophoresis the 0.5 kb bands were excised and purified as described previously, digested with NcoI and SalI and cloned into pnlacF at the NcoI and SalI sites. The insert was checked for errors by sequencing and plasmid was prepared by Promega Maxipep. Vector sequence was removed by digestion with HindIII and SalI.

2.7.2 DNA purification for injection

DNA was prepared by Qiagen midiprep or Promega Wizard Maxiprep. Vector sequences were removed by restriction digest of 50-70 µg of plasmid. The digested plasmids were electrophoresed on 0.8% low melting point agarose gel and the bands corresponding to the vector-free fragments were excised and weighed. The agarose was digested with agarase (Boehringer Mannheim) by incubation at 65°C for 15 min with 0.04 vol. 25X agarase buffer. The temperature was adjusted to 45°C before the addition of 0.8 U agarase/100 µl followed by incubation for 1 h. The DNA was then purified with an Elutip-D column (Schleicher & Schuell) according to the manufacturer's instructions, followed by ethanol precipitation and resuspension in sterile injection buffer (0.1 mM EDTA, pH 8, 10 mM Tris HCl, pH 7.5). To remove particles, the injection buffer was Millipore filtered (0.22 µm) twice before use and all microfuge tubes were washed twice with injection buffer before

use, vortexed each wash and then the remaining injection buffer was flicked out. The A_{260} of the DNA solution was measured with a Pharmacia spectrophotometer and the concentration of the DNA was calculated. This value was checked by electrophoresis on a 1% agarose gel and the intensity compared to that of a high mass ladder (Gibco BRL) by UV transillumination. Dialysis was performed on 10 µg DNA in a "waterbug" (Orr et al., 1995) against 1 liter of injection buffer for 48-72 h with 3 changes of the buffer. The concentration of the recovered DNA was calculated again after comparison to the intensity of a high mass ladder following electrophoresis and UV transillumination. The purified DNA was then diluted with filtered injection buffer to obtain a concentration of 2.5 µg/ml. The DNA was centrifuged (13,000 rpm) for 10 min to pellet any particles and the top portion was stored in aliquots in precleaned microfuge tubes. The aliquots were stored at -70°C.

2.7.3 Production of transgenic mice

To produce transgenic mice, transgenes (Prx1-nlacZ, Prx2-nlacZ, and Prx3-nlacZ) were introduced into the C57BL6 mouse genome by standard pronuclear microinjection (Hogan et al., 1994). Female F1 (C57BL6 X CBA hybrid mice) hybrids were superovulated and mated with F1 hybrid males. The oviducts from plugged mice were removed and placed in M2 medium (Sigma). Fertilized eggs were released from a swollen ampulla by tearing the tissue with fine forceps and transferred to a dish containing 300 µg/ml hyaluronidase (Sigma) in M2 for a few minutes to remove the cumulus (follicle) cells and then transferred to fresh M2. Embryos were injected with the transgene, briefly incubated in M16 (Sigma) before transfer to the oviducts of pseudo-pregnant foster mothers. The injections and embryo transfers were performed by Professor P.J. Brophy. Mice were kept in the Department of Veterinary Pathology Animal House, University of Edinburgh in an isolation room. Breeding and tail biopsies were performed by Ms. Linda Ferguson

as well as assistance with transgene screening. Tail clips were taken from possible founders at ~postnatal-day 21 and genomic DNA was extracted.

2.7.4 Genomic DNA extraction from tail biopsies

Each tail clip was placed in a 1.5 ml screw-top vial containing 0.5 ml of lysis buffer (100 mM EDTA, 0.125% SDS, 1 mg/ml proteinase K (Boehringer Mannheim, 50 mM Tris HCl, pH 8) overnight at 55°C. An equal volume of phenol/chloroform (1:1) was added and the vial was gently mixed to form an emulsion. The vials were placed on a rotating mixer for 10 min followed by centifugation at 5000 rpm for 5 min. The aqueous phase was removed with a yellow tip (small point cut off to prevent shearing of genomic DNA) and transferred to a fresh screw-top vial. The phenol/chloroform extraction step was repeated followed by extraction with chloroform to remove any phenol. The aqueous phase was removed and the genomic DNA was precipitated with 1/10 vol. 3 M sodium acetate pH 6 and 2 vol. ethanol. After centrifugation the DNA was washed with 70% cold ethanol to remove salts, and resuspended in 100 µl TE. The A_{260} was measured and the concentration was calculated. Genomic DNA was stored at 4°C.

2.7.5 Transgene screening by PCR

The primers synthesized for genomic PCR were: a forward primer Lac 1 and a reverse primer Lac 2 which produced a 500 bp product [Leconte, 1996 #7]. A 50 µl PCR reaction consisted of 240 ng template, 0.5 µM primers, 5 µl Dynazyme 10x buffer, 0.2 mM dNTPs, 1U Dynazyme polymerase (Flowgen). A control without template was included. The PCR conditions were: 94°C denaturation for 1 min, 55°C annealing for 30 s, and 72°C extension for 30 s for one cycle, followed by 28 cycles of 94°C denaturation for 30 s, 55°C annealing for 30 s, 72°C extension for 30 s. The last cycle consisted of 72°C denaturation for 30 s, 55°C annealing for 30

s, and 72°C extension for 4 min. An aliquot of the reaction (9 µl) was run on 1% agarose gel in TAE buffer containing 0.5 µg/ml ethidium bromide and visualized by UV transillumination.

2.7.6 Transgene screening by Southern blotting

Genomic DNA (10 µg) was digested overnight at 37°C with 50 U EcoRI (Gibco BRL) containing 2.5 µg/ml BSA. The digests were resolved by 0.8% agarose gel electrophoresis. Resolved samples were then transferred to nylon membrane (Micron Separations Inc.) using a VacuGene XL blotting unit (Pharmacia Biotech). The DNA was depurinated in 0.25 M HCl for 5 min, denatured in 1.5 M NaCl, 0.5 M NaOH for 20 min and then neutralized in 1.5 M NaCl, 0.5 M Tris HCl pH 8 for 20 min followed by 20X SSC for 1 h. The membrane was baked at 80°C for 2 h.

Probe preparation

A 2 kb probe was prepared by restriction digestion of placF DNA with SstI followed by BamHI. The DNA was resolved by 1% agarose gel electrophoresis in TAE buffer and the 2 kb band was excised and purified using the Qiaex II gel extraction kit. The concentration of the probe was determined by comparison with a low mass ladder (Gibco BRL) following gel electrophoresis in 1% agarose and UV transillumination. The probe was labelled (50 ng) with [α^{32}P] dCTP by random priming (Gibco BRL).

Pre-hybridization

After briefly wetting the membrane with distilled water, it was placed in a 50 ml screw-top centrifuge tube and covered with Quikhyb (5 mls, Stratagene). The centrifuge tube was placed in a glass hybridization roller tube which was then rotated in a hybridization oven (Techne Hybridizer HD-1B) at 65°C for 30 min.

Hybridization

After the addition of 1 mg of sheared salmon sperm DNA (Stratagene), the labelled probe was boiled for 8 min and immediately added to the Quikhyb in the tube and hybridized for 2 h at 65°C.

Post-hybridization washes

The membrane was washed twice with 2x SSC containing 0.1% SDS for 10 min each at room temperature and twice with 0.2x SSC containing 0.1% SDS for 30 min each at 65°C. The membrane was wrapped in Saran Wrap and exposed to X-ray film (Agfa Curix) in an X-ray cassette with an intensifying screen for 2-3 d. Autoradiographs were developed with Kodak LX24 followed by Kodak Industrex fixer.

2.7.7 β-galactosidase histochemistry

Mice were perfused through the left ventricle with heparinized saline followed by freshly prepared 4% paraformaldehyde in 0.1 M phosphate buffer pH 7.3. For β-galactosidase staining tissues were quickly removed and placed in freshly prepared 2% paraformaldehyde, 0.2% glutaraldehyde, 2 mM $MgCl_2$, 5 mM EGTA in 0.1 M sodium phosphate buffer pH 7.4 at 4°C for 1 h (Hogan et al., 1994). Embryos older than E13 and adult brain were cut saggitally with a scalpel blade before immersion in fixative. Tissues were rinsed three times, for 30 min each, with a buffer containing 2 mM $MgCl_2$, 0.01% sodium deoxycholate, 0.02% NP-40 in 0.1 M sodium phosphate buffer pH 7.3. The staining reaction was performed by incubating the tissue overnight at 37°C in 1 mg/ml X-gal (Gibco BRL), 5 mM $K_3Fe(CN)_6$ and 5 mM $K_4Fe(CN)_6$ in the rinse buffer. After washing in PBS, postfixation was performed overnight in 10% formalin. The tissue was photographed as whole mount preparations on an Olympus SZH10 stereo microscope. Teased fibres were prepared of sciatic and trigeminal nerves and mounted in 80% glycerol. Embryos and brains were cryoprotected with 25%

sucrose and frozen in isopentane cooled in liquid nitrogen and 15 μm sections were cut on a cryostat. Sections were briefly counterstained with 1% Orange G (w/v) in 2% tungstophosphoric acid.

2.8 STRAINS OF ANIMALS USED IN THE WORK

The rats were of the Wistar strain. All mouse tissues and embryos were from F1 hybrid mice which were produced from C57BL/6 and CBA mice. *Periaxin*-null mutant mice were produced at the Centre for Genome Research, Edinburgh University and were the result of targetted deletion of the *Prx* locus in ES cells which were subsequently injected into C57BL/6 blastocysts. Heterozygous offspring were backcrossed to the parental C57BL/6 strain before intercrossing at the F3 and F4 generations. Mice homozygous for the mutant allele were identified by Southern blotting.

Results

3.1 IMMUNOLOCALIZATION OF L-PERIAXIN AND S-PERIAXIN

The myelin-forming Schwann cell is a polarized epithelial cell with distinct membrane domains that contain proteins with discrete localizations (Kidd et al., 1994; Trapp et al., 1995). P0, MBP, and PMP-22 have all been localized to compact myelin, whereas MAG, spectrin, and F-actin are associated with the periaxonal cytoplasmic region apposing the axon (Trapp et al., 1989b). There are also several proteins expressed in the uncompacted regions of the Schwann cell, the Schmidt-Lanterman incisures and paranodal loops, such as MAG, E-cadherin, and connexin-32 (Trapp and Quarles, 1982; Fannon et al., 1995; Scherer et al., 1995). In order to determine the localization of L-periaxin and S-periaxin and ascertain in which regions of the Schwann cell the proteins may be functionally important immunofluorescence and immunogold electron microscopy was performed.

3.1.1 L-periaxin localization in early postnatal peripheral nerve by immunogold electron microscopy

Using a post-embedding immunogold technique, sections of early postnatal rat sciatic nerve, (postnatal-day 1, 4 and 7) were immunolabelled with the affinity-purified anti-peptide antibody, 170pep1, followed by a secondary antibody coupled to 10 nm colloidal gold. The anti-170pep1 was raised against a synthetic peptide which comprised amino acids 713 to 728 in the repeat region of L-periaxin only.

During early ensheathment at postnatal-day 1 in the rat, at a time when the Schwann cell-axon unit is in a one-to-one relationship but myelin sheath formation has not yet occurred, gold particles linked to antibodies that recognize L-periaxin strongly decorated the Schwann cell plasma membranes. As the mesaxon spirals around the axon forming several complete turns, L-periaxin labelling was evident on all of the cytoplasm-filled membranes within the spiral (Fig. 16A and 16B).

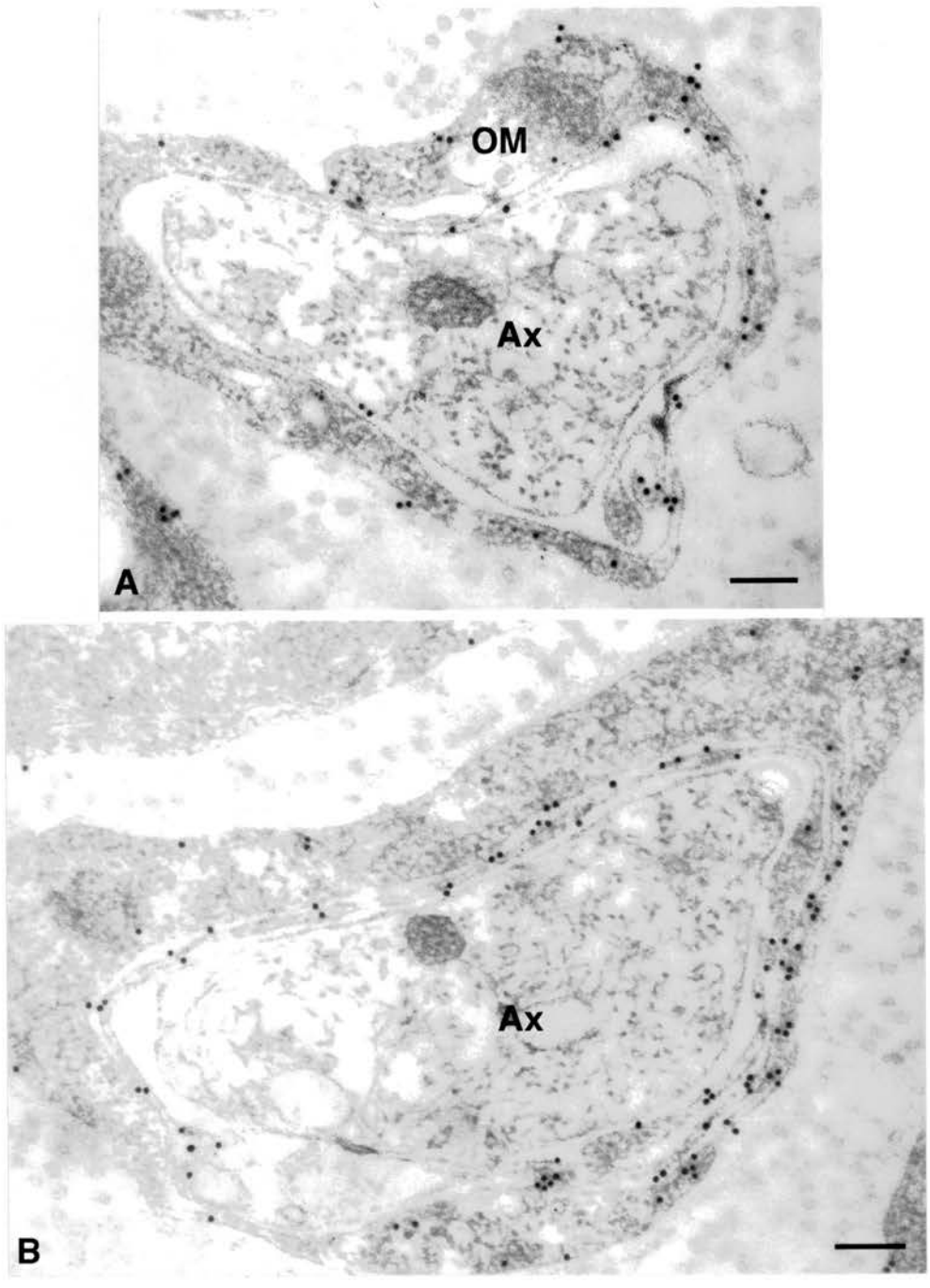

Figure 16. Immunolocalization of L-periaxin during early ensheathment at the electron microscopic level. At an early stage of axonal ensheathment, in rat postnatal-day 1 sciatic nerve, L-periaxin can be detected on the uncompacted Schwann cell membranes including the membranes of the inner and outer mesaxons (OM). The Schwann cell in (A) has completed a half turn around the axon (Ax) and in the cell in (B) approximately two turns. The Schwann cell plasma membrane is also labelled. Bar, 200 nm.

Slightly later in the development of the rat sciatic nerve at postnatal-day 4, immunogold particles were detected on the periaxonal membranes of the myelin sheath as well as the abaxonal membranes (apposing the basal lamina) (Fig. 17A, 17B). The localization on periaxonal membranes was similar to that previously described for MAG (Trapp et al., 1989a; Trapp et al., 1989b; Trapp et al., 1988). When sections were labelled using antisera directed against the major myelin protein P0 and MAG and compared with sections labelled with anti-170pep1, L-periaxin and MAG localized to the same periaxonal compartment (Fig. 18A and 18B). Like MAG, L-periaxin was excluded from compact myelin (Fig. 17A, 17B, and 18A) which indicates that L-periaxin does not play a role in the compaction of the myelin sheath. In contrast, P0, the major glycoprotein of peripheral myelin, was concentrated throughout compact myelin (Fig. 18C). L-periaxin was also detected in other regions of the Schwann cell including the Schwann cell plasma membrane (Fig. 17A), in the cytoplasm-filled outer loops or uncompacted region of the myelin sheath (Fig. 17B, 19A) and in Schmidt-Lanterman incisures (Fig. 19B), the cytoplasmic channels that traverse the myelin sheath. L-periaxin colocalized with MAG in the Schmidt-Lanterman incisures of sections that were double-labelled for both proteins (Fig. 20).

In the regions of the sheath that flank the node of Ranvier, L-periaxin was detected on the uncompacted cytoplasm-filled membranes of the paranodes but not in the loops which directly appose the axolemma where the electron-densities are known to be rich in the protein CASPR/paranodin (Fig. 21A, 21B) (Menegoz et al., 1997; Peles et al., 1997). The electron-dense adherens-type junctional cytoplasmic plaques that are in register across Schmidt-Lanterman incisures and paranodal loops were strongly labelled with an antiserum directed against E-cadherin (Fig. 22B, 22C) (Fannon et al., 1995) but were not labelled by L-periaxin (Fig. 22A).

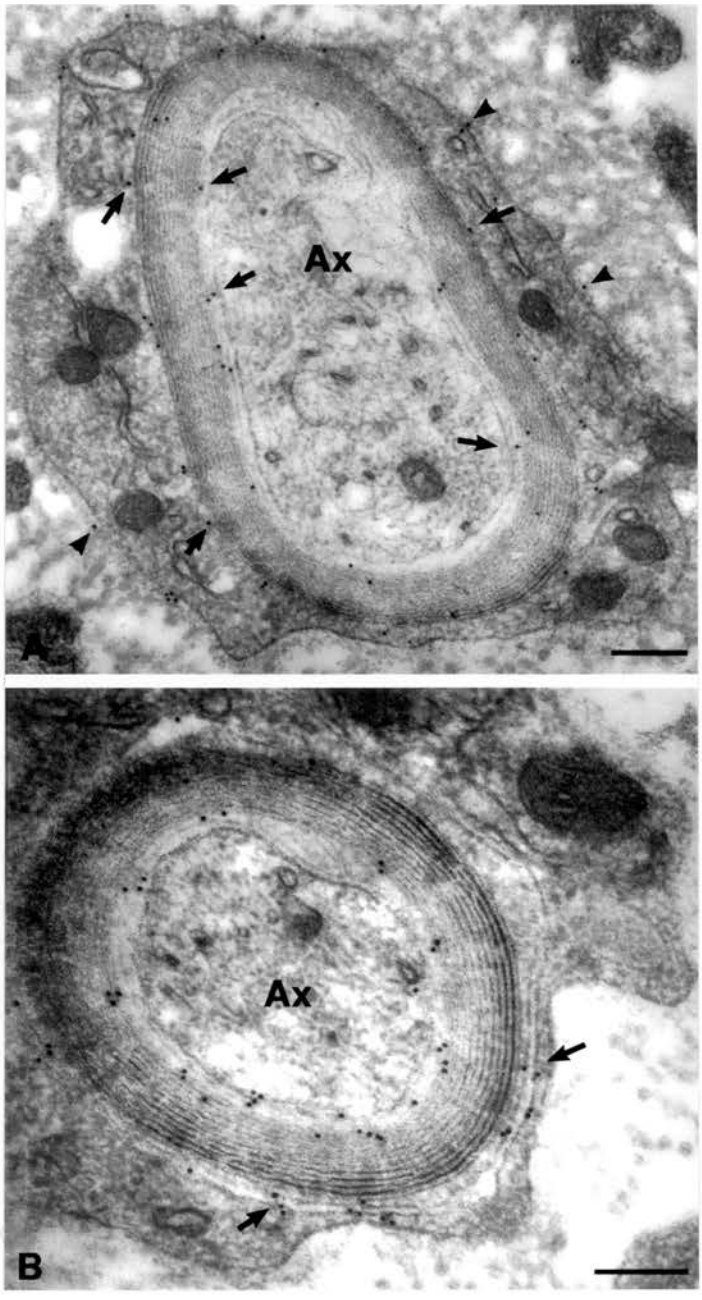

Figure 17. Localization of L-periaxin in postnatal-day 4 sciatic nerve by immunoelectron microscopy. (A) Immunogold particles are specifically localized to the periaxonal and abaxonal (apposing the basal lamina) myelin membranes (arrows) and the Schwann cell plasma membrane (arrowhead). (B) In a Schwann cell where the outer mesaxon is visible, gold particles decorate the apposing membranes (arrows). Ax, axon. Bar, 200 nm.

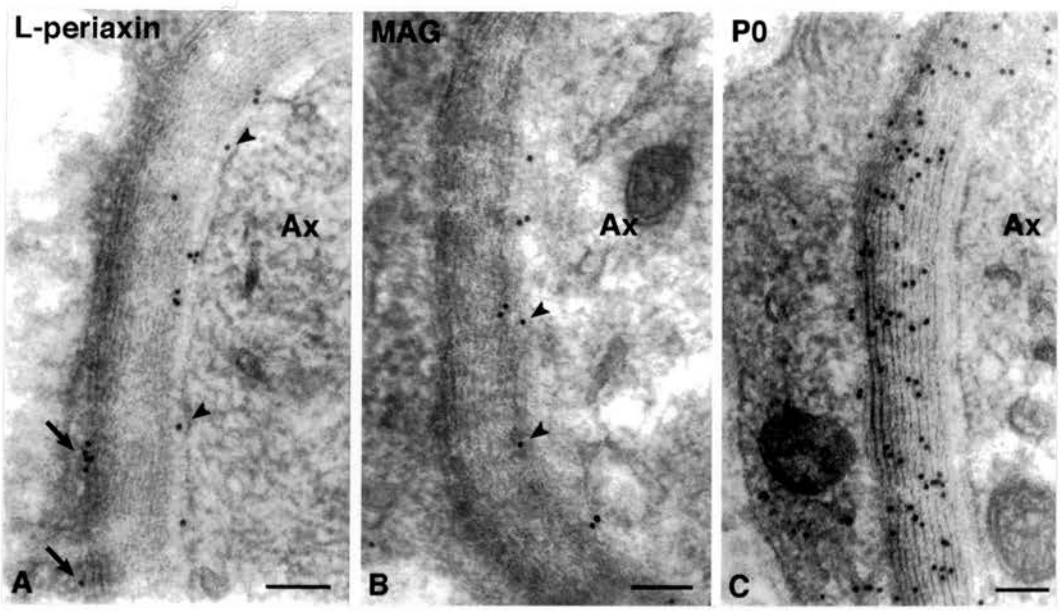

Figure 18. Comparison of L-periaxin, MAG and P0 localization in postnatal-day 4 sciatic nerve by immunoelectron microscopy. (A) L-periaxin is primarily localized to the periaxonal membranes (arrowheads). A few gold particles are also seen on the abaxonal membranes (arrows). (B) Like L-periaxin, MAG is localized to the periaxonal membranes (arrowheads). L-periaxin and MAG are excluded from compact myelin. (C) In contrast, P0 is localized to the compact myelin sheath. Ax, axon Bar, 200 nm.

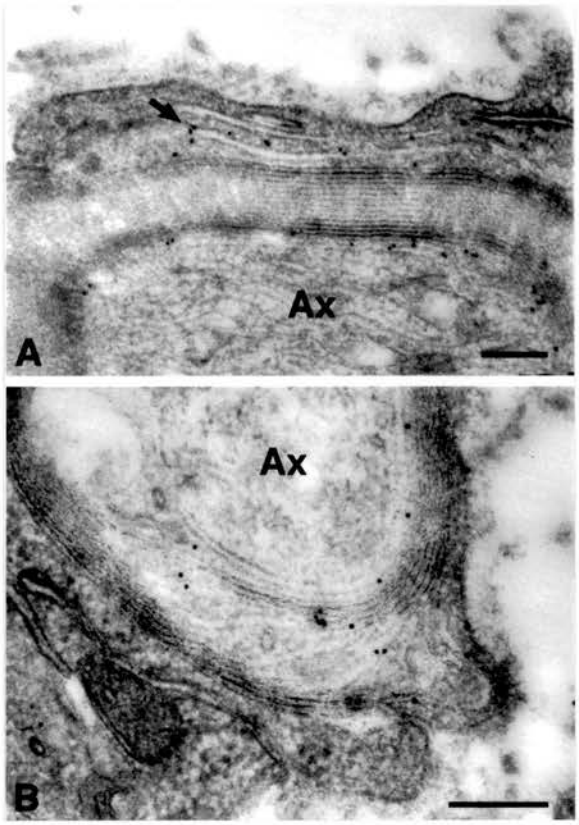

Figure 19. L-periaxin is localized to the uncompacted channel network of Schwann cells by immunogold electron microscopy. In postnatal-day 4 sciatic nerve, gold particles decorate uncompacted regions of the sheath (A, arrow) including Schmidt-Lanterman incisures (B). Ax, axon. Bar, 200 nm.

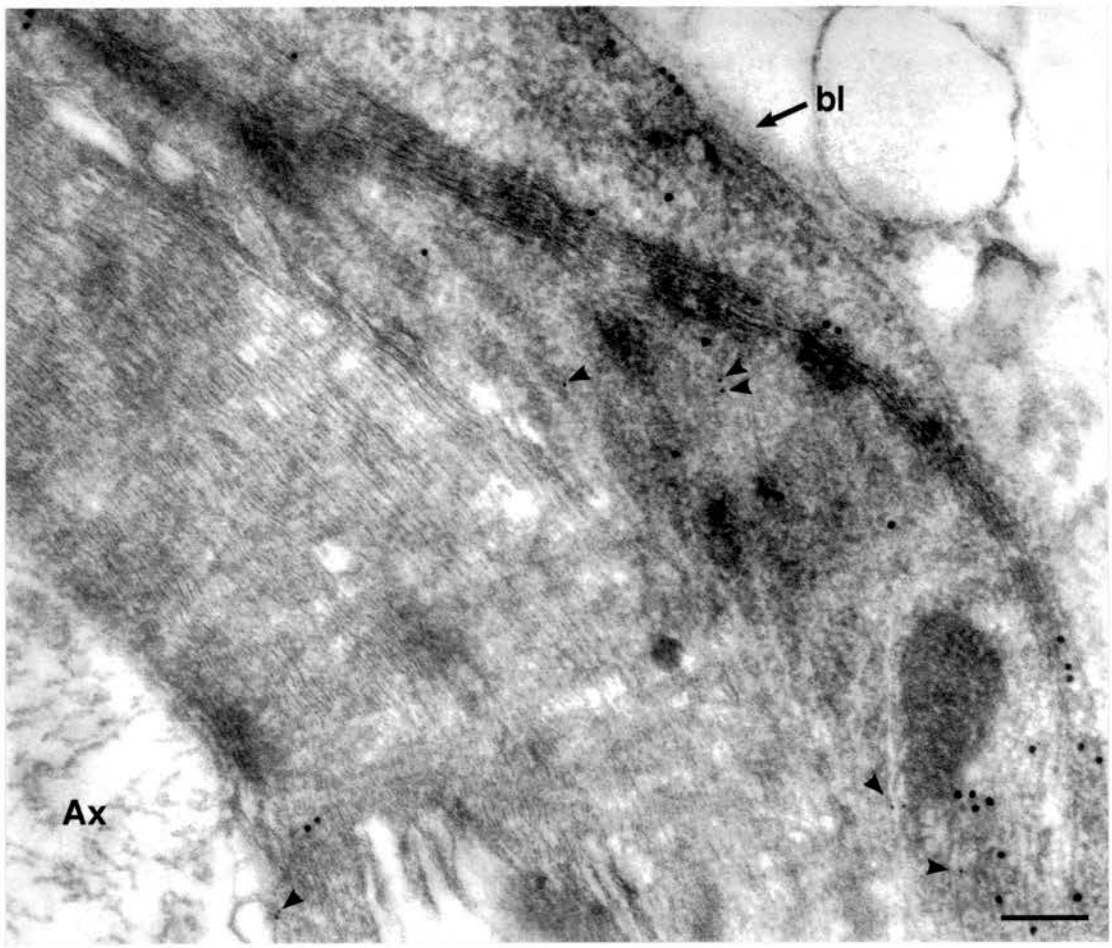

Figure 20. Colocalization of L-periaxin and MAG in Schmidt-Lanterman incisures by double-label immunogold electron microscopy. In postnatal-day 28 trigeminal nerve, L-periaxin (10 nm gold particles) and MAG (5 nm gold particles, arrowheads) are seen over the uncompacted channels of a Schmidt-Lanterman incisure. Compact myelin is devoid of labelling. Ax, axon; bl, basal lamina. Bar, 200 nm.

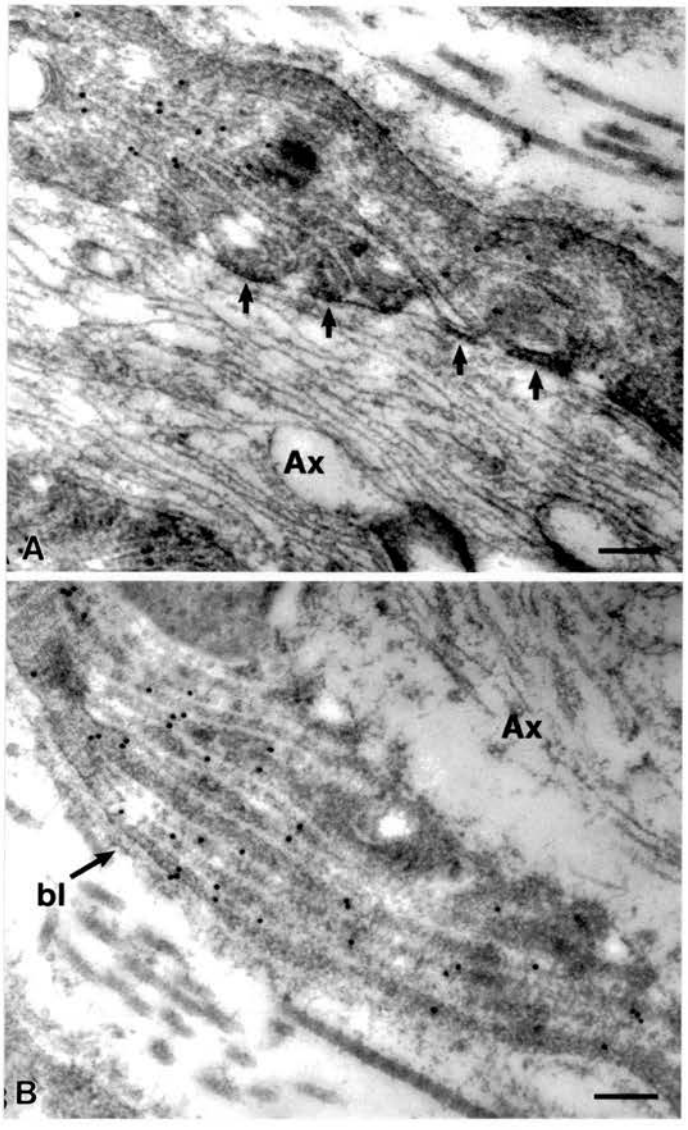

Figure 21. L-periaxin immunogold localization at the paranode. In sections of postnatal-day 5 sciatic nerve L-periaxin is localized to the paranodal uncompacted membranes (A and B) but is not present in the loops which appose the axolemma where electron densities are apparent (A, arrows). Ax, axon; bl, basal lamina. Bar, 200 nm.

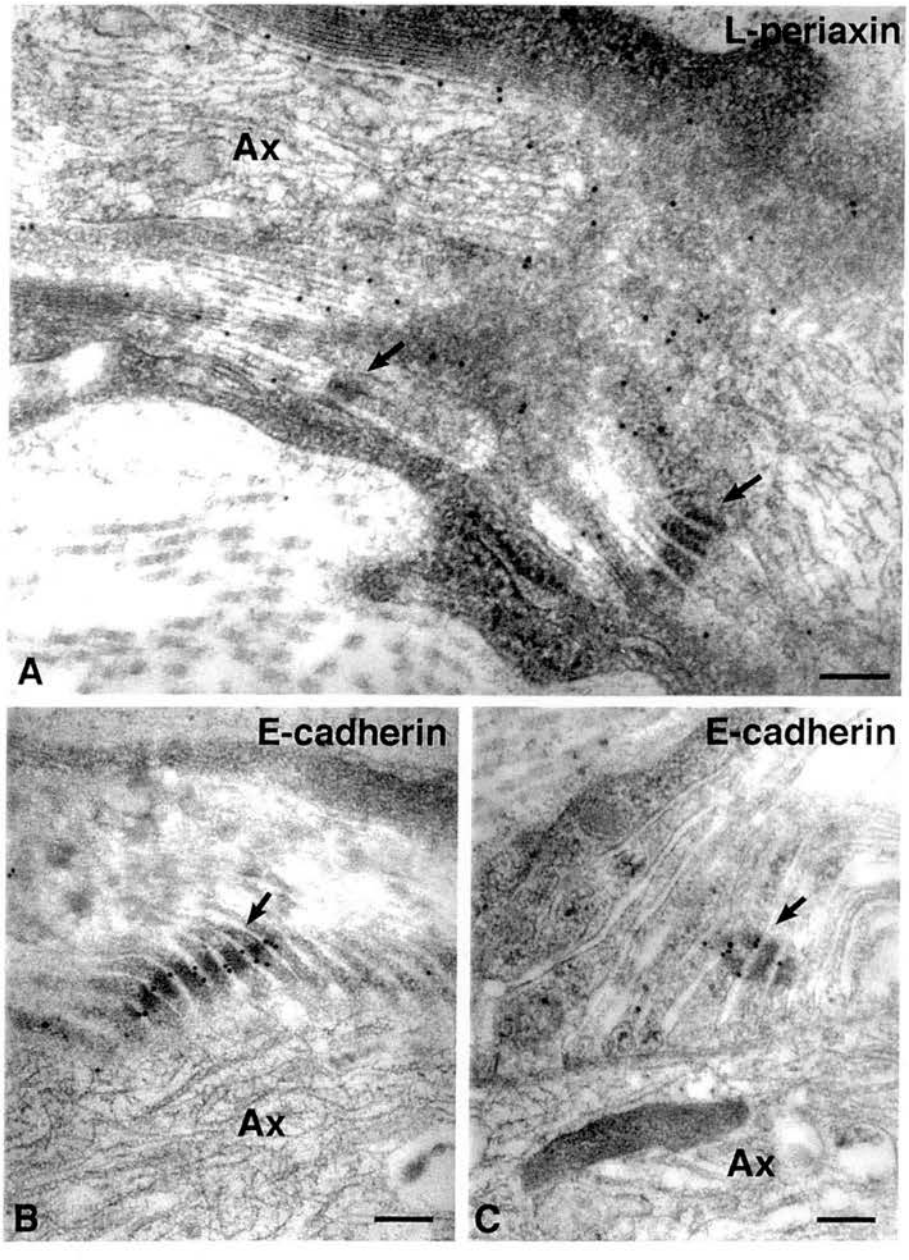

Figure 22. Adherens-type junctional complexes are labelled by antibodies against E-cadherin but not L-periaxin. In postnatal-day 8 sciatic nerve the electron-dense cytoplasmic plaques that are in register across paranodal loops are labelled with antibodies for E-cadherin (B and C) but not L-periaxin (A, arrow). Ax, axon. Bar, 200 nm.

3.1.2 L-periaxin is exclusively expressed by myelin-forming Schwann cells in peripheral nerve

There are two major types of Schwann cells in peripheral nerve, the myelin-forming Schwann cells which express P0, MBP, and MAG, and the non-myelin-forming which lack these proteins but express NGFR, GAP-43, L1, and N-CAM. To determine if L-periaxin is expressed in the non-myelin-forming population of Schwann cells, double-label immunofluorescence confocal microscopy was performed on cryosections of postnatal-day 1 mouse sciatic nerve with antisera to L-periaxin and GAP-43. As demonstrated in Fig 23, L-periaxin does not colocalize with GAP-43 indicating that it is not a constituent of non-myelin-forming Schwann cells.

To confirm this finding at the electron microscopic level immunogold stained sections of postnatal-day 4 rat sciatic nerve were examined. L-periaxin labelling was not detected over non-myelin-forming Schwann cells which ensheathe multiple axons (Fig. 24). Only Schwann cells in a one-to-one relationship with an axon, i.e. myelin-forming Schwann cells, were labelled. Consistent with these observations, the non-myelin-forming Schwann cells of the cervical sympathetic trunk also do not express L-periaxin (Scherer et al., 1995). The cervical sympathetic trunk is predominantly composed of non-myelin-forming Schwann cells (Aguayo et al., 1976).

3.1.3 L-periaxin localization in later postnatal peripheral nerve demonstrates a shift during development

When sections of adult mouse sciatic nerve were compared with sections from sciatic nerves of younger animals just after the most active phase of myelination, a change in the pattern of labelling was observed. Transverse cryosections of postnatal-day 20 (Fig. 25A and 25B) and adult (Fig. 25C and 25D) mouse sciatic nerves immunolabelled with anti-170pep1 (Fig. 25A, 25B, 25C, 25D)

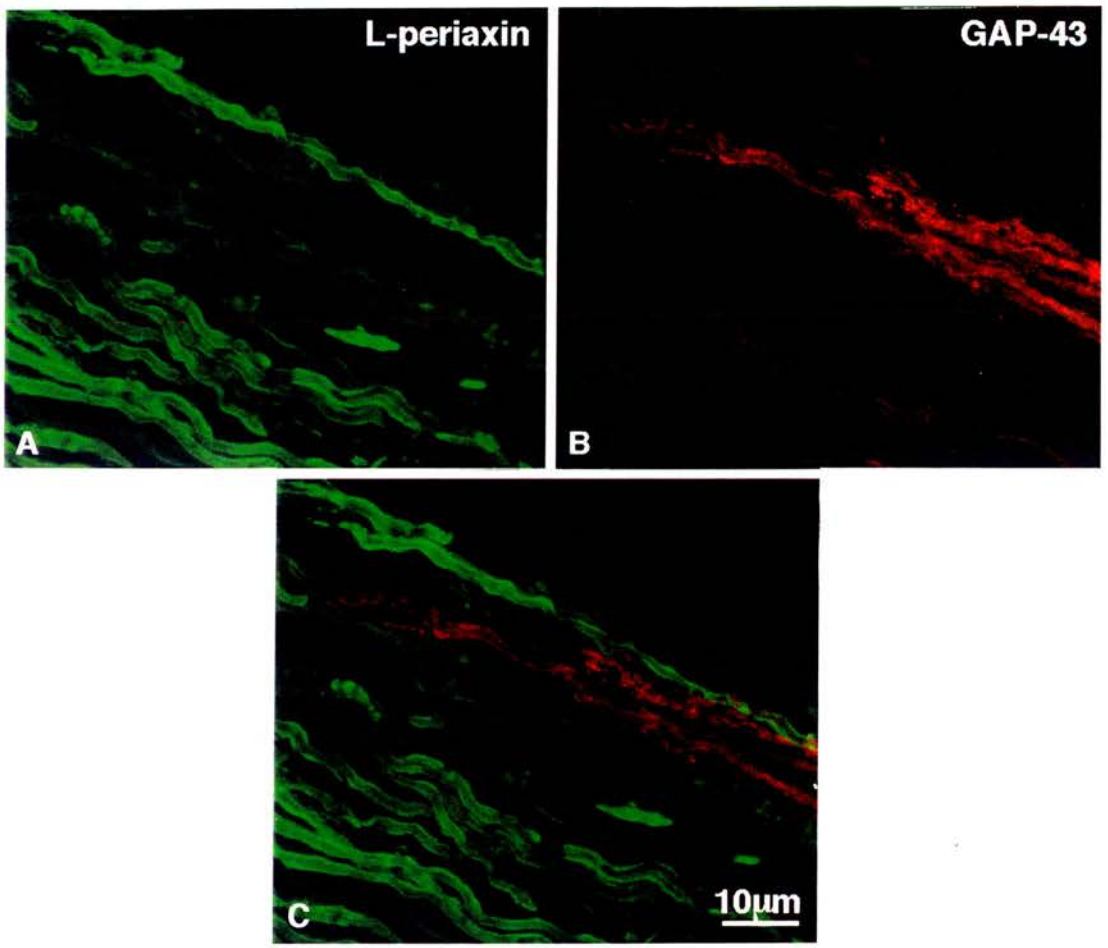

Figure 23. Immunofluorescence localization of L-periaxin and GAP-43 in mouse sciatic nerve. Longitudinal cryosections of postnatal-day 1 sciatic nerve were immunolabelled for L-periaxin (A, fluorescein) and GAP-43 (B, Texas red) to label non-myelin-forming Schwann cells and examined by confocal microscopy. The GAP-43 positive cells (B) do not colocalize with L-periaxin positive cells which is evident in the combined image (C) demonstrating that L-periaxin is exclusively expressed by myelin-forming Schwann cells in peripheral nerves. Bar, 10 µm.

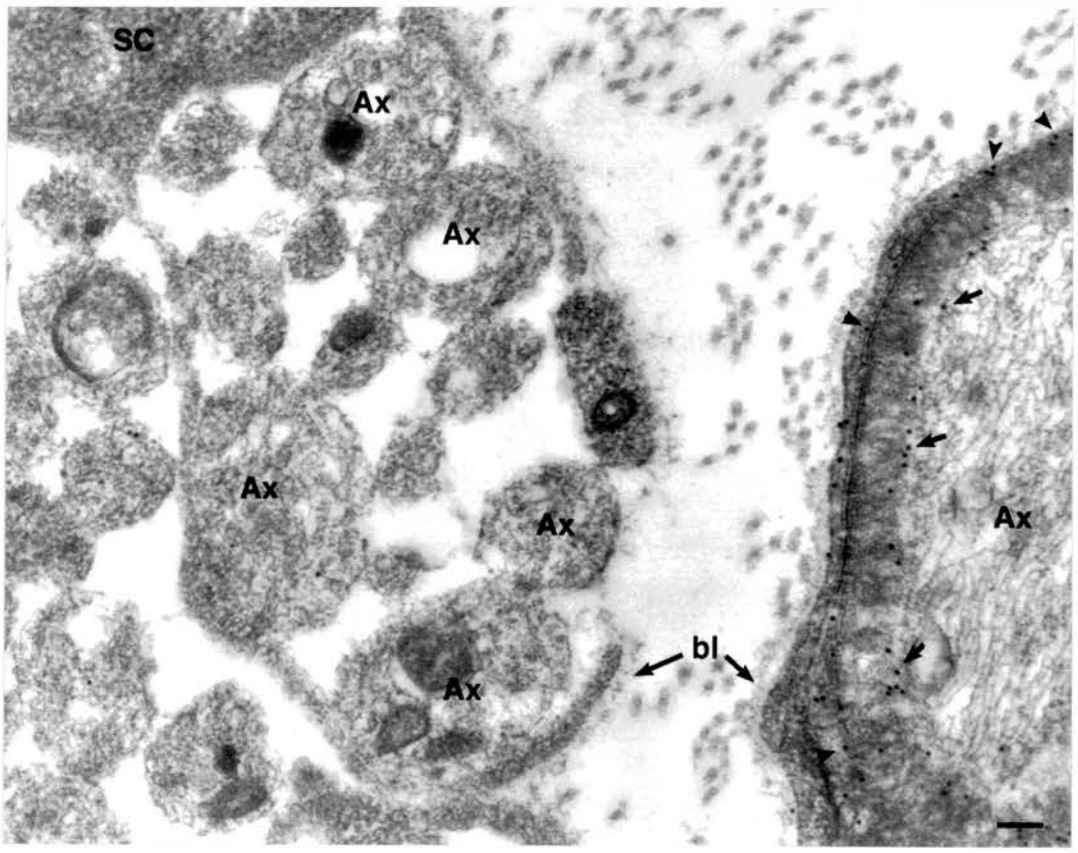

Figure 24. L-periaxin is exclusively expressed by myelin-forming Schwann cells. Immunogold electron microscopy of sections of postnatal-day 4 rat sciatic nerve for L-periaxin showed that non-myelin-forming Schwann cell processes which ensheathe multiple axons (left) are not labelled whereas the periaxonal (arrows) and abaxonal (arrowheads) membranes of the myelin-forming cell (right), are labelled. Ax, axon; bl, basal lamina. Bar, 200 nm.

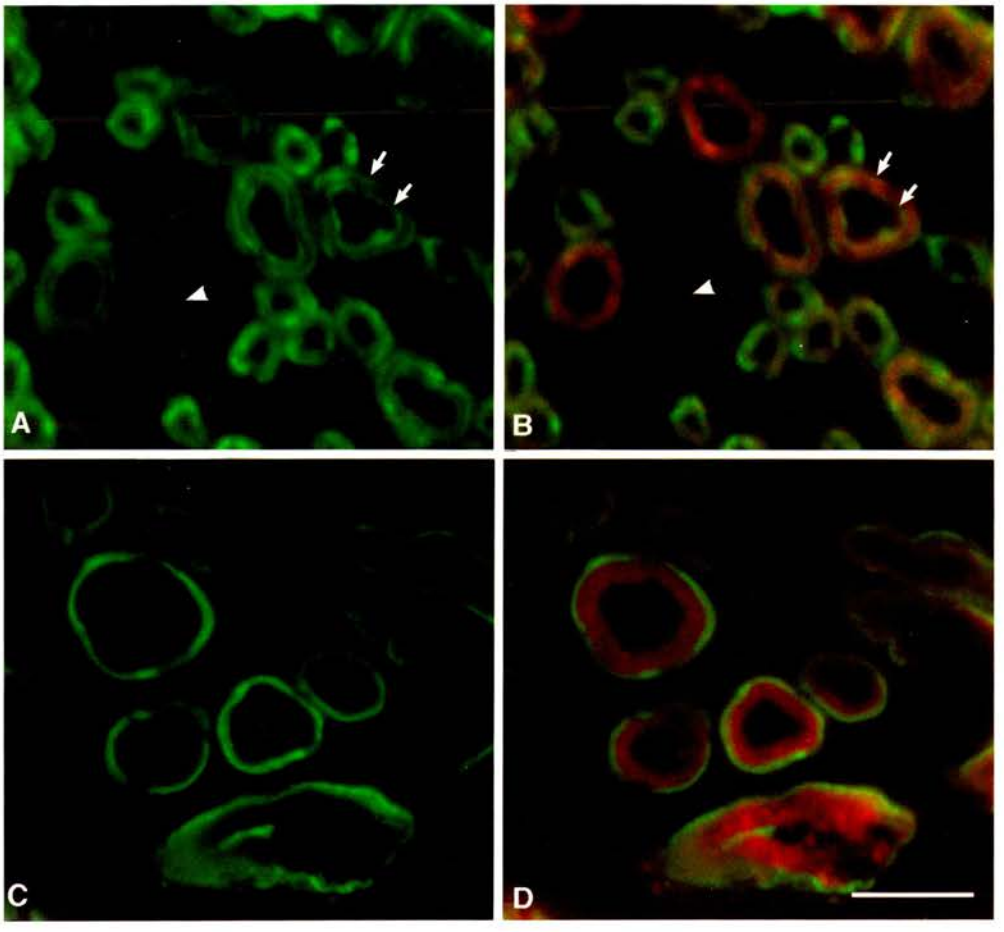

Figure 25. Immunofluorescence localization of L-periaxin and MBP in postnatal-day 20 and adult mouse sciatic nerve. (A, B) A transverse section of postnatal-day 20 mouse sciatic nerve, double-labelled for L-periaxin (A, fluorescein) and MBP (B combined image, Texas red). L-periaxin is localized to the plasma membrane (arrowhead) as well as the abaxonal and adaxonal membranes (arrows) of myelinating Schwann cells. MBP labeling is restricted to the myelin sheath and shows no co-localisation. (C, D) A transverse section of adult mouse sciatic nerve double-labelled for L-periaxin (C, fluorescein) and MBP (D combined image, Texas red) demonstrates that L-periaxin is concentrated in the abaxonal membranes and is absent from the adaxonal membranes as seen at postnatal-day 20. Bar, 5 μm.

and antisera directed against MBP (Fig. 25B, 25D) were examined by confocal immunofluorescence microscopy. In large diameter fibres at postnatal-day 20, L-periaxin immunostaining was observed in the adaxonal and abaxonal regions of the myelin sheath (Fig. 25A, 25B) which was visualized by immunolabelling of MBP (Fig. 25B). In small diameter fibres where the axons were thinly myelinated, the immunolabelling appeared to colocalize with MBP but this was probably a consequence of the resolution limitations of the microscope. In direct contrast in adult nerve, L-periaxin was concentrated in the abaxonal Schwann cell membranes (Fig. 25C, 25D) on the outside of the MBP^+ compact myelin sheath (Fig. 25D. This suggests that during development of peripheral nerves L-periaxin is lost from the periaxonal collar and becomes concentrated in the abaxonal region of the sheath.

The developmental shift in localization of L-periaxin was confirmed by immunogold electron microscopy. In postnatal-day 7 trigeminal nerve, L-periaxin was localized to the adaxonal and abaxonal membranes (Fig. 26A) but by postnatal-day 28 a striking redistribution in L-periaxin localization was observed (Fig. 26B). Antibodies against L-periaxin predominantly labelled the abaxonal membranes but not the adaxonal or periaxonal membranes, thus confirming the localization observed by light microscopy. Immunogold particles were detected on the Schwann cell plasma membrane and the outer membrane of the myelin sheath at both developmental ages investigated (Fig. 26A and 26B).

Earlier work on L-periaxin had suggested that the protein was cytoskeleton-associated due to its presence in the Triton X-100-insoluble fraction of PNS myelin. Since I had demonstrated L-periaxin in periaxonal membranes during development in the same region where Trapp and co-workers (Trapp et al., 1989b) have previously localized two components of the actin cytoskeleton, F-actin and spectrin, I wanted to investigate the localization of L-periaxin in relation to F-actin during postnatal nerve development.

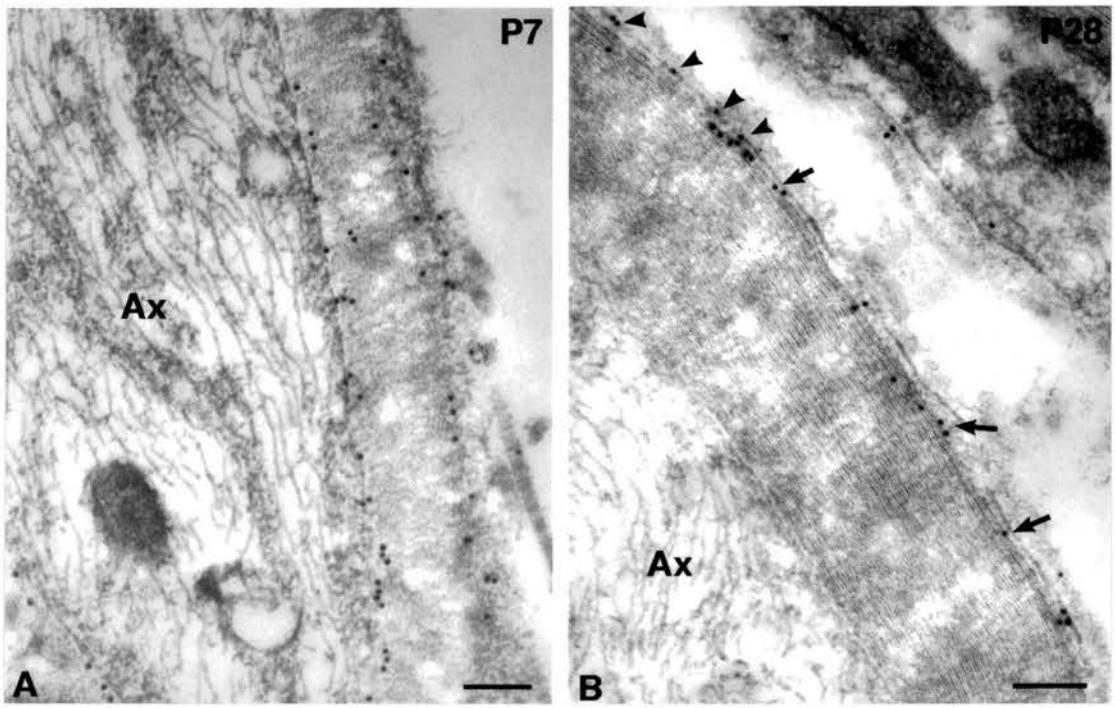

Figure 26. Comparison of L-periaxin immunogold localization in sections of postnatal-day 7 and postnatal-day 28 trigeminal nerve. (A) Immunogold particles are detected on abaxonal and adaxonal myelin membranes in postnatal-day 7 sections. (B) A concentration of gold particles on the abaxonal myelin membranes (arrows) demonstrates a redistribution of L-periaxin during nerve development. Gold particles are also evident on the plasma membrane (arrowheads).
Bar, 200 nm.

Using immunofluorescence to localize L-periaxin and rhodamine phalloidin binding to localize F-actin, stained cryosections from early postnatal rat sciatic nerve were compared with cryosections from adult nerve. At early ages, F-actin colocalizedwith L-periaxin in myelinated fibres (Fig. 27A, 27B, 27C). F-actin was also present in other locations presumed to be non-myelin-forming Schwann cells and the endothelial cells of blood vessels. The exact regions of co-localization around the myelin sheath in these young nerves were difficult to resolve at the light microscopic level but there appeared to be co-localization in the region apposing the axon and at the plasma membrane. In contrast, in the adult nerve L-periaxin and F-actin colocalized at the abaxonal and plasma membranes but not at the adaxonal membrane where F-actin is readily detectable (Fig. 27D, 27E, 27F). F-actin and L-periaxin are colocalized in the Schmidt-Lanterman incisures which are strongly labelled for both proteins. This indicates that during the early development of peripheral nerves L-periaxin localizes to all membrane/cytoplasmic channel regions where there are actin-cytoskeletal components but later in development this is not the case. Interestingly Trapp and co-workers demonstrated spectrin localization by immuno-gold microscopy (Trapp et al., 1989b) to the abaxonal membranes, adaxonal membranes and uncompacted cytoplasmic channels, the same regions where L-periaxin is localized indicating that L-periaxin may be associated with microfilaments.

Teased fibres from adult sciatic nerves were immunolabelled for L-periaxin and MAG to examine the cytoplasmic channels of Schmidt-Lanterman incisures and paranodal loops in the fully developed internode. L-periaxin colocalized with MAG in Schmidt-Lanterman incisures (Fig. 28A, 28B, 28C) by immunofluorescence confocal microscopy. There is some periaxin present at the paranodal regions but it is not closely associated with the MAG-positive paranodal loops (Fig. 28D, 28E, 28F). L-periaxin is also evident at the node of Ranvier which is most likely plasma membrane staining of Schwann cell microvilli (Fig. 28D).

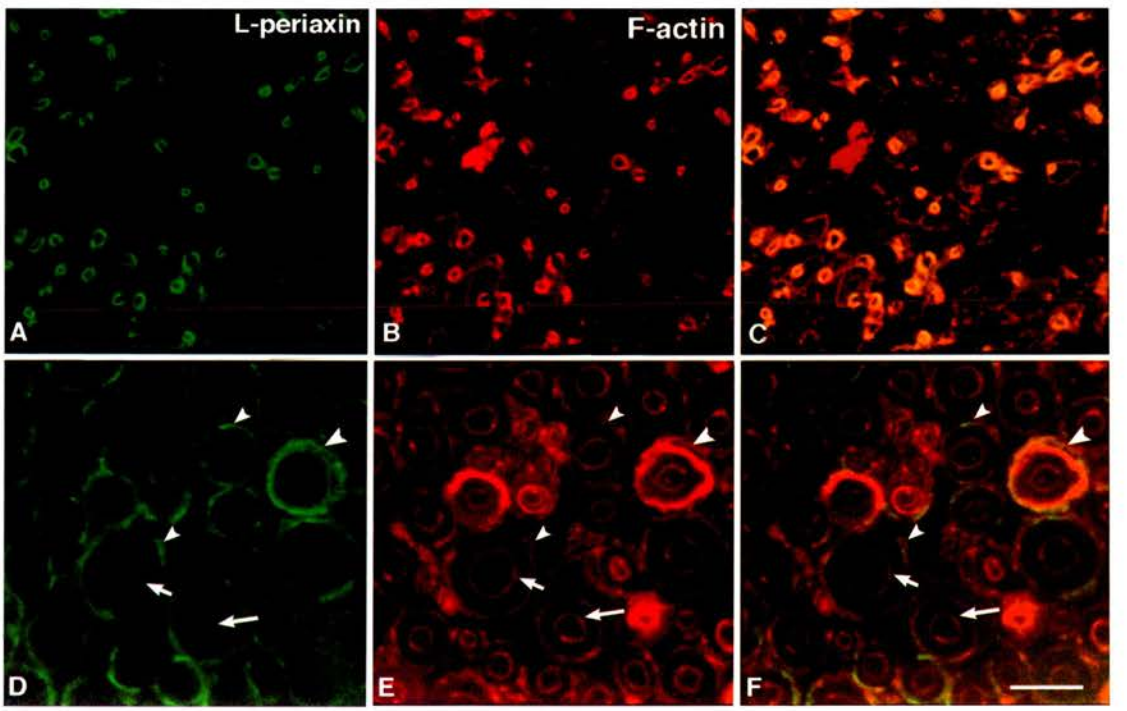

Figure 27. L-periaxin localization by immunofluorescence and F-actin localization by phalloidin binding during development and in the adult sciatic nerve. Transverse cryosections of postnatal-day 7 (A, B, C) and adult (D, E, F) rat sciatic nerve were immunolabeled for L-periaxin (fluorescein) and phalloidin (rhodamine) which binds to F-actin and examined by confocal microscopy. In postnatal-day 7 sections L-periaxin (A) and F-actin (B) colocalize (C, combined) whereas in adult sections F-actin is present in the periaxonal cytoplasm (E, arrows) but not L-periaxin (D, arrows). In abaxonal regions L-periaxin and F-actin colocalized (D, E, F, arrowheads).

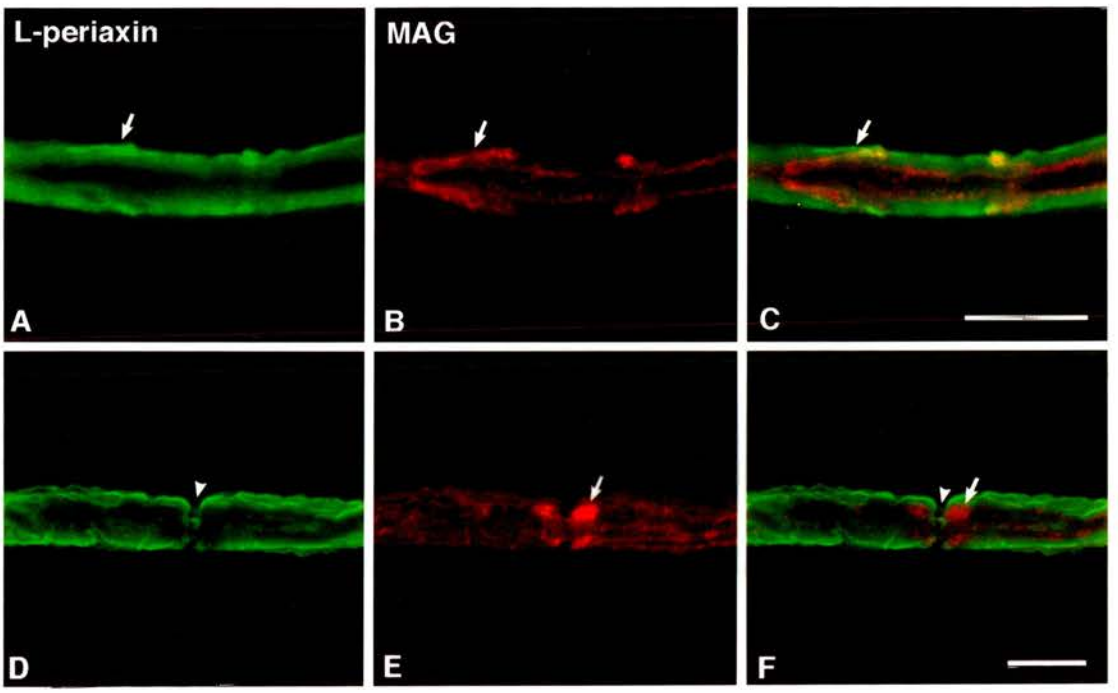

Figure 28. Colocalization of L-periaxin and MAG in Schmidt-Lanterman incisures and paranodes of teased fibres from adult mouse sciatic nerve. (A, B) Teased sciatic nerve fibres were double-labelled for L-periaxin (A and D, fluorescein) and MAG (B and E, Texas red) and examined by confocal microscopy. L-periaxin (A) and MAG (C) are colocalized (C, combined image) in the Schmidt-Lanterman incisures (arrows) whereas the paranodal loops which are labelled for MAG (E, arrow) do not colocalize with L-periaxin (F). L-periaxin labels the plasma membrane of Schwann cell microvilli at the node (arrowhead; D and F). Bar, 200 nm.

3.1.4 L-periaxin is not exposed on the Schwann cell surface

From hydrophobicity plots of the deduced amino acid sequence, L-periaxin is not predicted to possess transmembrane domains and is therefore not believed to be an integral membrane protein (Gillespie et al., 1994). In order to confirm that L-periaxin is not exposed at the extracellular surface of the Schwann cell, immunofluorescence on unpermeabilized cells and cell-surface biotinylation experiments were performed.

Transfected 33B cells permanently expressing L-periaxin were prepared by liposome-mediated transfection (method in section 2.4.1). Colonies were isolated and expanded and clone 25 was selected which expressed high levels of L-periaxin protein as detected by immunofluorescence screening. Cells from clone 25 were metabolically labelled with [^{35}S] methionine and immuneprecipitated with anti-170pep1. A protein of the same M_r as L-periaxin was obtained (Fig 29A) demonstrating that the stable transfectants were expressing full length protein.

Schwann cells from short-term cultures and cells from 33B clone 25 permanently expressing L-periaxin were immunostained without detergent permeabilization to determine if L-periaxin was exposed on the cell surface. Four different L-periaxin antisera were used, p170, 170pep1, NTerm, CTerm, which recognize different regions of the protein (see Materials and Methods, Table 1). No staining was detected whereas labelling occurred with all four antibodies if the cells were first permeabilized with Triton X-100 (data not shown).

The surface of cells from clone 25 was biotinylated (method in section 2.4.5) to confirm the result by immunofluoresence. No biotinylated cell surface proteins were immuneprecipitated with anti-170pep1 after probing with streptavidin HRP (Fig. 29B lane 1). When cells from clone 25 were first permeabilized with Triton X-100, biotinylated periaxin was detected by immuneprecipitation with anti-170pep1 followed by probing with streptavidin HRP (Fig. 29B lane 2). These data confirm that L-periaxin is not exposed on the cell surface.

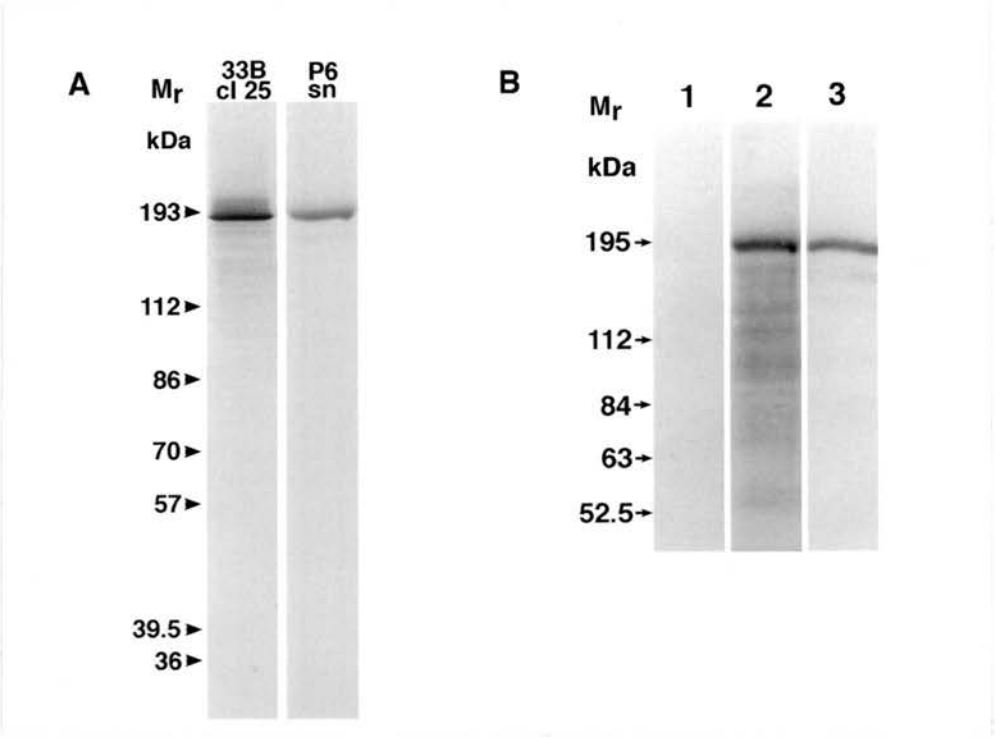

Figure 29. Cell surface biotinylation of 33B cells permanently expressing L-periaxin. 33B cells (clone 25) were examined for protein expression prior to cell surface biotinylation studies. **(A)** 33B cells (clone 25) and postnatal-day 6 sciatic nerve were metabolically labelled with [^{35}S]methionine, solubilized in SDS, immunoprecipitated with anti-170pep1 and analyzed by SDS-PAGE. Proteins of the same M_r were obtained from both 33B cells and sciatic nerve. **(B)** Cells from clone 25 were biotinylated before (Lane 1) and after permeabilization with Triton X-100 (Lane 2), immuneprecipitated with anti-170pep1, separated by SDS-PAGE , and probed with steptavidin HRP (Lane 1 and 2) or anti170pep1 (Lane 3). No biotinylated cell surface proteins were immuneprecipitated with anti-170pep1 (Lane A). When cells were permeabilized before biotinylation then immuneprecipitated with anti-170pep1 and probed with either streptavidin HRP (Lane 2) or anti-170pep1 (Lane 3), proteins of the same M_r are apparent. Molecular mass standards are indicated on the left.

3.1.5 The S-periaxin isoform is expressed in the Schwann cell cytoplasm in neonatal sciatic nerve

Immunofluorescence analysis of postnatal-day 20 murine sciatic nerve had demonstrated that S-periaxin was localized to the Schwann cell cytoplasm (Dytrych et al., 1998). In order to determine the localization of S-periaxin in neonatal sciatic nerve, teased fibres from postnatal-day 1 mouse sciatic nerve were prepared and immunolabelled with a specific antibody to S-periaxin which was raised against a synthetic peptide corresponding to the C-terminal 23 amino acids unique to mouse S-periaxin, anti-SPeri (Dytrych et al., 1998), and with an antibody to the 160 kDa neurofilament protein NF-M to immunolabel the axons. Teased fibres were also immunolabelled with antibodies to L-periaxin, anti-170pep1, and NF-M for comparison. L-periaxin was expressed in the membranes apposing the NF-M positive axon and on the plasma membrane (Fig. 30C, 30D). In contrast, S-periaxin was diffusely expressed in the Schwann cell cytoplasm (Fig. 30A, 30B). In some fibres there was a concentration of S-periaxin in discrete regions of myelinating fibres (Fig. 30E) which colocalized with MAG (Fig. 30F) suggesting that these regions may be where the cytoplasmic channels of Schmidt-Lanterman incisures will develop.

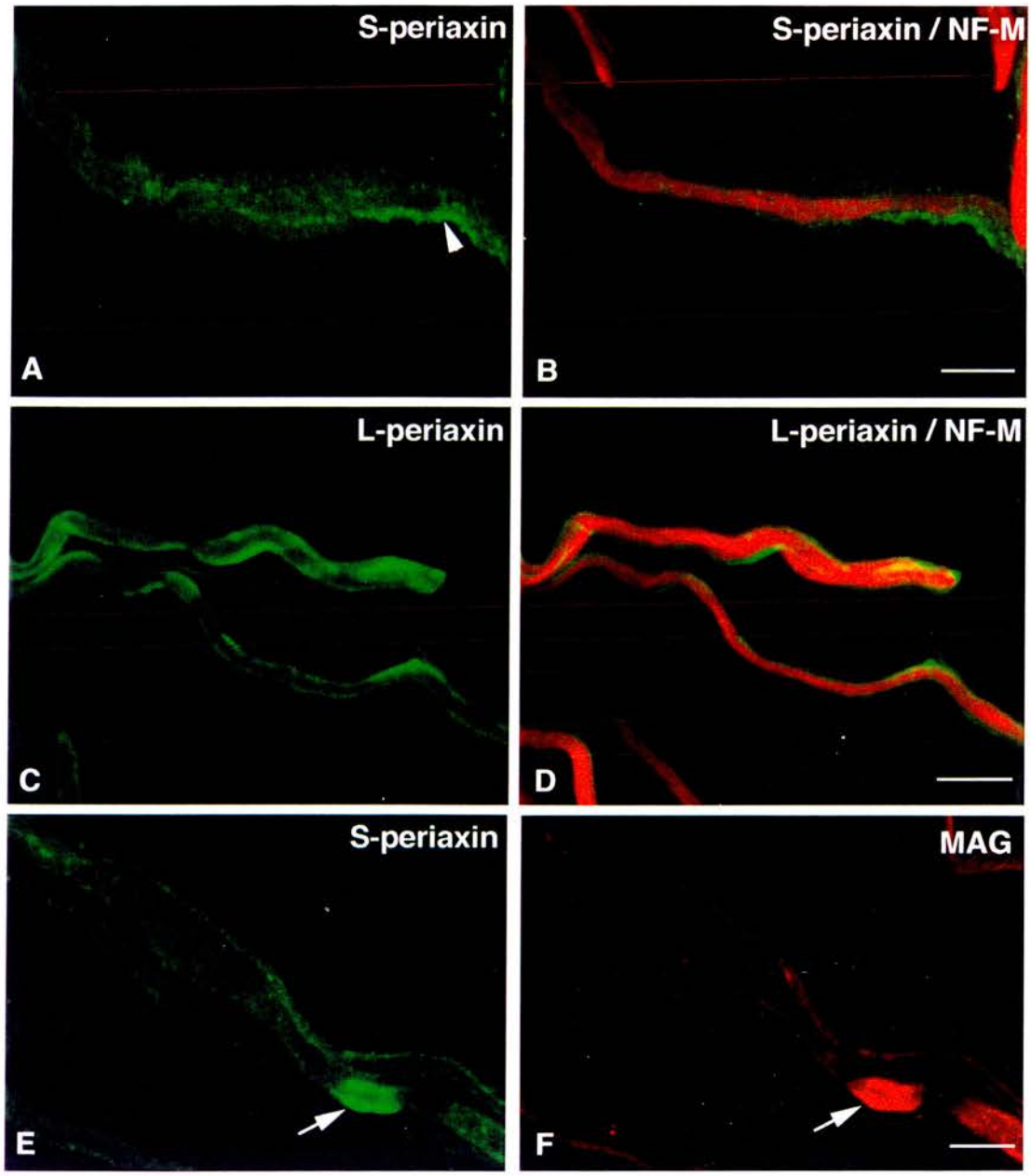

Figure 30. Comparison of the localization of S-periaxin and L-periaxin in teased fibres of postnatal-day 1 mouse sciatic nerve. Teased fibres were double-labelled for S-periaxin (A, fluorescein) and NF-M (B, Texas red; combined image) or L-periaxin (C, fluorescein) and NF-M (D, Texas red; combined image) and examined by confocal microscopy. S-periaxin (A) is diffusely distributed within the Schwann cell cytoplasm with concentrations (arrowhead) around the axon labelled by NF-M. In contrast, L-periaxin (C) is concentrated in the membranes ensheathing the axon and at the plasma membrane. When immunofluorescence was performed on teased fibres double-labeled for S-periaxin (E, fluorescein) and MAG (F, Texas red) discrete concentrations of S-periaxin colocalized with MAG (arrows). Bar, 5 μm.

3.1.6 Summary

In this chapter I have demonstrated that L-periaxin is expressed by myelin-forming Schwann cells in discrete domains that are developmentally regulated. In early postnatal nerve it is concentrated in the adaxonal and abaxonal membranes, but as the myelin sheath matures, L-periaxin became predominantly localized to the abaxonal Schwann cell membrane. L-periaxin is also localized to uncompacted regions of the sheath. I have confirmed that L-periaxin is not exposed on the cell surface by cell surface biotinylation but is closely associated with the cytoplasmic face of the Schwann cell plasma membrane by its localization with immunogold. I have also shown that both isoforms of periaxin are expressed at an early stage in the postnatal peripheral nerve and that S-periaxin is present throughout the Schwann cell cytoplasm. Both proteins are excluded from the myelin sheath after compaction.

3.2 EMBRYONIC EXPRESSION

Schwann cells are derived from the neural crest. The neural crest is a group of migratory cells which emerges from the neuroepithelium as it folds to form the dorsal neural tube. Crest cells give rise to a diverse population of cell types of which the Schwann cell is but one (LeDouarin, 1982). In the rat hindlimb, embryonic Schwann cell development spans about a week from approximately E14 to birth at E21. In the murine PNS the period corresponds to E12 to E18 since Schwann cell differentiation occurs earlier in the mouse. Cells isolated from E14 rat hind limb nerves have a distinct phenotype intermediate between neural crest cells and Schwann cells which has been called the Schwann cell precursor (Jessen et al., 1994). At around E16 in the rat sciatic nerve the precursor cells differentiate to form embryonic Schwann cells (Jessen et al., 1994; Mirsky and Jessen, 1996) which in turn become either myelin-forming or non-myelin-forming Schwann cells in the mature PNS.

The major peripheral myelin protein P0 has been shown to be expressed very early in the Schwann cell lineage of chickens (Bhattacharyya et al., 1991) and rats (Zhang et al., 1995) and more recently Lee and co-workers (Lee et al., 1997). demonstrated P0 mRNA and low levels of protein in a subpopulation of migrating neural crest cells, Schwann cell precursors, and embryonic Schwann cells in the rat. Both protein products of the *periaxin* gene are expressed in neonatal rodent peripheral nerve, therefore I wanted to investigate whether the gene is expressed during embryonic development because L-periaxin protein expression appears to precede that of other myelin proteins both in the neonate and during remyelination after sciatic nerve crush (Scherer et al., 1995).

3.2.1 L-periaxin mRNA and protein is expressed in the embryonic sciatic nerve

Periaxin mRNA expression was examined by *in situ* hybridization on transverse cryo-sections though the lumbro-sacral regions of E12.5 to E16.5 mouse embryos which included the developing sciatic nerves. The probe recognized sequences (nts 1500-2500) present in both the 4.6 and 5.2 kb mRNAs. The only isoform-specific sequence, 0.6 kb, was unique to S-periaxin mRNA. Antisense [^{35}S]-labelled riboprobes generated signals after 2 weeks exposure whereas in the same period the sense [^{35}S]-labelled riboprobes generated no signal above background. Serial sections probed for P0 mRNA were also examined for comparison.

At E12.5, at a time when all of the cells in the hind limb nerves would be Schwann cell precursors, no periaxin labelling was observed (data not shown). A low level signal for periaxin mRNA was first detected in E13.5 sections (Fig 31A). The positive cells were in the developing sciatic nerve. By E14.5 there were more cells labelled with a stronger signal (Fig. 31C) indicating that periaxin mRNAs are first expressed in embryonic Schwann cells after they differentiate from precursor cells. In addition to peripheral nerve labelling, there was a discrete layer of labelled cells in the body wall which was more evident at E15.5 (Fig. 31E). The sense control had no signal (Fig. 31F). By comparison, P0 mRNA expression was strong at E13.5 (Fig. 31B). A strong signal was seen in the dorsal root ganglia, the dorsal and ventral roots, and the peripheral nerves including the developing sciatic nerve (Fig. 31B, 31D).

The expression of L-periaxin protein in embryonic sciatic nerves was examined by immunofluorescence on transverse cryosections through the trunk of mouse embryos. Double-label immunofluorescence was performed with anti-170pep1 and NF-M as an axonal marker to identify the sciatic nerve. The vast majority of cells in E13.5 sciatic nerve were L-periaxin negative although a few positive cells were observed in some embryos (Fig. 32A). Many L-periaxin positive

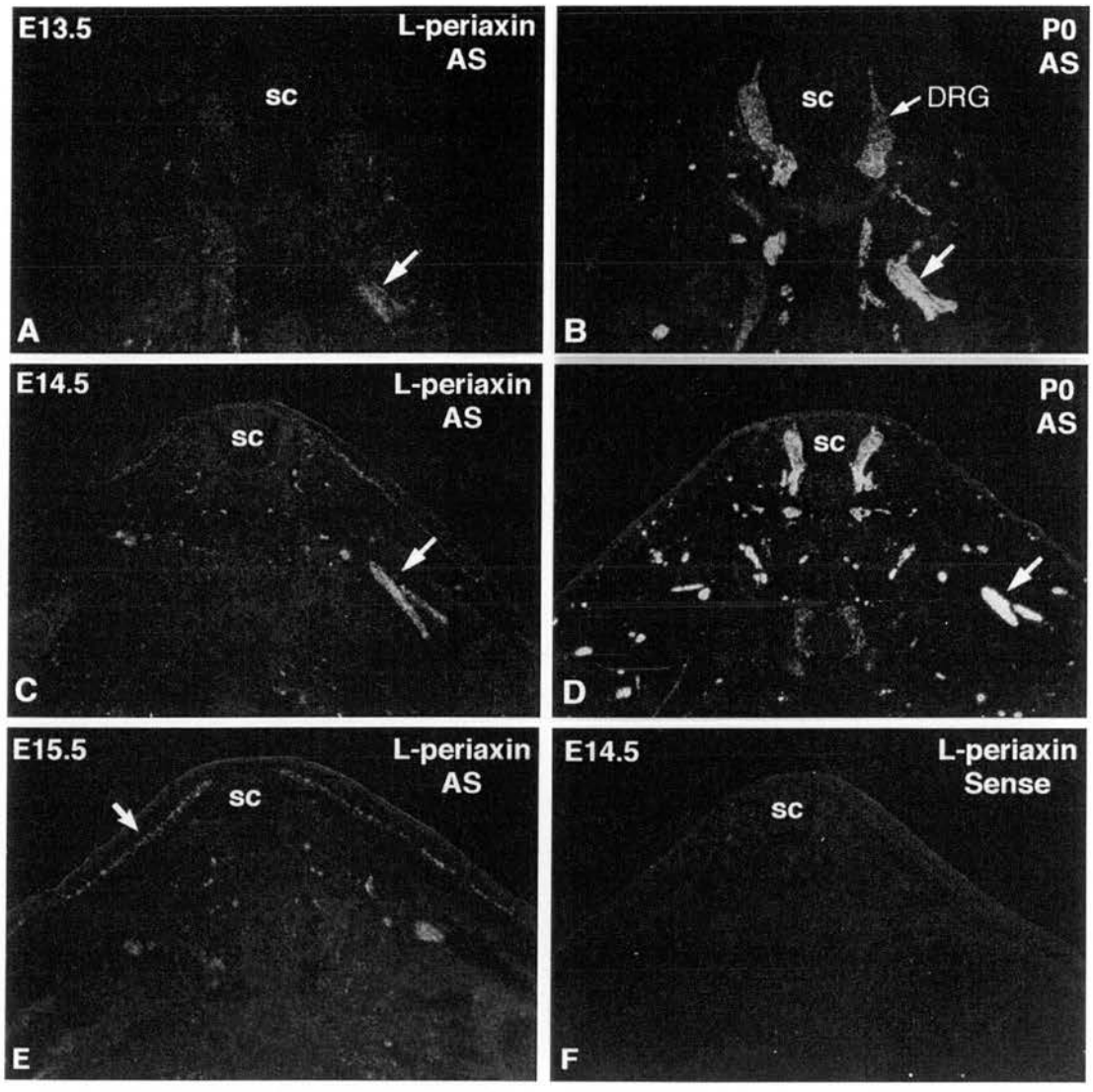

Figure 31. Comparison of periaxin and P0 mRNA expression by *in situ* hybridization during embryonic development. *In situ* hybridization was performed on transverse trunk sections from mouse embryos at E13.5 (A, B), E14.5 (C, D, F), and E15.5 (E) using antisense riboprobes for periaxin (A, C, E,) and P0 (B, D) and a sense riboprobe for periaxin (F). Periaxin mRNA is first detected in a few cells in E13.5 developing sciatic nerve (A, arrow) but by E14.5 more cells expressing periaxin mRNA are apparent (C, arrow). A discrete row of cells expressing periaxin mRNA is seen in the body wall in E15.5 sections (E, arrow). In comparison, P0 mRNA expression is strong in the sciatic nerve (arrow), dorsal roots, dorsal root ganglia, and other nerve trunks in E13.5 (B) and E14.5 (D) sections. sc, spinal cord; DRG, dorsal root ganglion; AS, anti-sense.

Figure 32. Immunofluorescence localization of L-periaxin in developing sciatic nerves of mouse embryos. Transverse cryosections through the trunks of E13.5, E14.5 and E17.5 embryos were double-labeled with anti-170pep1 (A, C, E; fluorescein) and NF-M (B, D, F; Texas red) to label axons and examined by confocal microscopy. Very few L-periaxin labeled cells are present in the sciatic nerve at E13.5 (A) where most of the cells are Schwann cell precursors. By E14.5 many L-periaxin labelled cells are apparent (C) in the NF-M positive sciatic nerve (D). The L-periaxin immunoreactivity is concentrated in the nuclei but by E17.5, L-periaxin is concentrated at the Schwann cell membranes (E) ensheathing axons (F). Bar, 50 μm.

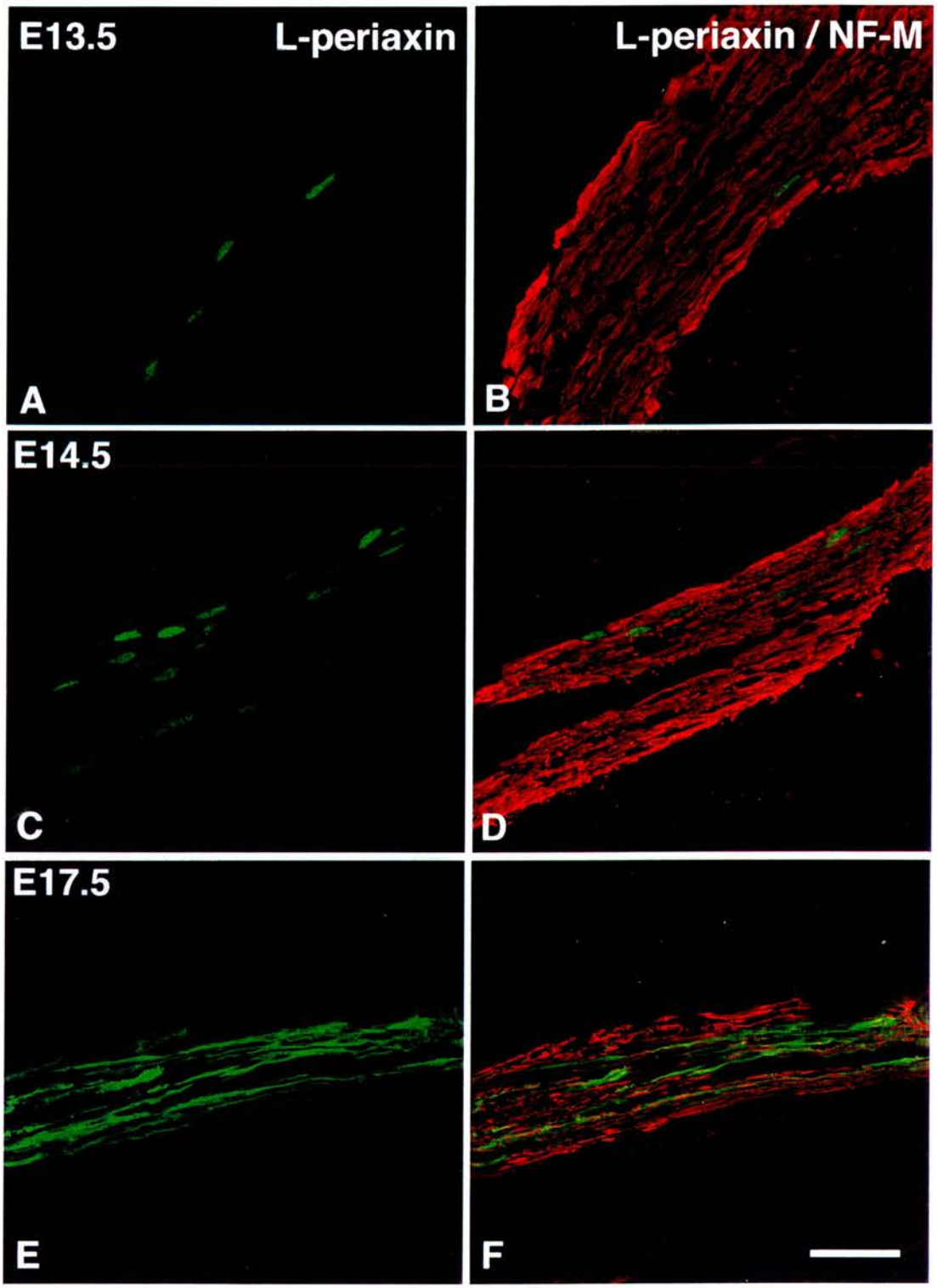
E13.5
L-periaxin
L-periaxin / NF-M
A
B
E14.5
C
D
E17.5
E
F

cells were observed at E14.5 (Fig. 32C). The most intense labelling was seen in the nuclei although cytoplasmic staining was also detected. The same staining pattern persisted until E17.5 where there was an up-regulation of membrane associated L-periaxin and no nuclear immunolabelling (Fig. 32E). Therefore, protein expression correlates well with mRNA expression demonstrating that L-periaxin is first expressed in the early embryonic Schwann cell immediately after differentiation from its precursor cell.

3.2.2 S-periaxin mRNA is first expressed at postnatal-day 1

The riboprobe used for the previously described *in situ* hybridization studies recognized both mRNA species, the 4.6 kb which encodes L-periaxin and the 5.2 kb mRNA which encodes S-periaxin. Specific S-periaxin mRNA expression was examined by *in situ* hybridization on transverse cryosections though the lumbro-sacral region of E16.5 mouse embryos which included the sciatic nerve, E17.5 and postnatal-day 1 sciatic nerves, and postnatal-day 2 hindlimb. The [^{35}S]-labelled riboprobe used recognized a sequence present in a 0.6 kb region of the 5.2 kb mRNA unique to S-periaxin. Antisense [^{35}S]-labelled riboprobes generated signals after 2 weeks exposure whereas the sense [^{35}S]-labelled riboprobes generated no signal above background.

There was no signal above background with longer exposure of 3 weeks in E16.5 embryo sections (Fig. 33A). The first positive cells were observed in postnatal-day 1 mouse sciatic nerve (Fig. 33B) sections demonstrating that S-periaxin expression occurs later than the L-periaxin isoform. These data also demonstrate that the early embryonic mRNA which was observed with a [^{35}S]-labelled riboprobe which recognizes both mRNAs was detecting the 4.6 kb mRNA exclusively in those early embryonic Schwann cells and body wall cells.

Ultrastructural examination of embryonic Schwann cells in E16.5 mouse sciatic nerves (Fig. 34A) when L-periaxin is expressed demonstrates that all of the

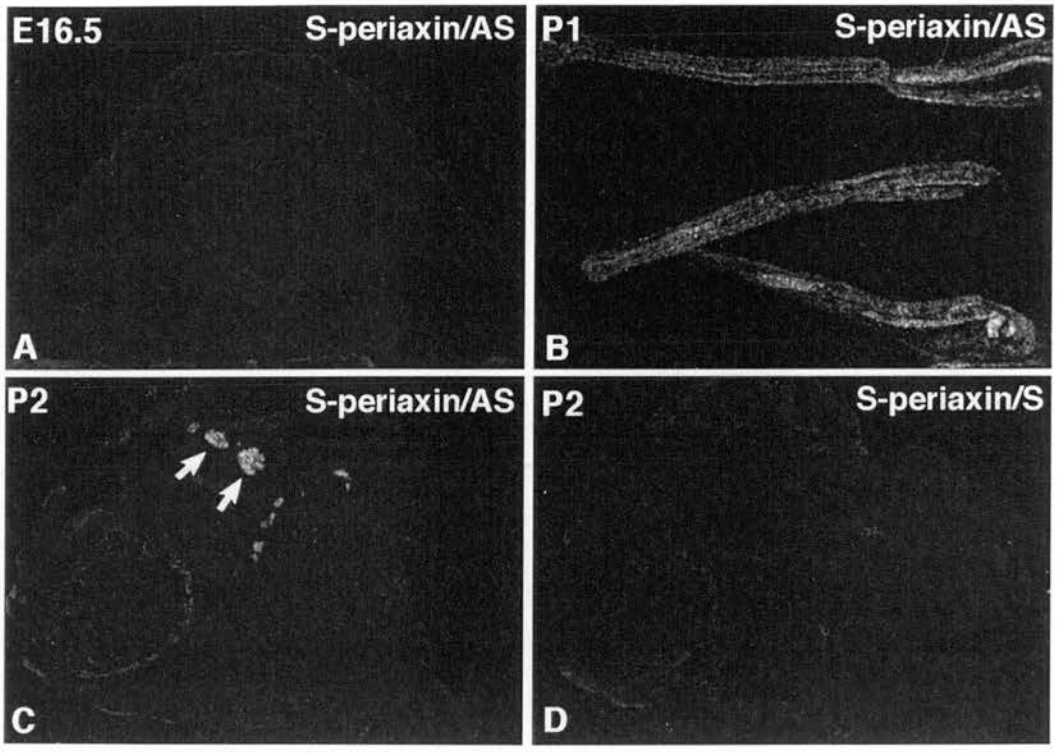

Figure 33. S-periaxin mRNA expression in murine sciatic nerve by *in situ* hybridization. *In situ* hybridization was performed on transverse cryosections through the trunk of E16.5 embryos (A), postnatal-day 1 (P1) sciatic nerve cryosections (B) and postnatal-day 2 transverse hindlimb cryosections (C, D) using an antisense riboprobe unique to S-periaxin (A, B, C) and a sense control (D). In cryosections through E16.5 sciatic nerve there was no signal for S-periaxin mRNA (A). S-periaxin mRNA is first detected in P1 sciatic nerve (B). In P2 hindlimb sections, the sense riboprobe (D) generated no signal above background when compared to a serial section using the antisense riboprobe (C). AS, anti-sense; S, sense. Bar, 200 μm.

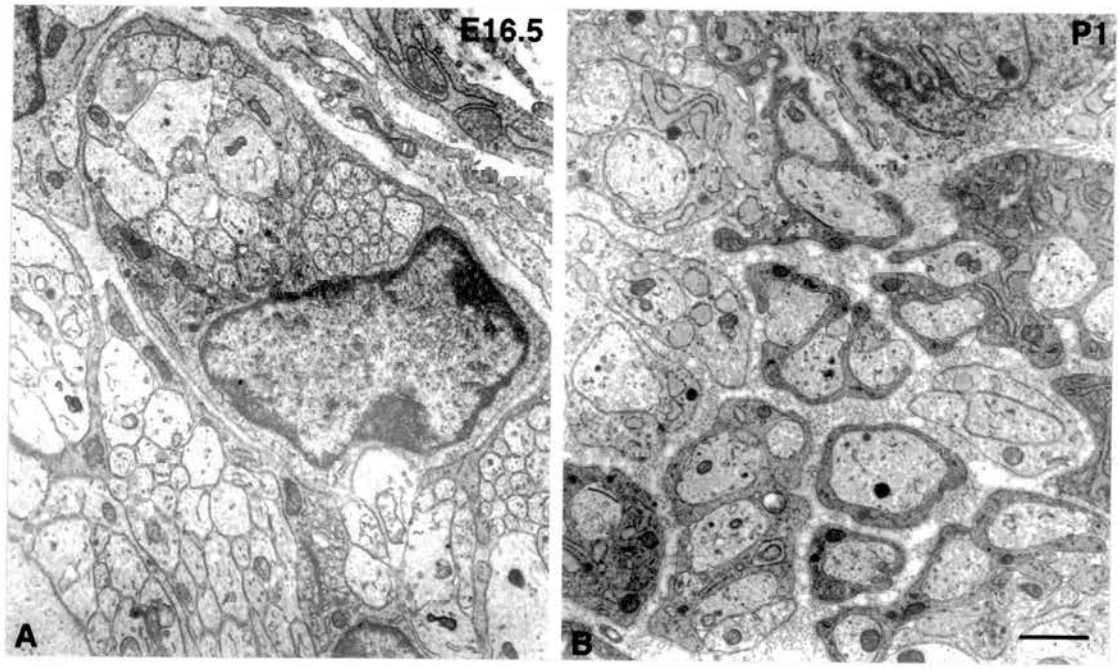

Figure 34. Electron micrographs of transverse sections from E16.5 and postnatal-day 1 sciatic nerve. (A) Embryonic Schwann cells in E16.5 sciatic nerves ensheathe multiple small axons. (B) Schwann cells in postnatal-day 1 sciatic nerve are mainly in a1:1 relationship with axons. Bar, 1 μm.

Schwann cells ensheathe multiple small axons whereas at postnatal-day 1 when S-periaxin is expressed, many Schwann cells are observed in 1:1 relationships with axons (Fig 34B).

3.2.3 L-periaxin expression in embryonic Schwann cells in a predominantly non-myelinating nerve

P0, the major PNS myelin protein, was shown to be expressed very early in development, in a population of neural crest cells, Schwann cell precursor cells and embryonic Schwann cells (Lee et al., 1997). P0 mRNA was also present in most of the embryonic Schwann cells of the rat cervical sympathetic trunk and was then down-regulated during development (Lee et al., 1997). The cervical sympathetic trunk in the adult is composed of around 95% non-myelin-forming Schwann cells (Lee et al., 1997). P0 was also expressed in satellite cells in the dorsal root ganglia. Therefore, P0 is expressed in all embryonic Schwann cells regardless of their fate.

Since L-periaxin is only expressed in myelin-forming Schwann cells in the neonate and is expressed in embryonic Schwann cells long before they form a 1:1 relationship with an axon, I wanted to determine if L-periaxin was a very early marker of the myelin-forming Schwann cell or like P0 was expressed in all embryonic Schwann cells.

In order to determine whether all embryonic Schwann cells express L-periaxin, dissociated cell cultures isolated from embryonic mouse sciatic nerves were prepared and immunolabelled with an embryonic Schwann cell marker, to label all Schwann cells, and L-periaxin. Embryonic Schwann cells express the proteins S100 (Jessen et al., 1994) and O4 (Mirsky et al., 1990). Since several monoclonal antibodies to S100 protein did not immunostain mouse Schwann cells reliably, the monoclonal antibody O4, which recognizes among other things, the lipid antigen sulfatide on embryonic, neonatal, and adult myelin-forming and non-myelin-forming Schwann cells in the rat (Mirsky et al., 1990), was chosen for these

studies. Short-term cultures were used because L-periaxin is down-regulated with other myelin proteins after longer times in culture in the absence of growth factors or agents that elevate intracellular cAMP (Morgan et al., 1991; Shuman et al., 1988). Sciatic nerves were removed from E16.5 mouse embryos, dissociated, and plated on coverslips. After the cells had adhered to the coverslip and spread, they were labelled with O4 antibody. The coverslips were fixed and immunolabelled with anti-170pep1 followed by secondary antibodies (Fig. 35A, 35B, 35C, 35D). Positive cells were counted from 3 experiments which showed that 88.6 ± 3.7% of the O4 positive cells expressed L-periaxin. Therefore 11.4% of the Schwann cells did not express L-periaxin. Two possible explanations exist. One possibility is that L-periaxin is expressed only in Schwann cells destined to be myelin-forming and the 11.4% L-periaxin$^-$ O4$^+$ cells may represent a population of cells destined to remain non-myelin-forming. Another possibility is that L-periaxin is expressed in all embryonic Schwann cells at some time point during development whether they are destined to myelinate later or not and in the window of time in which the counts were done there were cells which had not yet begun to express the protein.

To distinguish between these two possibilities, L-periaxin expression was examined in the cervical sympathetic trunk where most of the Schwann cells in the adult are non-myelin-forming. In transverse sections through E16.5 mouse embryos very few L-periaxin positive cells were observed (Fig. 36A and 36C) when compared with serial sections labelled with a polyclonal antibody directed against S100 (Fig. 36D and 36F). In contrast, in the vagus nerve, which is myelinated in the mature animal, many L-periaxin positive Schwann cells were observed (Fig. 36A and 36C). When E16.5 cervical sympathetic trunks were removed and longitudinally cryosectioned, and immunolabelled for L-periaxin in combination with propidium iodide, which binds to DNA and thus labels all nuclei, more L-periaxin positive cells were observed (Fig. 37A, 37C). The labelled cells were not distributed evenly in the trunk (Fig. 37D, 37F) and areas with no positive labelling

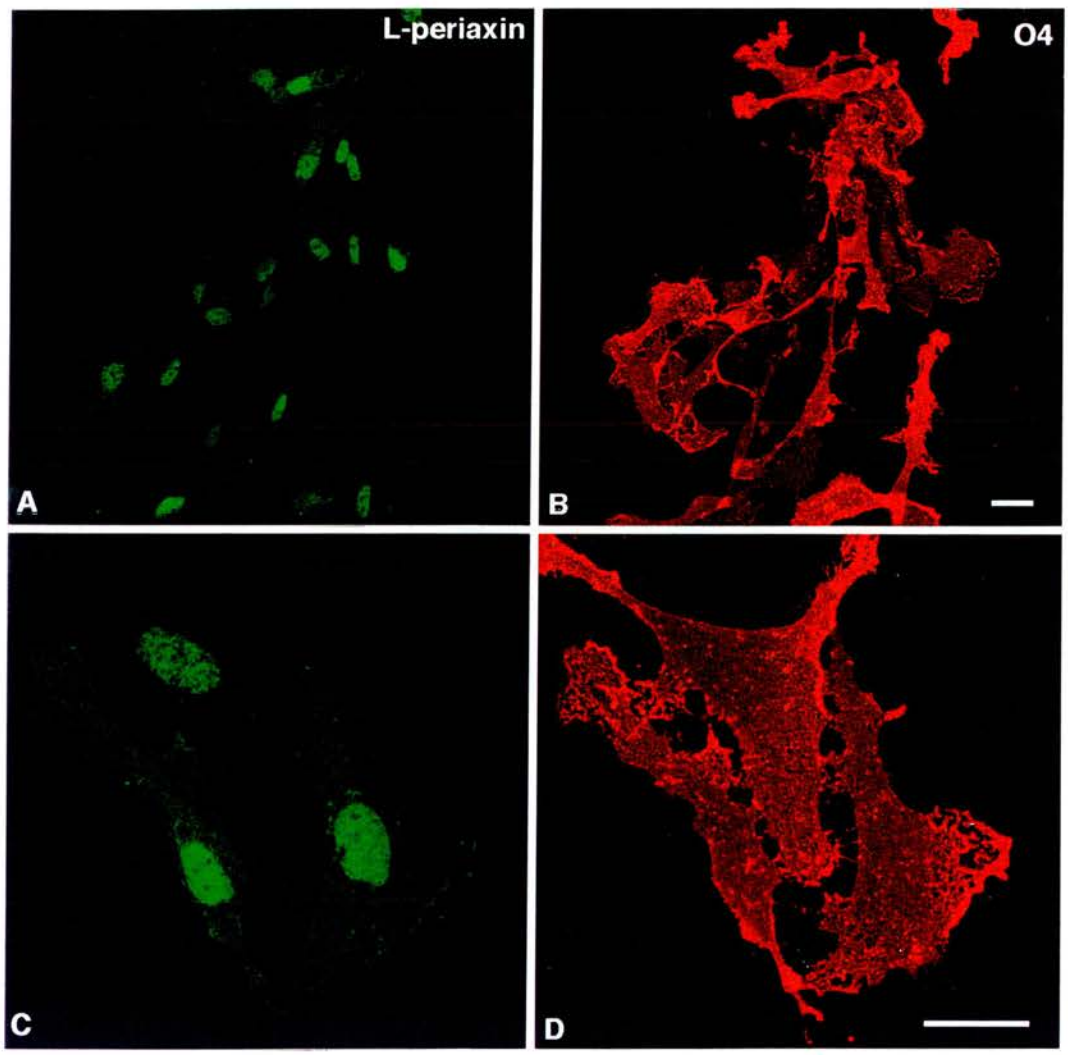

Figure 35. Immunofluorescence localization of L-periaxin and O4 in dissociated E16.5 sciatic nerve cultures. Sciatic nerves were dissociated, placed in short-term culture and immunolabeled with O4 (B, D; Texas red) as a marker for embryonic Schwann cells and L-periaxin (A, C; fluorescein). Most of the O4 positive cells are L-periaxin positive. L-periaxin labeling is predominantly nuclear but some cytoplasmic labeling is apparent (C). Bar, 20 μm.

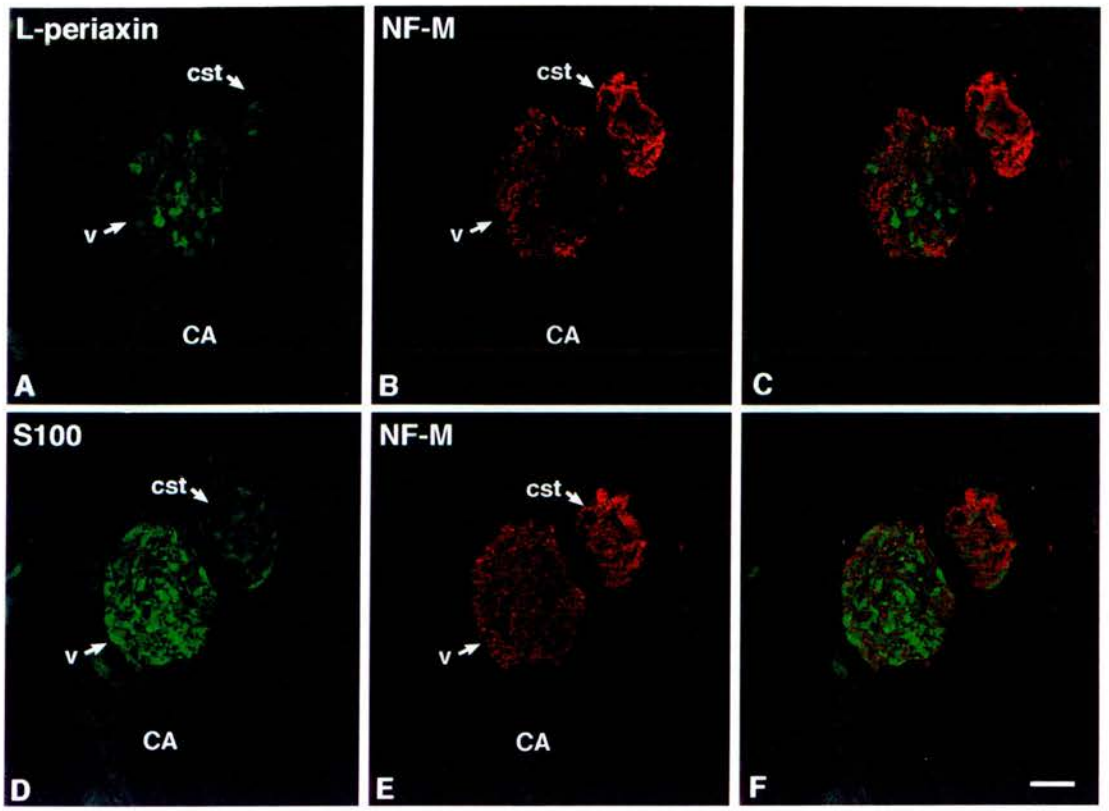

Figure 36. Comparison of the immunofluorescence localization of L-periaxin and S100 in Schwann cells in the embryonic cervical sympathetic trunk (cst) and vagus nerve (v). Serial transverse sections through the cervical region of E16.5 mouse embryos were immunolabeled for L-periaxin (A; fluorescein) and NF-M (Texas red; B C, combined) or S100 (D; fluorescein) and NF-M (Texas red; E, F, combined) and examined by confocal microscopy. A few L-periaxin$^+$ cells are present in the cst, whereas many such cells are present in the vagus nerve (A), in contrast an antibody against S100 labelled all the Schwann cells in both the cst and vagus nerves (D). CA, carotid artery. Bar, 20 μm.

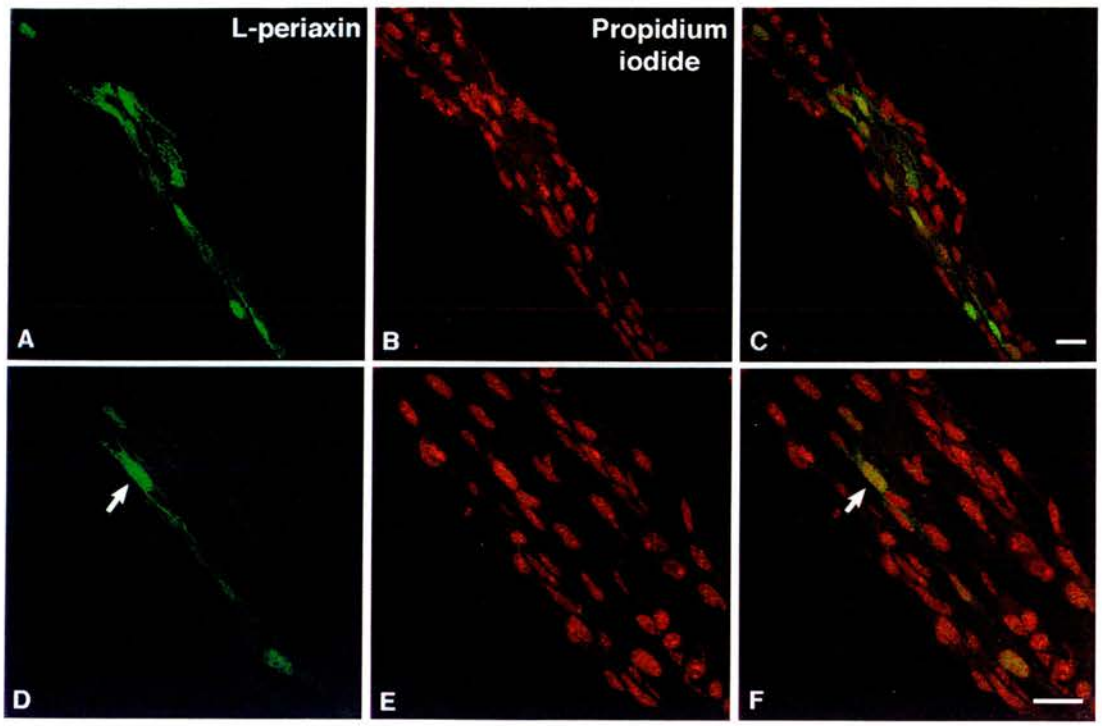

Figure 37. Localization of L-periaxin in E16.5 cervical sympathetic trunk by immunofluorescence confocal microscopy. Longitudinal cryosections of E16.5 mouse cervical sympathetic trunks were immunolabeled for L-periaxin (A, D; fluorescein) and nuclei were labeled with propidium iodide (B, E; red). The majority of the cells were not labelled but there were L-periaxin labelled Schwann cells with some sections containing more L-periaxin positive cells (A) than other sections (B). The immunoreactivity was concentrated in nuclei (D, E, F; arrow). Bar, 20 μm.

were evident. About 20% of the Schwann cells in the trunk were L-periaxin positive at this stage of development. These results indicate that L-periaxin protein is not expressed in the majority of the embryonic Schwann cells destined to be non-myelin-forming.

In situ hybridization studies were performed on transverse sections through the cervical sympathetic trunk of E16.5 and postnatal-day 1 mice to determine if L-periaxin mRNA was present in the Schwann cells of a predominantly non-myelinated nerve. In most sections from E16.5 embryos no positive cells were detected but in one section there were a few weakly positive cells when compared with the more strongly labelled vagus nerve which is destined to be myelinated (Fig. 38C, 38D). By postnatal-day 1 positive cells were not observed in the sympathetic trunk (Fig. 38G, 38H). However, because of the relatively small numbers of embryonic Schwann cells in cervical sympathetic trunk transverse sections, longitudinal sections were examined and compared with sections of vagus nerve. There appeared to be a weak signal in some cells at E16.5 (Fig. 38A, 38B) and P1 (38E, 38F) which correlated with the proportion of cells in which L-periaxin protein was observed. Therefore L-periaxin mRNA expression in cells of the sympathetic trunk is not down-regulated by postnatal-day 1. This weak labelling (Fig 38I) is in marked contrast to that observed in the vagus nerve at E16.5 (Fig. 38J). The vagus nerve has a much higher cell density than the sympathetic trunk which could account for some of the difference in the intensity of labelling, nevertheless individual cells were much more intensely labelled in the vagus. In addition, upon examination of E16.5 transverse sections a few cells were observed which expressed L-periaxin mRNA in the wall of the developing esophagus which are probably enteric Schwann cells (Fig. 38K, 38L). These results suggest that L-periaxin is expressed at very low levels in a subset of embryonic Schwann cells which is not destined to myelinate. Indeed, both L-periaxin mRNA (Fig. 31C) and

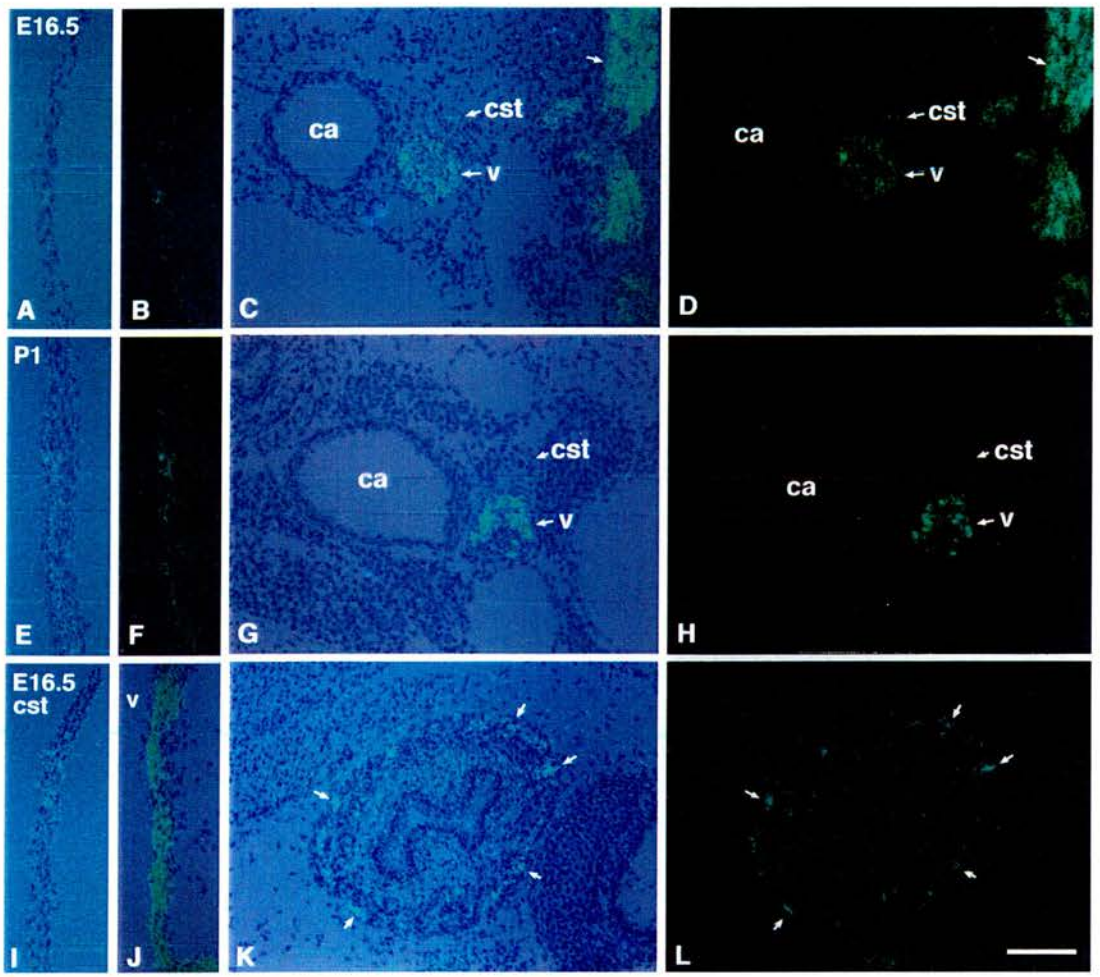

Figure 38. Localization of L-periaxin mRNA in the cervical sympathetic trunk (cst). *In situ* hybridization was performed on longitudinal cryosections of the cst (A, B, I) and vagus nerve (v; J) at E16.5 and postnatal-day 1 (E, F) and transverse sections at E16.5 (C, D,) and postnatal-day 1 (G, H) and examined by epifluorescence microscopy. At E16.5 very sparse labeling is evident in the cst in longitudinal sections (A, B) and transverse sections (C, D; arrow, nerve trunk) compared with the strongly labeled vagus nerve (C, D, J). Labeling was observed in the longitudinal sections of cst at postnatal-day 1 (E, F) but not in transverse sections (G, H). Labeling is also observed in the muscularis externa of the esophagus (arrows; K, L) which are probably glial cells in the myenteric plexus. ca, carotid artery. Bar, 50 μm.

protein were not even detectable in the satellite cells of the dorsal root ganglia which constitute another population of Schwann cells that do not myelinate.

3.2.4 The L-periaxin protein expressed in embryonic sciatic nerve is the full length protein

Since antibodies raised against N-terminal and C-terminal peptides of L-periaxin did not immunolabel early embryonic Schwann cells, I wanted to confirm that the protein recognized by anti-170pep1 was the same size as the protein originally identified in mature peripheral nerves. Sciatic nerves were removed from E15.5 mouse embryos (23 nerves/lane) and postnatal-day 3 (P3) mice and subjected to SDS-PAGE electrophoresis. After transfer to PVDF membrane and blotting with anti-170pep1, the bands were visualized by enhanced chemiluminescence. The band observed in the blot of E15.5 nerves (Fig. 39) had the same mobility as the P3 control demonstrating that the protein in embryonic nerves was indistinguishable in size from L-periaxin. The reason why the N and C terminal peptide antibodies did not immunolabel embryonic nerves might be related to the sensitivity of the antisera or the conformation of the protein at this stage of development.

3.2.5 L-periaxin is transiently expressed in skeletal muscle

A striking finding from the *in situ* hybridization studies on developing mouse embryos was the discrete layer of cells in the body wall that were labelled using the periaxin riboprobe (Fig. 31E, 40A, 40B) which first appeared labelled at E14.5 (Fig. 31C). These cells were not present in the sections labelled with the P0 riboprobe. Silver grains were also observed over elongated cells (Fig. 40A, 40B) that were not associated with peripheral nerves and L-periaxin immunolabelling on embryo sections revealed labelled cells that were not associated with NF-M positive axons. Transverse sections through E15.5 embryos were immunolabelled with anti-

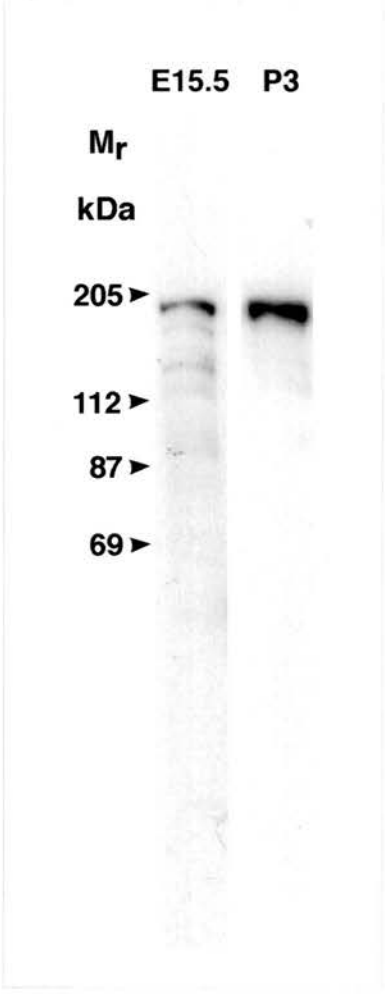

Figure 39. Western blot analysis of L-periaxin from embryonic sciatic nerves. Sciatic nerves from E15.5 and postnatal-day 3 (P3) mouse sciatic nerves were analyzed by SDS PAGE. Following transfer to PVDF membrane and blotting with anti-170pep1, the bands were visualized with enhanced chemiluminescence. The M_r of E15.5 nerves and P3 nerves were the same demonstrating that the embryonic L-periaxin is the full length protein. Molecular mass standards are indicated on the left.

Figure 40. Localization of L-periaxin mRNA and protein in a population of cells not associated with peripheral nerves. *In situ* hybridization was performed on transverse cryosections of E16.5 embryos using a riboprobe for periaxin (A, B). Elongated cells were labeled as well as cells in the body wall (arrows). Transverse cryosections of E15.5 mouse embryos were immunolabeled for L-periaxin (fluorescein) and nuclei were labeled with propidium iodide (red). A layer of L-periaxin labeled cells were present in the body wall (arrows; C, D) and in the developing hindlimb (arrows; E, F) which were not associated with peripheral nerves (n). Occasionally elongated multinucleated cells were labeled (G, H) which had the appearance of myotubes. L-periaxin was also evident in the nuclei of these cells (E, F, G, H). Bar, A, B- 50 μm; C to H- 20 μm.

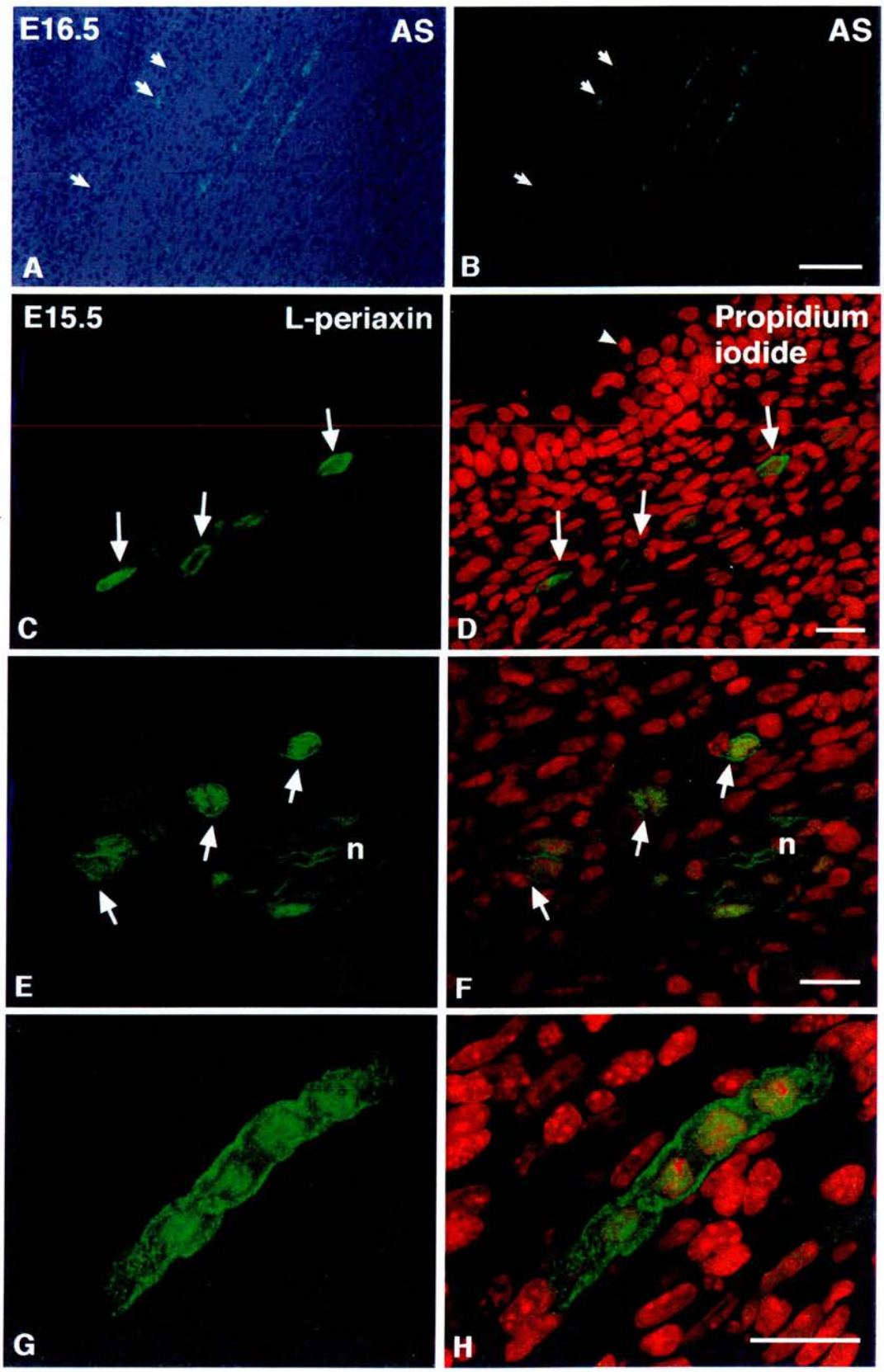
E16.5
AS
A
AS
B
E15.5
L-periaxin
C
Propidium
iodide
D
n
E
n
F
G
H

170pep1 and labelled with propidium iodide. L-periaxin labelling was observed on the plasma membrane of a layer of cells in the body wall (Fig. 40C and 40D). Other labelled cells were observed that had nuclear labelling as well as plasma membrane labelling (Fig. 40E and 40F). Occasionally large multinucleated cells were labelled which had the appearance of myotubes (Fig. 40G and 40H).

To positively identify the labelled cells, double-label immunofluorescence microscopy was performed using anti-170pep1 and a monoclonal antibody that recognized myosin heavy chain (MHC) which is present in skeletal muscle cells. The L-periaxin positive cells in the body wall (Fig. 41A) were also labelled by MHC (Fig. 41B). Only a subset of muscle cells in the body wall expressed L-periaxin.

Previous work showed that L-periaxin was not present in adult rat skeletal muscle by Western blotting (Gillespie et al., 1994). Since L-periaxin was expressed in embryonic muscle, the expression during postnatal development was examined by immunofluorescence on muscles of the mouse hind limb. L-periaxin staining was observed in cells which colocalized with MHC in postnatal-day 4 limb muscle (Fig. 41C and 41E). At postnatal-day 8, few L-periaxin labelled cells were observed and no labelled cells were observed at postnatal-day 10 (data not shown), demonstrating that L-periaxin is transiently expressed in a subset of skeletal muscle cells during embryonic development and early postnatal life.

3.2.6 Analysis of embryonic muscle in *periaxin*-null mice

Embryos from mice with a targeted disruption of the *periaxin* gene by homologous recombination were examined to confirm that the antibody to L-periaxin and the [^{35}S] periaxin riboprobe used for *in situ* hybridization studies were recognizing products of the *periaxin* gene in embryonic muscle. Cryosections from E15.5 *periaxin*-null embryos and wild type embryos were immunolabelled with anti-170pep1 and anti-NF-M. There were no L-periaxin labelled cells in the NF-M positive sciatic nerve (Fig. 42A and 42B). When the muscle cells in the body wall

Figure 41. Localization of L-periaxin and myosin heavy chain (MHC) in skeletal muscle by immunofluorescence microscopy. Transverse cryosections through the body wall of E16.5 mouse embryos and postnatal-day 4 hindlimbs were double-labeled for L-periaxin (A, C, E; fluorescein) and MHC (B, D, F; Texas red) and examined by confocal microscopy. The L-periaxin labelled cells in the body wall (B) and limb muscle (D, low magnification; F, high magnification) colocalized with MHC. Bar, 20 μm.

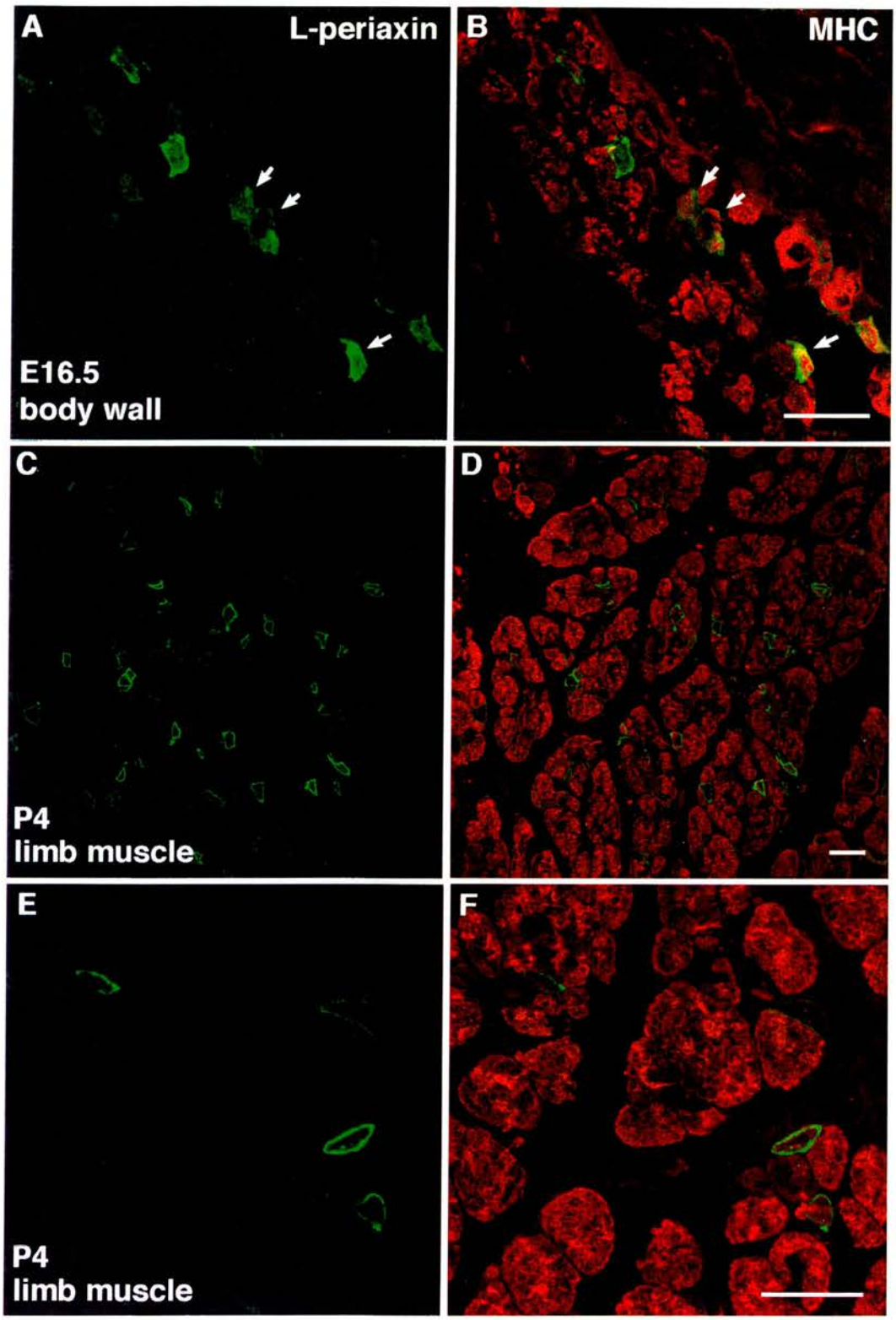
A
L-periaxin
B
MHC
E16.5
body wall
C
D
P4
limb muscle
E
F
P4
limb muscle

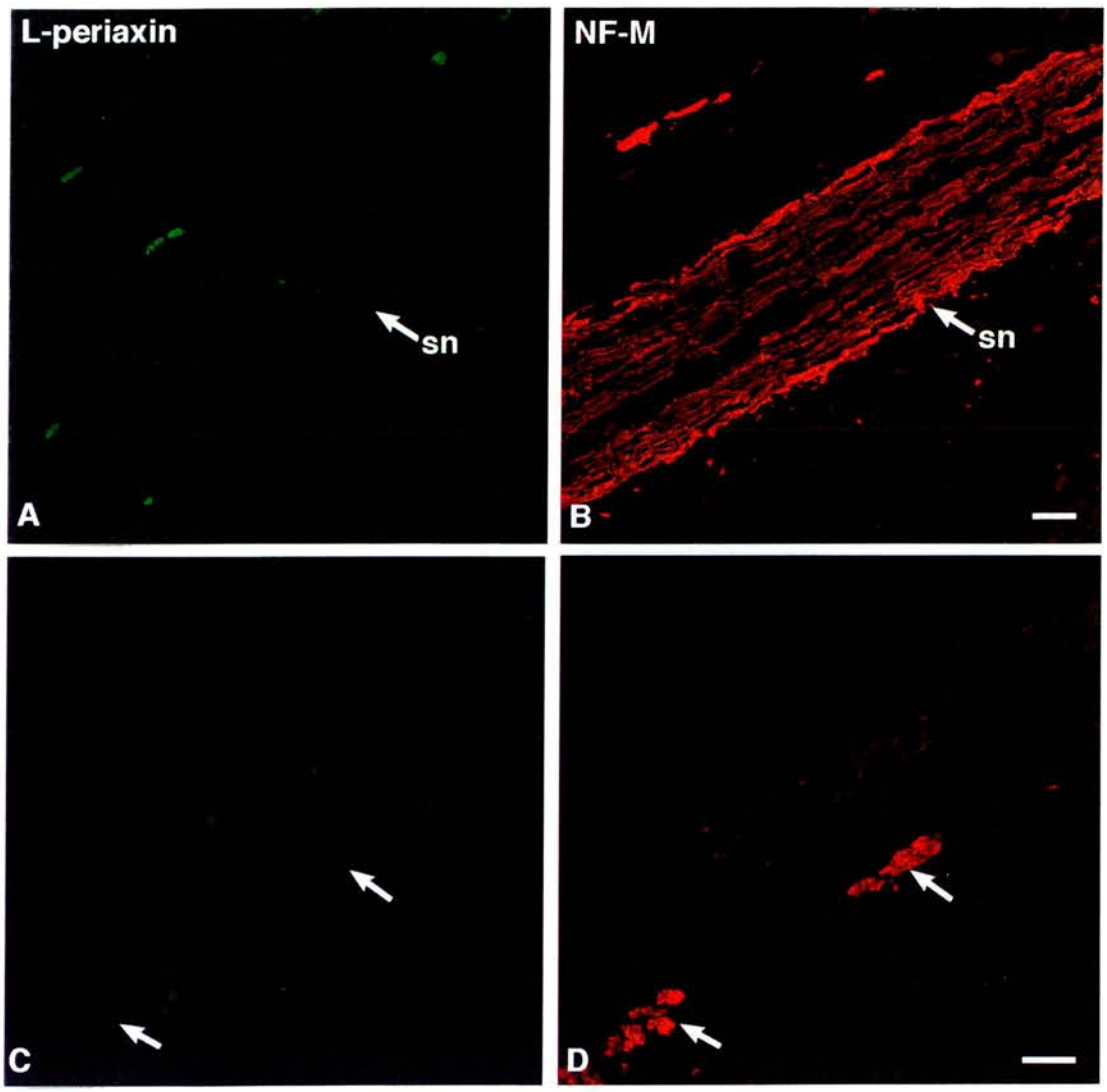

Figure 42. Schwann cell and skeletal muscle cell L-periaxin expression are products of the same gene. Double-label immunofluorescence localization of L-periaxin and NF-M in transverse cryosections through the trunk of E15.5 *periaxin* null embryos were examined by confocal microscopy. There were no positive L-periaxin immunolabeled cells in the body wall (C; fluorescein), or sciatic nerve (sn; A, fluorescein) which was identified by NF-M$^+$ axons (Texas red). arrows, NF-M positive axons. Bar, 20 μm.

(Fig 42C) and skeletal muscle cells were examined, no L-periaxin positive cells were detected. These data conclusively demonstrate that the periaxin mRNA and protein observed in embryonic Schwann cells and muscle cells are the products of the same gene.

3.2.7 Summary

L-periaxin mRNA and protein were found to be first expressed in embryonic Schwann cells coinciding with the developmental switch from precursor cell to embryonic Schwann cell which occurs at E14 in the mouse. That these cells were indeed Schwann cells was confirmed by double-label immunocytochemistry on dissociated embryonic sciatic nerve cultures using O4 as a Schwann cell marker. Interestingly, the protein was predominantly expressed in Schwann cell nuclei until E17.5 when it assumed a predominantly plasma membrane localization.

It seems very likely that L-periaxin is largely expressed by embryonic Schwann cells that are destined to be myelin-forming in the mature nerve since most of the Schwann cells in the embryonic sciatic nerve, as detected by O4 immunostaining, express L-periaxin. However, there was a small population of cells which was $O4^+$, L-$periaxin^-$ suggesting that these cells may be destined to become non-myelin-forming Schwann cells. In the cervical sympathetic trunk, where most of the Schwann cells are non-myelin-forming in the adult, about 20% of the cells were L-$periaxin^+$ at E16.5. This is a higher percentage than would be predicted by comparison with the adult nerve if L-periaxin were a marker for myelin-forming embryonic Schwann cells. Nevertheless, cells in the cervical sympathetic trunk are still proliferating at this stage of development and they continue to divide until around postnatal-day 15, whereas the rate of proliferation in myelin-forming cells drops off at birth (Stewart et al., 1993). Thus the cells which are L-periaxin positive in the E16.5 cervical sympathetic trunk may represent those cells destined to be myelin-forming whereas the L-periaxin negative cells may

have a non-myelin-forming fate and may continue to proliferate until postnatal-day 15. An alternative scenario is that L-periaxin may be expressed at basal levels in embryonic Schwann cells destined to be non-myelin-forming and then down-regulated in the adult, as occurs for P0. P0 mRNA is expressed at basal levels in most of the embryonic Schwann cells in the cervical sympathetic trunk whereas L-periaxin mRNA and protein are expressed at low levels in a subset of the embryonic Schwann cells. P0 is also expressed in satellite cells in the dorsal root ganglia whereas periaxin is not. Because L-periaxin mRNA was observed in cells which appear to be enteric glia it seems likely that there is a basal level of L-periaxin mRNA expression in some Schwann cells which do not form myelin.

I have shown that S-periaxin mRNA and protein are not expressed during embryonic development and are first expressed at postnatal-day 1 in the mouse. The relative abundance of the two mRNAs is difficult to evaluate by *in situ* hybridization since the probe used for the smaller mRNA recognizes both species. Northern analysis in postnatal-day 5 rats (Gillespie et al., 1994) and postnatal-day 3 mice (L. Dytrych, PhD thesis) demonstrate that the two distinct mRNAs are of equal abundance.

L-periaxin was previously thought to be exclusively expressed by myelin-forming Schwann cells (Scherer et al., 1995). I have now shown that L-periaxin is expressed transiently in skeletal muscle, first appearing at E14.5 in the mouse. The lack of L-periaxin immunoreactivity in the *periaxin* null mutant embryo confirmed the mRNA and protein detected in Schwann cells and skeletal muscle were both products of the *periaxin* gene.

3.3 NUCLEAR EXPRESSION OF L-PERIAXIN

During embryogenesis it was surprising to find that L-periaxin was expressed in the nuclei of embryonic Schwann cells. Strikingly this expression was very sharply developmentally regulated. A similar expression pattern has been observed for myelin basic proteins (MBPs) (Allinquant et al., 1991; Hardy et al., 1996; Pedraza, 1997; Pedraza et al., 1997) in oligodendrocytes. In immature oligodendrocytes exon II-containing MBPs are partially localized to the nucleus and as oligodendrocytes mature the MBP isoforms are translocated from the nucleus. The authors suggest that nuclear entry of these MBP isoforms may be the initiating mechanism for myelination. Since L-periaxin is expressed before MBP in embryonic Schwann cells, it was of great interest to study the nuclear localization of the protein further.

3.3.1 The localization of L-periaxin is predominantly nuclear in embryonic Schwann cells

The localization of L-periaxin and propidium iodide to detect cell nuclei was examined by confocal immunofluorescence on cryosections from mouse embryonic E15.5 nerve trunks and on teased mouse sciatic nerves at E15.5. Many L-periaxin positive nuclei (Fig. 43A) were observed which colocalized with propidium iodide positive nuclei (Fig. 43B and 43C). L-periaxin labelling of the plasma membranes was demonstrated more clearly in teased sciatic nerve (Fig. 43D and 43F). It is also evident in Fig. 43A and 43D that there was a greater abundance of the protein in nuclei than in other cellular regions.

3.3.2 L-periaxin protein expression is developmentally regulated

Short-term dissociated cultures of mouse embryonic Schwann cells and mouse neonatal Schwann cells were prepared to compare the cellular distribution of

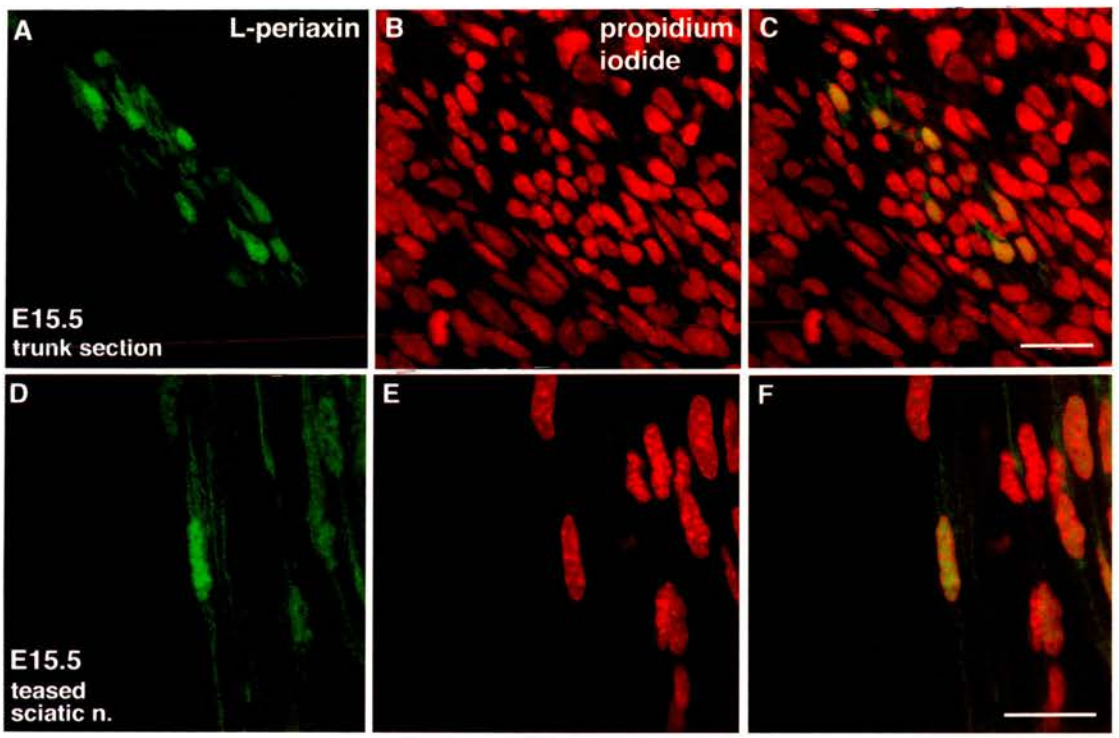

Figure 43. Immunolocalization of L-periaxin in embryonic Schwann cell nuclei. Transverse cryosections through the trunk and teased sciatic nerve fibres were immunolabeled with anti-170pep1 and stained with propidium iodide to label nuclei and were examined by confocal microscopy. L-periaxin (A, C; fluorescein) colocalizes with propidium iodide (B, E; red) stained nuclei in peripheral nerve trunks (A, B; C, combined) and teased fibres (D, E; F, combined). In the teased fibre preparation L-periaxin is also seen in Schwann cell processes (D). Bar, 20 μm.

L-periaxin by immunofluorescence confocal microscopy. At E16.5 strong nuclear labelling was observed (Fig. 44A) with the nucleolus devoid of immunostaining. However by postnatal-day 1 the protein redistributed to the cytoplasm and plasma membrane (Fig. 44B). These data demonstrate that L-periaxin is targeted to different cellular compartments during Schwann cell development .

3.3.3 Nuclear L-periaxin is not the consequence of programmed cell death.

To examine whether L-periaxin expression in the nucleus of embryonic Schwann cells reflected the fact that these cells were undergoing programmed cell death, terminal deoxynucleotide transferase mediated UTP nick end-labelling (TUNEL) was performed on E15.5 cryosections of mouse sciatic nerve in combination with L-periaxin immunofluorescence. The L-periaxin positively labelled nuclei were not TUNEL labelled (Fig. 45A, 45B, 45C). Hence nuclear L-periaxin does not reflect fragmented DNA indicative of dying cells.

3.3.4 Nuclear targeting of L-periaxin is affected by cell contact

When the L-periaxin cDNA was transiently transfected into heterologous cells or used to make stable transfectants, the majority of the protein produced was localized to the nucleus. To examine whether cell density affects the nuclear targeting of L-periaxin, low density and high density cultures of 33B cells permanently expressing L-periaxin were prepared and immunolabelled. Cells in low density cultures displayed strong nuclear labelling (Fig. 46A) and like the embryonic cultured Schwann cells, the nucleoli were devoid of labelling. In contrast, nuclear labelling was not observed when cells were grown at high density where the labelling was cytoplasmic (Fig. 46B).

To test whether this process was reversible and the cytoplasmic L-periaxin would be retargeted to nuclei, a high density monolayer was damaged by scraping with a blue pipette tip. This process allowed cells to migrate into the cell-free

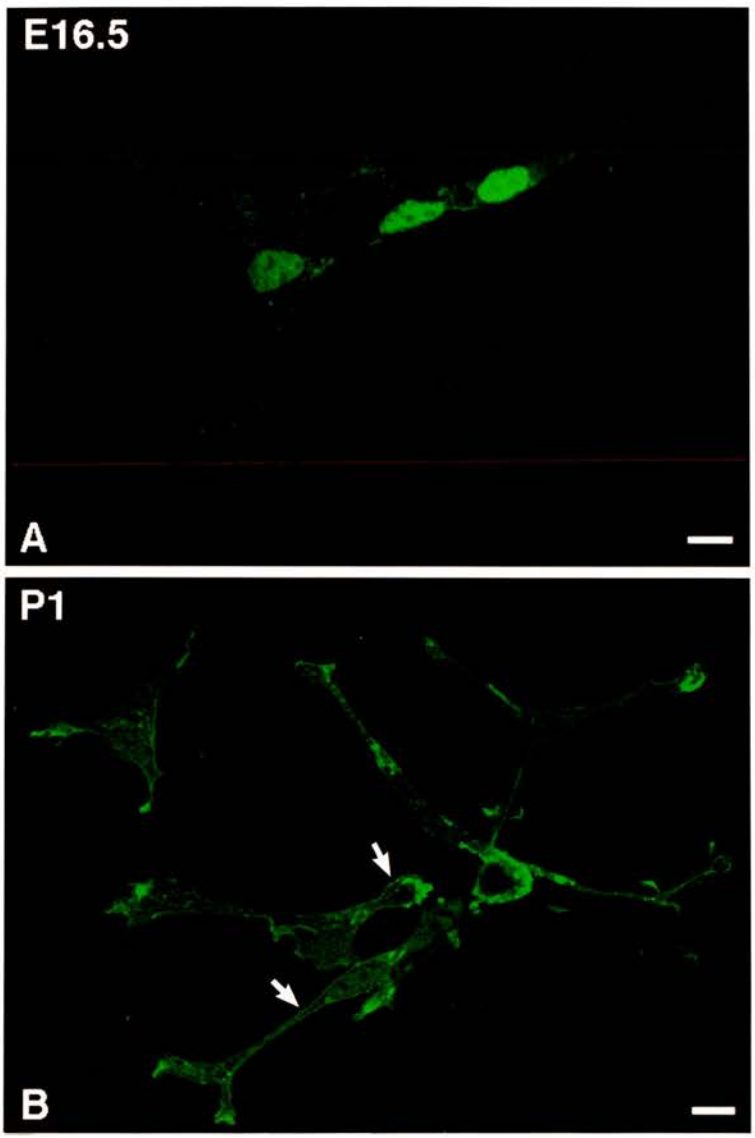

Figure 44. Nuclear expression of L-periaxin in embryonic and neonatal cultured Schwann cells by immunofluorescence microscopy. Cultured Schwann cells from E16.5 and postnatal-day 1 (P1) sciatic nerves were immunolabeled with anti-170pep1 and examined by confocal microscopy. At E16.5 L-periaxin is predominantly nuclear (A) whereas at P1 the cytoplasm and plasma membrane are labeled (B). Bar, 10 μm.

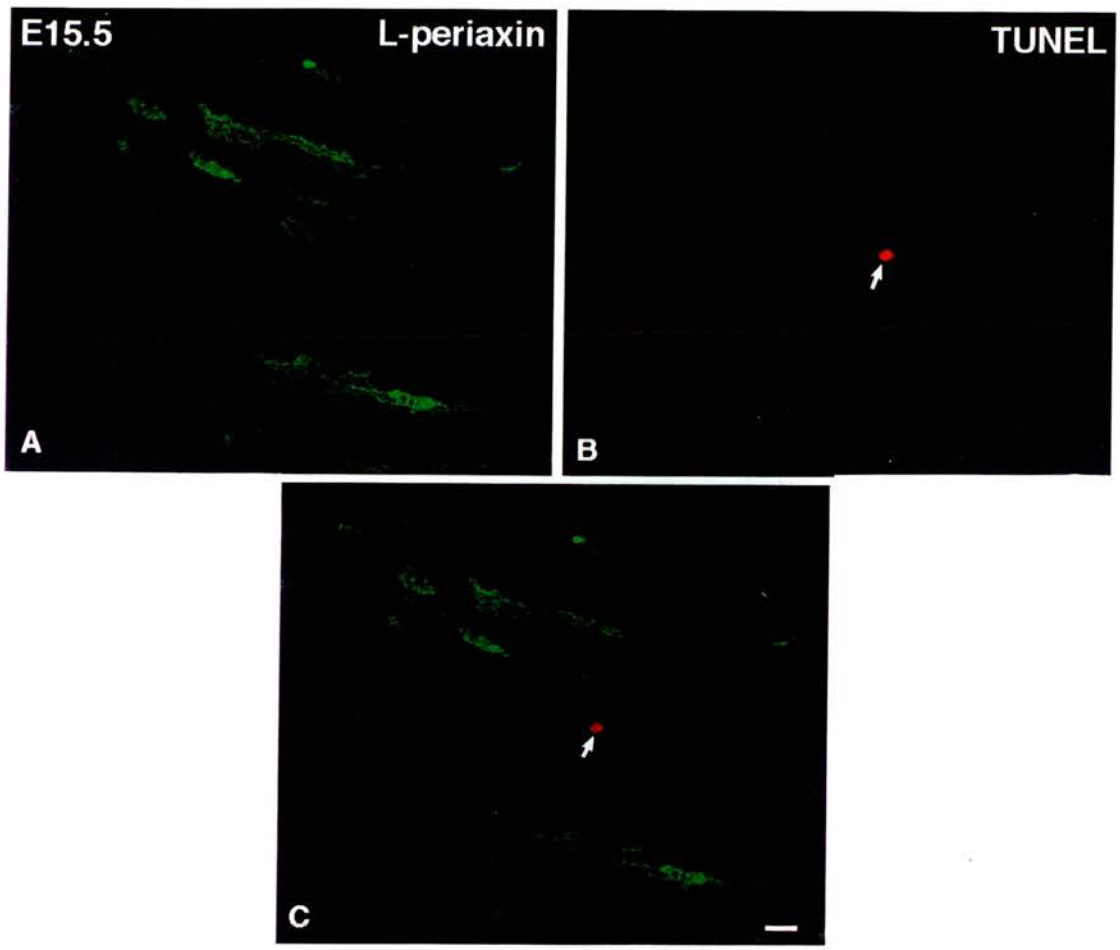

Figure 45. Nuclear L-periaxin expression is not the result of apoptosis. Cryosections of E15.5 sciatic nerves were labeled for L-periaxin (fluorescein) and TUNEL (Texas red) and examined by confocal microscopy. L-periaxin labeled cells (A) do not colocalize with TUNEL labeled nuclei (B; C, combined). Bar, 10 μm.

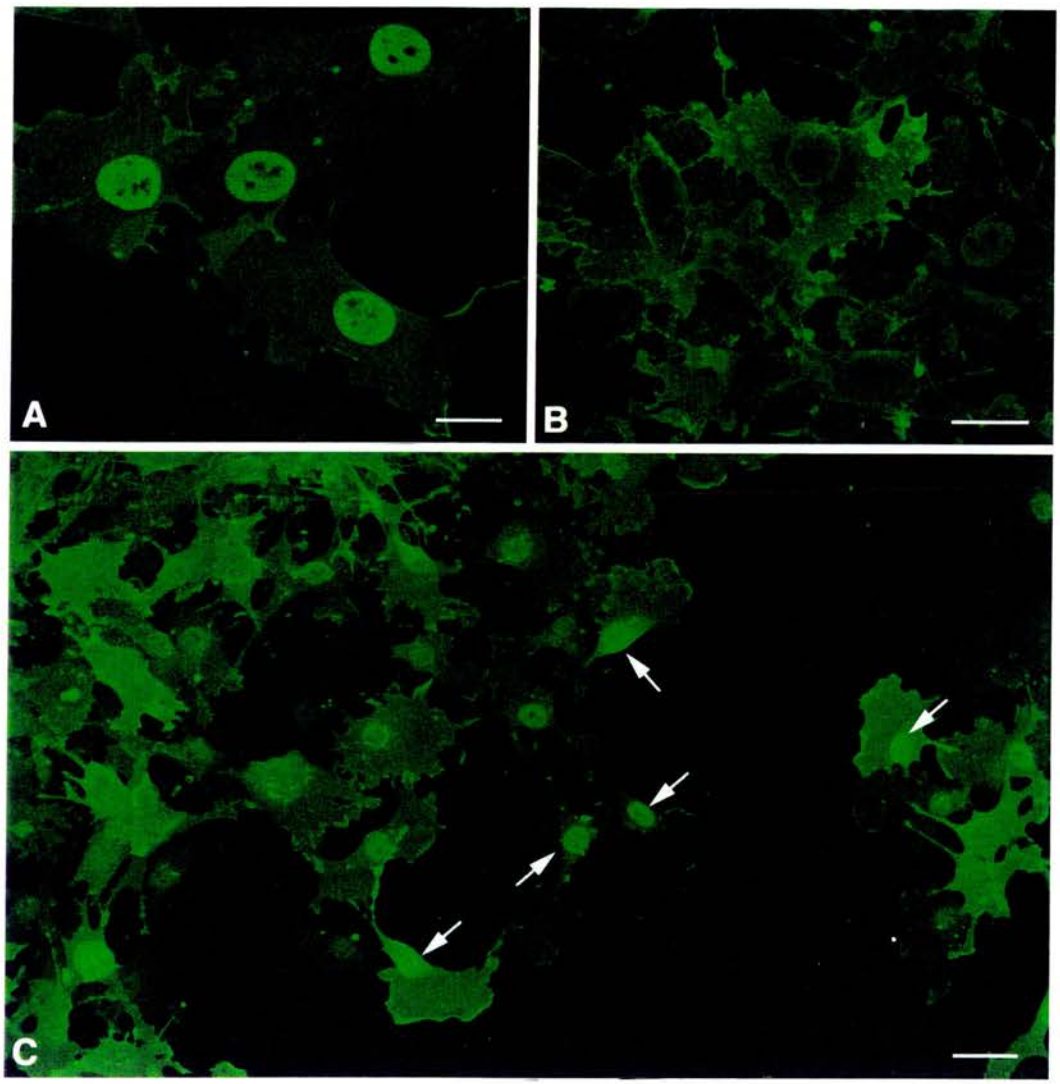

Figure 46. The nuclear localization of L-periaxin is affected by cell-cell contact. Low density and high density cultures of permanently-expressing 33B cells were immunolabeled with anti-170pep1 and examined by confocal microscopy. Cells grown at low density (A) displayed mainly nuclear L-periaxin whereas cells in high density cultures (B) had mainly cytoplasmic L-periaxin. Two hours after a high density culture was wounded (C), cells with nuclear L-periaxin were seen in the cell-free space (arrows). Bar, A, B, 20 μm; C, 50 μm.

space. Cells which displayed nuclear labelling were observed migrating into the cell-free space 2 h after scraping the monolayer (Fig. 46C).

These results demonstrate that cell-cell contact prevents nuclear targeting of L-periaxin and that translocation from the nucleus is reversible.

3.3.5 L-periaxin has a PDZ modular protein-binding domain at its extreme N-terminus

The domain structure of L-periaxin was described by Gillespie et al., 1994 and previous database searches had not revealed any sequence similarities to any known proteins. In the process of searching for a possible nuclear localization signal, a database search using the deduced amino acid sequence of L-periaxin revealed a region of 52 amino acids in the extreme N-terminus of L-periaxin with a 49% identity with the tight junction protein ZO-1 (Itoh et al., 1993; Willott et al., 1993). This identity with ZO-1 was extremely interesting because like L-periaxin, ZO-1 was targeted to the nucleus. However, of more functional significance ZO-1 is a member of a family of proteins with a modular protein-binding domain called the PDZ domain which is implicated in mediating signal transduction. And most importantly the region of identity with L-periaxin was within the PDZ domain. When a comparison of the N-terminus of L-periaxin with other PDZ domains from various proteins was conducted (Fig. 47), it was clear that L-periaxin possessed a PDZ domain from amino acids 14 to 98.

PDZ domains were originally identified based on sequence similarity in **P**SD-95, the post-synaptic density protein, the Drosophila septate junction protein **D**iscs-Large (dlg), and **Z**O-1 (Cho et al., 1992; Woods and Bryant, 1991; Willott et al., 1993). Proteins with PDZ domains interact with the cytoplasmic tail of integral membrane proteins (Saras and Heldin, 1996) and the cytoskeleton (Sheng, 1996) and particularly relevant for this work, most of these proteins have been localized to the plasma membrane (Sheng, 1996).

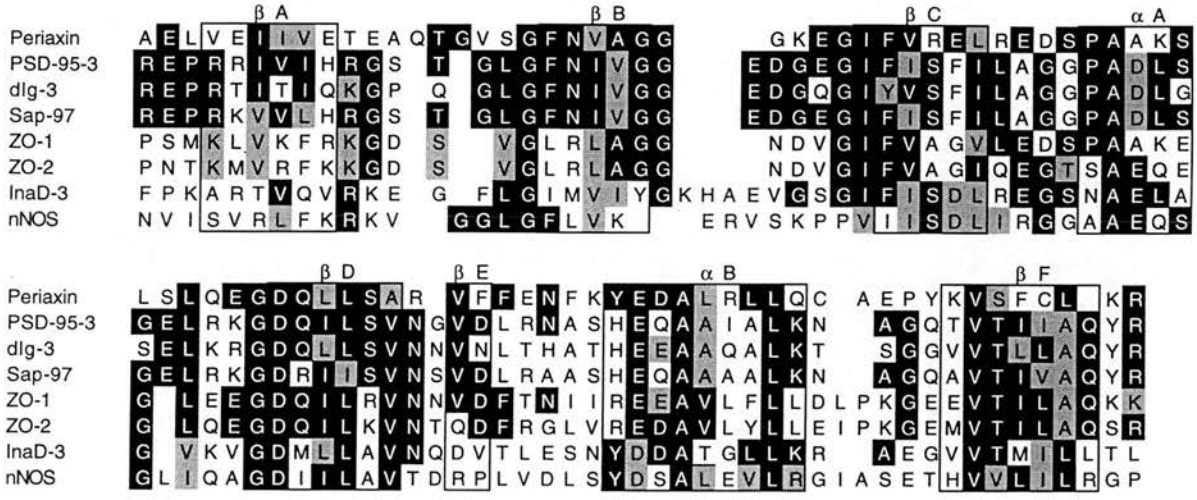

Figure 47. Identification of a PDZ domain at the N-terminus of L- and S-periaxin. The sequence of mouse L- and S-periaxin between amino acids 14 and 98 was compared with PDZ domains in the nNOS (residues 14-100) (Bredt et al., 1991), PSD-95 (residues 309-393) (Cho et al., 1992), discs-large (dlg) (residues 482-566), (Woods et al., 1991), SAP97 (residues 461-545) (Müller et al., 1995), ZO-1 (residues 408-491) (Willott et al., 1993), ZO-2 (residues 93-176) (Jesaitis et al., 1994), and InaD (residues 361-447) (Shieh et al., 1996). The eight segments within the domain comprising six β strands and two α-helices (Doyle et al., 1996). Black blocks show amino acid identity and grey shading indicates conservative substitutions.

3.3.6 The basic domain of L-periaxin is responsible for nuclear targeting

In an effort to identify a region of L-periaxin that was responsible for nuclear targeting, cDNA constructs were prepared with deleted regions and cloned into an expression vector for transient transfection studies. Three constructs were prepared with deletions in the entire N-terminus (PrxΔ3) including the PDZ domain, the repeat region (PrxΔ1), and the entire C terminus (PrxΔ2) of the protein.

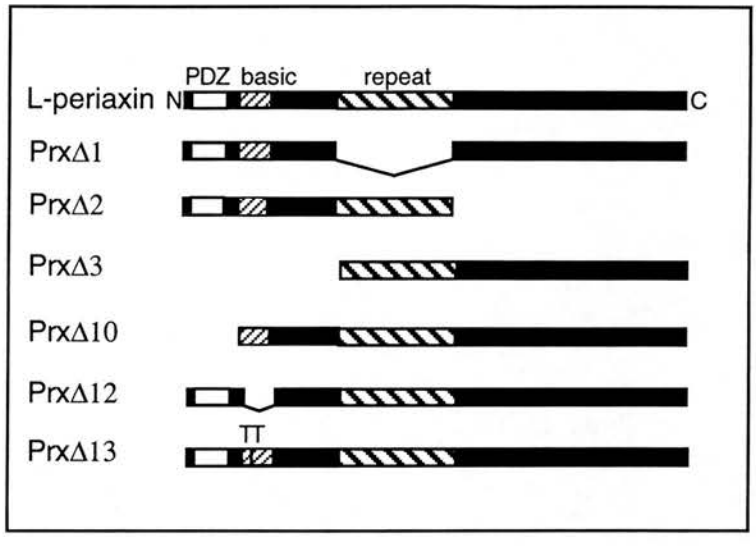

Domain structure of L-periaxin and deletion mutants

After transient transfection in 33B cells it was clear that nuclear targeting was only abolished in the construct in which the N-terminus was deleted (data not shown). The deleted region in the N-terminus comprised two domains, the PDZ and the basic domains. Constructs were prepared which deleted the PDZ domain (PrxΔ10) and the basic domain (PrxΔ12). Liposome-mediated transient transfections were performed on Hela cells, 33B cells and Schwann cells prepared from primary cultures. Immunofluorescence was performed using anti-170pep1 for cells transfected with the full length L-periaxin and PrxΔ12, and anti-NTerm for cells transfected with PrxΔ1. As shown in Fig. 48 using the full length L-periaxin (Fig. 48A, 48D, 48G) and the repeat region deletion PrxΔ1 (Fig. 48C, 48F, 48I) as controls, only the basic domain deletion PrxΔ12 dramatically abolished nuclear

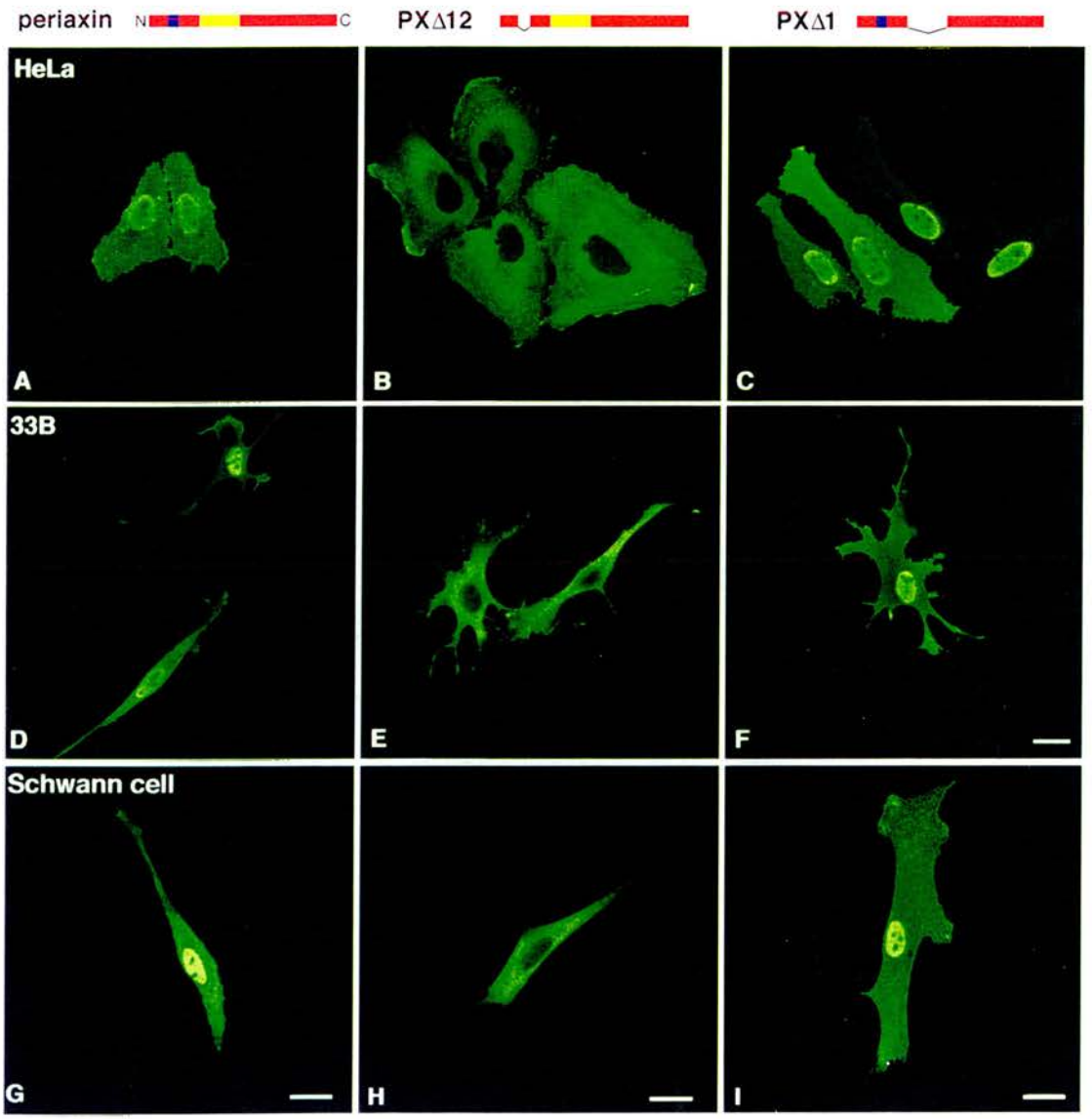

Figure 48. The basic domain of L-periaxin is responsible for nuclear targeting. Hela cells (A, B, C), 33B cells (D, E, F) and Schwann cells (G, H, I) were transfected with the full length L-periaxin cDNA (A, D, G), PrxΔ12 (lacking the encoded basic domain) (B, E, H) and PrxΔ1 (lacking the encoded repeat region) (C, F, I). A schematic of the constructs are shown on the top panel. Immunofluorescence was performed with anti-170pep1 for the full length protein and PrxΔ12, and anti-NTerm for PrxΔ1 and examined by confocal microscopy. Nuclear staining was observed in all cell types examined with the full length L-periaxin (A, D, G) and PrxΔ1 (C, F, I). Only cytoplasmic staining was observed in all cell types transfected with PrxΔ12 (B, E, H). Bar, 20 μm.

staining in Hela cells (Fig. 48B), 33B cells (Fig. 48E), and Schwann cells (Fig. 48H). Therefore the basic domain of L-periaxin appears to be responsible for nuclear targeting.

3.3.7 The basic domain of L-periaxin targets green fluorescent protein (GFP) to the nucleus

GFP from the jellyfish *Aequorea victoria* has been used as a tag to trace the translocation of proteins in living cells (Ogawa et al., 1995). In order to confirm that the basic domain was responsible for nuclear targeting of L-periaxin the 234 bp basic domain was fused to GFP under the control of the CMV promoter (BD-GFP) in order to monitor the location of the basic domain-GFP fusion protein in living cells. After transient transfection of GFP alone in Hela cells (Fig. 49A), 33B cells (Fig. 49C), and Schwann cells (Fig. 49E) a strong green fluorescence was observed uniformly distributed throughout the cytoplasm and nucleus. In contrast, BD-GFP accumulated only in the nucleus (Fig. 49B, 49D, 49F) demonstrating that the basic domain of L-periaxin was sufficient to target GFP to the nucleus. It is interesting to note that BD-GFP also accumulates in the nucleolus which may be due to the high affinity that basic peptides have for B23, the major acidic nucleolar protein (Breeuwer and Goldfarb, 1990; Goldfarb, 1988).

3.3.8 The basic domain of L-periaxin contains a putative nuclear localization signal (NLS)

The deduced amino acid sequence of the basic domain of L-periaxin contains a lysine-rich stretch (underlined), nts 136-139, which may be a part of a NLS. It also has an arginine-rich stretch (underlined) closer to the end of the domain at nts 185-187.

118 KGPRAKVAKLNIQSLSPV<u>KKKK</u>MVIGTLGTPADLAPVDV

EFSFPKFSRLRRGLKADAVKGPVPAAPA<u>RRR</u>LQLPRLRVR 196

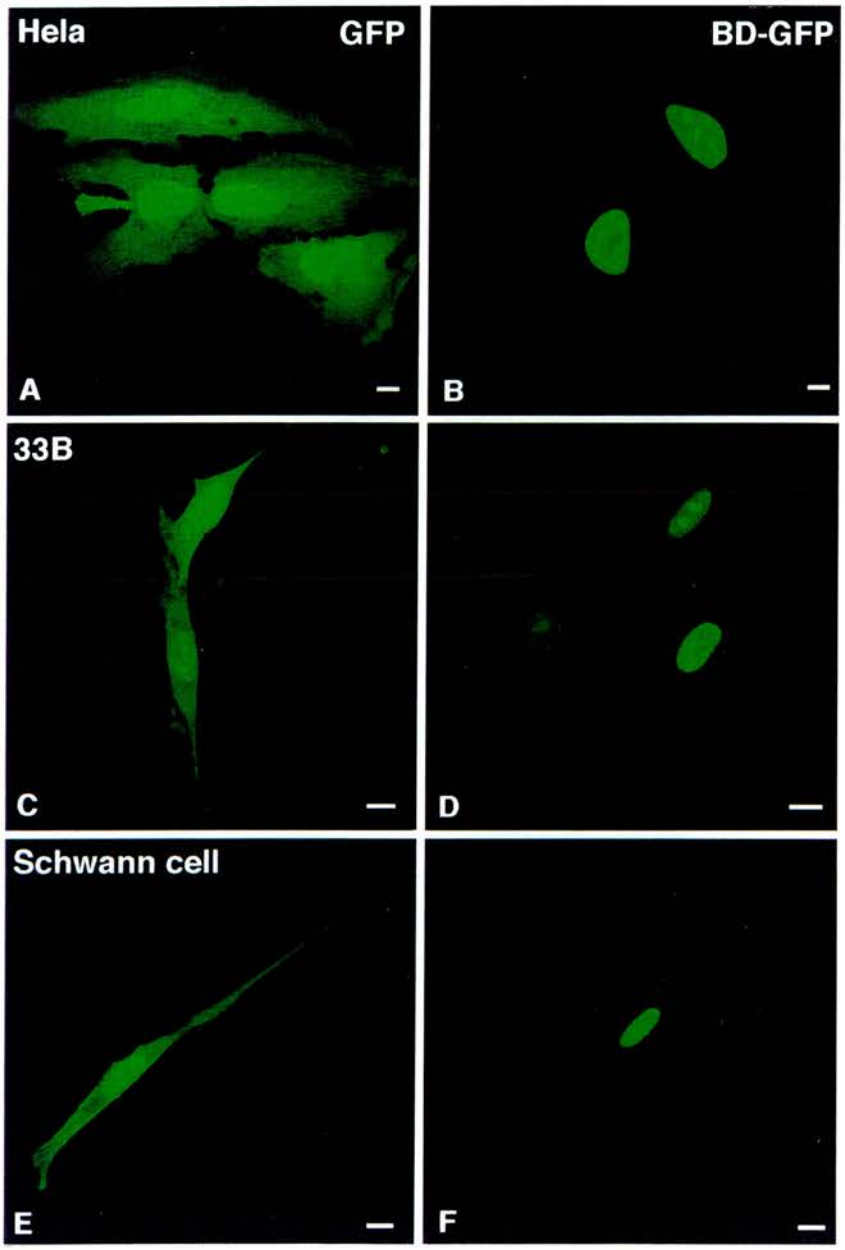

Figure 49. The basic domain of L-periaxin targets GFP to the nucleus. Hela cells (A, B), 33B cells (C, D,) and Schwann cells (E, F) were transfected with either GFP (A, C, E) or BD-GFP (B, D, F) and examined by confocal microscopy. GFP was distributed throughout the nuclei and cytoplasm of all cell types examined (A, C, E) whereas BD-GFP was confined to nuclei (B, D, F). Bar, 10 μm.

The amino acid sequence of the basic domain was compared to the sequences of classic NLSs both single, as in the SV40 large T antigen (Kalderon et al., 1984), and the bipartite forms (Lodish et al., 1995). The 4 lysines at nts 136-139 could be a NLS. To test whether the stretch of lysines were responsible for nuclear localization, two of the lysines were mutated to threonines in the full length cDNA and transfected into several cell lines to observe the localization of the mutated protein. The mutated protein was still located in the nucleus (data not shown) demonstrating that mutating two amino acids of a highly basic region did not prevent nuclear import.

Single	L-periaxin	PVKKKKMV
	SV40 T antigen	PPKKKRKV
	adenovirus E1a	KRPRP
Bipartite	Nucleoplasmin	KR(10)KKKK
	mouse poly-ADP-ribose polymerase	RK(11)KKK

It is important to note that NLSs have been described which do not fall into the classic NLS, both single or bipartite, category. It is possible that the stretch of lysines and the stretch of arginines can both act together as a NLS.

3.3.9 The energy requirements of nuclear translocation

The energy released by ATP hydrolysis is essential for import of a protein with a NLS across a nuclear pore into the nucleus (Lodish et al., 1995). Pedraza and co-workers found in their work on the nuclear translocation of MBP that it was an active process requiring energy (Pedraza et al., 1997). Schwann cells and Hela cells transiently expressing BD-GFP were used to observe if nuclear transport was affected by energy depletion. Cells were incubated at 37°C in glucose-free medium containing 2-deoxyglucose (an inhibitor of glycolysis) and sodium azide (an inhibitor of mitochondrial electron transport) for 1 and 2 h. After 2 h incubation

some cells were allowed to recover for 2 h in the presence of glucose. After Schwann cells were depleted of energy for 1 (Fig. 50B) and 2 h (Fig. 50C) there was transport arrest of BD-GFP because cytoplasmic protein was visible but a strong nuclear localization was still observed indicating that the arrest may be partial or that some of the BD-GFP protein was bound in the nucleus and remained there after energy depletion. Upon recovery after energy depletion, all of the protein translocated back to the nucleus (Fig. 50D). These results demonstrate that energy depletion has an effect on nuclear translocation since significant labelling was seen in the cytoplasm of depleted cells. Small proteins lacking NLSs diffuse into the nucleus independent of the energy charge of the cell (Breeuwer and Goldfarb, 1990). However this seems unlikely for BD-GFP since GFP alone remained partially in the cytoplasm. It seems more likely that the basic domain targets GFP to the nucleus where the protein binds to a nuclear component.

3.3.10 Nuclear L-periaxin is insoluble in non-ionic detergent

Because L-periaxin was shown to be in the Triton X-insoluble fraction of PNS myelin (Gillespie et al., 1994) and present in Schwann cell cytoskeletons prepared from cultured postnatal sciatic nerve (B. Kelly, personal communication) it was presumed to be associated with a component of the cellular cytoskeleton. Since some of the BD-GFP remained in the nucleus during energy depletion experiments I wanted to determine whether L-periaxin was bound to a component of the nuclear cytoskeleton.

To examine if nuclear L-periaxin was soluble in non-ionic detergent, cell cultures of permanently expressing 33B cells (clone 25) were extracted with 0.5% Triton X-100 in a cytoskeleton stabilization buffer. After fixation and immunolabelling, immunofluorescence confocal microscopy was performed. As evident in Fig. 51A and 51B nuclear L-periaxin remains associated with the Triton X-100-insoluble residue indicating that the protein is bound to a nuclear structure.

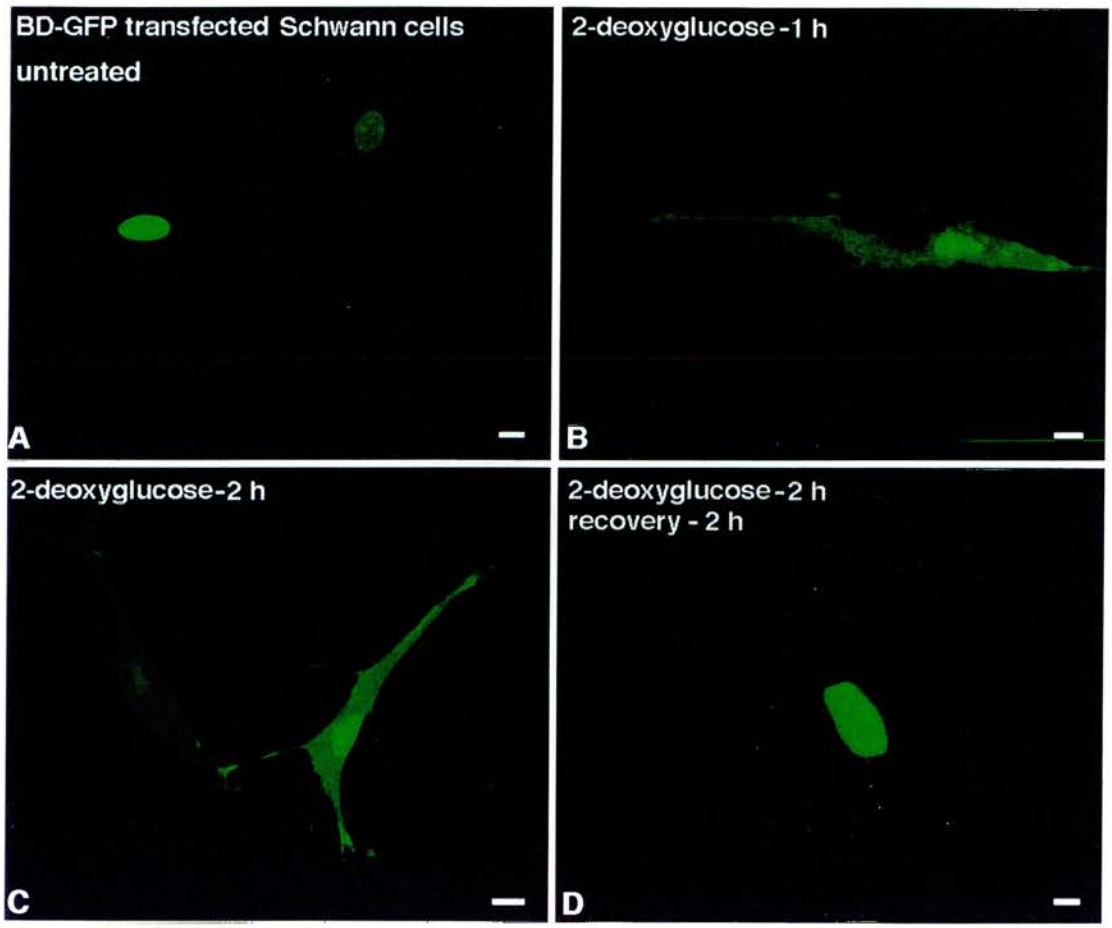

Figure 50. The nuclear targeting of BD-GFP fusion protein is affected by energy depletion. Cultured Schwann cells transiently transfected with BD-GFP were incubated in medium (A) or glucose-free medium containing 2-deoxyglucose for 1 h (B) or 2 h (C). Cells were also incubated for 2 h with 2-deoxyglucose followed by 2 h in medium containing glucose (D). After fixation cultures were examined by confocal microscopy. After incubation with 2-deoxyglucose for 1 or 2 h, BD-GFP fusion protein was observed in the cytoplasm and nucleus (B, C) whereas control (A) or cells after recovery in glucose (D) displayed only nuclear fluorescence. Bar, 10 μm.

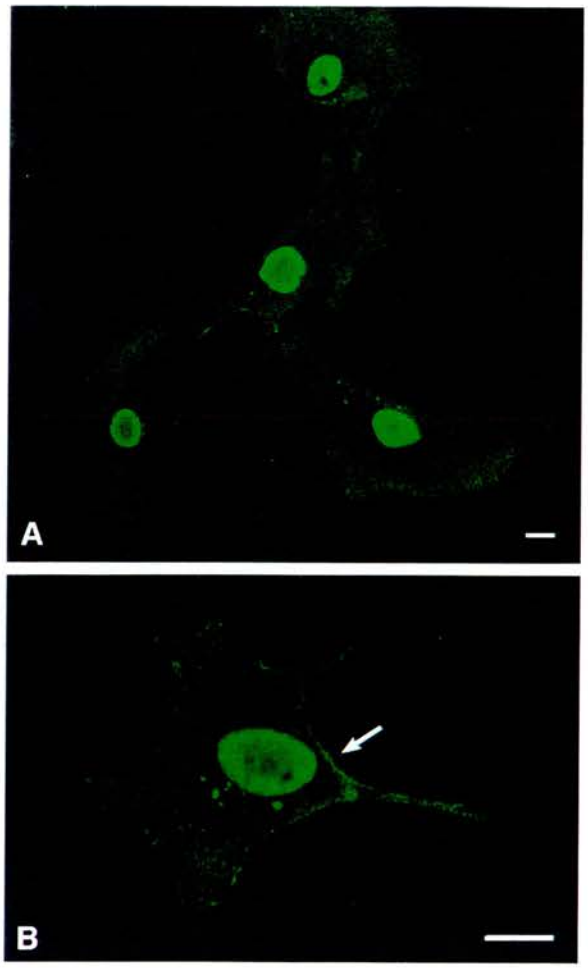

Figure 51. Nuclear L-periaxin is insoluble in non-ionic detergent. Permanently L-periaxin expressing 33B cells were immunolabeled for L-periaxin after Triton X-100 extraction and examined by confocal microscopy. (A) L-periaxin (fluorescein) remains associated with the nucleus. At higher magnification, L-periaxin is also seen associated with the cytoskeleton and plasma membrane (B; arrow). Bar, 10 μm.

The structure does not appear to be the nuclear lamina as the protein was detected throughout the nucleus.

Another membrane-associated protein with PDZ domains, the tight junction protein ZO-1, redistributes to the nucleus *in vitro* in cells plated at low density and is found in nuclei *in vivo* in distinct regions of the intestinal villus (Gottardi et al., 1996). In contrast to L-periaxin, nuclear ZO-1 is soluble in Triton X-100 whereas the protein is insoluble when targeted to tight junctions (Gottardi et al., 1996).

3.3.11 Summary

L-periaxin is expressed predominantly in the nucleus of embryonic Schwann cells *in vivo* and *in vitro* in short-term cultures. This nuclear localization is developmentally regulated and by E17.5, it was no longer observed. Embryonic Schwann cells displaying L-periaxin in their nuclei were not undergoing programmed cell death.

When L-periaxin was transfected into heterologous cells, the protein was transported to the nucleus. Cell-cell contact inhibited nuclear translocation and the process was reversible. The basic domain in L-periaxin was shown to be responsible for nuclear targeting because the mutant protein with the basic domain deleted did not localize to the nucleus. The role of the basic domain in nuclear targeting was confirmed by the use of a GFP fusion protein containing the basic domain which translocated to the nucleus. The nuclear import of BD-GFP was shown to require energy because cytoplasmic staining was observed after energy depletion even though all of the nuclear BD-GFP did not redistribute to the cytoplasm. Nuclear L-periaxin binds to a nuclear component and is insoluble in non-ionic detergent. Examination of the basic domain sequence revealed two possible NLSs.

A modular protein-protein binding PDZ domain was identified at the extreme N-terminus of the protein. Like other PDZ containing proteins, L-periaxin

is localized to the cytoplasmic side of the plasma membrane and probably, like other PDZ containing proteins, the PDZ domain binds to the cytoplasmic tail of an integral membrane protein in the Schwann cell plasma membrane. The PDZ domain is also present in the smaller isoform, S-periaxin, which has a cytoplasmic distribution suggesting that other factors influence PDZ-protein binding.

3.4 TRANSGENESIS

While this work was in progress, the structure of the murine *periaxin* gene was determined (Dytrych et al., 1998). It was shown by Dytrych et al., 1998 that the mouse promoter is TATA-less, contains a single transcription initiation site, a CAAT box consensus sequence (-86 to -76), and an octomer motif (-236 to -243) which may be a binding site for the POU family of transcription factors two of which are present in Schwann cells, Oct-1 and Oct-6 (Blanchard et al., 1996). They also identified a sequence (-317 to -306) with homology to the GCRE element present in the promoters of other myelin genes.

Transcriptional regulation is important for understanding the stage and cell specific expression of genes. Since I had shown that the *periaxin* gene was exclusively expressed in myelin-forming Schwann cells in the adult, embryonic Schwann cells and a subset of skeletal muscle cells in the embryo up to postnatal-day 8, I sought to identify by transgenesis the regulatory elements in the *periaxin* gene responsible for cell specific expression.

3.4.1 Preparation of LacZ constructs

The E. coli *LacZ* gene was used as a reporter gene so that the localization of the transgene could be identified at the cellular level by β–galactosidase histochemistry. The SV40 large T-antigen NLS (Lanford et al., 1988) was used to target β-galactosidase to the nucleus. Each transgene was inserted into pLacF and pnLacF (with NLS) plasmids (see Materials and Methods, 2.7.1). In these plasmids a segment of the mouse *protamine-1* gene (mP1) provides an intron and a polyadenylation site (Peschon et al., 1987). The following constructs were prepared from the *periaxin* genomic clone HH1: Prx1-nlacZ which contained 5.5 kb

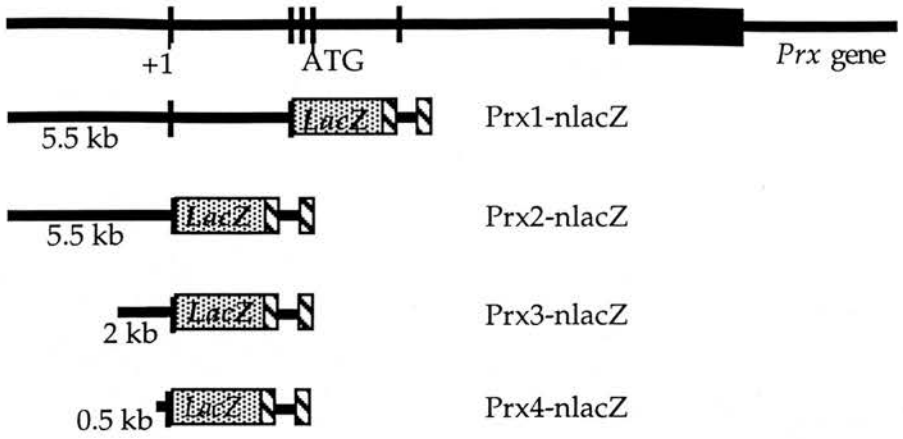

Structure of the *periaxin* gene and transgenes

upstream of the transcription initiation site, exon 1, intron 1 and exon 2; Prx2-nlacZ which was the same as Prx1-nLacZ except it lacked intron 1 and exon 2; Prx3-nlacZ which contained 2 kb upstream of the transcription initiation site and exon 1; and Prx4-nlacZ contained exon 1 and 500 bp upstream.

3.4.2 Prx1-4 lacZ constructs drive transcription in cultured cells upon transient transfection

Transient transfections were performed on primary cultures of rat Schwann cells and NIH 3T3 cultured cells. Gene expression was analysed by β–galactosidase histochemistry. All 4 of the constructs were able to drive transcription in Schwann cells and NIH 3T3 cells. Prx3-nlacZ and Prx4-nlacZ transgenes were expressed in many Schwann cell nuclei (Fig. 52E and 52G) and NIH 3T3 cell nuclei (Fig. 52F and 52H). Prx2-nlacZ was expressed in a larger number of NIH 3T3 cells (Fig. 52D) than was Prx2-lacZ in Schwann cells (Fig. 52C). In contrast, very few (1 or 2 per coverslip) Prx1-nlacZ expressing cells were found in both NIH 3T3 cells (Fig. 52B) and Schwann cells (Fig. 52A).

The Schwann cell cultures used for these transfections were de-differentiated cells that had been induced with forskolin to up-regulate L-periaxin expression. High concentrations of forskolin to raise intracellular cAMP was added

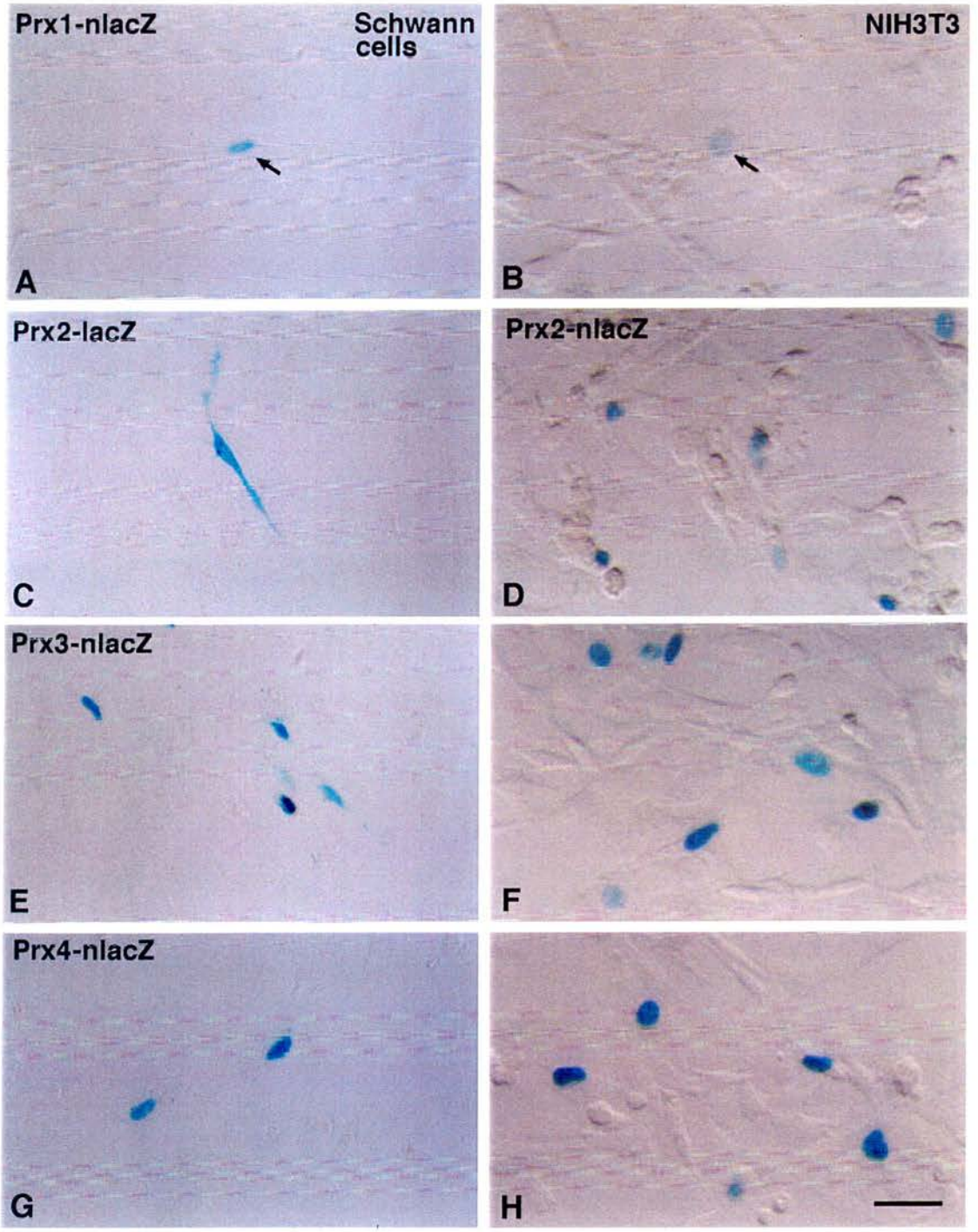

Figure 52. Expression of Prx-lacZ constructs by transfection in Schwann cells and NIH3T3 cells. β-galactosidase histochemistry was performed on transiently transfected Schwann cells (A, C, E, G) and NIH3T3 cells (B, D, F, H) using periaxin promoter/LacZ constructs Prx1-nlacZ (A, B), Prx2-lacZ on Schwann cells (C) and Prx2-nlacZ on NIH3T3 cells (D), Prx3-nlacZ (E, F), and Prx4-nlacZ (G, H). Arrows mark lightly stained cells. Bar, 50 μm.

to the culture medium both before and after transfection to induce myelin gene expression (Kelly et al., 1992; Morgan et al., 1991; Shuman et al., 1988). In spite of this only 40-50% of the Schwann cells expressed L-periaxin by immunofluorescence. Therefore over half of the cells in the cultures do not reflect the *in vivo* myelin-forming Schwann cell phenotype. Nevertheless, these data do show that these constructs are able to drive transcription.

3.4.3 Prx2-nlacZ transgene is expressed in myelin-forming Schwann cells in peripheral nerves in transgenic mice

Vector sequences were removed from the transgenes in pnLacF before purification for microinjection into the pronucleus of murine fertilized eggs by standard techniques (Hogan et al., 1994). The fertilized eggs were produced from an F1 hybrid (C57BL6 X CBA) cross. Genomic DNA was prepared from tail biopsies and screened by PCR and Southern blot analysis for the presence of the transgene. PCR primers gave a 500 bp product from the *LacZ* gene and a 2 kb probe from the *LacZ* gene was used for Southern blotting. An example of each screen is shown in Fig. 53.

Seven founder mice were identified by PCR followed by Southern screening after which sciatic and trigeminal nerves from all lines were examined after β–galactosidase histochemistry. Two of the founders did not pass the transgene to the next generation suggesting that they were mosaic in germline tissues. Two of the five remaining lines had positive β–galactosidase staining in some cells in the sciatic (Fig. 54A) and trigeminal nerves. Teased nerve preparations from sciatic nerve demonstrated β–galactosidase stained nuclei in myelin-forming Schwann cells (Fig. 54B and 54C). Not all myelin-forming Schwann cells expressed the transgene and in one line there were very few cells with positively stained nuclei indicating that the penetrance of this transgene was partial. Therefore it was concluded that the Prx2-

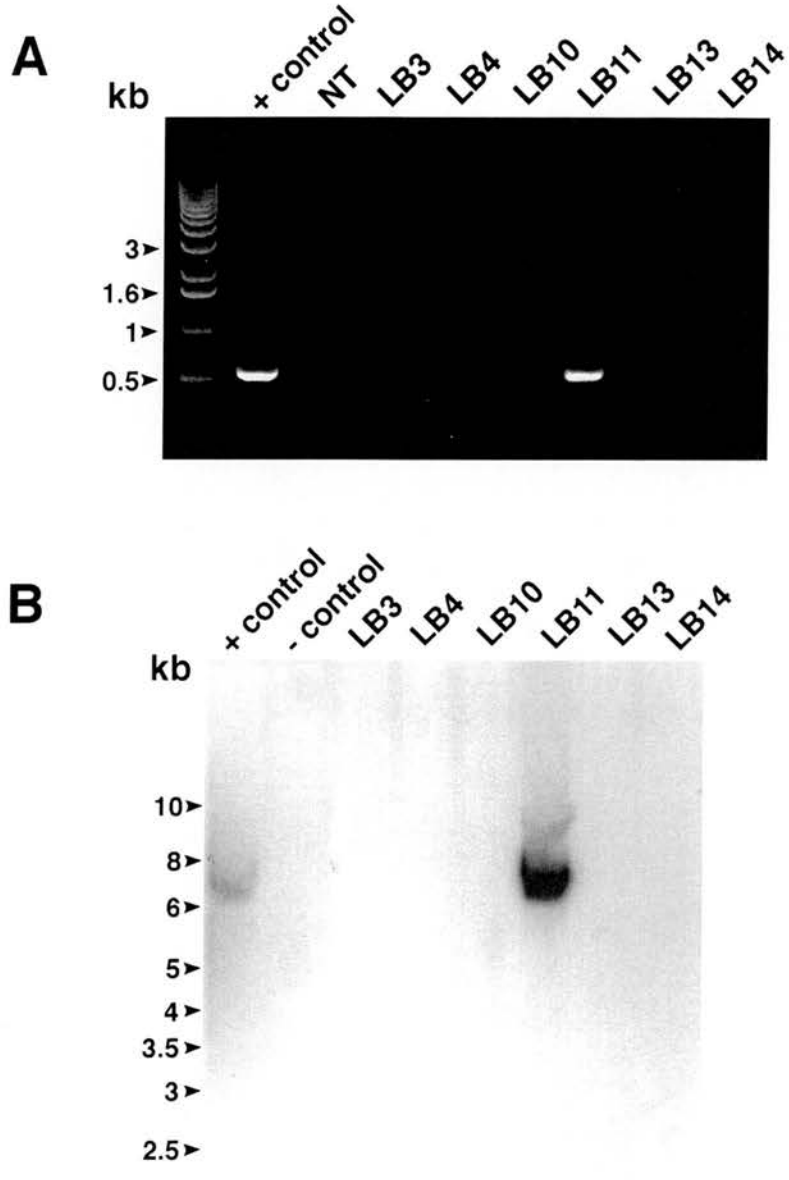

Figure 53. PCR and Southern blot analysis used for transgene screening. (A) PCR was performed on 240 ng of genomic DNA from mouse tail biopsies using Lac1 and Lac2 primers followed by 1% agarose gel electrophoresis. One kb ladder is on the left. NT, PCR with no DNA. (B) Southern analysis of 10 µg of EcoRI digested genomic DNA from mouse tail biopsies probed with a 2 kb fragment of *LacZ*. One kb ladder is on the left.

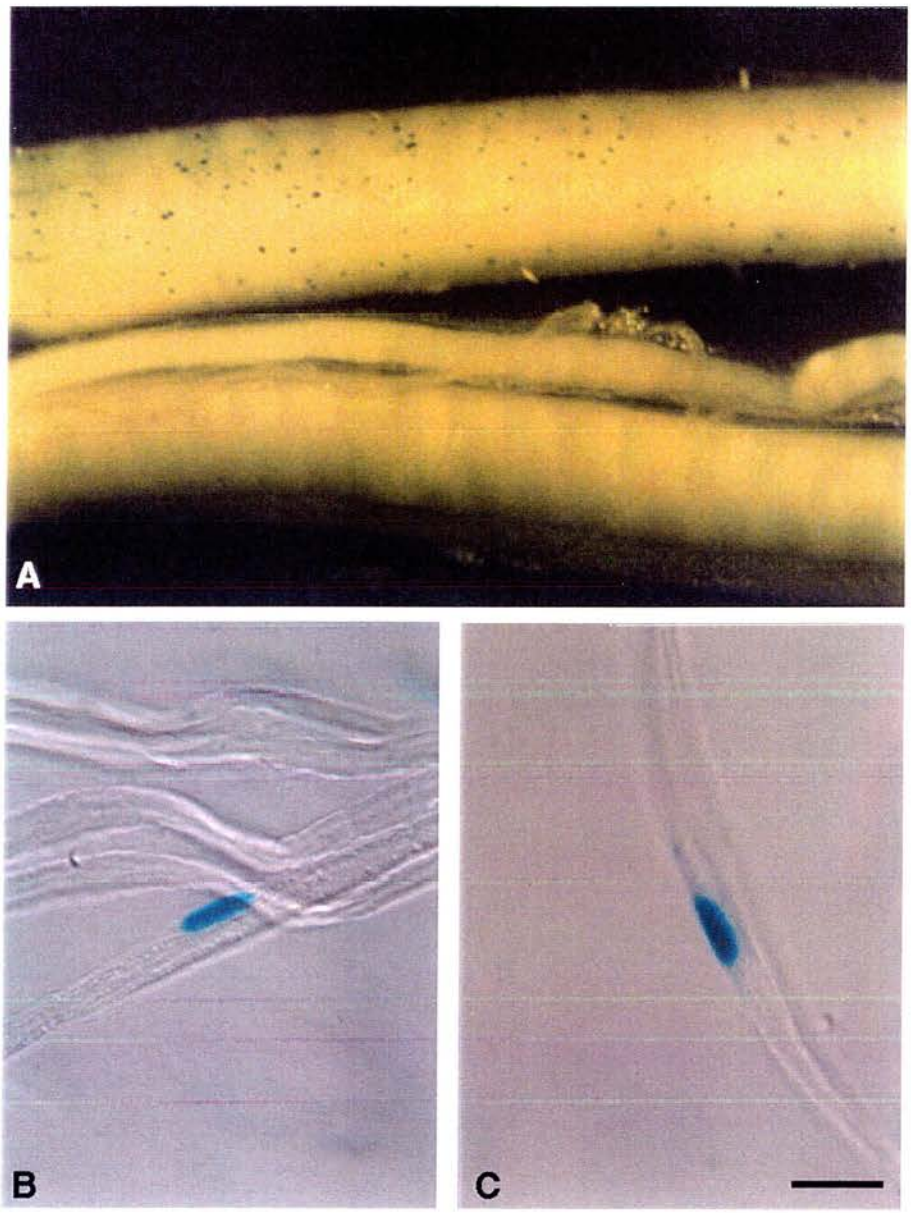

Figure 54. Prx2-nlacZ expression in sciatic nerve. (A) β-galactosidase staining of sciatic nerves from transgenic line TF11 (top) and wild type mice (bottom). (B and C) Teased fibres from a β-galactosidase stained sciatic nerve from a TF11 line mouse showing nuclear staining. Bar, 20 μm.

nlacZ transgene did not include all of the essential regulatory elements needed for Schwann cell expression.

3.4.4 Prx2-nlacZ transgene is expressed in the central nervous system

To assess if the transgene was expressed in other tissues, E17.5 embryos and tissues from adult mice were subjected to β–galactosidase histochemistry. Interestingly the brains from 4 lines displayed β–galactosidase staining including the ones where the transgene was expressed in peripheral nerve.

Prx2 lines	PNS	CNS
TF11	+	+
TL1	-	-
TM3	-	+
TO11	-	+
TO33	+	+

The regions of the brain with β–galactosidase stained nuclei were different in all of the lines (Fig. 55). No other tissues had specific nuclear β–galactosidase staining. These data suggest that the *periaxin* gene has a silencing element which is not located in the 5.5 kb promoter. Negative regulatory elements that repress neuronal genes in non-neuronal cells and neuronal cells have been demonstrated for several genes (reviewed in Schoenherr and Anderson, 1995).

3.4.5 Prx3-nlacZ transgene is also expressed in the CNS but not in the PNS

Five Prx3-nlacZ founder mice were identified by PCR and Southern blot analysis and peripheral nerve, brain, and other tissues were examined for β–galactosidase positively stained nuclei. The Prx3-nlacZ transgene was not expressed in the sciatic and trigeminal nerves of mice from all the lines examined.

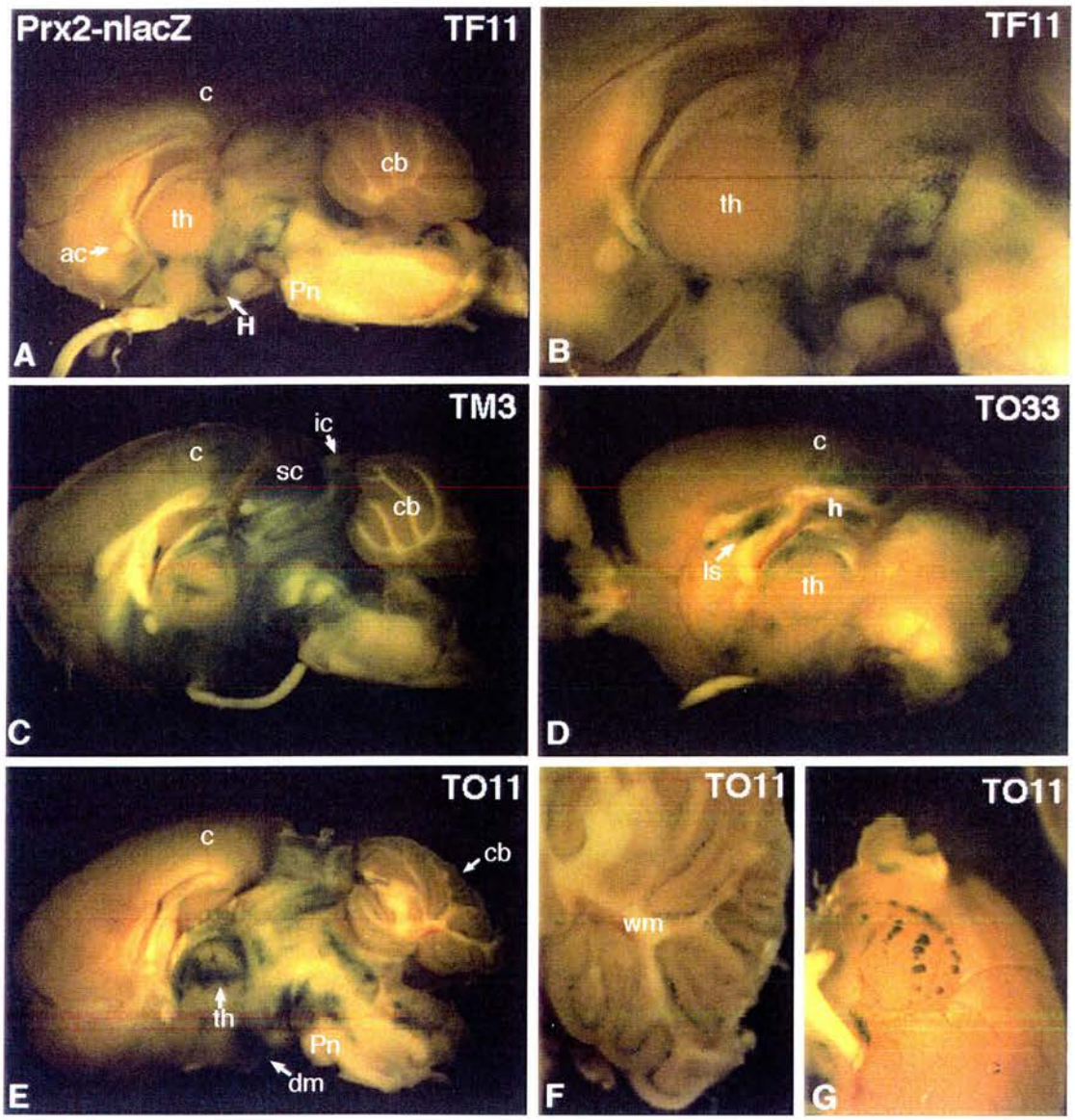

Figure 55. Prx2-nlacZ expression in brain. Brains from 4 lines, TF11, TM3, TO33, and TO11, of Prx2-nlacZ transgenic mice were sagittally sliced and stained as whole mount preparations for β-galactosidase histochemistry. Rostral is to the left (A to E). (F) cerebellum. (G) anterior surface of the cortex. ac, anterior commissure; c, cortex; cb, cerebellum; dm, dorsal medial hypothalamic nucleus; H, hypothalamus; h, hippocampus; ic, inferior colliculus; ls, lateral septal nucleus; Pn, pontine nucleus; sc, superior colliculus; th, thalamus, wm, white matter.

Prx3 lines	PNS	CNS
TP41	-	+
TQ1	-	-
TR3	-	+
TS4	-	-
TT1	-	-

As in Prx2-nlacZ transgenics, expression in the brain was exhibited by two of the five lines (Fig. 56A, 56B, 56C, 56D) and cell nuclei were stained by β–galactosidase histochemistry (Fig. 56D inset). CNS expression was not unexpected after the results obtained with Prx2-lacZ transgenic mice, thereby confirming that there is very likely a neural silencer in the *periaxin* gene. These transgenic data show that the 2 kb periaxin promoter may not contain the regulatory elements needed to drive Schwann cell expression *in vivo*. Since only two of the lines showed any transgene expression analysis of additional lines will be necessary to see if the transgene is expressed in the PNS.

3.4.6 Prx1-nlacZ transgene is expressed in both the PNS and CNS

Five Prx1-nlacZ founder mice were identified by PCR and Southern blotting and PNS and CNS tissues from three of the lines were subjected to β–galactosidase histochemistry. All three lines expressed the transgene in the CNS and one line, TV1, expressed the transgene in Schwann cells in the PNS.

Prx1 lines	PNS	CNS
TW1	-	+
TV1	+	+
TY31	-	+

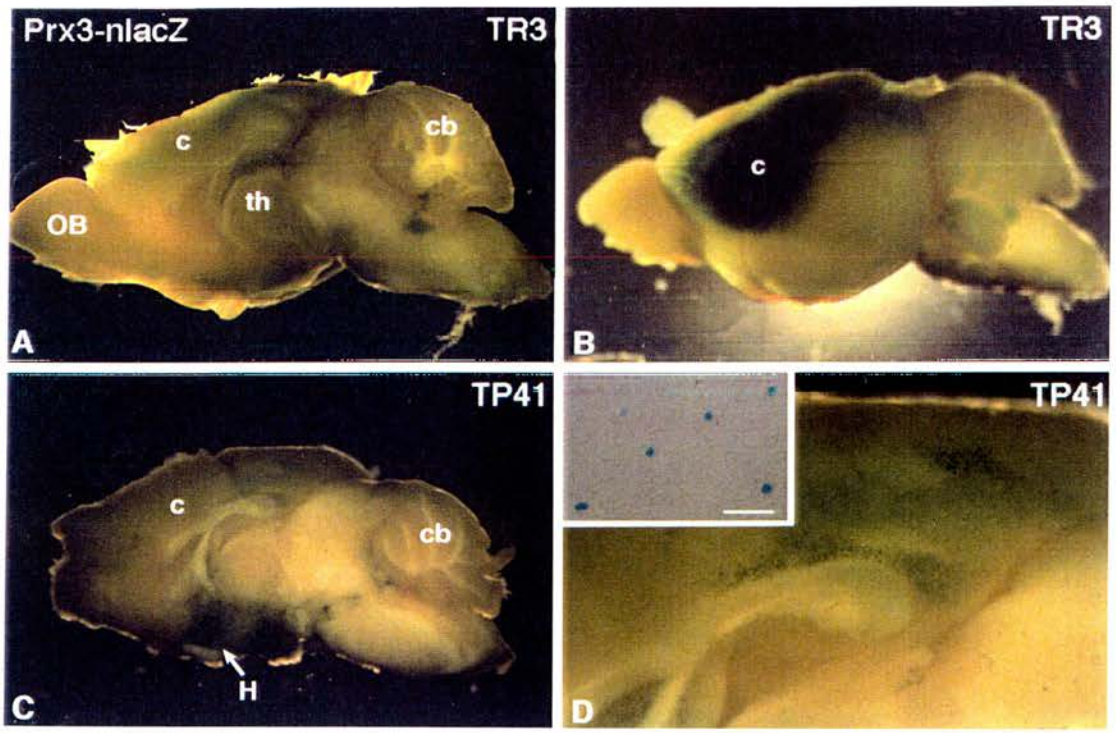

Figure 56. Prx3-nlacZ expression in brain. Brains from 2 lines, TR3 (A, B) and TP41 (C, D), of Prx3-nlacZ transgenic mice were sagittally sliced and stained as whole mount preparations for β-galactosidase histochemistry. c, cortex; cb, cerebellum; H, hypothalamus; OB, olfactory bulb. Inset in (D) shows nuclear β-galactosidase staining in cells in the cortex. Bar, 50 μm.

Almost all Schwann cells in the sciatic nerves displayed *LacZ* expression (Fig. 57C). Teased fibres of sciatic nerve showed that all myelinated internodes observed had Schwann cells with positively stained nuclei (Fig. 57D). Expression was also observed in the dorsal and ventral roots but not in the dorsal root ganglia (Fig. 57B). The brain of Prx1-nlacZ transgenic mice showed strong expression of the transgene in the choroid plexus (Fig. 57A) and weaker staining in the cerebellum, inferior colliculus, and thalamus. These results indicate that the neural silencer is not in the first intron of the *periaxin* gene.

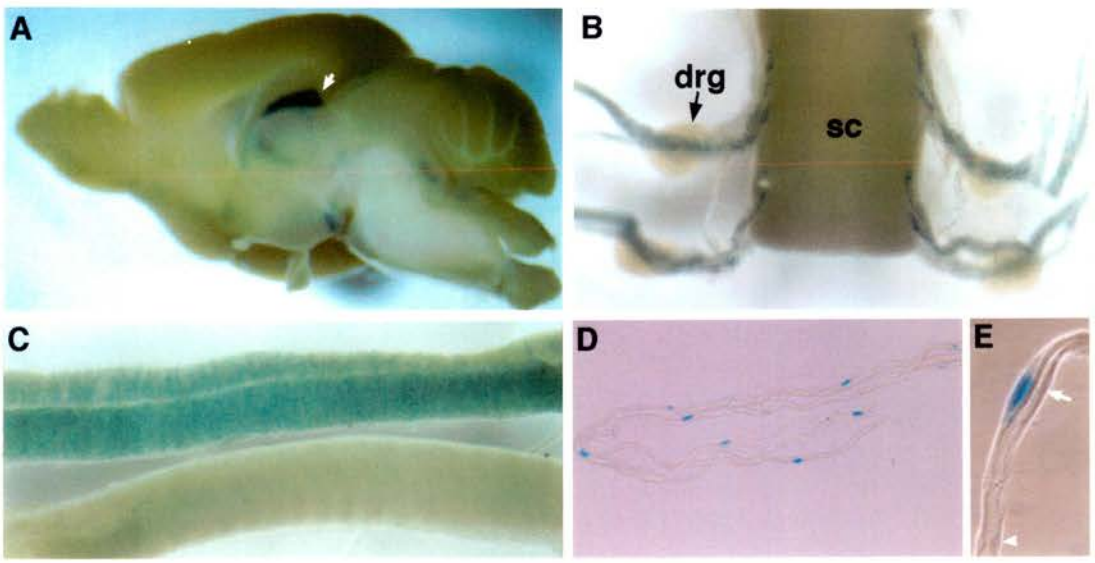

Figure 57. Prx1-nlacZ expression in the CNS and PNS. Tissues from line TV1 Prx1-nlacZ transgenic mice were stained as whole mount preparations for β-galactosidase. In the brain (A) strong labeling is evident in the choroid plexus (arrow), with weaker labeling in the thalamus, cerebellum and inferior colliculus. In the PNS, the ventral roots are stained (B) but not the spinal cord (sc) or the dorsal root ganglia (arrow). A β-galactosidase-positive sciatic nerve from TV1 (C; top nerve) is compared with a control sciatic nerve (C; lower nerve). Teased sciatic nerve fibres have positively stained nuclei (D; low magnification, E; high magnification, arrow- myelin sheath; arrowhead- Schmidt-Lanterman incisure).

3.5.7 Summary

Experiments to analyse the regulation of the *periaxin* gene were undertaken by generating transgenic mice. Four constructs were prepared from the *periaxin* gene using *LacZ* as a reporter gene. The constructs were initially used in transient transfection experiments to evaluate expression in Schwann cells and a fibroblast cell line. The results from the transfections were inconclusive because I was not able to reproduce the phenotype of a myelin-forming Schwann cell in culture in order to best compare the expression of the transgenes with that of fibroblasts. But the transfection experiments did show that the promoter constructs could drive the expression of the *LacZ* gene. Also it is known that the requirements for tissue-specific expression in cultured cells do not necessarily reflect the requirements in transgenic mice (Hoyle et al., 1994).

Transgenic mice were generated from three of the *periaxin* gene constructs. Analysis of five lines of mice with the Prx2-nlacZ transgene where *LacZ* was driven by 5.5 kb of the *periaxin* promoter showed that regulatory elements were missing for correct PNS expression even though there was some expression in myelin-forming Schwann cells. Analysis of other tissues for β–galactosidase expression also demonstrated that a neural silencer was very likely present in some part of the *periaxin* gene because the transgene was expressed in the CNS. The pattern of CNS expression was different in each line examined. Variation in expression within lines is frequently observed due to the influence of surrounding sequences in different chromosomal sites in which the transgene is inserted (Bonnerot et al., 1990). Analysis of mice expressing the Prx1-nlacZ transgene which contained the first intron of the *periaxin* gene showed similar results to the Prx2-lacZ transgenics with respect to CNS expression indicating that a neural silencer was not present in the first intron. One line of Prx1-nLacZ transgenic mice showed correct PNS expression in myelin-forming Schwann cells. Mice expressing the transgene driven by 2 kb of the *periaxin* promoter also expressed the transgene in the CNS but in contrast to

Prx2-nlacZ transgenics these mice did not show any PNS expression suggesting that more than 2 kb of the *periaxin* promoter may be necessary to drive any Schwann cell expression.

Discussion

4. DISCUSSION

In this thesis the stage at which L-periaxin and S-periaxin mRNA and protein are expressed in developing peripheral nerve was established. L-periaxin is developmentally regulated and relocates during development to the abaxonal surface of the Schwann cell-axon unit. The protein has a cortical localization in mature Schwann cells but in embryonic Schwann cells it is targeted to the nucleus. The basic domain of L-periaxin was shown to be responsible for nuclear targeting. A PDZ domain was identified in the extreme N-terminus of both S- and L-periaxin which is likely to be at least partly responsible for the association of L-periaxin with the plasma membrane of the Schwann cell. The regulation of the *periaxin* gene was studied by transgenesis by which it was shown that a region 5.5 kb upstream from the transcription initiation site could direct expression to myelinating Schwann cells. The expression of the reporter gene in cells of the central nervous system indicates the presence of a neural silencer in the *periaxin* gene.

4.1 Periaxin, PDZ proteins and signalling

Immunogold localization of L-periaxin demonstrated that during early myelination the protein is concentrated in the abaxonal and adaxonal membranes of the Schwann cell but as myelin sheaths mature it becomes concentrated in the abaxonal plasma membrane. Therefore, after the active phase of myelination L-periaxin is lost from the periaxonal membranes. This shift may reflect some functional or structural change in the periaxonal collar during sheath maturation and suggests that L-periaxin may be involved in membrane-protein interactions that serve to stabilize the myelin sheath. Nevertheless, at all stages of myelination L-periaxin was present at the Schwann cell plasma membrane apposing the basal lamina. This cortical localization of L-periaxin along with the presence of a PDZ domain in the N-terminus suggests that the protein may be involved in signalling

mechanisms at the plasma membrane which in early developmental stages might reflect axon-glial signalling.

Proteins involved in signalling cascades often contain protein-protein interaction domains that promote the assembly of macromolecular complexes. These specialized regions include Src homology (SH2 and SH3) domains, pleckstrin-homology (PH) domains, phosphotyrosine-binding (PTB) domains, and PDZ domains. Many proteins with PDZ domains, or that interact with PDZ proteins, localize to the plasma membrane and interact with the cytoplasmic tails of membrane proteins. Biochemical evidence suggests that the PDZ domain functions as a protein-binding module that mediates interactions between intracellular complexes and plasma membrane receptors (Sheng, 1996). Therefore PDZ domain proteins may provide a structural framework for recruiting proteins into membrane-bound complexes as has been shown for PSD-95, which mediates K^+ channel (Kim et al., 1995) and NMDA receptor clustering (Kornau et al., 1995).

Thus far, it has been suggested that PDZ domains have two major functions, primarily on the basis of their interactions with plasma membrane proteins and their presence in known signalling molecules such as *dlg* tumour suppressor protein (Fanning and Anderson, 1996), neuronal nitric oxide synthase (Brenman et al., 1996) and the FAP-1 protein tyrosine phosphatase (Sato et al., 1995). First, PDZ proteins may act as organizers of cortical transduction complexes in which the domain serves as a scaffold on which the macromolecular signalling complex is assembled. These complexes have been termed transducisomes (Tsunoda et al., 1997). Secondly, they may function as linker proteins that structurally and functionally connect transmembrane proteins with the actin cytoskeleton via actin-binding proteins such as protein 4.1 (Lue et al., 1994). The cytoskeleton association of L-periaxin based on its insolubility in non-ionic detergent was important in the initial identification of this protein (Gillespie et al., 1994).

PDZ domains are believed to share a common three-dimensional structure which has recently been determined for the third PDZ domain of PSD-95 and which has been shown to interact with a sequence found at the carboxy-terminus of certain plasma membrane proteins (Doyle et al., 1996). Binding occurs through a β-sheet-antiparallel interaction whereby the carboxy-terminal amino acid of the transmembrane protein fits into a hydrophobic pocket in the folded PDZ module at the carboxylate binding loop which is formed by the βB strand and the αB helix. Although the complementary binding site for some PDZ domains is the consensus peptide sequence (S/T)XV, others recognize somewhat different sequences and can even form homophilic clusters with the PDZ domains of other proteins (Songyang et al., 1997). The divergence of the periaxin PDZ domain in the C-terminal carboxylate binding loop, particularly within the GLGF sequence that lines the peptide-binding groove suggests that periaxin may represent a new type of PDZ protein with a distinct binding specificity.

PDZ domains have been organized into two groups based on the identity of the first residue in the αB helix (αB1) (Songyang et al., 1997). This residue confers binding specificity at the -2 position of the binding peptide. Group I PDZ domains have a basic residue at the αB1 position and the subgroup IA are those domains with a histidine in this position. Group II PDZ domains lack a basic residue at αB1. Periaxin falls into Group II with a tyrosine residue at position 77 in the αB region (αB1) (Fig. 58, depicted as yellow boxes). The PDZ domain of neuronal nitric oxide synthase (nNOS) also has a tyrosine residue at position 77 in the sequence (αB1) and has been shown to bind tightly to peptides ending in D-X-V (Stricker et al., 1997). Preference for aspartic acid at the -2 peptide position was mediated by Y^{77} and when the sequence $Y^{77}D^{78}$ was changed to $H^{77}E^{78}$ the binding specificity of peptide was altered from D-X-V to T-X-V (Stricker et al., 1997). Because periaxin has the identical residue at position αB1 as nNOS it seems highly likely that the protein with which periaxin interacts has a C-terminal D-X-V/X motif. Although

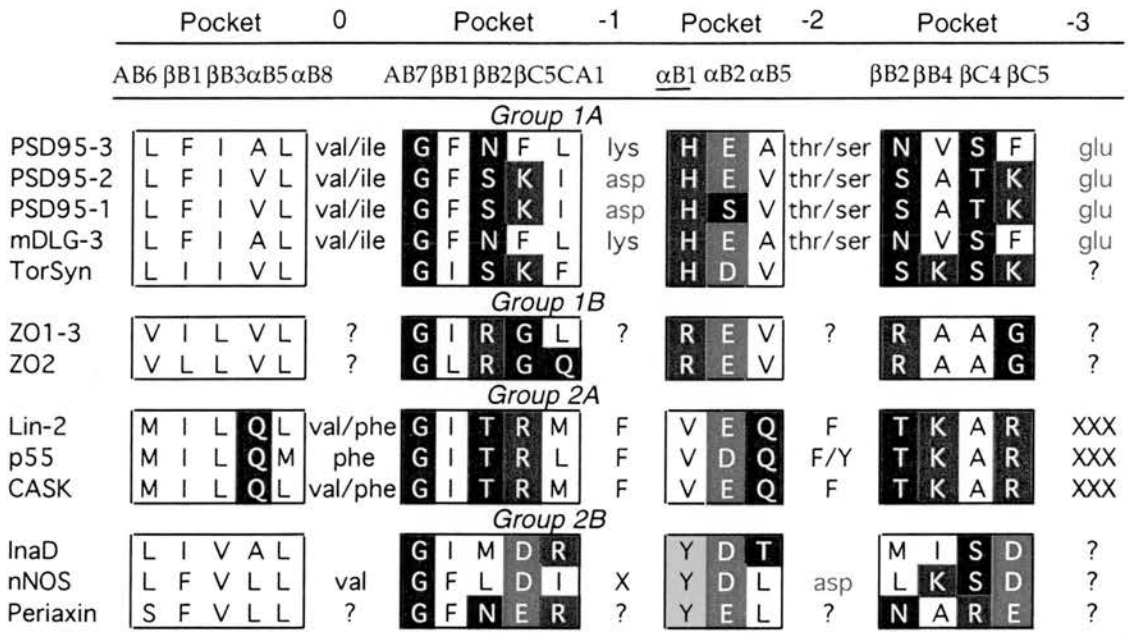

Figure 58. Position of the amino acids in the PDZ domains of different proteins that are likely to bind to the C-terminal sequence of their binding partners. Basic residues-blue, acidic residues- red, hydrophilic residues- green, hydrophobic residues-white. Modified from Songyang et al., 1997.

the PDZ domain of periaxin differs in the carboxylate binding loop from other PDZ proteins it appears that most of the residues which comprise the pocket at position 0 (which select valine) are highly conserved except for the residue at position AB6 (serine) which may account for a different binding specificity at position 0 (V/X) when compared to other PDZ domains.

The identification of a PDZ domain in the periaxin proteins is a significant step forward in progress to determining the function not only of periaxin but also of other PDZ domain-containing proteins. This PDZ domain may either participate in the membrane-protein interactions that are required to promote spiralization or it may function in recruiting proteins to a cortical scaffold important in transmembrane signalling. S-periaxin is not concentrated at the plasma membrane but is distributed throughout the cytoplasm of the Schwann cell suggesting that its PDZ domain may not be sufficient to ensure cortical targeting. Indeed this may reflect an entirely distinct function for this smaller isoform. The unique C-terminus of S-periaxin may target the protein away from the plasma membrane. Another possibility is that the functional periaxin PDZ domain is larger than the consensus domain. The consensus PDZ domain contains approximately 80 amino acids. The third PDZ domain of PSD-95 is functionally active as a 101 amino acid polypeptide but the functional nNOS PDZ domain requires an additional 30 amino acids (Stricker et al., 1997). The PDZ domain of periaxin encompasses amino acids 14 to 98 and the S-periaxin isoform is 148 amino acids in length. Thus it is possible that the periaxin PDZ domain requires a longer sequence than the minimum PDZ domain to promote binding specificity.

Although most PDZ proteins are localized to the cell cortex, there is an increasing recognition that they do not always function at the plasma membrane. A possible role in in nuclear signalling has been suggested by the fact that the tight junction-associated protein Z0-1 localizes to the nucleus before it is recruited to sites of cell-cell contact (Gottardi et al., 1996). Another example is SIP-1, a nuclear

binding partner for the transcriptional factor SRY, which is a PDZ protein that is thought to participate in a macromolecular transcription complex (Poulat et al., 1997).

4.2 Nuclear targeting of L-periaxin

The classical nuclear import pathway involves two steps: NLS-dependent binding to the nuclear pore complex followed by energy-dependent translocation through the pore (Newmeyer and Forbes, 1988; Richardson et al., 1988). NLS-dependent binding occurs in the cytoplasm through a NLS receptor which is comprised of a heterodimer composing importin-α (or α-karyopherin) and importin-β (or β-karyopherin) (reviewed in Görlich and Mattaj, 1996; Nigg, 1997). First the NLS binds to the importin-α subunit then the entire complex docks at the nuclear pore whereby the importin-β subunit binds to nucleoporins. The translocation of the complex through the nuclear pore occurs by an energy-dependent process which involves the GTPase Ran/TC4 (Moore and Blobel, 1993). In addition NLS-independent and importin-independent pathways have also been described but their mechanisms are still unclear (Fagotto et al., 1998).

L-periaxin is mainly localized to the nucleus in embryonic Schwann cells. Transient expression of L-periaxin in several cell lines including primary Schwann cells also revealed nuclear localization of the protein. The basic domain of L-periaxin was shown to be responsible for nuclear targeting and was sufficient to target GFP to the nucleus. Nuclear translocation was shown to require energy indicating that it is an active process. Indeed, it is unlikely that nuclear translocation is the result of diffusion for a protein of a molecular mass of 147 kDa such as L-periaxin. Small proteins can diffuse through the nuclear pore complex but proteins above 40 to 60 kDa are prevented and can only enter the nucleus in an active manner (Görlich and Mattaj, 1996). Therefore an active transport process through the nuclear pore complex usually requires a NLS although a "piggyback"

mechanism can occur in which a protein enters the nucleus by interacting with a NLS-containing protein (Dingwall et al., 1982). Examination of the deduced amino acid sequence of the basic domain of L-periaxin revealed two putative NLSs, one in a lysine-rich region, the other enriched in arginine residues. There is also another region of 10 amino acids that has 50% lysine and arginine residues content and lies between the two former regions. Mutation of two of the lysine residues in one putative NLS did not abolish nuclear import. It is possible that the two remaining lysines along with the stretch of arginines or the third arginine/lysine-rich region can still act as a bipartite NLS. Therefore it will be interesting to mutate all four lysines and then examine nuclear import as well as mutating the arginines. It remains to be determined whether any of these putative NLSs can direct nuclear entry on their own.

4.3 Cell-cell contact, nuclear localization and signalling

Nuclear localization in heterologous cells was shown to be regulated by cell-cell contact. L-periaxin was targeted to the nucleus when cells were grown at low density but not at high density. Therefore cell contact inhibited nuclear translocation and one signal for nuclear translocation may be the loss of cell-cell contact. This was shown to be the case *in vitro* because wounding the monolayer generated cell-free areas in which adjacent cells were observed with nuclear accumulation of L-periaxin. This result raises the possibility that cell density in embryonic nerve versus postnatal nerve may regulate nucleocytoplasmic distribution of the protein.

The nuclear accumulation of L-periaxin in embryonic Schwann cells is sharply developmentally regulated and by E17.5 nuclear L-periaxin is no longer observed. In embryonic nerve Schwann cells envelop many axons but at around postnatal-day 1 they form a 1:1 relationship with axons. A transitional stage in this process may occur at E17.5 just prior to the Schwann cell singling out an axon to

ensheathe. Axonal signals may regulate this event and L-periaxin may be involved in this signalling. The Schwann cell is always in close contact with axons. Therefore, the only other cell-cell contact that this cell has is with itself when it surrounds an axon and with other Schwann cells at the node of Ranvier where their microvilli interdigitate. It is possible that this "autotypic" contact inhibits nuclear accumulation of L-periaxin.

Because cells in low density cultures are dividing more frequently than cells in high density cultures it is possible that cell proliferation may be responsible for nuclear accumulation. This appears unlikely because the peak of DNA synthesis in Schwann cells *in vivo* occurs between E19 and E20 in the rat (Stewart et al., 1993) which is just after the time when nuclear L-periaxin is lost. Therefore nuclear expression of L-periaxin does not correlate with cell proliferation.

Perhaps the most attractive hypothesis to explain the nuclear localization of L-periaxin in embryonic Schwann cells may be in the context of its binding to a plasma membrane protein via the PDZ domain. It is possible that this "binding partner" is not expressed before E17.5 in which case L-periaxin is translocated to the nucleus by default. In the presence of this "binding partner", L-periaxin is prevented from nuclear translocation and is tethered to the plasma membrane. Therefore when L-periaxin is transfected into heterologous cells, in the absence of its "binding partner", it is transported to the nucleus. It will of course be very interesting to identify the protein which binds to the PDZ domain of periaxin and determine if its expression pattern correlates with this hypothesis. Other PDZ proteins are found in cell nuclei. ZO-1 translocates to the nucleus in response to inhibition of cell-cell contact (Gottardi et al., 1996), hDlg (human discs large) localizes to cell nuclei as well as sites along membranes and p55 localizes to the nucleus of epithelial cells (Lutchman et al., 1997). Several membrane-associated proteins such as the focal adhesion localizing protein zyxin and the adherens junction-associated protein β-catenin have been shown to exhibit transient nuclear

localization (Fagotto et al., 1998). The functional significance of the nuclear translocation of these proteins is as yet unknown but they may modulate signalling pathways from the plasma membrane to the nucleus.

4.4 The phenotype of embryonic Schwann cells

The phenotypes of myelin-forming and non-myelin-forming Schwann cells are quite distinct in the adult. However the nature of the precise signals that determine this divergence of fate are still not clear. I was interested to determine if there were phenotypic differences in embryonic Schwann cells which might indicate if their fate were predetermined. Because L-periaxin is a gene expressed exclusively by myelin-forming Schwann cells in the adult PNS and is expressed in embryonic Schwann cells well before myelination and the expression of myelin specific genes, it was a candidate as a marker for embryonic cells destined for a myelin-forming fate. On the other hand, P0 is expressed widely in embryonic Schwann cells regardless of their fate and is even expressed in satellite cells of the DRG. It has been suggested that there may be a P0 inhibitory signal which regulates *P0* gene expression in non-myelin-forming cells later in development (Lee et al., 1997). The *P0* gene is expressed at much higher levels in the embryo than L-periaxin therefore Lee and co-workers were able to detect two distinct populations of cells expressing P0 mRNA: these were cells with basal levels in the embryo and cells with much higher levels during myelination. When the amounts of L-periaxin mRNA in cells of the predominantly non-myelin-forming sympathetic trunk were compared with cells in a nerve trunk that becomes myelinated, a significant difference in expression levels was detected indicating that L-periaxin like P0 may be expressed at basal levels in embryonic Schwann cells destined not to myelinate. L-periaxin was also expressed in cells in the embryonic gut wall which are probably enteric glia, but, in contrast to P0, L-periaxin is not expressed in DRG satellite cells. Therefore the satellite cells of the DRG appear to have a distinct phenotype when compared to other types of

Schwann cells. Interestingly, in the *ErbB3* null mutant, all Schwann cells in peripheral nerves and enteric glia were absent but DRG satellite cells differentiated normally, indicating that the ErbB3 receptor is not responsible for the regulation of satellite cell development and that these cells may comprise a distinct Schwann cell lineage.

The transcription factor Krox-20 is expressed only in Schwann cells that are myelin-forming in the adult and is expressed in the embryonic Schwann cells that are destined to be myelin-forming. Krox-20 is first expressed at around E15.5 in sciatic nerve (Topilko et al., 1994) which is later than L-periaxin. Interestingly as was found for L-periaxin, the satellite cells of the DRG do not express Krox20 *in vivo* but when these cells are put into culture Krox-20 expression is induced which suggests that negative regulation restricts Krox20 expression in satellite cells *in vivo* (Topilko et al., 1996). Therefore embryonic DRG satellite cells have a distinct phenotype from Schwann cells, they are L-periaxin$^-$, Krox-20$^-$, P0$^+$, S100$^+$ and are unlike non-myelin-forming Schwann cells as demonstrated by the phenotype of the *ErbB3* mutant mouse (Riethmacher et al., 1997).

4.5 L-periaxin expression in skeletal muscle

L-periaxin mRNA and protein are detected in embryonic skeletal muscle cells at the same time that the mRNA and protein are detected in peripheral nerves. The expression was shown to be specific because of the absence of skeletal muscle expression in the *periaxin* null mutant embryo. The protein is developmentally regulated in muscle cells and its localization closely resembles that in Schwann cells in that it is detected in the cortical region of the cell and in the nucleus in the embryo but postnatally it is only localized at the cell cortex. Unlike the pattern of Schwann cell expression, L-periaxin was not expressed in all skeletal muscle cells at any time point examined and its appearance was transient. This raised the possibility that L-periaxin is expressed in a skeletal muscle stem cell or satellite cell and it will be

particularly interesting to determine if L-periaxin is re-expressed in muscle during regeneration after injury.

4.6 Gene regulation and silencing

To elucidate the molecular mechanisms that are involved in PNS myelination it is important to analyze the transcriptional regulatory components of Schwann cell-specific genes. The generation of transgenic mice constitutes a powerful means of examining the molecular mechanisms of gene regulation *in vivo*. I sought to identify DNA sequences in the *periaxin* gene that are sufficient to direct Schwann cell-specific expression. Transfection experiments demonstrated that all of the constructs were expressed in both Schwann cells and heterologous cells. We proceeded with the generation of transgenic mice in spite of these results because the requirements in cultured cells and transgenic mice are in some cases different. In retrospect, these transfection results demonstrate that the regulatory elements necessary to restrict expression to Schwann cells were not present in any of the periaxin-LacZ constructs tested which is what was later observed by transgenesis. On the other hand, 2 kb of the *periaxin* promoter was sufficient for Schwann cell expression in cultured Schwann cells but Schwann cells expression was not observed by transgenesis indicating that the Schwann cell transfection paradigm used in these studies does not adequately reflect the *in vivo* situation.

Transgenic mice were produced using different *periaxin-LacZ* constructs. I was able to show that correct PNS expression may require more than 2 kb of the *periaxin* promoter indicating the presence of a transcriptional regulatory element between -2 kb and -5.5 kb that is required for Schwann cell expression. However additional transgenic lines will have to be analyzed to be certain that the 2 kb promoter is not sufficient for PNS expression. Using 5.5 kb of the *periaxin* promoter only partial PNS expression was observed suggesting that regulatory elements which enhance *periaxin* expression were missing. When the first intron of the

periaxin gene was included in the construct with the 5.5 kb promoter one transgenic line showed correct PNS expression. It is known that introns can play a role in facilitating transcription by 10 to 100-fold in transgenic mice (Brinster et al., 1988). The first intron of the *periaxin* gene very likely contains an enhancer element which increases Schwann cell-specific expression.

Introns also are known to contain gene silencing elements and negative regulation of neuronal gene transcription has been described for an increasing number of neuronal genes (Hoyle et al., 1994; Kallunki et al., 1995; Wuenschell et al., 1990). Many studies have shown that the deletion of certain regulatory regions from constructs in which neuronal-specific expression was expected resulted in expression in non-neuronal cells. This has been shown for the superior cervical ganglion 10 (SCG-10) gene (Wuenschell et al., 1990), the type II sodium channel gene (Chong et al., 1995), and the nicotinic acetylcholine receptor β2 subunit gene (Bessis et al., 1997) among others. A consensus neural restrictive silencer element (NRSE) was identified and a zinc finger protein known as neural restrictive silencer factor (NRSF) or RE-1-silencing transcription factor (REST) was shown to bind to NRSE and silence NRSE-containing genes in non-neuronal cells (Chong et al., 1995; Schoenherr and Anderson, 1995). REST is expressed in most non-neuronal cells and in neuronal precursors but is down-regulated in neurons during development. Recent studies have revealed REST in specific regions of the adult rat brain suggesting that it acts as a negative regulator and counteracts positive regulators to modulate gene expression in neurons as well as non-neuronal cells (Palm et al., 1998). The L1 gene which is expressed by both neurons and Schwann cells has recently been shown to contain a NRSE which is located in the second intron (Kallunki et al., 1997). For optimal silencing in non-neural cells it was found that sequences in the first intron were required along with the promoter and the NRSE in the second intron. Other transcriptional repressive elements have been identified and recently a novel repressive element in the GAP-43 gene, the nNOS gene, and a

25 kDA synaptosomal-associated protein gene has been described which is located downstream of the TATA box (Weber and Skene, 1997). Repressive elements may also regulate transcription of the myelin *PLP* gene. Transfection studies demonstrated that the first intron is required for oligodendrocyte specificity (Wight and Dobretsova, 1997). In an even more complex example, transgenic mice generated with different 5' regions of the dopamine β-hydroxylase gene demonstrated that tissue-specific expression is mediated by positive regulatory elements while negative elements refine the cell-specific expression to the appropriate neurons (Hoyle et al., 1994).

Transgenic mice generated using all three *periaxin-lacZ* constructs showed CNS expression of the transgene. This indicates that negative regulation may also play a role in modulating *periaxin* gene expression. Transgenic mice generated with the Prx1-nlacZ construct which included sequences from the entire first intron also displayed CNS expression indicating that the sequences which silence expression in the CNS are not located in the 4.9 kb first intron or in the 5.5 kb proximal promoter. The second intron (88 nt) and the third intron (116 nts) are relatively small but the fourth (2.9 kb) and the fifth (7.5 kb) introns are considerably larger. These two large introns are the obvious places in which to look for a NRSE in future work. The data from these transgenic mice experiments indicate that periaxin gene regulation is complex and involves regulatory elements located upstream, within the first intron and in as yet unidentified regions.

FUTURE WORK

The identification of a PDZ domain in periaxin opens up an exciting area of future work. Since PDZ proteins are believed to act as organizers of transduction complexes and function as scaffolds on which macromolecular signalling complexes are assembled, it is important to identify the other components of the periaxin signalling complex or transducisome. The first step in unraveling this complex would be to identify the polypeptide(s) which bind(s) to the periaxin PDZ domain. Other binding partners for PDZ proteins have been identified using the yeast two-hybrid system with the PDZ domain as bait (Nishimune et al., 1996). It will also be interesting to see if the periaxin PDZ domain has unique structural features which might explain the cytoplasmic localization of the smaller isoform. Therefore once the binding partner is found it will be possible to see if the functional periaxin PDZ domain requires amino acids in addition to the identified consensus sequence.

The sequence responsible for nuclear targeting of L-periaxin can be identified by further deletion and mutation experiments. Because the detergent-insolubility of nuclear L-periaxin suggests that it is binding to some nuclear component it will be particularly interesting to see if it binds to DNA. This could be determined by DNA footprinting experiments. It will also be interesting to explore the significance of the nuclear localization of L-periaxin in the embryo.

It will be important to perform transection experiments on adult mice in which the cervical sympathetic trunk is transected and examined at a later time point to detect if loss of axonal contact in non-myelin-forming cells results in the expression of L-periaxin mRNA at a basal level as has been shown to occur for P0. This type of experiment may be able to definitively answer the question whether L-periaxin is a marker for embryonic Schwann cells in peripheral nerves destined to myelinate.

The *periaxin* gene is essential for normal peripheral nerve function (Gillespie et al., paper in preparation). The transcriptional elements responsible for Schwann cell-specific expression of *periaxin* are important to identify and further fine mapping of the 5' positive regulatory elements necessary for Schwann cell expression which are probably located in the -2 kb to -5.5 kb region will be essential. The negative regulatory elements which suppress CNS expression will also be important to identify in the context of this myelin gene as well as for our understanding of gene regulation in the PNS in general. This work provides a basis for these future studies which will help to characterize the requirements for the regulation of *periaxin* which is now known to be an essential gene for the assembly and stability of the Schwann cell-axon unit in the vertebrate peripheral nervous system.

References

REFERENCES

Adams, C. W. M., Davidon, A. N., and Gregson, N.A. (1963). Enzyme inactivity of myelin: histochemical and biochemical evidence. J. Neurochem. *10*, 383-395.

Adlkofer, K., Frei, R., Neuaberg, D. H., Zielasek, J., Toyka, K. V., and Suter, U. (1997). Heterozygous peripheral myelin protein 22- deficient mice are affected by a progressive demyelinating peripheral neuropathy. J. Neurosci. *17*, 4662-4671.

Adlkofer, K., Martini, R., Aguzzi, A., Zielasek, J., Toyka, K. V., and Suter, U. (1995). Hypermyelination and demyelinating peripheral neuropathy in *Pmp22*-deficient mice. Nature Genet. *11*, 274-280.

Agrawal, H. C., and Agrawal, D. (1991). Proteolipid protein and DM-20 are synthesized by Schwann cells, present in myelin membrane, but they are not fatty acylated. Neurochem. Res. *16*, 855-858.

Aguayo, A. J., Chavron, L., and Bray, G. M. (1976). Potential of Schwann cells from unmyelinated nerves to produce myelin: a quantitative ultrastructural and radiographic study. J. Neurocytol. *5*, 565-573.

Ali, S. A., and Steinkasserer, A. (1995). PCR-ligation-PCR-mutagenesis: a protocol for creating gene fusions and mutations. Biotechniques *18*, 746-750.

Allinquant, B., Staugaitis, S. M., D'Urso, D., and Colman, D. R. (1991). The ectopic expression of myelin basic protein isoforms in Shiverer oligodendrocytes: implications for myelinogenesis. J. Cell Biol. *113*, 393-403.

Anderson, T. J., Montague, P., Nadon, N., Nave, K.-A., and Griffiths, I. R. (1997). Modification of Schwann cell phenotype with PLP transgenes: evidence that the PLP and DM20 isoproteins are targeted to different cellular domains. J. Neurosci. Res. *50*, 13-22.

Anzini, P., Neuberg, D. H., Schachner, M., Nelles, E., Willecke, K., Zielasek, J., Toyka, K., Suter, U., and Martini, R. (1997). Structural abnormalities and deficient maintenance of peripheral nerve myelin in mice lacking the gap junction protein connexin32. J. Neurosci. *17*, 4545-4561.

Arquint, M., Roder, J., Chia, L. S., Down, J., Wilkinson, D., Bayley, H., Braun, P., and Dunn, R. (1987). Molecular cloning and primary structure of myelin-associated glycoprotein. Proc. Natl. Acad. Sci. USA *84*, 600-604.

Aruga, J., Okano, H., and Mikoshiba, K. (1991). Identification of the new isoforms of mouse myelin basic protein: the existence of exon 5a. J. Neurochem. *56*, 1222-1226.

Baechner, D., Liehr, T., Hameister, H., Altenberger, H., Grehel, H., Suter, U., and Rautenstrauss, B. (1995). Widespread expression of the peripheral myelin protein-22 gene (PMP22) in neural and non-neural tissues during murine development. J. Neurosci. Res. *42*, 733-741.

Bansal, R., Warrington, A. E., Gard, A. L., Ranscht, B., and Pfeiffer, S. E. (1990). Characterization of monoclonal antibodies O1, O4, R-mAb used in the analysis of oligodendrocyte development. Ann. N.Y. Acad. Sci. *605*, 409-411.

Barbarese, E., Carson, J. H., and Braun, P. E. (1978). Accumulation of the four myelin basic proteins in the mouse brain during development. J. Neurochem. *31*, 779-782.

Barbu, M. (1990). Molecular cloning of cDNAs that encode the chicken P0 protein: evidence for early expression in avians. J. Neurosci. Res. *25*, 143-151.

Baroffio, A., Dupin, E., and Le Douarin, N. M. (1988). Clone-forming ability and differentiation potential of migratory neural crest cells. Proc. Natl. Acad. Sci. USA *85*, 5325-5329.

Barton, D. E., Arquint, M., Roder, J., Dunn, R., and Francke, U. (1987). The myelin-associated glycoprotein gene: mapping to human chromosome 19 and mouse chromosome 7 and expression in quivering mice. Genomics *1*, 107-112.

Bergoffen, J., Scherer, S. S., Wang, S., Scott, M. O., Bone, L. J., Paul, D. L., Chen, K., Lensch, M. W., Chance, P. F., and Fischbeck, K. H. (1993). Connexin mutations in X-linked Charcot-Marie-Tooth disease. Science *262*, 2039-2042.

Bermingham, J. R. J., Scherer, S. S., O'Connell, S., Arroyo, E., Kalla, K. A., Powell, F. L., and Rosenfeld, M. G. (1996). Tst-1/Oct-6/SCIP regulates a unique step in peripheral myelination and is required for normal respiration. Genes Dev. *10*, 1751-1762.

Berryman, M. A., Porter, W. R., Rodewald, R. D., and Hubbard, A. L. (1992). Effects of tannic acid on antigenicity and membrane contrast in ultrastructural immunocytochemistry. J. Histochem. Cytochem. *40*, 845-857.

Bessis, A., Champtiaux, N., Chatelin, L., and Changeux, J. P. (1997). The neuron-restrictive silencer element: a dual enhancer/silencer crucial for patterned expression of a nicotinic receptor gene in the brain. Proc. Natl. Acad. Sci. USA *94*, 5906-5911.

Bhattacharyya, A., Frank, E., Ratner, N., and Brackenbury, R. (1991). P0 is an early marker of the Schwann cell lineage in chickens. Neuron *7*, 831-844.

Billings-Gagliardi, S., Webster, H. d. F., and O'Connell, M. F. (1974). *In vivo* and electron microscopic observations in Schwann cells in developing tadpole nerve fibers. Am. J. Anat. *141*, 375-392.

Blanchard, A. D., Sinanan, A., Parmantier, E., Zwart, R., Broos, L., Meijer, D., Meier, C., Jessen, K. R., and Mirsky, R. (1996). Oct-6 (SCIP/Tst-1) is expressed in Schwann cell precursors, embryonic Schwann cells, and postnatal myelinating Schwann cells: comparison with Oct-1, Krox-20, and Pax-3. J. Neurosci. Res. *46*, 630-640.

Boll, F. (1877). Studi sulle imagini microscopiche della fibra nervosa midollare. Atti Accad. Naz. Lincei Rc. Ser. *3 (I)*, 75.

Bollensen, E., and Schachner, M. (1987). The peripheral myelin glycoprotein P0 expresses the L2/HNK-1 and L3 carbohydrate structures shared by neural adhesion molecules. Neurosci. Lett. *82*, 77-82.

Bonnerot, C., Grimber, G., Briand, P., and Nicolas, J.-F. (1990). Patterns of expression of position-dependent integrated transgenes in mouse embryo. Proc. Natl. Acad. Sci. USA *87*, 6331-6335.

Bosio, A., Binczek, E., Haupt, W. F., and Stoffel, W. (1998). Composition and biophysical properties of myelin lipid define the neurological defects in galactocerebroside- and sulfatide-deficient mice. J. Neurochem. *70*, 308-315.

Bosio, A., Binczek, E., and Stoffel, W. (1996). Functional breakdown of the lipid bilayer of the myelin membrane in central and peripheral nervous system by disrupted galactocerebroside synthesis. Proc. Natl. Acad. Sci. USA *93*, 13280-13285.

Braun, P. E., Sandillon, D., Edwards, A., Matthieu, J. M., and Privat, A. (1988). Immunocytochemical localization by electron microscopy pf 2',3'-cyclic nucleotide 3'-phosphodiesterase in developing oligodendrocytes of normal and mutant brain. J. Neurosci. *8*, 3057-3066.

Breeuwer, M., and Goldfarb, D. S. (1990). Facilitated nuclear transport of histone H1 and other small nucleophilic proteins. Cell *60*, 999-1008.

Brenman, J. E., Chao, D. S., Gee, S. H., McGee, A. W., Craven, S. E., Santillano, D. R., Wu, Z. Q., Huang, F., Xia, H. H., Peters, M. F., Froehner, S. C., and Bredt, D. S. (1996). Interaction of nitric-oxide synthase with the postsynaptic density protein PSD-95 and α-1-syntrophin mediated by PDZ domains. Cell *84*, 757-767.

Brinster, R. L., Allen, J. M., Behringer, R. R., Gelinas, R. E., and Palmiter, R. D. (1988). Introns increase transcriptional efficiency in transgenic mice. Devel. Biol. *85*, 836-840.

Brockes, J. P., Lemke, G. E., and Balzer, D. R. J. (1980). Purification and preliminary characterization of a glial growth factor from the bovine pituitary. J. Biol. Chem. *255*, 8374-8377.

Brockes, J. P., Raff, M. C., Nishiguchi, D. J., and Winter, J. (1980). Studies on cultured rat Schwann cells. III. Assays for peripheral myelin proteins. J. Neurocytol. *9*, 67-77.

Brophy, P. J., Boccaccio, G. L., and Colman, D. R. (1993). The distribution of myelin basic protein mRNAs within myelinating oligodendrocytes. Trends Neurosci. *16*, 515-521.

Brostoff, S. W., Karkhanis, Y. D., Carlo, D. J., Reuter, W., and Eylar, E. H. (1975). Isolation and partial charcterization of the major proteins of rabbit sciatic nerve myelin. Brain Res. *86*, 449-458.

Brown, A., and Lemke, G. (1997). Multiple regulatory elements control transcription of the peripheral myelin protein zero gene. J. Biol. Chem. 272, 28939-28947.

Bruzzone, R., White, T. W., Scherer, S. S., Fischbeck, K. H., and Paul, D. L. (1994). Null mutations of connexin 32 in patients with X-linked Charcot-Marie-Tooth disease. Neuron *13*, 1253-1260.

Bunge, M. B. (1993). Schwann cell regulation of extracellular matrix biosynthesis and assembly. In Peripheral Neuropathy, P. J. Dyck, P. K. Thomas, J. Griffin, P. A. Low and J. Poduslo, eds. (Philadelphia: W.B. Saunders), pp. 299-316.

Bunge, M. B., Clark, M. B., Dean, A. C., Eldridge, C. F., and Bunge, R. P. (1990). Schwann cell function depends upon axonal signals and basal lamina components. Ann. N.Y. Acad. Sci. *580*, 281-287.

Burden, S., and Yarden, Y. (1997). Neuregulins and their receptors: a versatile signaling module in organogenesis and oncogenesis. Neuron *18*, 847-855.

Campagnoni, A. T., Pribyl, T. M., Campagnoni, C. W., Kampf, K., Amur-UmarJee, S., Landry, C. F., Handley, V. W., Newman, S. L., Garbay, B., and Kitamura, K. (1993). Structure and developmental expression of Golli-mbp, a 105-kilobase gene that encompasses the myelin basic protein gene and is expressed in cells in the oligodendrocyte lineage in the brain. J. Biol. Chem. *286*, 4930-4938.

Carenini, S., Montag, D., Cremer, H., Schachner, M., and Martini, R. (1997). Absence of the myelin-associated glycoprotein (MAG) and the neural cell adhesion molecule (N-CAM) interferes with the maintenance, but not with the formation of peripheral myelin. Cell Tissue Res. *287*, 3-9.

Carrasco, D., and Bravo, R. (1994). In situ hybridization of frozen sections using ^{35}S-labeled riboprobes. In Cell Biology: A Laboratory Handbook, J. E. Celis, ed. (London: Academic Press), pp. 466-476.

Carraway, K. L. I., and Burden, S. J. (1995). Neuregulins and their receptors. Curr. Opin. Neurobiol. *5*, 606-612.

Carraway, K. L. I., and Cantley, L. C. (1994). A neu acquaintance for erbB3 and erbB4: a role for receptor heterodimerization in growth signaling. Cell *78*, 5-8.

Carson, J. H., Worboys, K., Ainger, K., and Barbarese, E. (1997). Translocation of myelin basic protein mRNA in oligodendrocytes requires microtubules and kinesin. Cell Motil. Cytoskel. *38*, 318-328.

Carson, J. I., Nielson, M. L., and Barbarese, E. (1983). Developmental regulation of myelin basic protein expression in mouse brain. Devel. Biol. *96*, 485-492.
542

Carter, B. D., Kaltschmidt, C., Kaltschmidt, B., Offenhauser, N., Bohm-Mattaei, R., Baeuerle, P. A., and Barde, Y. A. (1996) Selective activation of NF-kappa B by nerve growth factor through the neurotrophin receptor p75. Science 272, 542-545.

Chance, P. F., Alderson, M. K., Leppig, K. A., Lensch, M. W., Matsunami, N., Smith, B., Swanson, P. D., Odelberg, S. J., Disteche, C. M., and Bird, T. D. (1993). DNA deletion associated with hereditary neuropathy with liability to pressure palsies. Cell *72*, 143-151.

Chiu, S. Y., and Richie, J. M. (1980). Potassium channels at nodal and internodal axonal membrane of mammalian myelinated fibres. Nature *284*, 170-171.

Cho, K. O., Hunt, C. A., and Kennedy, M. B. (1992). The rat brain post-synaptic density fraction contains a homolog of the Drosophila Discs-Large tumor suppressor protein. Neuron *9*, 929-942.

Chong, J. A., Tapia-Ramírez, J., Kim, S., Toledo-Aral, J. J., Zheng, Y., Boutros, M. C., Altshuller, Y. M., Frohman, M. A., Kraner, S. D., and Mandel, G. (1995). REST: a mammalian silencer protein that restricts sodium channel gene expression to neurons. Cell *80*, 949-957.

Coetzee, T., Fujita, N., Dupree, J., Shi, R., Blight, A., Suzuki, K., and Popko, B. (1996). Myelination in the absence of galactocerebroside and sulfatide: normal structure with abnormal function and regional instability. Cell *86*, 209-219.

Colman, D. R., Kreibich, G., Frey, A. B., and Sabatini, D. D. (1982). Synthesis and incorporation of myelin polypeptides into CNS myelin. J. Cell Biol. *95*, 598-608.

Cox, H. K., Deleon, D. V., Angerer, L. M., and Angerer, R. C. (1984). Detection of mRNAs in sea urchin embryos by *in situ* hybridization using asymmetric RNA probes. Dev. Biol. *101*, 485-502.

Curtis, R., Stewart, H. J. S., Hall, S. M., Wilkin, G. P., Mirsky, R., and Jessen, K. R. (1992). GAP-43 is expressed by nonmyelin-forming Schwann cells of the peripheral nervous system. J. Cell Biol. *116*, 1455-1464.

D'Eustachio, P., Colman, D. R., and Salzer, J. L. (1988). Chromosomal location of the mouse gene that encodes the myelin-associated glycoproteins. J. Neurochem. *50*, 589-593.

D'Urso, D., Brophy, P. J., Staugaitus, S. M., Gillespie, C. S., Frey, A. B., Stempak, J. G., and Colman, D. R. (1990). Protein zero of peripheral nerve myelin: biosynthesis, membrane insertion and evidence for homotypic interaction. Neuron *2*, 449-460.

D'Urso, D., and Müller, H. W. (1997). Ins and outs of peripheral myelin protein-22: mapping transmembrane topology and intracellular sorting. J. Neurosci. Res. *49*, 551-562.

D'Urso, D., Prior, R., Greiner-Petter, R., Gabreels-Festen, A. A. W. M., and Muller, H. W. (1998). Overloaded endoplasmic reticulum-Golgi compartments, a possible pathomechanism of peripheral neuropathies caused by mutations of the peripheral myelin protein PMP22. J. Neurosci. *18*, 731-740.

Daniloff, J. K., Levi, G., Grumet, M., Reiger, R., and Edelman, G. M. (1986). Altered expression of neuronal cell adhesion molecules induced by nerve injury and repair. J. Cell Biol. *103*, 929-945.

Davies, A. M. (1998). Neuronal survival: early dependence on Schwann cells. Curr. Biol. *8*, R15-R18.

Davis, J. Q., Lambert, S., and Bennett, V. (1996). Molecular composition of the node of Ranvier: identification of ankyrin-binding cell adhesion molecules neurofasin (mucin+/Third FNIII domain-) and NrCAM at nodal axon segments. J. Cell Biol. *135*, 1355-1367.

de Ferra, F., Engh, H., Hudson, L., Kamholz, J., Puckett, C., Molineaux, S., and Lazzarini, R. A. (1985). Alternative splicing accounts for the four forms of myelin basic protein. Cell *43*, 721-727.

Debellard, M. E., Tang, S., Mukhopadhyay, G., Shen, Y. J., and Filbin, M. T. (1996). Myelin-associated glycoprotein inhibits axonal regeneration from a variety of neurons via interaction with a sialoglycoprotein. Mol. Cell. Neurosci. *7*, 89-101.

Devereaux, J. P., Haeberli, P., and Smithies, O. (1984). A comprehensive set of sequence analysis programs for the VAX. Nucl. Acids Res. *12*, 387-395.

DeWaegh, S. M., Lee, V. M. Y., and Brady, S. T. (1992). Local modulation of neurofilament phosphorylation, axonal caliber, and slow axonal-transport by myelinating Schwann cells. Cell *68*, 451-463.

Dieperink, M. E., O'Neill, A., Magnoni, G., Wellman, R. L., Heinrikson, R. L., Zurcher-Neely, H. A., and Stefansson, K. (1992). SAG: A Schwann cell membrane glycoprotein. J. Neurosci. *12*, 2177-2185.

Ding, Y., and Brunden, K. R. (1994). The cytoplasmic domain of myelin protein P0 interacts with negatively charged phospholipid bilayers. J. Biol. Chem. *269*, 10764-10770.

Dingwall, C., Sharnick, S. V., and Laskey, R. A. (1982). A polypeptide domain that specifies migration of nucleoplasmin into the nucleus. Cell *30*, 449-458.

Dong, Z., Brennan, A., Liu, N., Yarden, Y., Lefkowitz, G., Mirsky, R., and Jessen, K. R. (1995). Neu differentiation factor is a neuron-glia signal and regulates survival, proliferation, and maturation of rat Schwann cell precursors. Neuron *15*, 585-596.

Doyle, D. A., Lee, A., Lewis, J., Kim, E., Sheng, M., and MacKinnon, R. (1996). Crystal structures of a complexed and peptide-free membrane protein-binding domain: Molecular basis of peptide recognition by PDZ. Cell *85*, 1067-1076.

Dugandzija-Novakovic, S., Koszowski, A. G., Levinson, S. R., and Shrager, P. (1995). Clustering of sodium channels and node of Ranvier formation in remyelinating axons. J. Neurosci. *15*, 492-502.

Duncan, I. D., Hammang, J. P., and Trapp, B. D. (1987). Abnormal compact myelin in the myelin-deficient rat: absence of proteolipid protein correlates with a defect in the intraperiod line. Proc. Natl. Acad. Sci. USA *84*, 6287-6291.

Dupin, E., Baroffio, A., Dulac, C., Cameron-Curry, P., and Le Douarin, N. M. (1990). Schwann-cell differentiation in clonal cultures of the neural crest, as evidenced by the anti-Schwann cell myelin protein monoclonal antibody. Proc. Natl. Acad. Sci. USA *87*, 1119-1123.

Dupin, E., Ziller, C., and Le Douarin, N. M. (1998). The avian embryo as a model in developmental studies: chimeras and *in vitro* clonal analysis. In Curr. Top. in Dev. Biol., F. de Pablo, A. Ferrús and C. Stern, eds.: Academic Press), pp. 1-35.

Dyck, P. J., Chance, P., Lebo, R., and Carney, J. A. (1993). Hereditary motor and sensory neuropathies. In Peripheral Neuropathy, P. J. Dyck, P. K. Thomas, J. W. Griffin, P. A. Low and J. F. Poduslo, eds. (Philadelphia: W.B. Saunders), pp. 1094-1136.

Dytrych, L., Sherman, D. L., Gillespie, C. S., and Brophy, P. J. (1998). Two PDZ proteins encoded by the murine periaxin gene are the result of alternative intron

retention and are differentially targeted in Schwann cells. J. Biol. Chem. *273*, 5794-5800.

Edelman, G. M. (1983). Cell adhesion molecules. Science *219*, 450-457.

Eichberg, J., and Iyer, S. (1996). Phosphorylation of myelin proteins: recent advances. Neurochem. Res. *21*, 527-535.

Einheber, S., Zanazzi, G., Ching, W., Scherer, S. S., Milner, T. A., Peles, E., and Salzer, J. L. (1997). The axonal membrane protein Caspr, a homologue of Neurexin IV, is a component of the septate-like paranodal junctions that assemble during myelination. J. Cell Biol. *139*, 1495-1506.

Everly, J. L., Brady, R. O., and Quarles, R. H. (1973). Evidence that the major protein of rat sciatic nerve myelin is a glycoprotein. J. Neurochem. *21*, 329.

Fabrizi, C., Kelly, B. M., Gillespie, C. S., Schlaepfer, W. W., Scherer, S. S., and Brophy, P. J. (1997). Transient expresion of the neurofilament proteins NF-L and NF-M by Schwann cells is regulated by axonal contact. J. Neurosci. Res. *50*, 291-299.

Fagotto, F., Glück, U., and Gumbiner, B. M. (1998). Nuclear localization signal-independent and importin/karyopherin-independent nuclear import of β-catenin. Curr. Biol. *8*, 181-190.

Fanning, A. S., and Anderson, J. M. (1996). Protein-protein interactions - PDZ domain networks. Curr. Biol. *6*, 1385-1388.

Fannon, A. M., Sherman, D. L., Ilyina-Gragerova, G., Brophy, P. J., Friedrich, V. L., and Colman, D. R. (1995). Novel E-cadherin-mediated adhesion in peripheral nerve:Schwann cell architecture is stabilized by autotypic adherens junctions. J. Cell Biol. *129*, 189-202.

Felgner, J., Martin, M., Tsai, Y., and Felgner, P. L. (1993). Cationic lipid-mediated transfection in mammalian cells: "Lipofection". J. Tiss. Cult. Meth. *15*, 63-68.

Fernandez-Valle, C., Gorman, D., Gomez, A. M., and Bunge, M. B. (1997). Actin plays a role in both changes in cell shape and gene expression associated with Schwann cell myelination. J. Neurosci. *17*, 241-250.

Figlewicz, D. A., Quarles, R. H., Johnson, D., Barbarash, G. R., and Sternberger, N. H. (1981). Biochemical demonstration of the myelin- associated glycoprotein in the peripheral nervous system. J. Neurochem. *37*, 749-758.

Filbin, M. T., and Tennekoon, G. I. (1993). Both P0-molecules must be glycosylated for homophilic adhesion. J. Cell Biol. *122*, 451-459.

Filbin, M. T., and Tennekoon, G. I. (1990). High level of expression of the myelin protein P0 in Chinese hamster ovary cells. J. Neurochem. *55*, 500-505.

Filbin, M. T., and Tennekoon, G. I. (1993). Homophilic adhesion of the myelin P0 protein requires glycosylation of both molecules in the homophilic pair. J. Cell Biol. *122*, 451-459.

Filbin, M. T., and Tennekoon, G. I. (1991). The role of complex carbohydrates in adhesion of the myelin protein, P0. Neuron *7*, 845-855.

Filbin, M. T., Walsh, F. S., Trapp, B. D., Pizzey, J. A., and Tennekoon, G. I. (1990). Role of myelin P0 protein as a homophilic adhesion molecule. Nature *344*, 871-872.

Fraher, J. P. (1978). Quantitative studies on the maturation of central and peripheral parts of individual ventral motoneuron axons. I. Myelin sheath and axon calibre. J. Anat. *126*, 509-522.

Frail, D. E., and Braun, P. E. (1984). Two developmentally regulated messenger RNAs differing in their coding region may exist for the myelin associated glycoprotein. J. Biol. Chem. *259*, 14857-14863.

Frail, D. E., Webster, H. d. F., and Braun, P. E. (1985). Developmental expression of the myelin-associated glycoprotein in the peripheral nervous system is different from that in the central nervous system. J. Neurochem. *45*, 1308-1310.

Frank, E., and Sanes, J. R. (1991). Lineage of neurons and glia in chick dorsal root ganglia: analysis *in vivo* with a recombinant retrovirus. Development *111*, 895-908.

Fraser, S. E., and Bronner-Fraser, M. (1991). Migrating neural crest cells in the trunk of the avian embryo are multipotent. Development *112*, 913-920.

Friede, R. L., and Samorajski, T. (1967). Relation between the number of myelin lamellae and axon circumference in fibers of vagus and sciatic nerves of mice. J. Comp. Neurol. *130*, 223-231.

Fruttiger, M., Montag, D., Schachner, M., and Martini, R. (1995). Crucial role for the myelin associated glycoprotein in the maintenance of axon-myelin assembly. Eur. J. Neurosci. *7*, 511-515.

Fujita, N., Sato, S., Kurihara, T., Kuwano, R., Sakimura, K., Inuzuka, T., Takahashi, Y., and Miyatake, T. (1989). cDNA cloning of mouse myelin-associated glycoprotein: a novel alternative splicing pattern. Biochim. Biophys. Res. Commun. *165*, 1162-1169.

Garbern, J. Y., Cambi, F., Tang, X.-M., Sima, A. A. F., Vallat, J. M., Bosch, E. P., Lewis, R., Shy, M., Sohi, J., Kraft, G., Chen, K. L., Joshi, I., Leonard, D. G. B., Johnson, W., Raskind, W., Dlouhy, S. R., Pratt, V., Hodes, M. E., Bird, T., and Kamholz, J. (1997). Proteolipid protein is necessary in peripheral as well as central myelin. Neuron *19*, 205-218.

Gassmann, M., Casagranda, F., Orioli, D., Simon, H., Lai, C., Klein, R., and Lemke, G. (1995). Aberrant neural and cardiac development in mice lacking the ErbB4 neuregulin receptor. Nature *378*, 390-394.

Gavrilovic, J., Brennan, A., Mirsky, R., and Jessen, K. R. (1995). Fibroblast growth factors and insulin growth factors combine to promote survival of rat Schwann cell precursors without induction of DNA synthesis. Eur. J. Neurosci. *7*, 77-85.

Geren, B. B. (1954). The formation from the Schwann cell surface of myelin in peripheral nerves of chick embryos. Exp. Cell. Res. *7*, 558.

Ghabriel, M. N., and Allt, G. (1981). Incisures of Schmidt-Lanterman. Prog. Neurobiol. *17*, 25-58.

Giese, K. P., Martini, R., Lemke, G., Soriano, P., and Schachner, M. (1992). Mouse P0 gene disruption leads to hypomyelination, abnormal expression of recognition molecules and degeneration of myelin and axons. Cell *71*, 565-576.

Gillespie, C. S., Lee, M., Fantes, J. F., and Brophy, P. J. (1997). The gene encoding the Schwann cell protein periaxin localises on mouse chromosome 7 (*Prx*). Genomics *41*, 297-298.

Gillespie, C. S., Sherman, D. L., Blair, G. E., and Brophy, P. J. (1994). Periaxin, a novel protein of myelinating Schwann cells with a possible role in axonal ensheathment. Neuron *12*, 497-508.

Goldfarb, D. S. (1988). Karyophilic peptides: applications to the study of nuclear transport. Cell Biol. Int. Rep. *12*, 809-832.

Görlich, D., and Mattaj, I. W. (1996). Nucleocytoplasmic transport. Science *271*, 1513-1518.

Gottardi, C. J., Arpin, M., Fanning, A. S., and Louvard, D. (1996). The junction-associated protein, zonula occludens-1, localizes to the nucleus before the maturation and during the remodeling of cell-cell contacts. Proc. Natl. Acad. Sci. USA *93*, 10779-10784.

Gould, R. M., Byrd, A. L., and Barbarese, E. (1995). The number of Schmidt-Lanterman incisures is more than doubled in *shiverer* PNS myelin sheaths. J. Neurocytol. *24*, 85-98.

Gould, R. M., and Mattingly, G. (1990). Regional localization of RNA and protein metabolism in Schwann cells *in vivo*. J. Neurocytol. *19*, 285-301.

Goulding, M. D., Chalepakis, G., Deutsch, U., Erselius, J. R., and Gruss, P. (1991). Pax-3, a novel murine DNA binding protein expressed during early neurogenesis. EMBO J. *10*, 135-147.

Gow, A., Friedrich, V. L. J., and Lazzarini, R. A. (1992). Myelin basic protein gene contains separate enhancers for oligodendrocyte and Schwann cell expression. J. Cell Biol. *119*, 605-616.

Greenfield, S., Brostoff, S., Eylar, E. H., and Morell, P. (1973). Protein composition of myelin of the peripheral nervous system. J. Neurochem. *20*, 1207-1216.

Griffin, J. W., Li, C. Y., Macko, C., Ho, T. W., Hsieh, S. T., Xue, P., Wang, F. A., Cornblath, D. R., McKhann, D. R., and Asbury, A. K. (1996). Early nodal changes in the acute motor axonal neuropathy pattern of the Guillain-Barré syndrome. J. Neurocytol. *25*, 33-51.

Griffiths, I. R., Dickinson, P., and Montague, P. (1995). Expression of the proteolipid protein gene in glial cells of the post-natal peripheral nervous system of rodents. Neuropath. Appl. Neurobiol. *21*, 97-110.

Griffiths, I. R., Mitchell, L. S., McPhilemy, K., Morrison, S., Kyriakides, E., and Barrie, J. A. (1989). Expression of myelin protein genes in Schwann cells. J. Neurocytol. *18*, 345-352.

Grinspan, J. B., Marchionni, M. A., Reeves, M., Coulaloglou, M., and Scherer, S. S. (1996). Axonal interactions regulate Schwann cell apoptosis in developing peripheral nerve: neuregulin receptors and the role of neuregulins. J. Neurosci. *16*, 6107-6118.

Hahn, A. F., Chang, Y., and Webster, H. d. F. (1987). Development of myelinated nerve fibers in the sixth cranial nerve of the rat: a quantitative electron microscope study. J. Comp. Neurol. *250*, 491-500.

Hall, S. M., and Williams, P. L. (1970). Studies on the 'incisures' of Schmidt and Lanterman. J. Cell Sci. *6*, 767-791.

Haney, C., Snipes, G. J., Shooter, E. M., Suter, U., Garcia, C., Griffin, J. W., and Trapp, B. D. (1996). Ultrastructural distribution of PMP22 in Charcot-Marie-Tooth disease type 1A. J. Neuropath. Exp. Neurol. *55*, 290-299.

Hardy, R. J., Lazzarini, R. A., Colman, D. R., and Friedrich, V. L. J. (1996). Cytoplasmic and nuclear localization of myelin basic proteins reveals heterogeneity among oligodendrocytes. J. Neurosci. Res. *46*, 246-257.

Harkin, J. C. (1964). A series of desmosomal attachments in the Schwann sheath of myelinated mammalian nerves. Z. Zellforsch. Mikrosk. Anat. *64*, 189-195.

Hayasaka, K., Himoro, M., Sato, W., Takada, G., Uyemura, K., Shimizu, N., Bird, T. D., Conneally, P. M., and Chance, P. F. (1993). Charcot-Marie-Tooth neuropathy type 1B is associated with muations of myelin P0 gene. Nature Genet. *5*, 31-34.

Hayasaka, K., Nanao, K., Tahara, M., Sato, W., Takada, G., Miura, M., and Uyemura, K. (1991). Isolation and sequence determination of cDNA encoding the major structural protein of human peripheral myelin. Biochem. Biophys. Res. Commun. *180*, 515-518.

He, X., Gerrero, R., Simmons, D. M., Park, R. E., Lin, C. R., Swanson, L. W., and Rosenfeld, M. G. (1991). Tst-1, a member of the POU domain gene family, binds the promoter of the gene encoding the cell surface adhesion molecule P0. Mol. Cell. Biol. *11*, 1739-1744.

He, X., Treacy, M. N., Simmons, D. M., Ingraham, H. A., Swanson, L. W., and Rosenfeld, M. G. (1989). Expression of a large family of POU-domain regulatory genes in mammalian brain development. Nature *340*, 35-42.

Henry, E. W., Cowen, J. S., and Sidman, R. L. (1983). Comparison of Trembler and Trembler-J mouse phenotypes: varying severity of peripheral hypomyelination. J. Neuropath. Exp. Neurol. *42*, 688-706.

Henry, E. W., and Sidman, R. L. (1988). Long lives for homozygous trembler mutant mice despite virtual absence of peripheral nerve myelin. Science *241*, 344-346.

Hilmi, S., Fournier, M., Valeins, H., Gandar, J. C., and Bonnet, J. (1995). Myelin P0 glycoprotein: identification of the site phosphorylated in vitro and in vivo by endogenous protein kinases. J. Neurochem. *64*, 902-907.

Hiscoe, H. B. (1947). The distribution of nodes and incisures in normal and regenerating nerve fibers. Anat. Rec. *99*, 447-476.

Hogan, B., Beddington, R., Costantini, F., and Lacy, E. (1994). Manipulating the Mouse Embryo: A Laboratory Manual, 2nd Edition: Cold Spring Harbor Laboratory Press).

Hoyle, G., Mercer, E. H., Palmiter, R. D., and Brinster, R. L. (1994). Cell-specific expression from the human dopamine β-hydroxylase promoter in transgenic mice is controlled via a combination of positive and negative regulatory elements. J. Neurosci. *14*, 2455-2463.

Ichimura, T., and Ellisman, M. H. (1991). Three-dimentional fine structure of cytoskeletal-membrane interactions at nodes of Ranvier. J. Neurocytol. *20*, 667-681.

Ikenaka, K., Katagawa, T., and Mikoshiba, K. (1992). Selective expression of DM-20, an alternatively spliced myelin proteolipid protein gene product, in developing nervous system and non-glial cells. J. Neurochem. *58*, 2248-2253.

Ionasescu, V., Searby, C., and Ionasescu, R. (1994). Point mutations of the connexin32 (GJB1) gene in X-linked dominant Charcot-Marie-Tooth neuropathy. Human Mol. Genet. *3*, 355-358.

Ishaque, A., Roomi, M. W., Szymanska, I., Kowalski, S., and Eylar, E. (1980). The P0 glycoprotein of peripheral nerve myelin. Can. J. Biochem. *58*, 913-921.
Itoh, M., Nagafuchi, A., Yonemura, S., Kitani-Yasuda, T., Tsukita, S., and Tsukita, S. (1993). The 220 kD protein colocalizing with cadherins in non-epithelial cells is identical to ZO-1, a tight junction-associated protein in epithelial cells: cDNA cloning and electron microscopy. J. Cell Biol. *121*, 491-502.

Jaegle, M., Mandemakers, W., Broos, L., Zwart, R., Karis, A., Visser, P., Grosveld, F., and Meijer, D. (1996). The POU factor Oct-6 and Schwann cell differentiation. Science *273*, 507-510.

Jessen, K. R., Brennan, A., Morgan, L., Mirsky, R., Kent, A., Hashimoto, Y., and Gavrilovic, J. (1994). The Schwann cell precursor and its fate: a study of cell death and differentiation during gliogenesis in rat embryonic nerves. Neuron *12*, 509-527.

Jessen, K. R., and Mirsky, R. (1992). Schwann cells: early lineage, regulation of proliferation and control of myelin formation. Curr. Opin. Neurobiol. *2*, 575-581.

Jessen, K. R., Mirsky, R., and Morgan, L. (1987). Axonal signals regulate the differentiation of non-myelin-forming Schwann cells: an immunohistochemical study of galactocerebroside in transected and regenerating nerves. J. Neurosci. *7*, 3362-3369.

Jessen, K. R., Morgan, L., Brammer, M., and Mirsky, R. (1985). Galactocerebroside is expressed by myelin-forming Schwann cells *in situ*. J. Cell Biol. *101*, 1135-1143.

Jin, J.-J., Nikitin, A. Y., and Rajewsky, M. F. (1993). Schwann cell lineage-specific *neu* (*erbB*-2) gene expression in the developing rat nervous system. Cell Growth Diff. *4*, 227-237.

Joe, E. H., and Angelides, K. (1992). Clustering of voltage-dependent sodium channels on axons depends on Schwann cell contact. Nature *356*, 333-335.

Johnson, P. W., Abramow-Newerly, W., Seilheimer, B., Sadoul, R., Tropak, M. B., Arquint, M., Dunn, R. J., Schachner, M., and Roder, J. C. (1989). Recombinant myelin-associated glycoprotein confers neural adhesion and neurite outgrowth function. Neuron *3*, 377-385.

Jordan, M., Schallhorn, A., and Wurm, F. M. (1996). Transfecting mammalian cells: optimization of critical parameters affecting calcium-phosphate precipitate formation. Nucleic Acids Research *24*, 596-601.

Kalderon, D., Roberts, B., Richardson, W., and Smith, A. (1984). A short amino acid sequence able to specify nuclear localization. Cell *39*, 499-509.

Kallunki, P., Edelman, G. M., and Jones, F. S. (1997). Tissue-specific expression of the L1 cell adhesion molecule is modulated by the neural restrictive silencer element. J. Cell Biol. *138*, 1343-1354.

Kallunki, P., Jenkinson, S., Edelman, G. M., and Jones, F. S. (1995). Silencer elements modulate the expression of the gene for the neuron-glia adhesion molecule, Ng-CAM. J. Biol. Chem. *270*, 21291-21298.

Kaplan, M. R., Meyer-Franke, A., Lambert, S., Vennett, V., Duncan, I. D., Levinson, S. R., and Barres, B. A. (1997). Induction of sodium channel clustering by oligodendrocytes. Nature *386*, 724-728.

Kelly, B. M., Gillespie, C. S., Sherman, D. L., and Brophy, P. J. (1992). Schwann cells of the myelin-forming phenotype express neurofilament protein NF-M. J. Cell Biol. *118*, 397-410.

Kidd, G. J., Andrews, S. B., and Trapp, B. D. (1994). Organization of microtubules in myelinating Schwann cells. J. of Neurocytol. *23*, 801-810.

Kim, E., Niethammer, M., Rothschild, A., Jan, Y. N., and Sheng, M. (1995). Clustering of Shaker-type K^+ channels by interaction with a family of membrane-associated guanylate kinases. Nature *378*, 85-88.

Kimura, M., Sato, M., Akatsuka, A., Nozawa-Kimura, S., Takahashi, R., Yokoyama, M., Nomura, T., and Katsuki, M. (1989). Restoration of myelin formation by a single type of myelin basic protein in transgenic *shiverer* mice. Proc. Natl. Acad. Sci. USA *86*, 5661-5665.

Kioussi, C., Gross, M. K., and Gruss, P. (1995). Pax3: a paired domain gene as a regulator in PNS myelination. Neuron *15*, 553-562.

Kioussi, C., and Gruss, P. (1996). Making of a Schwann. Trends Genet. *12*, 84-86.

Kirschner, D. A., and Ganser, A. L. (1980). Compact myelin exists in the absence of basic protein in the Shiverer mutant mouse.. Nature *283*, 207-209.

Kirschner, D. A., and Ganser, A. L. (1982). Myelin labelled with mercuric chloride:Asymmetric localization of phosphatidylethanolamine plasmalogen. J. Mol. Biol. *157*, 635-658.

Kirschner, D. A., Ganser, A. L., and Caspar, D. L. D. (1984). Diffraction studies of molecular organization and membrane interactions in myelin. In Myelin, P. Morell, ed. (New York: Plenum Press), pp. 51-95.

Kitamura, K., Newman, S. L., Campagnoni, C. W., Verdi, J. M., Mohandas, T., Handley, V. W., and Campagnoni, A. T. (1990). Expression of a novel transcript of the myelin basic protein gene. J. Neurochem. *54*, 2032-2041.

Kitamura, K., Suzuki, M., and Uyemura, K. (1976). Purification and partial characterization of two glycoproteins in bovine peripheral nerve myelin membrane. Biochim. Biophys. Acta. *455*, 806-816.

Klugmann, M., Schwab, M. H., Pühlhofer, A., Schnieder, A., Zimmermann, F., Griffiths, I. R., and Nave, K.-A. (1997). Assembly of CNS myelin in the absence of proteolipid protein. Neuron *18*, 59-70.

Kordeli, E., Lambert, S., and Bennett, V. (1995). AnkyrinG: a new ankyrin gene with neural-specific isoforms localized at the axonal initial segment and node of Ranvier. J. Biol. Chem. *270*, 2352-2359.

Kornau, H. C., Schenker, L. T., Kennedy, M. B., and Seeburg, P. H. (1995). Domain interaction between NMDA receptor subunits and the postsynaptic density protein PSD-95. Science *269*, 1737-1740.

Kozak, M. (1996). Interpreting cDNA sequences: some insights from studies on translation. Mammalian Genome *7*, 563-574.

Kruse, J., Mailhammer, R., Wernecke, H., Faissner, A., Sommer, I., Goridis, C., and Schachner, M. (1984). Neural cell adhesion molecules and myelin-associated glycoprotein share a common carbohydrate moiety recognized by monoclonal antibodies L2 and HNK-1. Nature *311*, 153-155.

Kulkens, T., Bolhuis, P. A., Wolterman, R. A., Kemp, S., te Nijenhuis, S., Valentijn, L. J., Hensels, G. W., Jennekens, F. G. I., de Visser, M., Hoogendijk, J. E., and Baas, F. (1993). Deletion of the serine 34 codon from the major peripheral myelin protein P0 gene in Charcot-Marie-Tooth disease type 1B. Nature Genet. *5*, 35-39.

Künemund, V., Jungalwala, F. B., Fischer, G., Chou, D. K. H., Keilhauer, G., and Schachner, M. (1988). The L2/HNK-1 carbohydrate of neural cell adhesion molecules is involved in cell interactions. J. Cell Biol. *106*, 213-223.

Lai, C., Brow, M. A., Nave, K. A., Noronha, A. B., Quarles, R. H., Bloom, F. E., Milner, R. J., and Sutcliffe, J. G. (1987). Two forms of 1B236/myelin-associated glycoprotein, a cell adhesion molecule for post-natal neural development, are produced by alternative splicing. Proc. Natl. Acad. Sci. USA *84*, 4337-4341.

Landry, C. F., Ellison, J. A., Pribyl, T. M., Campagnoni, C., Kampf, K., and Campagnoni, A. T. (1996). Myelin basic protein gene expression in neurons: developmental and regional changes in protein targeting within neuronal nuclei, cell bodies and processes. J. Neurosci. *16*, 2452-2462.

Lanford, R. E., White, R. G., Dunham, R. G., and Kanda, P. (1988). Effect of basic and nonbasic amino acid sunstitutions on transport induced by simian virus 40 T-antigen synthetic peptide nuclear transport signals. Mol. Cell Biol. *8*, 2722-2729.

Langley, J. N., and Anderson, H. K. (1903). On the union of the fifth cervical nerve with the superior cervical ganglion. J. Physiol. *30*, 439-442.

Lanterman, A. J. (1877). Ueber den feineren Bau der Markhaltigen Nervenfasern. Arch. Mikrosk. Anat. *13*, 1.

LeBlanc, A. C., and Poduslo, J. F. (1990). Axonal modulation of myelin gene expression in the peripheral nerve. J. Neurosci. Res. *26*, 317-326.

LeDouarin, N. M. (1993). Embryonic neural chimeras in the study of brain development. Trends Neurosci. *16*, 64-72.

LeDouarin, N. M. (1982). The Neural Crest (Cambridge: Cambridge University Press).

LeDouarin, N. M., and Smith, J. (1988). Development of the peripheral nervous system from the neural crest. Annu. Rev. Cell Biol. *4*, 375-404.

Lee, K. F., Simon, H., Chen, H., Bates, B., Hung, M. C., and Hauser, C. (1995). Requirement for neuregulin receptor erbB2 in neural and cardiac development. Nature *378*, 394-398.

Lee, M.-J., Brennan, A., Blanchard, A., Zoidl, G., Dong, Z., Tabemero, A., Zoidl, C., Dent, M. A. R., Jessen, K. R., and Mirsky, R. (1997). P0 is constitutively expressed in the rat neural crest and embryonic nerves and is negatively and positively regulared by axons to generate non-myelin-forming and myelin-forming Schwann cells, respectively. Mol. Cell. Neurosci. *8*, 336-350.

Lees, M. B., and Brostoff, S. W. (1984). Proteins of Myelin. In Myelin, P. Morell, ed. (New York: Plenum Press), pp. 197-224.

Lemke, G. (1992). Myelin and myelination. In An introduction to molecular neurobiology, Z. W. Hall, ed. (Sunderland, MA: Sinauer Associates, Inc.), pp. 281-309.

Lemke, G., and Axel, R. (1985). Isolation and sequence of a cDNA encoding the major structural protein of peripheral myelin. Cell *40*, 501-508.

Lemke, G., and Chao, M. (1988). Axons regulate Schwann cell expression of the major myelin and NGF receptor genes. Development *102*, 499-504.

Lemke, G., Lamar, E., and Patterson, J. (1988). Isolation and analysis of the gene encoding peripheral myelin protein zero. Neuron *1*, 73-83.

Lemke, G. E., and Brockes, J. P. (1984). Identification and purification of glial growth factor. J. Neurosci. *4*, 75-83.

Levi, A. D., Bunge, R. P., Lofgren, J. A., Meima, L., Hefti, F., Nikolics, K., and Sliwkowski, M. X. (1995). The influence of heregulins on human Schwann cell proliferation. J. Neurosci. *15*, 1329-1340.

Li, C., Tropak, M. B., Gerial, R., Clapoff, S., Abramow-Newerly, W., Trapp, B., Peterson, A., and Roder, J. (1994). Myelination in the absence of myelin-associated glycoprotein. Nature *369*, 747-750.

Lodish, H., Baltimoe, D., Berk, A., Zipursky, S. L., Matsudaira, P., and Darnell, J. (1995). Organelle Biogenesis: the mitochondrion, chloroplast, peroxisome and nucleus. In Molecular Cell Biology (New York: Scientific American Books), pp. 843.

Loring, J. F., and Erickson, C. A. (1987). Neural crest pathways in the trunk of the chick embryo. Dev. Biol. *121*, 220-236.

Lue, R., Marfatia, S. M., Branton, D., and Chishti, A. H. (1994). Cloning and characterization of hdlg: the human homolog of the *Drosophila* discs-large tumour suppressor binds to protein 4.1. Proc. Natl. Acad. Sci. USA *91*, 9818-9822.

Lunn, E. R., Scourfield, J., Keynes, R. J., and Stern, C. (1887). The neural tube origin of ventral root sheath cells in the chick embryo. Development *101*, 247-254.

Lupski, J. R., Montes de Oca-Luna, R., Slaugenhaupt, S., Pentau, L., Guzzetta, V., Trask, B. J., Saucedo-Cardenas, O., Barker, D. F., Killian, J. M., Garcia, C. A., Chakravarti, A., and Patel, P. I. (1991). DNA duplication associated with Charcot-Marie-Tooth disease type 1A. Cell *66*, 219-232.

Lutchman, M., Peel, D., Kim, A. C., Bryant, P. J., and Chishti, A. H. (1997). Nuclear localization of protein 4.1 and the MAGUK family members p55 and hDlg. Mol. Biol Cell *8*, 1021.

MacGarry, R. C., Helfand, S. L., Quarles, R. H., and Roder, J. C. (1983). Recognition of myelin-associated glycoprotein by the monoclonal antibody HNK-1. Nature *306*, 376-379.

Maggio, B., and Yu, R. K. (1992). Modulation by glycosphingolipids of membrane-membrane interaction induced by myelin basic protein and mellitin. Biochim. Biophys Acta. *112*, 105-114.

Magyar, J. P., Martini, R. R., T., Aguzzi, A., Adkofer, K., Dembic, Z., Zielasek, J., Toyka, K. V., and Suter, U. (1996). Impaired differentiation of Schwann cells in transgenic mice with increased *PMP22* gene dosage. J. Neurosci. *16*, 5351-5360.

Manfioletti, G., Ruaro, M. E., Del Sal, G., Philipson, L., and Schneider, C. (1990). A growth arrest-specific (gas) gene codes for a membrane protein. Mol. Cell Biol. *10*, 2924-2930.

Marchionni, M. A., Goodearl, A. D. J., Chen, M. S., Bermingham-McDonogh, O., Kirk, C., Hendricks, M., Danehy, F., Misumi, D., Sudhalter, J., Kobayashi, K., Wroblewski, D., Lynch, C., Baldassare, M., Hiles, I., Davis, J. B., Hsuan, J. J., Totty, N. F., Otsu, M., McBurney, R. N., Waterfield, M. D., Stroobant, P., and Gwynne, D. (1993). Glial growth factors are alternatively spliced erbB2 ligands expressed in the nervous system. Nature *362*, 312-318.

Martenson, R. E., and Uyemura, K. (1992). Myelin P2, a neuritogenic member of the family of cytoplasmic lipid-binding proteins. In Myelin: Biology and Chemistry, R. E. Martenson, ed: (CRC Press), pp.509-528.

Martini, R., Mohajeri, M. H., Kasper, S., Giese, K. P., and Schachner, M. (1995). Mice doubly deficient in the genes for P0 and myelin basic protein show that both proteins contribute to the formation of the major dense line in peripheral nerve myelin. J. Neurosci. *15*, 4488-4495.

Martini, R., and Schachner, M. (1986). Immunoelectron microscopic localization of neural cell adhesion molecules (L1, N-CAM, and MAG) and their shared carbohydrate epitope and myelin basic protein in developing sciatic nerve. J. Cell Biol. *103*, 2439-2448.

Martini, R., and Schachner, M. (1988). Immunoelectron microscopic localization of neural cell adhesion molecules (L1, N-CAM, and myelin-associated glycoprotein) in regenerating adult mouse sciatic nerve. J. Cell Biol. *106*, 1735-1746.

Matsunami, N., Smith, B., Ballard, L., Lensch, M. W., Robertson, M., Albertson, H., Hanemann, C. O., Muller, H. W., Bird, T. D., White, R., and Chance, P. F. (1992). Peripheral myelin protein-22 gene maps in the duplication in chromosome 17p11.2 associated with Charcot-Marie-Tooth 1A. Nature Genet. *1*, 159-165.

McKerracher, L., David, S., Jackson, D. L., Kottis, V., Dunn, R. J., and Braun, P. E. (1994). Identification of myelin-associated glycoprotein as a major myelin-derived inhibitor of neurite growth. Neuron *13*, 805-811.

Meijer, D., Graus, A., Kraay, R., Langeveld, A., Mulder, M. P., and Grosveld, G. (1989). The octamer binding-factor Oct-6: cDNA cloning and expression in early embryonic cells. Nucl. Acids Res. *18*, 7357-7365.

Mendz, G. L. (1992). Structure and molecular interactions of myelin basic protein and its antigenic peptides. In Myelin: Biology and Chemistry, R. E. Martenson, ed.: (CRC Press), pp. 277-366.

Menegoz, M., Gaspar, P., Le Bert, M., Galvez, T., Burgaya, F., Palfrey, C., Ezan, P., Arnos, F., and Girault, J.-A. (1997). Paranodin, a glycoprotein of neuronal paranodal membranes. Neuron *19*, 319-331.

Messing, A., Behringer, R. R., Hammang, J. P., Palmiter, R. D., Brinster, R. L., and Lemke, G. (1992). P0 promoter directs expression of reporter and toxin genes to Schwann cells of transgenic mice. Neuron *8*, 507-520.

Messing, A., Behringer, R. R., Wrabetz, L., Hammang, J. P., Lemke, G., Palmiter, R. D., and Brinster, R. L. (1994). Hypomyelinating peripheral neuropathies ans schannomas in transgenic mice expressing SV40 T-antigen. J. Neurosci. *14*, 3533-3539.

Meyer, D., and Birchmeier, C. (1995). Multiple essential functions of neuregulin in development. Nature *378*, 386-390.

Meyer, D., Yamaai, T., Gattatt, A., Riethmacher-Sonnenberg, E., Kane, D., Theill, L. E., and Birchmeier, C. (1997). Isoform-specific expression and function of neuregulin. Development *124*, 3575-3586.

Mi, H., Deerinck, T. J., Ellisman, M. H., and Schwartz, T. L. (1995). Differential distribution of closely related potassium channels in rat Schwann cells. J. Neurosci. *15*, 3761-3774.

Mirsky, R., Dubois, C., Morgan, L., and Jessen, K. R. (1990). O4 and A007-sulfatide antibodies bind to embryonic Schwann cells prior to the appearance of galactocerebroside; regulation of the antigen by axon-Schwann cell signals and cyclic AMP. Development *109*, 105-116.

Mirsky, R., and Jessen, K. R. (1996). Schwann cell development, differentiation and myelination. Curr. Opin. Neurobiol. *6*, 89-96.

Mirsky, R., Winter, J., Abney, E. R., Pruss, R. M., J., G., and Raff, M. C. (1980). Myelin-specific proteins and glycolipids in rat Schwann cells and oligodendrocytes. J. Cell Biol. *84*, 483-494.

Molineaux, S. M., Engh, H., de Ferra, F., Hudson, L., and Lazzarini, R. A. (1986). Recombination within the myelin basic protein gene created the dysmyelinating shiverer mouse mutation. Proc. Natl. Acad. Sci. USA *83*, 7542-7546.

Montag, D., Giese, K. P., Bartsch, U., Martini, R., Lang, Y., Bluthmann, H., Karthigasan, J., Kirschner, D. A., Wintergerst, E. S., Nave, K. A., Zielasek, J., Toyka, K. V., Lipp, H. V., and Schachner, M. (1994). Mice deficient for the myelin-associated glycoprotein show subtle abnormalities in myelin. Neuron *13*, 229-246.

Monuki, E. S., Kuhn, R., and Lemke, G. (1993). Repression of the myelin Po gene by the POU transcription factor SCIP. Mech. Dev. *42*, 15-32.

Monuki, E. S., Kuhn, R., Weinmaster, G., Trapp, B. D., and Lemke, G. (1990). Expression and activity of the POU transcription factor SCIP. Science *249*, 1300-1303.

Monuki, E. S., Weinmaster, G., Kuhn, R., and Lemke, G. (1989). SCIP: A glial cell POU domain gene regulated by cyclic AMP. Neuron *3*, 783-793.

Moore, M. S., and Blobel, G. (1993). The GTP-binding protein Ran/TC4 is required for protein import in the nucleus. Nature *365*, 661-663.

Morgan, L., Jessen, K. R., and Mirsky, R. (1991). The effects of cAMP on differentiation of cultured Schwann cells: progression from an early phenotype ($O4^+$) to a myelin phenotype ($P0^+$, $GFAP^-$, $NCAM^-$, NGF-$receptor^-$) depends on growth inhibition. J. Cell Biol. *112*, 457-467.

Morrissey, T. K., Levi, A. D., Nuijens, A., Sliwkowski, M. X., and Bunge, R. P. (1995). Axon-induced mitogenesis of human Schwann cells involves heregulin and p185erbB2. Proc. Natl. Acad. Sci. USA *92*, 1431-1435.

Mukhopadhyay, G., Doherty, P., Walsh, F. S., Crocker, P. R., and Filbin, M. T. (1994). A novel role for myelin-associated glycoprotein, MAG, as an inhibitor for axonal regeneration. Neuron *13*, 757-767.

Murphy, P., Topilko, P., Schneider-Maunoury, S., Seitanidou, T., Baron-Van Evercooren, A., and Charnay, P. (1996). The regulation of Krox-20 expression reveals important steps in the control of peripheral glial cell development. Development *122*, 2847-2857.

Naef, R., Adlkofer, K., Lescher, B., and Suter, U. (1997). Aberrant protein trafficking in Trembler suggests a disease mechanism for hereditary human peripheral neuropathies. Mol. Cell Neurosci. *9*, 13-25.

Nakano, R., Fujita, N., Sato, S., Inuzuka, T., Sakimura, K., Ishiguro, H., Mishina, M., and Miyatake, T. (1991). Structure of mouse myelin-associated glycoprotein gene. Biochim. Biophys. Res. Commun. *178*, 282-290.

Narayanan, V., Barbosa, E., Randall, R. and Tennekoon, G. I. (1991). Structure of the mouse myelin P2 protein gene. J. Biol. Chem. *263*, 8332-8337.

Nave, K.-A. (1996). Myelin-specific genes and their mutations in the mouse. In Glial Cell Development: basic principles and clinical relevance, K. R. a. W. D. R. Jessen, ed. (Oxford, U.K.: Bios Scientific Publishers), pp. 141-164.

Nave, K.-A., Bloom, F. E., and Milner, R. J. (1987). Splice site selection in the proteolipid protein (PLP) gene transcript and primary structure of the DM-20 protein of the central nervous system myelin. Proc. Natl. Acad. Sci. USA *84*, 5665-5669.

Nelles, E., Butzler, C., Jung, D., Temme, A., Gabriel, H. D., Dahl, U., Traub, O., Stumpel, F., Jungermann, K., and Zielasek, J. (1996). Defective propagation of signals generated by sympathetic nerve stimulation in the liver of connexin32-deficient mice. Proc. Natl. Acad. Sci. USA *93*, 9565-9570.

Newman, S., Kitamura, K., and Campagnoni, A. T. (1987). Identification of a cDNA coding for a fifth form of myelin basic protein in mouse. Proc. Natl. Acad. Sci. USA *84*, 886-890.

Newmeyer, D. D., and Forbes, D. J. (1988). Nuclear import can be separated into distinct steps in vitro: nuclear pore binding and translocation. Cell *52*, 641-653.

Nicholson, G., Valentijn, L. J., Cherryson, A. K., Kennerson, M. L., Bragg, T. L., Dekroon, R. M., Ross, D. A., Pollard, J. D., Mcleod, J. G., Bolhuis, P. A., and Baas, F. (1994). A frame shift mutation in the PMP22 gene in hereditary neuropathy with liability to pressure palsies. Nature Genet. *6*, 263-266.

Nigg, E. A. (1997). Nucleocytoplasmic transport signals, mechanisms and regulation. Nature *386*, 779-787.

Nikam, S. S., Tennekoon, G. I., Christy, B., Yoshino, J. E., and Rutkowski, J. L. (1995). The zinc finger transcription factor Zif168/Egr-1 is essential for Schwann cell expression of the p75 NGF receptor. Mol. Cell. Neurosci. *6*, 337-348.

Nishimune, A., Nash, S. R., Nakanishi, S., and Henley, J. M. (1996). Detection of protein-protein interactions in the nervous system using the two-hybrid system. Trends Neurosci. *19*, 261-266.

Norton, W. T., and Cammer, W. (1984). Isolation and Characterization of Myelin. In Myelin, P. Morell, ed. (New York: Plenum Press), pp. 147-195.

Notterpek, L., Shooter, E. M., and Snipes, G. J. (1997). Upregulation of the endosomal-lysosomal pathway in the Trembler-J neuropathy. J. Neurosci. *17*, 4190-4200.

Ochoa, J. (1976). The unmyelinated nerve fibre. In The Peripheral Nerve, D. N. Landon, ed. (Lomdon: Chapman and Hall), pp. 19-76.

Ogawa, H., Inouye, S., Tsuji, F. I., Yasuda, K., and Umensono, K. (1995). Localization, trafficking, and temperature-dependence of the Aequorea green fluorescent protein in cultured vertebrate cells. Proc. Natl. Acad. Sci. USA *92*, 11899-11903.

Omori, Y., Mesnil, M., and Yamasaki, H. (1996). Connexin 32 mutations associated from X-linked Charcot-Marie-Tooth disease patients: functional defects and dominant negative effects. Mol. Biol. Cell *7*, 907-916.

Ong, R. L., and Yu, R. K. (1984). Interaction of ganglioside GM1 and myelin basic protein studied by 12C and1H nuclear magnetic resonance. J. Neurosci. Res. *12*, 377-393.

Orr, A., Ivanova, V. S., and Bonner, W. M. (1995). "Waterbug" dialysis. Biotechniques *19*, 204-206.

Owens, G. C., and Boyd, C. J. (1991). Expressing antisense P0 RNA in Schwann cells perturbs myelination. Development *112*, 639-649.

Owens, G. C., Boyd, C. J., Bunge, R. P., and Salzer, J. L. (1990). Expression of recombinant myelin-associated glycoprotein in primary Schwann cells promotes the initial investment of axons by myelinating Schwann cells. J. Cell Biol. *111*, 1171-1182.

Owens, G. C., and Bunge, R. P. (1989). Evidence for an early role for myelin-associated glycoprotein in the process of myelination. Glia *2*, 119-128.

Owens, G. C., and Bunge, R. P. (1990). Schwann cells depleted of galactocerebroside express myelin-associated glycoprotein and initiate but do not continue the process of myelination. Glia *3*, 118-124.

Owens, G. C., and Bunge, R. P. (1991). Schwann cells infected with a recombinant retrovirus expressing myelin-associated glycoprotein antisense RNA do not form myelin. Neuron *7*, 565-575.

Palm, K., Belluardo, N., Metsis, M., and Timmusk, T. (1998). Neuronal expression of zinc finger transcription factor REST/NRSF/XRB gene. J. Neurosci. *18*, 1280-1296.

Pareek, S., Suter, U., Snipes, G. J., Welcher, A. A., Shooter, E. M., and Murphy, R. A. (1993). Detection and processing of peripheral myelin protein PMP22 in cultured Schwann cells. J. Biol. Chem. *268*, 10372-10379.

Parmantier, E., Cabon, F., Braun, C., D'Durso, D., Müller, H. W., and Zalc, B. (1995). Peripheral myelin protein-22 is expressed in rat and mouse brain and spinal cord motoneurons. Eur. J. Neurosci. *7*, 1080-1088.

Pedraza, L. (1997). Nuclear transport of myelin basic protein. J. Neurosci. Res. *50*, 258-264.

Pedraza, L., Fidler, L., Staugaitis, S. M., and Colman, D. R. (1997). The active transport of myelin basic protein into the nucleus suggests a regulatory role in myelination. Neuron *18*, 579-589.

Pedraza, L., Owens, G. C., Green, L. A. D., and Salzer, J. L. (1990). The myelin-associated glycoprotein: membrane disposition, evidence of a novel disulfide linkage between immunoglobulin-like domains, and posttranslational palmitylation. J. Cell Biol. *111*, 2651-2661.

Peles, E., Nativ, M., Lustig, M., Grumet, M., Schilling, J., Martinez, R., Plowman, G. D., and Schlessinger, J. (1997). Identification ofa novel contactin-associated transmembrane receptor with multiple domains implicated in protein-protein interactions. EMBO J. *16*, 978-988.

Peles, E., and Yarden, Y. (1993). Neu and its ligands: from an oncogene to neural factors. BioEssays *15*, 815-824.

Peschon, J. J., Behringer, R. R., Brinster, R. L., and Palmiter, R. D. (1987). Spermatid-specific expression of protamine 1 in transgenic mice. Proc. Natl. Acad. Sci USA *84*, 5316-5319.

Peters, A., Palay, S. L., and Webster, H. d. F. (1991). The cellular sheaths of neurons. In The fine structure of the nervous system: neurons and their supporting cells (Oxford: Oxford University Press), pp. 212-272.

Peters, A., and Vaughn, J. E. (1970). Morphology and development of the myelin sheath. In Myelination, A. N. Davison and A. Peters, eds. (Springfield, Illinois: Charles C. Thomas), pp. 3-79.

Peterson, A. C., and Bray, G. M. (1984). Hypomyelination in the peripheral nervous system of shiverer mice and in shiverer-normal chimæra. J. Comp. Neurol. *227*, 348-356.

Peterson, R. G., and Grevner, R. W. (1978). Morphological localization of PNS myelin proteins. Brain Res. *152*, 17-29.

Peyron, F., Timsit, S., Thomas, J.-L., Kagawa, T., Ikenaka, K., and Zalc, B. (1997). In situ expression of PLP/DM-20, MBP, and CNP during embryonic and postnatal development of the jimpy mutant and of transgenic mice overexpressing PLP. J. Neurosci. Res. *50*, 190-201.

Pham-Dinh, D., Birling, M. C., Roussel, G., Dautigny, A., and Nussbaum, J. L. (1991). Proteolipid DM-20 predominates over PLP in peripheral nervous system. Neuroreport *2*, 89-92.

Poduslo, J. F., Berg, C. T., and Dyck, P. J. (1984). Schwann cell expression of a major myelin glycoprotein in the absence of myelin assembly. Proc. Natl. Acad. Sci. USA *81*, 1864-1866.

Poduslo, J. F., Berg, C. T., Ross, S. M., and Spencer, P. S. (1985). Regulation of myelination: axons not required for the biosynthesis of basal levels of the major myelin glycoprotein by Schwann cells in denervated distal segments of the adult cat sciatic nerve. J. Neurosci. Res. *14*, 177-185.

Poduslo, J. F., and Windebank, A. J. (1985). Differentiation-specific regulation of Schwann cell expression of the major myelin glycoprotein. Proc. Natl. Acad. Sci. USA *82*, 5987-5991.

Politis, M. J., Sternberger, N., Ederle, K., and Spencer, P. S. (1982). Studies on the control of myelinogenesis. J. Neurosci. 2, 1252-1266.

Poltorak, M., Sadoul, R., Keilhauer, G., Landa, C., Fahrig, T., and Schachner, M. (1987). Myelin-associated glycoprotein, a member of the L2/HNK-1 family of

neural cell adhesion molecules, is inolved in neuron-oligodendrocyte and oligodendrocyte-oligodendrocyte interaction. J. Cell Biol. *105*, 1893-1899.

Poulat, F., de Santa Barbara, P., Desclozeaux, M., Soullier, S., Moniot, B., Bonneaud, N., Boizet, B., and Berta, P. (1997). The human testis determining factor *SRY* binds a nuclear factor containing PDZ preotein interaction domains. J. Biol. Chem. *272*, 7167-7172.

Pribyl, T. M., Campagnoni, C. W., Kampf, K., Handley, V. W., McMahon, J., and Campagnoni, A. T. (1993). The human myelin basic protein gene is included within a 179-kilobase transcription unit: expression in the immune and central nervous system. Proc. Natl. Acad. Sci. USA *90*, 10695-10699.

Privat, A., Jacque, C., Bourre, J. M., Dupouey, P., and Baumann, N. (1979). Absence of the major dense line in the myelin of the mutant mouse 'shiverer'. Neurosci. Lett. *12*, 107-112.

Puckett, C., Hudson, L., Ono, K., Friedrich, V., Benecke, J., Dubois-Dalcq, M., and Lazzarini, R. A. (1987). Myelin-specific proteolipid protein is expressed in myelinating Schwann cells but is not incorporated into myelin sheaths. J. Neurosci. Res. *18*, 511-518.

Quarles, R. H. (1984). Myelin-associated glycoprotein in development and disease. Dev. Neurosci. *6*, 285-303.

Raff, M. C., Mirsky, R., Fields, K. L., Lisak, R. P., Dorfmann, S. H., Silberberg, D. H., Gregson, N. A., Liebowitz, S., and Kennedy, C. M. (1978). Galactocerebroside is a specific cell surface antigenic marker for oligodendrocytes in culture. Nature *274*, 813-816.

Ranscht, B., Clapshaw, P. A., Price, J., Noble, M., and Seifert, W. (1982). Development of oligodendrocytes and Schwann cells studies with a monoclonal antibody against galactocerebroside. Proc. Natl. Acad. Sci. USA *79*, 2709-2713.

Ranscht, B., Wood, P. M., and Bunge, R. P. (1987). Inhibition of in vitro peripheral myelin formation by monoclonal anti-galactocerebroside. J. Neurosci. *7*, 2936-2947.

Ranvier, L. (1871). Contributions a l'histologie et à là physiologie des nerfs periphèriques. C.R. Acad. Sci. *73*, 1168.

Rasband, M. N., Trimmer, J. S., Schwarz< T.L. Levinson, S. R., Ellisman, M. H., Schachner, M., and Shrager, P. (1998). Potassium channel distribution, clustering,and function in remyelinating rat axons. J. Neurosci. *18*, 36-47.

Readhead, C., Popko, B., Takahashi, N., Shine, H. D., Saavedra, R. A., Sidman, R. L., and Hood, L. (1987). Expression of a myelin basic protein gene in transgenic shiverer mice: correction of the dysmyelinating phenotype. Cell *48*, 703-712.

Richardson, W. D., Mills, A. D., Dilworth, S. M., Laskey, R. A., and Dingwall, C. (1988). Nuclear protein migration involves two steps: rapid binding to the nuclear envelope followed by slower translocation through nuclear pores. Cell *52*, 655-664.

Rickmann, M., Fawcett, J. W., and Keynes, R. J. (1985). The migration of neural crest cells and the growth of motor axons through the rostral half of the chick somite. J. Embryol. Exp. Morph. *90*, 437-455.

Riethmacher, D., Sonnenberg-Riethmacher, B., V., Yamaai, T., Lewin, G. R., and Birchmeier, C. (1997). Severe neuropathies in mice with targeted mutations in the ErbB3 receptor. Nature *389*, 725-730.

Ritchie, J. M. (1984). Physiological basis of conduction in myelinated nerve fibers. In Myelin, P. Morell, ed. (New York: Plenum Press), pp. 117-145.

Roa, B. B., Dyck, P. J., Marks, H. G., Chance, P. F., and Lupski, J. R. (1993). Dejerine-Sottas syndrome associated with point mutation in the peripheral myelin protein 22 (PMP22) gene. Nature Genet. *5*, 269-273.

Roach, A., Takahashi, N., Pravtcheva, D., Ruddle, F., and Hood, L. (1985). Chromosomal mapping of mouse myelin basic protein gene and structure and transcription of the partially deleted gene in shiverer mutant mice. Cell *42*, 149-155.

Rosen, C. L., Lisanti, M. P., and Salzer, J. L. (1992). Expression of unique sets of GPI-linked proteins by different primary neurons in vitro. J. Cell Biol. *117*, 617-627.

Rosenbluth, J. (1980). Peripheral myelin in the mouse mutant shiverer. J. Comp. Neurol. *193*, 729-739.

Rowe-Rendleman, C. L., and Eichberg, J. (1994). P0 phosphorylation in nerves from normal and diabetic rats: role of protein kinase C and turnover of phosphate groups. Neurochem. Res. *19*, 1023-1031.

Sadoul, D., Fahrig, T., Bartsch, U., and Schachner, M. (1990). Binding properties of liposomes containing the myelin-associated glycoprotein MAG to neural cell cultures. J. Neurosci. Res. *25*, 1-13.

Sakamoto, Y., Kitamura, K., Yoshimura, K., Nishijima, T., and Uyemura, K. (1987). Complete amino acid sequence of P0 protein in bovine peripheral nerve myelin. J. Biol. Chem. *262*, 4208-4214.

Salzer, J. L. (1997). Clustering sodium channels at the node of Ranvier: close encounters of the axon-glia kind. Neuron *18*, 843-846.

Salzer, J. L., and Colman, D. R. (1989). Mechanisms of cell adhesion in the nervous system: role of the immunoglobulin gene superfamily. Dev. Neurosci. *11*, 377-390.

Salzer, J. L., Holmes, W. P., and Colman, D. R. (1987). The amino acid sequences of the myelin associated glycoproteins: homology to the immunoglobulin gene superfamily. J. Cell Biol. *104*, 957-965.

Salzer, J. L., Pedraza, L., Brown, M., Struyk, A., Afar, D., and Bell, J. (1990). Structure and function of the myelin associated glycoprotein. Ann. N.Y. Acad. Sci *605*, 302-312.

Sambrook, J., Fritsch, E. F., and Maniatis, T. (1989). Molecular Cloning: A Laboratory Manual (Cold Spring Harbour, New York: Cold Spring Harbour Laboratory Press).

Sandrock, A. W. J., Goodearl, A. D. J., Yin, Q.-W., Chang, D., and Fischbach, G. D. (1995). ARIA is concentrated in nerve terminals at neuromuscular junctions and at other synapses. J. Neurosci. *15*, 6124-6136.

Sanger, F., Nicklen, S., and Coulson, A. R. (1977). DNA sequencing with chain-terminating inhibitors. Proc. Natl. Acad. Sci. *74*, 5463-5467.

Saras, J., and Heldin, C.-H. (1996). PDZ domains bind carboxy-terminal sequences of target proteins. Trends Biochem. Sci. *21*, 455-458.

Sato, T., Irie, S., Kitada, S., and Reed, J. C. (1995). Fap-1: A protein phosphatase that associates with Fas. Science *268*, 411-415.

Sawadogo, M., and Van Dyke, M. W. (1991). A rapid method for the purification of deprotected oligodeoxynucleotides. Nucl. Acids Res. *19*, 674.

Schachner, M., Kim, S. M., and Zehnle, R. (1981). Developmental expression in central and peripheral nervous system of oligodendrocyte cell surface antigens (O antigens) recognized by monoclonal antibodies. Dev. Biol. *83*, 328-338.

Scherer, S. S., Deschenes, S. M., Xu, Y.-T., Grinspan, J. B., Fischbeck, K. H., and Paul, D. L. (1995). Connexin 32 is a myelin-related protein in the PNS and CNS. J. Neurosci. *15*, 8281-8294.

Scherer, S. S., and Salzer, J. L. (1996). Axon-Schwann cell interactions during peripheral nerve degeneration and regeneration. In Glial Cell Development: basic principles and clinical relevance, K. R. Jessen and W. D. Richardson, eds. (Oxford: Bios Scientific Publishers), pp. 165-196.

Scherer, S. S., Wang, D., Kuhn, R., Lemke, G., Wrabetz, L., and Kamholz, J. (1994). Axons regulate Schwann cell expression of the POU transcription factor SCIP. J. Neurosci. *14*, 1930-1942.

Scherer, S. S., Xu, Y., Bannerman, P. G. C., Sherman, D. L., and Brophy, P. J. (1995). Periaxin expression in myelinating Schwann cells: modulation by axon-glial interactions and polarized localization during development. Development *121*, 4265-4273.

Scherer, S. S., Xu, Y.- T., Roling, D., Wrabetz, L., Feltri, M. L., and Kamholz, J. (1994). Expression of growth-associated protein-43 kD in Schwann cells is regulated by axon-Schwann cell interactions and cAMP. J. Neurosci. Res. *38*, 575-589.

Schlaepfer, W. W., and Myers, F. K. (1973). Relationship of myelin internode elongation and growth in the rat sural nerve. J. Comp. Neurol. *147*, 255-266.

Schmidt, H. D. (1874). On the construction of the dark or double-bordered nerve fiber. Mon. Microsc. J. *11*, 200.

Schneider-Schaulies, J., von Brunn, A., and Schachner, M. (1990). Recombinant peripheral myelin protein P0 confers both adhesion and neurite outgrowth-promotong properties. J. Neurosci. Res. *27*, 286-297.

Schober, R., Itoyama, J., Sternberger, N. H., Trapp, B. D., Richardson, E. P., Ashbury, A. K., Quarles, R. H., and Webster, H. d. F. (1981). Immunocytochemical study of P0 glycoprotein, P1, and P2 basic proteins and myelin-associated glycoprotein (MAG) in lesions of idiopathic polyneuritis. Neuropath. and Applied Neurobiol. *7*, 437-451.

Schoenherr, C. J., and Anderson, D. J. (1995). The neuron-restrictive silencer factor (NRSF): a coordinate repressor of multiple neuron-specific genes. Science *267*, 1360-1363.

Schwann, T. (1839). Mikroskopishe untersuchungen über die uebereinstimmung in der struktur und dem wachstum der tiere und pflanzen. (Berlin: Sander).

Sereda, M., Griffiths, I., Puhihofer, A., Stewart, H., Rossner, M. J., Zimmermann, F., Magyar, J. P., Schneider, A., Hund, E., Meinck, H. M., Suter, U., and Nave, K. A. (1996). A transgenic rat model of Charcot-Marie-Tooth disease. Neuron *16*, 1049-1060.

Shah, N. M., Marchionni, M. A., Isaacs, I., Stroobant, P., and Anderson, D. J. (1994). Glial growth factor restricts mammalian neural crest stem cells to a glial fate. Cell *77*, 349-360.

Shapiro, L., Doyle, J. P., Hensley, P., Colman, D. R., and Hendrickson, W. A. (1996). Crystal structure of the extracellular domain from P0, the major structural protein of peripheral nerve myelin. Neuron *17*, 435-449.

Sharma, K., Korade, Z., and Frank, E. (1995). Lat-migrating neuroepithelial cells from the spinal cord differentiate into sensory ganglion cells and melanocytes. Neuron *14*, 143-152.

Sheng, M. (1996). PDZs and receptor/channel clustering: rounding up the latest suspects. Neuron *17*, 575-578.

Shuman, S., Hardy, M., Sobue, G., and Pleasure, D. (1988). A cyclic AMP analogue induces synthesis of a myelin-specific glycoprotein by cultured Schwann cells. J. Neurochem. *50*, 190-194.

Shy, M. E., Shi, Y., Wrabetz, L., Kamholz, J., and Scherer, S. S. (1996). Axon-Schwann cell interactions regulate the expression of c-*jun* in Schwann cells. J. Neurosci. Res. *43*, 512-525.

Sieber-Blum, M., and Cohen, A. (1980). Clonal analysis of quail neural crest cells: they are pluripotent and differentiate in vitro in the absence of nonneural crest cells. Dev. Biol. *80*, 96-106.

Snipes, G. J., Suter, U., and Shooter, E. M. (1993). Human peripheral myelin protein-22 carries the L2/HNK-1 carbohydrate adhesion epitope. J. Neurochem. *61*, 1961-1964.

Snipes, G. J., Suter, U., Welcher, A. A., and Shooter, E. M. (1992). Characterization of a novel peripheral nervous system myelin protein (PMP-22/SR13). J. Cell Biol. *117*, 225-238.

Sommer, I., and Schachner, M. (1981). Monoclonal antibodies (O1 to O4) to oligodendrocyte cell surfaces: an immunocytological study in the central nervous system. Dev. Biol. *83*, 311-327.

Songyang, Z., Fanning, A. S., Fu, C., Xu, J., Marfatia, S. M., Chishti, A. H., Crompton, A., Chan, A. C., Anderson, J. M., and Cantley, L. C. (1997). Recognition of unique carboxy-terminal motifs by distinct PDZ domains. Science *275*, 73-77.

Spreyer, P., Kuhn, G., Hanemann, C. O., Gillen, C., Schaal, H., Kuhn, R., Lemke, G., and Muller, H. W. (1991). Axon-related expression of a Schwann cell transcript that is homologous to a 'growth arrest-specific' gene. EMBO J. *10*, 3661-3668.

Stahl, N., Harry, J., and Popko, B. (1990). Quantitative analysis of myelin protein gene expression during development in the rat sciatic nerve. Mol. Brain Res. *8*, 209-212.

Staugaitis, S. M., Smith, P. R., and Colman, D. R. (1990). Expression of myelin basic protein isoforms in nonglial cells. J. Cell Biol. *110*, 1719-1727.

Sternberger, N. H., Quarles, R. H., Itoyama, Y., and Webster, H. d. F. (1979). Myelin-associated glycoprotein demonstrated immunocytochemically in myelin and myelin-forming cells of developing rats. Proc. Natl. Acad. Sci. USA *76*, 1510-1514.

Stewart, H. J. S. (1995). Expression of c-Jun, Jun B, Jun D and cAMP response element binding protein by Schwann cells and their precursors *in vivo* and *in vitro*. Eur. J. Neurosci. *7*, 1366-1375.

Stewart, H. J. S., Mirsky, R., and Jessen, K. R. (1996). The Schwann cell lineage: embryonic and early postnatal development. In Glial Cell Development: basic principles and clinical relevance, K. R. a. W. D. R. Jessen, ed. (Oxford, U.K.: Bios Scientific Publishers), pp. 1-30.

Stewart, H. J. S., Morgan, L., Jessen, K. R., and Mirsky, R. (1993). Changes in DNA synthesis rate in the Schwann cell lineage *in vivo* are correlated with the precursor-Schwann cell transition and myelination. Eur. J. Neurosci. *5*, 1136-1144.

Stewart, H. J. S., Zoidl, G., Rossner, M., Brennan, A., Zoidl, C., Nave, K. A., Mirsky, R., and Jessen, K. R. (1997). Helix-loop-helix proteins in Schwann cells: a study of regulation and subcellular localization of Ids, REB, and E12/47 during embryonic and postnatal development. J. Neurosci. Res. *50*, 684-701.

Stoffel, W., and Bosio, A. (1997). Myelin glycolipids and their functions. Curr. Opin. Neurobiol. *7*, 654-661.

Stricker, N. L., Christopherson, K. S., Yi, B. A., Schatz, P. J., Raab, R. W., Dawes, G., Bassett, D. E. J., Bredt, D. S., and Li, M. (1997). PDZ domain of neuronal nitric oxide synthase recognizes novel C-terminal peptide sequences. Nature Biotech. *15*, 336-342.

Suter, U., and Snipes, G. J. (1995a). Biology and genetics of hereditary motor and sensory neuropathies. Annu. Rev. Neurosci. *18*, 45-75.

Suter, U., and Snipes, G. J. (1995b). Peripheral myelin protein 22: facts and hypotheses. J. Neurosci. Res. *40*, 145-151.

Suter, U., Snipes, G. J., Schoener-Scott, R., Welcher, A. A., Pareek, S., Lupski, J. R., Murphy, R. A., Shooter, E. M., and Patel, P. I. (1994). Regulation of tissue-specific expression of alternative peripheral myelin protein-22 (PMP22) gene transcripts by two promoters. J. Biol. Chem. *269*, 25795-25808.

Suter, U., Welcher, A. A., Ozcelik, T., Snipes, G. J., Kosaras, B., Francke, U., Billings-Gagliardi, S., Sidman, R. L., andShooter, E. M. (1992). Trembler mouse carries a point mutation in a myelin gene. Nature *356*, 241-243.

Suzuki, M., Sakamoto, Y., Kitamura, K., Fukunaga, K., Yamamoto, H., Miyamoto, E., andUyemura, K. (1990). Phosphorylation of P0 glycoprotein in peripheral nerve myelin. J. Neurochem. *55*, 1966-1971.

Suzuki, N., Rohdewohld, H., Neuman, T., Gruss, P., and Schöler, H. R. (1990). Oct-6: a POU transcription factor expressed in embryonal stem cells and in the developing brain. EMBO J. *9*, 3723-3732.

Syroid, D. E., Maycox, P. R., Burrola, P. G., Liu, N., Wen, D., Lee, K.-F., Lemke, G., and Kilpatrick, T. J. (1995). Cell death in the Schwann cell lineage and its regulation by neuregulin. Proc. Natl. Acad. Sci. USA *93*, 9229-9234.

Takahashi, N., Roach, A., Teplow, D. B., Prusiner, S. B., and Hood, L. (1985). Cloning and charcaterisation of the myelin basic protein gene from mouse: one gene can encode both 14 kd and 18.5 kd MBPs by alternate use of exons. Cell *42*, 139-148.

Tang, S., Woodhall, R. W., Shen, Y. J., de Bellard, M. E., Saffeil, J. L., Doherty, P., F.S., W., and Filbin, M. T. (1997). Soluble myelin-associated glycoprotein (MAG) found in vivo inhibits axonal regeneration. Mol. Cell. Neurosci. *9*, 333-346.

Taniuchi, M., Clark, H. B., and Johnson, E. M. (1986). Induction of nerve growth factor receptor in Schwann cells after axotomy. Proc. Natl. Acad. Sci. USA *83*, 4094-4098.

Taniuchi, M., Clark, H. B., Schweitzer, J. B., and Johnson Jr, E. M. (1988). Expression of nerve growth factor receptors by Schwann cells of axotomized peripheral nerves: ultrastructural location, suppression by axonal contact, and binding properties. J. Neurosci. *8*, 664-681.

Timmerman, V., Nelis, E., Van Hul, W., Nieuwenhuijsen, B. W., Chen, K. L., Ben Othman, K., Cullen, B., Leachz, R. J., Hanemann, C. O., De Jonghe, P., Raeymaekers, P., van Ommen, G. J., Martin, J. J., Muller, H. W., Vance, J. M., Fischbeck, K. H., and Van Broeckhoven, C. (1992). The peripheral myelin protein gene PMP22 is contained within the Charcot-Marie-Tooth disease type 1A duplication. Nature Genet. *1*, 171-175.

Timsit, S., Bally-Cuif, L., Colman, D. R., and Zalc, B. (1992). DM-20 mRNA is expressed during early embryonic development of the nervous system of the mouse. J. Neurochem. *58*, 1172-1175.

Timsit, S., Martinez, S., Allinquant, B., Peyron, F., Puelles, L., and Zalc, B. (1995). Oligodendrocytes originate in a restricted zone of the embryonic neural tube defined by DM20 mRNA expression. J. Neurosci. *15*, 1012-1024.

Topilko, P., Murphy, P., and Charnay, P. (1996). Embryonic development of Schwann cells: multiple roles for neuregulins along the pathway. Mol. Cell. Neurosci. *8*, 71-75.

Topilko, P., Schneider-Maunoury, S., Levi, G., Baron-Van Evercooren, A., Chennoufi, A. B. Y., Seitanidou, T., Babinet, C., and Charnay, P. (1994). Krox-20 controls myelination in the peripheral nervous system. Nature *371*, 796-799.

Towbin, H., Staehlin, T., and Gordon, J. (1979). Electrophoretic transfer of proteins from acrylamide gels to nitrocellulose: procedure and some applications. Proc. Natl. Acad. Sci. USA *76*, 4350-4354.

Trachtenberg, J. T., and Thompson, W. J. (1996). Schwann cell apoptosis at developing neuromuscular junctions is regulated by glial growth factor. Nature *379*, 174-177.

Trapp, B. D., Andrews, S. B., Cootauco, C., and Quarles, R. (1989a). The myelin-associated glycoprotein is enriched in multivesicular bodies and periaxonal membranes of actively myelinating oligodendrocytes. J. Cell Biol. *J. Cell Biol.*, 2417-2426.

Trapp, B. D., Andrews, S. B., Wong, A., O'Connell, M., and Griffin, J. W. (1989b). Co-localization of the myelin-associated glycoprotein and the microfilament components, F-actin and spectrin, in Schwann cells of myelinated nerve fibres. J. Neurocytol. *18*, 47-60.

Trapp, B. D., Hauer, P., and Lemke, G. (1988). Axonal regulation of myelin protein mRNA levels in actively myelinating Schwann cells. J. Neurosci. *8*, 3515-3521.

Trapp, B. D., Itoyama, Y., Sternberger, N. H., Quarles, R. H., and Webster, H. d. F. (1981). Immunocytochemical localization of P0 protein in Golgi complex membranes and myelin of developing rat Schwann cells. J. Cell Biol. *90*, 1-6.

Trapp, B. D., Kidd, G. J., Hauer, P. E., Mulrenin, E., Haney, C., and Andrews, S. B. (1995). Polarization of myelinating Schwann cell surface membranes: role of microtubules and the trans-Golgi network. J. Neurosci. *15*, 1797-1807.

Trapp, B. D., Moench, T., Pulley, M., Barbosa, E., Tennekoon, G., and Griffin, J. (1987). Spatial segregation of mRNA encoding myelin-specific proteins. Proc. Natl. Acad. Sci. USA *84*, 7773-7777.

Trapp, B. D., and Quarles, R. H. (1982). Presence of the myelin-associated glycoprotein correlates with alterations in the periodicity of peripheral myelin. J. Cell Biol., 877-882.

Trapp, B. D., Quarles, R. H., and Griffin, J. W. (1984a). Myelin-associated glycoprotein and myelinating Schwann cell-axon interaction in chronic B,B'-iminodipropionitrile neuropathy. J. Cell Biol. *98*, 1272-1278.

Trapp, B. D., Quarles, R. H., and Suzuki, K. (1984b). Immunocytochemical studies of quaking mice support a role for the myelin-associated glycoprotein in forming and maintaining the periaxonal space and periaxonal cytoplasmic collar of myelinating Schwann cells. J. Cell Biol. *99*, 594-606.

Tropak, M. B., Johnson, P. W., Dunn, R. J., and Roder, J. C. (1988). Differential splicing of MAG transcripts during CNS and PNS development. Mol. Brain Res. *4*, 143-155.

Tsunoda, S., Sierralta, J., Sun, Y., Bodner, R., Suzuki, E., Becker, A., Socolich, M., and Zuker, C. S. (1997). A multivalent PDZ-domain protein assembles signalling complexes in a G-protein-coupled cascade. Nature *388*, 243-249.

Vabnick, I., Messing, A., Chiu, S. Y., Levinson, S. R., Schachner, M., Roder, J., Li, C., Novakovic, S., and Shrager, P. (1997). Sodium channel distribution in axons of hypomyelinated and MAG null mice. J. Neurosci. Res. *50*, 321-336.

Vabnick, I., Novakovic, S. D., Levinson, S. R., Schachner, M., and Shrager, P. (1996). The clustering of axonal sodium channels during development of the peripheral nervous system. J. Neurosci. *16*, 4914-4922.

Valentijn, L. J., Baas, F., Wolterman, R. A., Hoogendijk, J. E., van den Bosch, N. H. A., Zorn, I., Gabreels-Festen, A. A. W. M., De Visser, M., and Bolhuis, P. A. (1992). Identical point mutations of PMP-22 in *Trembler-J* mouse and Charcot-Marie-Tooth disease type 1A. Nature Genet. *2*, 288-291.

Valentijn, L. J., Bolhuis, P. A., Zorn, I., Hoogendijk, J. E., van den Bosch, N., Hensels, G. W., Stanton, V. P., Housman, D. E., Fischbeck, K. H., Ross, D. A., Nicholson, G. A., Meershoek, E. J., Dauwerse, H. G., van Ommen, G. J., and Baas, F. (1992). The peripheral myelin gene PMP22/gas3 is duplicated in Charcot-Marie-Tooth disease type 1A. Nature Genet *1*, 166-170.

Vartanian, T., Goodearl, A., Viehöver, A., and Fischbach, G. (1997). Axonal neuregulin signals cells of the oligodendrocyte lineage through activation of HER4 and Schwann cells through HER2 and HER3. J. Cell Biol. *137*, 211-220.

Venable, J. H., and Coggeshall, R. (1965). A simplified lead citrate stain for use in electron microscopy. J. Cell Biol. *25*, 407.

Verity, A. N., and Campagnoni, A. T. (1988). Regional expression of myelin protein genes in the developing mouse brain: in situ hybridization studies. J. Neurosci. Res. *21*, 15-28.

Virchow, R. (1854). Ueber das ausgebreitete Vorkommen einer dem Nervenmark analogen Substanz in den tierischen Geweben. Viechows Arch. Pathol Anat. *6*, 562.

Vizoso, A. D., and Young, J. Z. (1948). Internode length and fibre diameter in developing and regenerating nerves. J. Anat. (London) *82*, 110.

Voyvodic, J. T. (1989). Target size regulates calibre and myelination of sympathetic axons. Nature *342*, 430-433.

Wang, H., Kunkel, D. D., Martin, T. M., Schwartzkroin, P. A., and Temperl, B. L. (1993). Heteromultimeric K+ channels in terminal and juxtaparanodal regions of neurons. Nature *365*, 75-79.

Warner, L. E., Hilz, M. J., Appel, S. H., Killian, J. M., Watters, G. V., Wheeler, C., Witt, D., Bodell, A., Nelis, E., Van Broeckhoven, C., and Lupski, J. R. (1996). Clinical phenotypes of different MPZ (P0) mutations may include Charcot-Marie-Tooth type 1B, Dejerine-Sottas, and congenital hypomyelination. Neuron *17*, 451-460.

Weber, J. R. M., and Skene, J. H. P. (1997). Identification of a novel repressive element that contributes to neuron-specific gene expression. J. Neurosci. *17*, 7583-7593.

Webster, H. d. F. (1971). The geometry of peripheral myelin sheaths during their formation and growth in rat sciatic nerves. J. Cell Biol. *48*, 348-367.

Webster, H. d. F., and Favilla, J. T. (1984). Development of peripheral nerve fibres. In Peripheral Neuropathy, P. J. Dyck, P. K. Thomas, E. H. Lambert and R. Bunge, eds. (Philadelphia: W. B. Saunders), pp. 329-359.

Weinberg, H. J., and Spencer, P. S. (1976). Studies on the control of myelinogenesis II. Evidence for neuronal regulation of myelin production. Brain Res. *113*, 363-378.

Welcher, A. A., Suter, U., De Leon, M., Snipes, G. J., and Shooter, E. M. (1991). A myelin protein is encoded by the homologue of a growth arrest-specific gene. Proc. Natl. Acad. Sci. USA *88*, 7195-7199.

Weston, J. A. (1991). Sequential segregation and fate of developmentally restricted intermediate cell populations in the neural crest lineage. Curr. Top. Devel. Biol. *25*, 133-153.

Wight, P. A., and Dobretsova, A. (1997). The first intron of the myelin proteolipid protein gene confers cell type-specific expression by a transcriptional repression mechanism in non-expressing cell types. Gene *201*, 111-117.

Wight, P. A., Duchala, C. S., Readhead, C., and Macklin, W. B. (1993). A myelin proteolipid protein-LacZ fusion protein is developmentally regulated and targeted to the myelin membrane in transgenic mice. J. Cell Biol. *123*, 443-454.

Wiley, C. A., and Ellisman, M. H. (1980). Rows of dimeric-particles within the axolemma and juxtaposed partcles within glia, incorporated into a new model for the paranodal glial-axonal junction at the node of Ranvier. J. Cell Biol. *84*, 261-280.

Wilkinson, D. G., Bailes, J. A., and McMahon, A. P. (1987). Expression of the proto-oncogene int-1 is restricted to specific neural cells in the developing mouse embryo. Cell *50*, 79-88.

Williams, A. F., and Barclay, A. N. (1988). The immunoglobulin superfamily-domains for cell surface recognition. Ann. Rev. Immunol. *6*, 381-405.

Willott, E., Balda, M. S., Fanning, A. S., Jameson, B., Van Itallie, C., and Anderson, J. (1993). The tight junction protein ZO-1 is homologous to the *Drosophila* discs-large tumor supressor protein of septate junctions. Proc. Natl. Acad. Sci. USA *90*, 7834-7838.

Wilson, R., and Brophy, P. J. (1989). Role for the oligodendrocyte cytoskeleton in myelination. J. Neurosci. Res. *22*, 439-448.

Wong, M. H., and Filbin, M. T. (1994). The cytoplasmic domain of the myelin P0 protein influences the adhesive interactions of its extracellular domain. J. Cell Biol. *126*, 1089-1097.

Wong, M. H., and Filbin, M. T. (1996). Dominant-negative effect of adhesion by myelin P0 protein truncated in its cytoplasmic domain. J. Cell Biol. *134*, 1531-1541.

Wood, J. G., and Dawson, R. M. C. (1973). A major myelin protein of sciatic nerve. J. Neurochem. *21*, 717-721.

Wood, J. G., and McLaughlin, J. (1975). The visualization of concavalin A binding sites in the intraperiod line of rat sciatic nerve myelin. J. Neurochem. *24*, 233-235.

Wood, P. M., and Bunge, R. P. (1975). Evidence that sensory axons are mitogenic for Schwann cells. Nature *256*, 662-664.

Woods, D. F., and Bryant, P. J. (1991). The Discs-Large tumor suppressor gene of Drosophila encodes a guanylate kinase homolog localized at septate junctions. Cell *66*, 451-464.

Wuenschell, C. W., Mori, N., and Anderson, D. J. (1990). Analysis of SCG10 gene expression in transgenic mice reveals that neural specificity is achieved through selective derepression. Neuron *4*, 595-602.

Yin, X., Peterson, J., Gravel, M., Braun, P. E., and Trapp. B. D. (1997). CNP overexpression induces aberrant oligodendrocyte membranes and inhibits MBP accumulation and myelin compaction. J. Neurosci. Res. *50*, 238-247.

You, K. H., Hseih, C. L., Hayes, C., Stahl, N., Francke, U., and Popko, B. (1991). DNA sequence, genomic organisation, and chromosomal localization of the mouse peripheral myelin protein zero gene:identification of polymorphic alleles. Genomics *9*, 751-757.

Zawerthal, W. (1874). Contribuzione allo studio anatomico della fibrea nervosa. Riv. Accad. Sci. Fis. Mat. (Napoli) *1*, 82.

Zhang, K., and Filbin, M. T. (1994). Formation of a disulfide bond in the immunoglobulin domain of the myelin P0 protein is essential for its adhesion. J. Neuroschem. *63*, 367-370.

Zhang, K., Merazga, Y., and Filbin, M. T. (1996). Mapping the adhesive domains of the myelin P0 protein. J. Neurosci. Res. *45*, 525-533.

Zhang, S.-M., Marsh, R., Ratner, N., and Brackenbury, R. (1995). Myelin glycoprotein P0 is expressed at early stages of chicken and rat embryogenesis. J. Neurosci. Res. *40*, 241-250.

Zorick, T. S., Syroid, D. E., Arroyo, E., Scherer, S. S., and Lemke, G. (1996). The transcription factors SCIP and Krox-20 mark distinct stages and cell fates in Schwann cell differentiation. Mol. Cell. Neurosci. *8*, 129-145.

Appendix

APPENDIX

List of publications containing work included in this thesis:

Gillespie, C. S., Sherman, D. L., Blair, G. E., and Brophy, P. J. (1994). Periaxin, a novel protein of myelinating Schwann cells with a possible role in axonal ensheathment. Neuron *12*, 497-508.

Fannon, A. M., Sherman, D. L., Ilyina-Gragerova, G., Brophy, P. J., Friedrich, V. L., and Colman, D. R. (1995). Novel E-cadherin-mediated adhesion in peripheral nerve:Schwann cell architecture is stabilized by autotypic adherens junctions. J. Cell Biol. *129*, 189-202.

Scherer, S. S., Xu, Y., Bannerman, P. G. C., Sherman, D. L., and Brophy, P. J. (1995). Periaxin expression in myelinating Schwann cells: modulation by axon-glial interactions and polarized localization during development. Development *121*, 4265-4273.

Dytrych, L., Sherman, D. L., Gillespie, C. S., and Brophy, P. J. (1998). Two PDZ proteins encoded by the murine periaxin gene are the result of alternative intron retention and are differentially targeted in Schwann cells. J. Biol. Chem. *273*, 5794-5800.

Neuron, Vol. 12, 497–508, March, 1994, Copyright © 1994 by Cell Press

Periaxin, a Novel Protein of Myelinating Schwann Cells with a Possible Role in Axonal Ensheathment

C. Stewart Gillespie,* Diane L. Sherman,*
G. Eric Blair,† and Peter J. Brophy*
*Department of Biological and Molecular Sciences
University of Stirling
Stirling FK9 4LA
Scotland
†Department of Biochemistry and Molecular Biology
Leeds University
Leeds LS2 9JT
England

Summary

We report the cloning and subcellular localization of a novel Schwann cell–specific protein of 147 kd that we have named periaxin. Periaxin has a remarkable domain of repetitive pentameric units in the primary sequence. It is expressed in the first uncompacted whorls of membrane that ensheathe the axon, and further synthesis of the protein in the rat sciatic nerve parallels the deposition of myelin. In mature myelin, periaxin colocalizes with the myelin-associated glycoprotein in the cytoplasm-filled periaxonal regions of the sheath but is excluded from compact myelin. We propose that periaxin has a role in axon–glial interactions, possibly by interacting with the cytoplasmic domains of integral membrane proteins such as myelin-associated glycoprotein in the periaxonal regions of the Schwann cell plasma membrane.

Introduction

Schwann cells undergo major morphological changes during the development of the peripheral nervous system (PNS) (Jessen and Mirsky, 1991). During their proliferative phase, they must insinuate themselves within axon bundles to establish a 1:1 relationship with individual axons, whereupon they extend longitudinally to form the future internode (Martin and Webster, 1973; Peters and Muir, 1959; Webster et al., 1973). Axonal signals play a vital role in the morphological and functional differentiation of Schwann cells. Axonal contact stimulates Schwann cell proliferation (Salzer and Bunge, 1980; Sobue and Pleasure, 1985) and basement membrane formation (Bunge et al., 1986) and is also critical for myelin synthesis (Brunden et al., 1990; Bunge et al., 1986; Lemke and Chao, 1988). The molecular basis of axon–Schwann cell interaction has yet to be elucidated but it is widely believed that the plasma membrane proteins L1, the myelin-associated glycoprotein (MAG), and P_0, all members of the immunoglobulin superfamily, have a role in the initiation of axonal ensheathment by Schwann cells (Doyle and Colman, 1993).

A myelinating Schwann cell envelops an adjacent axon with a layer of cytoplasm that is bounded by an extension of the Schwann cell plasma membrane. After several rounds of spiralization, cytoplasm is extruded by the apposition of the cytoplasmic surfaces of the membrane to allow compaction of the mature multilamellar sheath. However, even in mature compact myelin, Schwann cell cytoplasm does persist in channels called Schmidt–Lanterman incisures and in the adaxonal or periaxonal rim of the mature sheath (Bunge et al., 1989). The purpose of these cytoplasm-filled channels is unclear. They may serve as supply lines for the delivery of nutrients or membrane to the distal regions of the sheath. Alternatively, they may provide the submembranous scaffolding required for appropriately orienting or locating proteins within discrete regions of the periaxonal myelin membrane. Indeed, it has been proposed that MAG interacts with microfilaments via spectrin, which might account for the restricted localization of MAG in the myelin sheath (Trapp et al., 1989a).

The intracellular events that trigger the morphological differentiation of the Schwann cell following axon–glial interaction are largely unknown. The second messenger cyclic AMP may function in the signaling process because elevated levels of intracellular cyclic AMP can mimic some of the effects of axonal contact in cultured Schwann cells (Kelly et al., 1992; Morgan et al., 1991; Porter et al., 1986; Sobue and Pleasure, 1984; Sobue et al., 1986). Notwithstanding the evidence for cyclic AMP involvement, the intracellular targets for such signals, which presumably include the cytoskeleton, remain unknown.

We are interested in elucidating the intracellular events that drive axonal ensheathment following the interaction between the Schwann cell and the axon. In this paper, we report the molecular cloning of a PNS myelin protein with a size of 147 kd deduced from the sequence of a full-length cDNA clone. Because this protein is primarily localized in the periaxonal membranes of myelinating Schwann cells, we call it periaxin. Periaxin is relatively abundant but, unlike the major protein of PNS myelin P_0, it is not an integral membrane protein. Periaxin is implicated in the earliest stages of myelin deposition because it is detectable in the first layers of Schwann cell cytoplasm that ensheathe the axon. Since the physical properties of periaxin are those expected of a cytoskeleton-associated protein, we propose that periaxin might link the cytoskeleton with the cytoplasmic domains of integral membrane proteins (such as MAG) in the periaxonal regions of the Schwann cell plasma membrane.

Results

A Protein of M_r 170 kd Is an Abundant and Specific Component of Rat PNS Myelin

In a search for cytoskeletal and cytoskeleton-associated proteins of Schwann cells, we raised an anti-

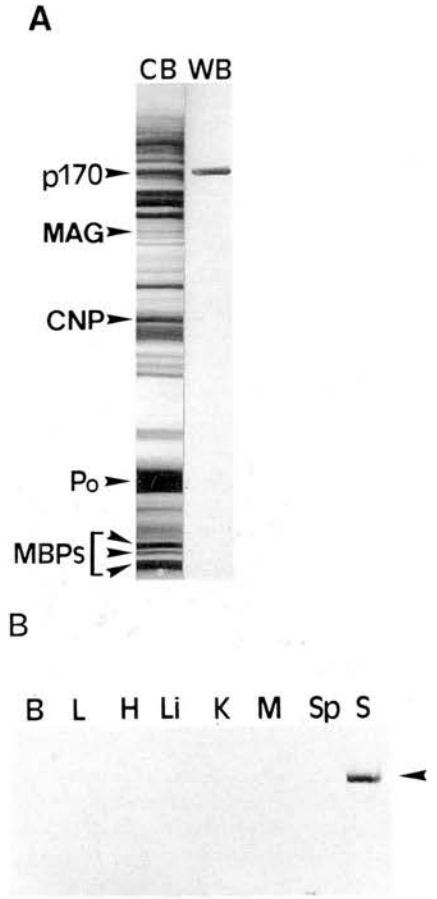

Figure 1. Identification of Periaxin as a Peripheral Nerve–Specific Protein with the Anti-p170 Antibody

(A) Rat sciatic nerve myelin was analyzed on 5%–17% gradient SDS–PAGE gels. One lane (CB) was stained with Coomassie blue (65 μg protein), and the other lane (WB) (1 μg protein) was transferred to nitrocellulose and immunostained with rabbit anti-p170 antibody. The immunoblot demonstrates that the anti-p170 antibody specifically recognizes a protein of M_r 170 kd.

(B) Homogenates of brain (B), lung (L), heart (H), liver (Li), kidney (K), muscle (M), spleen (Sp), and sciatic nerve (S) were homogenized in phosphate-buffered saline containing 0.1% Triton X-100. Aliquots of the homogenates (1 μg of protein for sciatic nerve; 15 μg of protein for all other tissues) were electophoresed by SDS–PAGE on 5%–17% gradient gels, transferred to nitrocellulose, and immunostained using rabbit anti-p170 antibody at 1:1000 dilution. Periaxin is clearly shown to be present only in peripheral nerve tissue.

body in rabbits against a high molecular weight, Triton X-100-insoluble protein of rat PNS myelin, which recognizes a protein with an estimated size of 170 kd (p170) by SDS–polyacrylamide gel electrophoresis (SDS–PAGE) (Figure 1A). When PNS myelin proteins are resolved by SDS–PAGE and stained with Coomassie blue, p170 appears to be a prominent constituent of PNS myelin in comparison with other well-characterized proteins such as MAG, 2′,3′-cyclic nucleotide 3′-phosphohydrolase, and the myelin basic proteins, although it is not as abundant as P_0, the major integral membrane of PNS myelin (Figure 1). The recovery of p170 in the myelin fraction is drastically reduced in the absence of proteinase inhibitors, and Western blot analysis shows that this is a consequence of extensive degradation (data not shown). In light of the fact that we subsequently localized p170 to the periaxonal membranes of PNS myelin, we have named it periaxin. In the rat, periaxin is exclusively found in the PNS (Figure 1B), and this pattern of expression is common to a variety of vertebrates, including human, pig, pigeon, cow, and Torpedo (data not shown).

Molecular Cloning and Sequence of Periaxin

To establish the primary structure of periaxin, several overlapping clones were isolated, and the sequence of a 4,657 bp cDNA clone pA1BG was established (Figure 2). This cDNA has a single long open reading frame and an initiation ATG within a strong Kozak concensus sequence (RNNATGG) (Kozak, 1991). The deduced sequence of 1389 amino acids would encode a protein of 147,063 daltons, which is at variance with the apparent size of the protein from SDS–PAGE. Therefore, we were concerned to ensure that another initiation methionine codon did not exist 5′ to the known sequence. This was particularly important to establish since there are no in-frame stop codons in the 5′ untranslated region of pA1BG. Repeated attempts by a variety of methods to isolate other cDNA clones, including rapid amplification of cDNA ends, did not extend the sequence further at the 5′ end. Although several clones were characterized, all terminated at their 5′ ends within a few nucleotides of the sequence shown in Figure 2. Further evidence that we had isolated a clone which encoded the full length of the protein came from in vitro transcription–translation experiments. These showed that the protein encoded by pA1BG has an identical M_r to the protein immunoprecipitated from a translation programmed with sciatic nerve mRNA (Figure 3A, lanes 1 and 2). Furthermore, the protein encoded by pA1BG is immunoprecipitated by anti-p170 antibody (Figure 3A, lane 3), which demonstrates that pA1BG does indeed encode periaxin. Since we had earlier found that the N-terminus of periaxin is blocked and not amenable to direct amino acid sequencing, we raised and affinity purified an antibody against a synthetic peptide corresponding to amino acids 713–728 (Figure 2) to confirm the correct reading frame of pA1BG independently. This antibody (anti-170pep1) recognizes periaxin in Western blot analysis, thus establishing the correct reading frame (Figure 3B).

Two distinct mRNAs are detected by Northern blot analysis (see Figure 7A). However, both mRNAs seem to be the product of a single gene, since only one major fragment is detected when genomic DNA is blotted after digestion with several restriction enzymes (Figure 4).

The Deduced Primary Structure

Neither the nucleotide nor the deduced amino acid sequence of periaxin is significantly similar to any

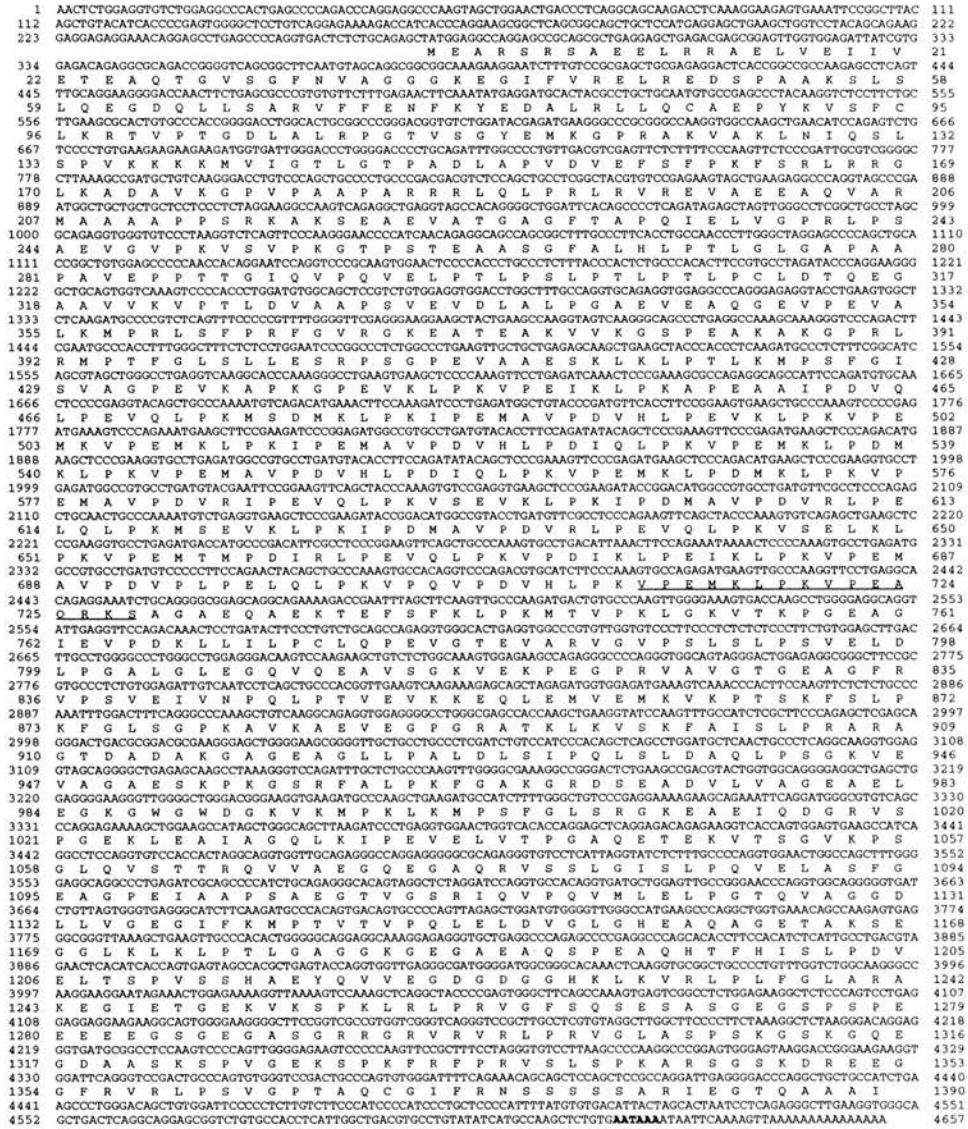

Figure 2. The Complete Nucleotide and Deduced Amino Acid Sequence of Rat Periaxin Clone pA1BG

The amino acid sequence was deduced from the first in-frame methionine, which also has a strong Kozak initiation consensus sequence RNNATGG. The underlined amino acid sequence denotes the 170pep1 peptide, and the sequence in bold type (AATAAA) indicates a polyadenylation signal. Periaxin contains 1389 amino acids (including the initiation methionine) and has a calculated molecular weight of 147,063.

other sequence in the GenBank or EMBL databases. The closest match at 18% similarity is shown by collagen type IV over a 600 amino acid region from amino acid 780 to the C-terminus of periaxin. It seems likely that this merely reflects the abundance of proline, serine, and glycine residues in that region of the protein. Overall, periaxin is slightly basic (pI, 8.6), but this obscures the presence of a highly basic domain near the N-terminus between amino acids 118 and 196 and an acidic region encompassed by residues 1036–1163 toward the C-terminus.

Periaxin does not appear to be an integral membrane protein. Hydrophobicity plots reveal no evidence for transmembrane hydrophobic domains in the sequence, and, although it does possess a single consensus N-glycosylation site at amino acid 1373, this site is not used since treatment with N-glycosidase F does not cause a shift in the mobility of the protein in SDS–PAGE (Figure 5). Under the same conditions, the major form of the glycoprotein MAG found in the PNS, S-MAG, is deglycosylated and shows a shift in M_r from 100,000 before deglycosylation to 67,000 after deglycosylation, which is close to the known size of the polypeptide (Frail et al., 1985) (Figure 5). There is a large number of potential phosphorylation sites in the protein: 11 for cyclic AMP kinase, 29 for glycogen synthase kinase 3, 2 for protein kinase C, and 11 for calmodulin kinase II. Comparison of secondary struc-

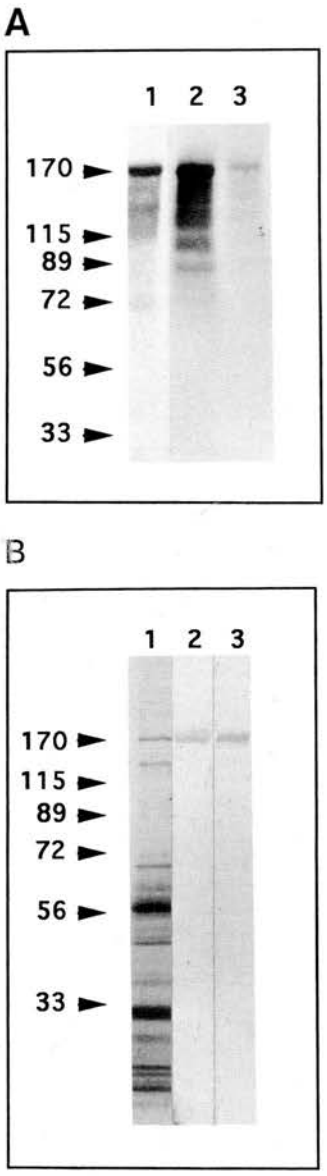

Figure 3. Confirmation That Periaxin Clone pA1BG Contains the Complete Coding Region and the Correct Open Reading Frame

(A) Comparison of the M_r of the protein made in translations programmed with sciatic nerve mRNA and mRNA transcribed from the pA1BG cDNA cloned into pSPORT 1 vector. The mRNAs were translated in a rabbit reticulocyte lysate, and the samples were as follows: lane 1, rat sciatic nerve translation products immunoprecipitated with anti-p170 antibody; lane 2, translation of pA1BG mRNA; lane 3, as for lane 2 but immunoprecipitated with anti-p170 antibody. A single major protein migrated with an M_r of 170 kd in all three lanes. This indicates that the entire coding region for periaxin is present in the pA1BG clone.

(B) Rat sciatic nerve myelin was electrophoresed on 5%–17% gradient gels and stained with Coomassie blue (lane 1; 40 μg of protein) or transferred to nitrocellulose (lanes 2 and 3). The blots (each containing 1 μg of protein) were immunostained using rabbit anti-p170 antibody (lane 2) and the rabbit anti-170pep1 antibody raised against the peptide sequence VPEMKLPKV-PEAQRKS (amino acids 713–728 of the deduced periaxin sequence). The anti-170pep1 antibody recognizes periaxin and confirms the correct reading frame of the deduced amino acid sequence.

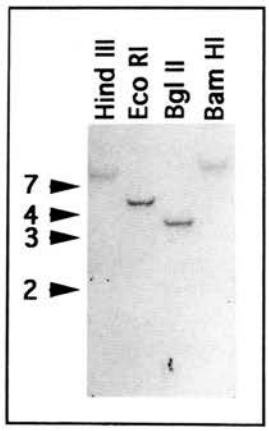

Figure 4. Southern Blot Analysis of the Periaxin Gene

Rat genomic DNA was digested with HindIII, EcoRI, BglII, and BamHI as indicated above each lane and electrophoresed on a 0.8% agarose gel. After transfer to Hybond-N membrane, the blot was hybridized with a pA1BG cDNA PCR fragment (nucleotides 1–265) that had been ^{32}P labeled by random priming. Molecular weight markers (kb) are indicated at the left margin. The presence of only one hybridizing band in each lane indicates a single copy periaxin gene.

ture predictions using the algorithms of Chou-Fassman and Robson-Garnier does not expose any consistent regions of α-helical structure.

The most remarkable feature of the primary structure of periaxin is the presence of a series of repeats throughout a rather long region comprising amino acids 430–730. The core repeat is a pentamer in which the variable amino acid is always either alanine or

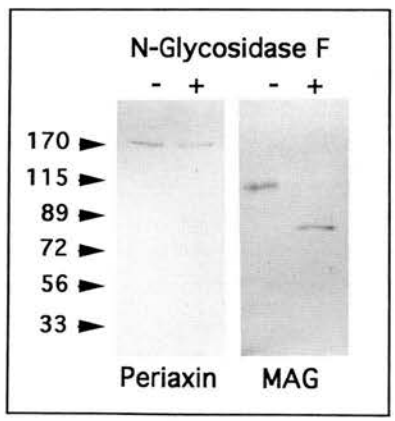

Figure 5. Periaxin Is Not N-Glycosylated

Rat sciatic nerve myelin was incubated at 37°C with (+) or without (−) N-glycosidase F as described in Experimental Procedures. The digests were electrophoresed on 5%–17% gradient gels and transferred to nitrocellulose. The blots were immunostained using rabbit anti-p170 or rabbit anti-MAG antibody as control. Incubation in the presence of N-glycosidase F did not alter the mobility of periaxin, indicating that there are no N-linked oligosaccharide chains present on the molecule. In contrast, cleavage of the N-linked oligosaccharides of MAG resulted in a large increase in the mobility of the protein.

A

432	GPEVK	APK	531	VPEMK		627	IPDMA	
440	GPEVK	LPK	536	LPDMK	LPK	632	VPDVR	
448	VPEIK	LPK	544	VPEMA		637	LPEVQ	LPK
456	APEAA		549	VPDVH		645	VSELK	LPK
461	IPDVQ		554	LPDIQ	LPK	653	VPEMT	
466	LPEVQ	LPK	562	VPEMK		658	MPDIR	
474	MSDMK	LPK	567	LPDMK	LPK	663	LPEVQ	LPK
482	IPEMA		575	VPEMA		671	VPDIK	
487	VPDVH		580	VPDVR		676	LPEIK	LPK
492	LPEVK	LPK	585	IPEVQ	LPK	684	VPEMA	
500	VPEMK		593	VSEVK	LPK	689	VPDVP	
505	VPEMK	LPK	601	IPDMA		694	LPELQ	LPK
513	IPEMA		606	VPDVR		702		VPQ
518	VPDVH		611	LPELQ	LPK	705	VPDVH	LPK
523	LPDIQ	LPK	619	MSEVK	LPK	713	VPEMK	LPK
						721	VPEAQ	

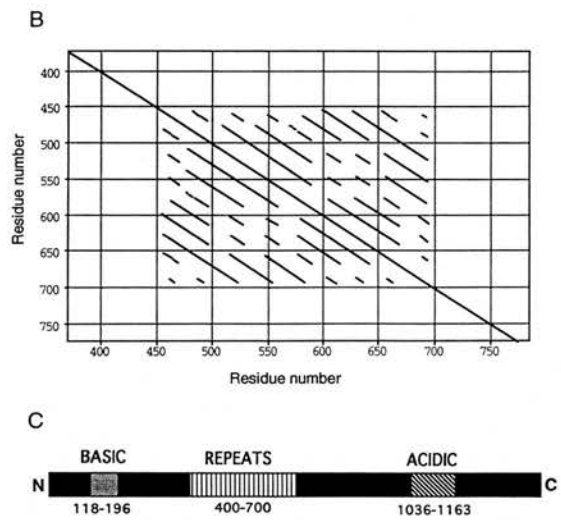

Figure 6. The Repeat Motif of Periaxin

(A) The smallest units in the repeat region are a pentapeptide and a tripeptide spacer. The pentapeptide comprised the following amino acids: aliphatic nonpolar:pro:glu or asp:aliphatic nonpolar:variable. The underlined sequences substitute serine for proline. The numbers refer to the position of the amino acids in the sequence shown in Figure 2.

(B) Dot matrix plot analysis showing the region between residues 430 and 730 that is rich in repeats. The periaxin amino acid sequence was compared with itself using the MacVector software package with a window size of 30 and a minimum score of 80%, and the results were plotted as a dot matrix. The repeat region is shown in expanded view to demonstrate the multiple repeated units. This was the only region in the protein to have a significant content of repeated sequences.

(C) The domain structure of periaxin. The repeat-rich region separates a strongly basic N-terminal segment from the acidic C-terminus.

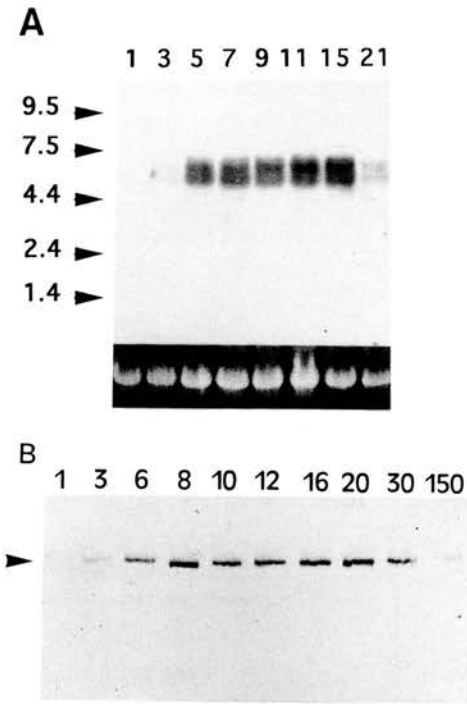

Figure 7. Periaxin Expression Parallels Myelination in Rat Sciatic Nerve

(A) Developmental expression of periaxin mRNA. Sciatic nerve total RNA from rats of various ages was electrophoresed (10 μg per lane) on a 1% formaldehyde agarose gel, transferred to Hybond-N membrane, and probed with a PCR fragment of the pA1BG cDNA (bases 1–265) that had been ^{32}P labeled by random priming. Postnatal ages (in days) are indicated at the top of the figure, and the ethidium bromide–stained 18S RNA in each lane is shown in the bottom panel to demonstrate that the RNA loadings are similar. Molecular weight markers are indicated at the left margin in kilobases. The levels of periaxin mRNA increase sharply at day 5 and peak at around day 15, following which periaxin mRNA becomes barely detectable by day 21.

(B) Immunoblot analysis of the developmental expression of periaxin. Sciatic nerves from rats of different ages were homogenized in phosphate-buffered saline containing 0.1% Triton X-100 and electrophoresed on 5%–17% gradient gels (5 μg of protein per lane), transferred to nitrocellulose, and immunostained with anti-p170 antibody. The postnatal ages (in days) are indicated at the top of each lane and show that periaxin protein expression increased steadily from birth and peaks between day 8 and day 20. The amounts of periaxin in sciatic nerve homogenates declined dramatically in the adult.

glutamine or one of the basic amino acids (Figure 6A), as follows:

aliphatic nonpolar:pro:glu or asp:aliphatic nonpolar:variable

Higher order repeats are also apparent, and these are most dramatically revealed by a dot matrix plot comparison of the periaxin amino acid sequence with itself (Figure 6B). This region appears to be less flexible than the rest of the polypeptide, as shown by analysis with the GCG and MacVector packages. Therefore, it may be that the repeat region serves to extend the protein, thus keeping the basic and acidic domains well separated (Figure 6C).

Developmental Expression of Periaxin in Sciatic Nerve

Both periaxin and its message are first detectable in sciatic nerve homogenates soon after birth (Figures 7A and 7B). Two distinct mRNAs of approximately 4.7 and 5.2 kb are detected by Northern blot analysis (Figure 7A). However, the relative amounts of these two

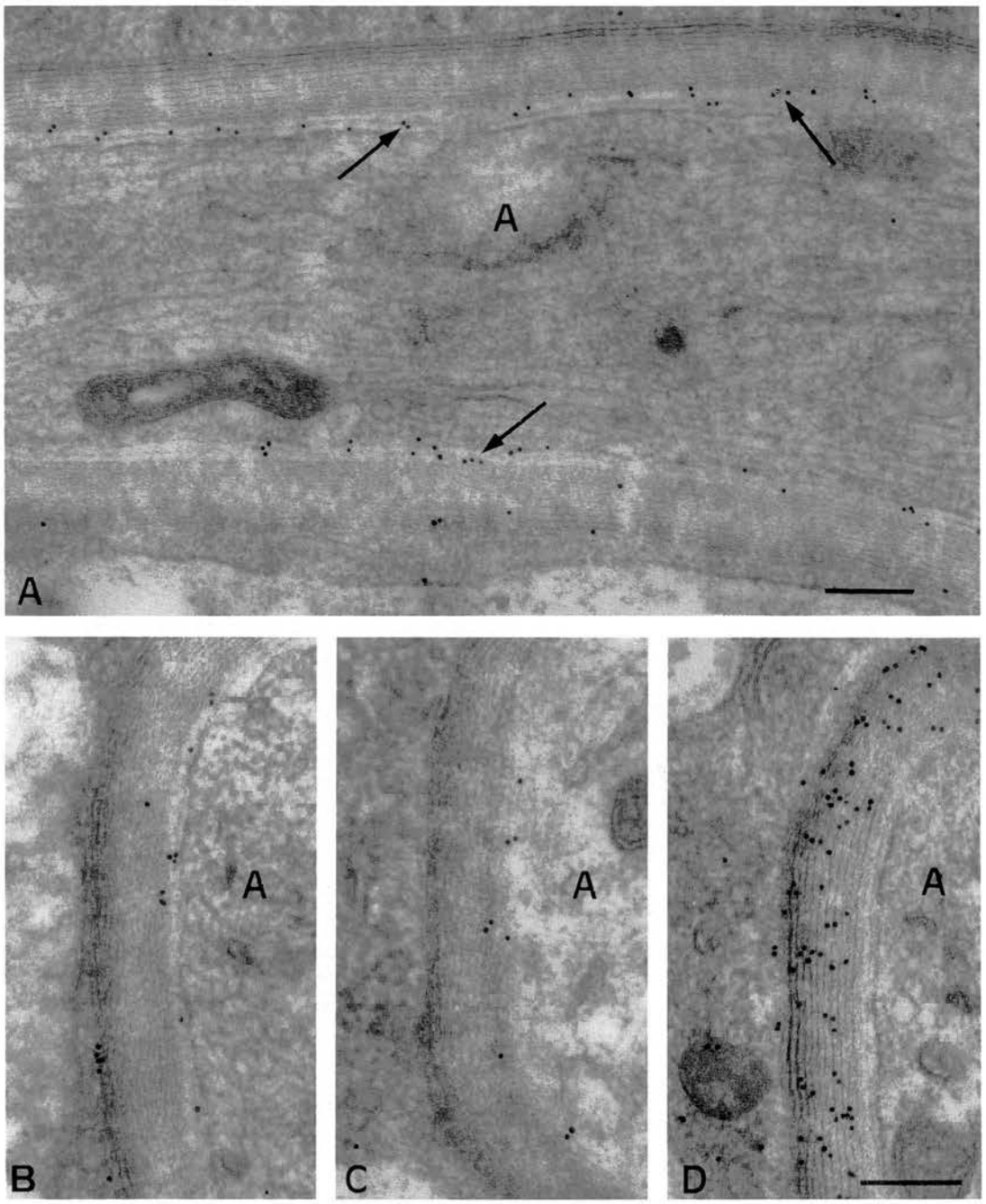

Figure 8. Comparison of Periaxin, MAG, and P_0 Localization in the Sciatic Nerves of 3- to 4-Day-Old Rats by Immunoelectron Microscopy
In longitudinal section, 10 nm gold particles are primarily localized to periaxonal myelin membranes in sciatic nerve (A, arrows). In transverse section, periaxin (B) colocalizes with MAG (C) in periaxonal membranes, whereas P_0 (D) is distributed throughout compact myelin. The axon (A) is indicated in each panel. Bar, 200 nm.

forms do not change during development, and it seems likely that they represent mRNAs with the same coding region but different-sized 3' untranslated sequences. It is presumed that the larger mRNA corresponds to a message with a longer untranslated region, and we have some preliminary evidence from the sequencing of another group of clones that this is the case.

Figure 7 shows that message and protein levels peak in the sciatic nerve between postnatal days 8 and 20; thereafter, they decline precipitously, which suggests that periaxin is primarily involved in the early phases of myelin deposition. The relative amounts of periaxin mRNA during the most active period of myelin deposition in the sciatic nerve parallel those of the major myelin protein P_0 (Lemke and Axel, 1985), although

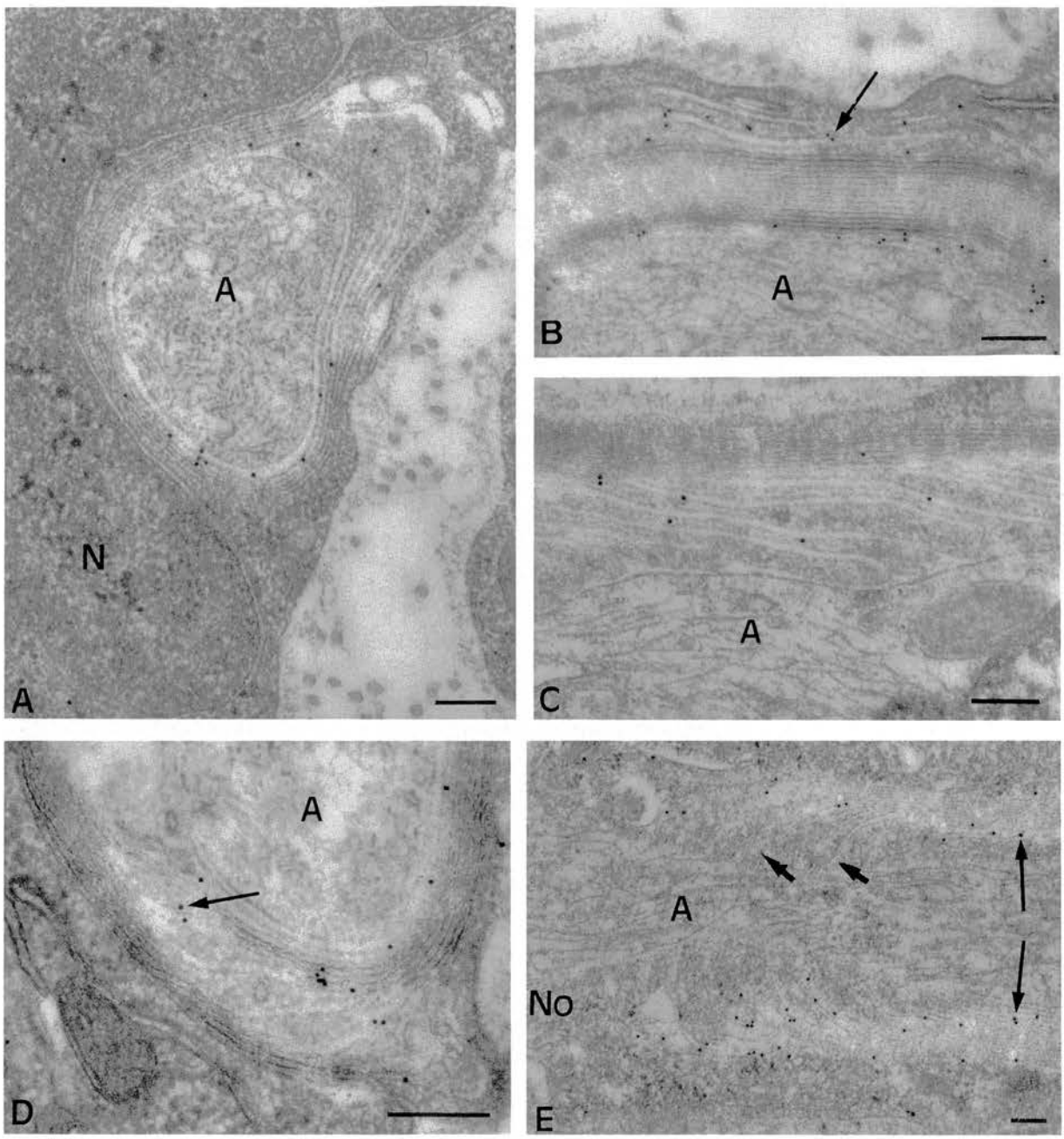

Figure 9. Immunoelectron Microscopic Detection of Periaxin in Uncompacted Myelin

A Schwann cell with a prominent nucleus (N) is shown at an early stage of axonal ensheathment in (A). Periaxin is present in the cytoplasm-filled tongues of myelin that surround the axon, but in regions where the membranes have compacted, it is restricted to the periaxonal membranes. Periaxin persists in abaxonal uncompacted layers of myelin (B, arrow) and in Schmidt-Lanterman incisures (C and D, arrow). Close to the nodal regions (No), periaxin is predominantly found in the periaxonal membranes of compact myelin (E, large arrows) and not in the paranodal loops (E, small arrows). The axon (A) is indicated in each panel. Bar, 200 nm.

the decline in periaxin mRNA in the adult nerve is more marked.

Subcellular Immunolocalization

To gain some insight into the function of periaxin, we investigated its localization in the myelin membrane at different stages of axonal ensheathment in the intact sciatic nerve by immunoelectron microscopy. In longitudinal sections of sciatic nerves stained with the affinity purified anti-peptide antibody, gold particles are localized to the periaxonal membranes of myelin (Figure 8A). Negligible labeling of compact myelin is observed. This localization is remarkably similar to that of MAG (compare Figures 8B and 8C), which has previously been documented by Trapp and coworkers (Trapp, 1988; Trapp et al., 1989a, 1989b; Trapp and

Quarles, 1984). By comparison, P_0, the major membrane glycoprotein of PNS myelin, is distributed throughout compact myelin (Figure 8D). The colocalization of periaxin and MAG suggests that they may interact in the periaxonal space.

Gold particles are distributed throughout the first three or four spirals of Schwann cell cytoplasm in nerves immunolabeled for periaxin at an early stage of axonal ensheathment (Figure 9A). However, Figure 9A also shows that in those regions of the sheath where the membranes are apposing, the gold particles appear to be localizing to the periaxonal membranes. In mature myelinated fibers, periaxin persists in the abaxonal noncompacted layers that are filled with Schwann cell cytoplasm (Figure 9B). A characteristic feature of the localization of MAG in the PNS is its enrichment in Schmidt–Lanterman incisures and paranodal loops in addition to the periaxonal region (Trapp, 1988; Trapp et al., 1989a, 1989b; Trapp and Quarles, 1984). In contrast, periaxin does not show the same type of distribution. Some periaxin is found in Schmidt–Lanterman incisures (Figures 9C and 9D), but it appears to be excluded from paranodal loops (Figure 9E).

Discussion

Neurons have a profound effect on the cell biology of the Schwann cell. However, the chain of events that determines the fate of the myelin-forming Schwann cell is still unclear. A prerequisite for unraveling the order of events will be the identification of the key genes that are expressed by the Schwann cell at the earliest stages of commitment to the myelin-forming path. In this paper, we demonstrate that a novel protein, periaxin, is detectable in the first layers of Schwann cell cytoplasm which encircle an axon during myelination. The extent of periaxin expression, both in terms of protein and mRNA, reflects the activity of PNS myelin deposition, and once the mature myelin sheath is established, the amount of the protein declines to barely detectable levels in the sciatic nerve. This suggests that periaxin has a role in ensheathment and spiralization but is perhaps less involved in the maintenance of the multilamellar structure in mature nerves.

The structure of periaxin provides some clues as to its function. It has a striking series of repetitive motifs in its deduced amino acid sequence, which are located to the C-terminal side of an N-terminal highly basic domain (Figure 6C). The only other region of the protein where there is a preponderance of acidic or basic amino acids is an acidic domain close to the C-terminus. The structural significance of the repeats has yet to be determined, but it is significant that repeated sequence units over quite long stretches of polypeptide sequence are particularly common amongst proteins which interact with the cytoskeleton (Matsudaira, 1991). This region is predicted to be rather rigid and relatively inflexible, and the repetitive sequence may serve as a spacer that would act to separate two functional domains, such as the acidic and basic regions of the protein, as has been proposed for the KDM repeats of the microtubule-associated protein MAP4 (West et al., 1991). By keeping the acidic and basic domains apart, they would be available for interaction with other polypeptide chains, including periaxin itself. Structure prediction programs indicate that periaxin has little secondary structure and a rather open linear conformation. Therefore, periaxin is an excellent prospective linker protein for coupling periaxonal proteins to elements of the Schwann cell cytoskeleton, particularly so since it has the solubility properties of a cytoskeleton-associated protein. Ensheathment and spiralization around the axon require drastic changes in cell shape, and the cytoskeleton is strongly implicated in the morphological differentiation of myelin-forming cells (Kelly et al., 1992; Vouyiouklis and Brophy, 1993; Wilson and Brophy, 1989).

There is considerable evidence that the integral membrane glycoprotein MAG is an adhesion molecule with a role in axonal–glial interaction (Owens and Bunge, 1991; Poltorak et al., 1987; Salzer and Colman, 1989; Salzer et al., 1987), particularly at early stages of myelination (Martini and Schachner, 1988; Owens and Bunge, 1989). In contrast with MAG, P_0 appears to be primarily concerned with myelin compaction (D'Urso et al., 1990; Filbin et al., 1990; Giese et al., 1992). It has been proposed that the C-terminal tail of MAG and the actin cytoskeleton are linked, possibly by means of the actin-binding protein spectrin (Trapp et al., 1989b). These interactions might have several functional implications. First, a strong association between the cytoplasmic surface of the periaxonal membrane and the cytoskeleton could provide the anchor points for microfilament attachment. These sites could then serve as the foci through which the force generated by the microfilament system might be transduced to drive the spiralization of myelin (Trapp et al., 1989b). Second, the necessity for the presence of Schwann cell cytoplasm between the periaxonal membranes might require a structure that could act as a physical spacer, thus preventing apposition and membrane compaction, as first suggested by Trapp and Quarles (1982). Third, the assembly of integral membrane proteins into domains is believed to be determined by their connections to the cortical cytoskeleton (Luna and Hitt, 1992). In these domains, such proteins could, for example, function optimally as intercellular adhesion molecules. The localization of periaxin to the first uncompacted spirals which surround the Schwann cell, together with its exclusion from compact myelin, suggests that it may have a role in one or more of these possible functions, perhaps by means of interactions with integral membrane proteins such as MAG. Periaxin itself does not appear to be an integral membrane protein with a transmembrane domain. Therefore, it probably copurifies with the myelin membrane owing to its association with other proteins. Although periaxin colocalizes with MAG in the periaxonal mem-

branes, it is significant that it does not show the enrichment in the paranodal regions or Schmidt-Lanterman incisures which is found for MAG in the PNS (Trapp, 1988; Trapp et al., 1989a, 1989b; Trapp and Quarles, 1982, 1984). From the relative intensities of Coomassie blue staining after SDS-PAGE, it can be concluded that there is much more periaxin than MAG in PNS myelin. Therefore, the fact that periaxin is not enriched in the paranodal loops and the Schmidt-Lanterman incisures does not preclude the possibility that there is sufficient periaxin to interact with MAG in these locations.

A particularly intriguing finding from this work is that periaxin is exclusively found in the PNS in all species examined. These observations raise the important question of how myelination in the PNS and CNS differs and what features of the cell biology of the Schwann cell might account for the requirement for periaxin expression at an early stage of axonal ensheathment. Myelin compaction occurs almost immediately after membrane ensheathment in the CNS, whereas in the PNS the cytoplasm is extruded more gradually, presumably to prevent apposition of the cytoplasmic surfaces of the growing myelin membrane (Field et al., 1968). Therefore, the presence of periaxin in the Schwann cell may promote ensheathment by preventing premature compaction.

Periaxin is a quantitatively significant component of PNS myelin. Therefore, it is perhaps surprising that this protein has not been described previously, since the protein composition of myelin, both in the CNS and the PNS, has been the subject of intense study. The extreme susceptibility of periaxin to proteolysis during the isolation of myelin may account for this dearth of knowledge. A protein with a similar M_r to periaxin has been described in Schwann cells induced by axonal contact, which was identified as a glycoprotein from lectin binding studies (Shuman et al., 1986, 1988). A second protein called Schwann cell-associated glycoprotein with an M_r of 170 kd from SDS-PAGE has been described by Western blot analysis and by immunocytochemistry at the light level in a separate report (Dieperink et al., 1992). Although it is possible that Schwann cell-associated glycoprotein and periaxin are related, the fact that the former is believed to be a transmembrane glycoprotein, whereas periaxin is not, makes this possibility less likely (Dieperink et al., 1992). As is apparent from Figure 1, there are several proteins in the vicinity of the 170 kd marker in SDS-PAGE separations of rat PNS myelin, and it seems likely that Schwann cell-associated glycoprotein is one of the other proteins in that region of the gel.

In summary, we have identified a novel protein with a pattern of developmental expression and subcellular localization consistent with its having an important role in the ensheathment of axons by Schwann cells. Further characterization of the function of this protein should help to elucidate the molecular mechanisms that underlie the engagement and ensheathment of nerve fibers by Schwann cells in the PNS. The availability of the cDNA that encodes periaxin and a knowledge of its amino acid sequence will now permit a more detailed analysis of its function in myelination.

Experimental Procedures

Isolation of Myelin

Myelin was prepared from CNS tissues of several species as previously described (Gillespie et al., 1989). PNS tissues were frozen in liquid nitrogen, pulverized, and homogenized in a 10 mM HEPES (pH 7.4) buffer containing 0.85 M sucrose and 3 mM dithiothreitol to which was added a proteinase inhibitor cocktail comprising of phenylmethylsulfonyl fluoride (2 mg/ml), leupeptin (10 μg/ml), chymostatin (0.7 mg/ml), antipain (10 μg/ml), pepstatin (15 nM), Nα-p-tosyl-L-lysine chloromethyl ketone (0.5 mM), benzamidine (10 μg/ml), EDTA (1 mM), and EGTA (1 mM). The homogenate was centrifuged at 4000 × g for 10 min at 4°C. Sucrose (0.25 M) in the same buffer used for homogenization was layered over the supernatant, and this was centrifuged at 80,000 × g for 90 min at 4°C. Myelin was collected at the interface between the two sucrose layers and osmotically shocked by resuspension in 20 vol of ice-cold water with the proteinase inhibitor cocktail. The myelin suspension was centrifuged at 10,000 × g for 30 min, and the pellet was shocked twice more.

Antibodies

The anti-p170 antibody was raised in rabbits against p170 purified by electroelution from polyacrylamide gels after SDS-PAGE of PNS myelin (Hunkapiller et al., 1984) and was used at a dilution of 1:1000 for Western blot analysis. A mouse polyclonal antibody was also generated against the same antigen. A rabbit antibody (170pep1) was raised against a synthetic peptide VPEMKLPKVPEAQRKS, a generous gift from Prof. N. Groome, Department of Biology, Oxford Brookes University, which comprised amino acids 713-728 of the complete periaxin sequence. To enhance its antigenicity, the peptide was coupled to Keyhole Limpet hemocyanin by standard techniques. Anti-170pep1 antibody was affinity purified by chromatography on a column of peptide coupled to CNBr-activated Sepharose (Sigma Chemical Company, Poole, England) and was used at 1:50 for immunoblotting. Affinity purified rabbit anti-MAG and anti-P_0 antibodies were a generous gift from Prof. D. R. Colman, Brookdale Centre for Molecular Biology, Mount Sinai Medical Center, NY.

Western Blot Analysis

Proteins were analyzed by SDS-PAGE on 5%-17% gradient polyacrylamide gels using the buffer system of Laemmli (1970). The separated proteins were then electrotransferred to nitrocellulose according to the method of Towbin et al. (1979). The nitrocellulose was blocked by incubation for 3 hr with 0.2% (w/v) gelatin in phosphate-buffered saline containing 0.1% (v/v) Triton X-100. Proteins were detected by incubation with appropriately diluted primary antibodies in blocking buffer followed by goat anti-rabbit IgG-horseradish peroxidase conjugate (Scottish Antibody Production Unit, Carluke, Scotland). After washing 3 times with blocking buffer and once with phosphate-buffered saline, immunoreactive proteins were detected using 3,3'-diaminobenzidine HCl and H_2O_2 (Sigma) as substrates in 50 mM Tris-HCl (pH 7.4). The peroxidase reaction was terminated with 2% SDS.

Deglycosylation of Myelin Proteins

Rat sciatic nerve myelin (20 μg of protein for MAG; 4 μg for periaxin) was solubilized in 1% SDS, 1% b-mercaptoethanol by boiling for 2.5 min. After cooling, the samples were divided into two equal aliquots, and each was diluted to 98 μl in 20 mM EDTA, 1% Nonidet P-40, and 0.1 M phosphate buffer (pH 6.3). N-Glycosidase F (2 μl; 0.4 U; Boehringer Mannheim, Lewes, England) was added to one set of samples, water was added to the other set, and all were incubated overnight at 37°C. Each sample was electrophoresed on 5%-17% gradient gels (Laemmli, 1970), and after transfer to nitrocellulose, the blots were immuno-

stained with either rabbit anti-MAG (1:500 dilution) or rabbit anti-p170 (1:1000) antibody.

Isolation and Characterization of cDNA Clones from Rat Sciatic Nerve Libraries

Total RNA was isolated from the sciatic nerves of 10-day-old rats using RNazol B following the manufacturer's instructions (Biogenesis, Bournemouth, England). Poly(A)$^+$ RNA was purified (Aviv and Leder, 1972) and used to construct a λgt11 cDNA library (Kelly et al., 1992), in which 3×10^5 recombinants were screened with the anti-p170 antibody (Young and Davis, 1983). Six positive clones were identified with a goat anti-rabbit antibody conjugated to horseradish peroxidase (North East Laboratories, Uxbridge, England). After plaque purification, one of the clones, pC2, was subcloned into M13 mp18 and mp19 vectors (Pharmacia, Milton Keynes, England) and sequenced by the chain termination technique (Sanger et al., 1977) using Sequenase (Cambridge Bioscience, Cambridge, England). An additional 3×10^5 recombinants were then screened by hybridization using a digoxigenin-labeled HindIII-ApaI fragment (nucleotides 1796–2677 of the pA1BG cDNA) according to the manufacturer's instructions (Boehringer Mannheim). One clone (pD5) was sequenced and found to have a 5′ end at nucleotide 1128 of the pA1BG sequence, but it lacked the poly(A) tail. A PstI fragment of this clone (nucleotides 1228–2457) was labeled with digoxigenin and used to screen 2.5×10^5 recombinants from a unidirectional postnatal day 5 rat sciatic nerve cDNA library constructed in SalI–NotI double-digested λgt22A (GIBCO BRL, Paisley, Scotland) following the manufacturer's instructions. Of the 12 clones isolated and plaque purified, the largest (pBG), which comprised almost all of the full-length pA1BG cDNA (from base 41 up to and including the poly[A] tail), was subcloned into the pSPORT 1 plasmid (GIBCO BRL) for restriction site analysis. Large restriction fragments encompassing the entire pBG clone were directionally subcloned into M13 phagescript (Stratagene, Cambridge, England) mp18 and mp19 vectors, and both strands were sequenced using a combination of unidirectional deletions (Henikoff, 1984) and specific oligonucleotide primers complementary to the derived DNA sequence.

To obtain more sequence 5′ to pBG, a random primed postnatal day 15 rat sciatic nerve library was constructed using 150 ng of random hexamers (GIBCO BRL) to prime first strand synthesis. Following second strand synthesis and the addition of EcoRI–NotI adaptors, the cDNA was ligated into EcoRI-digested λgt11 (Promega, Southampton, England) and packaged using Gigapack Gold packaging extracts (Stratagene). A portion of the library (3×10^5 recombinants) was screened using a digoxigenin-labeled cDNA probe derived from the extreme 5′ end of pBG (nucleotides 41–598 of the pA1BG sequence), and 10 positive clones were identified. On sequencing both strands of one of the clones, pA1, an extension of 40 bases at the 5′ end of pBG was obtained. The full-length clone pA1BG was obtained by ligating the SalI–SstII fragment (5′ end) from pA1 to the SstII–NotI (3′ end) fragment of pBG, and the resulting construct was subcloned into pSPORT 1 for further analysis. To determine whether a full-length clone might possess additional nucleotides 5′ to pA1BG, the remainder of the random primed λgt11 cDNA library was amplified (Sambrook et al., 1989), and aliquots equivalent to 1×10^5 pfu were subjected to polymerase chain reaction (PCR) using a combination of λgt11 forward and reverse primers (New England Biolabs, CP Laboratories, Hertfordshire, England), a pA1BG-specific primer (5′-TAGCTCTGCAGAGAGTCACC-3′), and a pA1BG-specific nested primer (5′-TGATGTACAGCTGTAAGCCGG-3′). In addition, the 5′ rapid amplification of cDNA ends protocol (Frohman et al., 1988) was performed with dCTP as the terminal transferase substrate, 5′-GGCCACGCGTCGACTAGTAC$(G)_{16}$-3′ as the PCR anchor primer, and the pA1BG-specific primers described above. Each PCR was subjected to 30 cycles of amplification with 2.5 U of Taq polymerase (GIBCO BRL) in a total volume of 100 μl of a buffer supplied by the manufacturer.

The MacVector (IBI, Cambridge, England) and University of Wisconsin GCG software packages (Devereaux et al., 1984) were used for sequence analysis.

Northern and Southern Blot Analyses

Poly(A)$^+$ RNA was electrophoresed on 1% formaldehyde agarose gels (Kroczek and Siebert, 1990) and transferred to Hybond-N membrane (Amersham, Aylesbury, England) by vacuum blotting in 20× SSC. The filters were probed for 1.5 hr in QuikHyb solution (Stratagene) with a PCR fragment spanning bases 1–265 of the pA1BG clone that had been ^{32}P labeled by random priming (Feinberg and Vogelstein, 1983). The blots were washed to a final stringency of 0.1× SSC at 65°C.

Genomic DNA for Southern blots was isolated from rat liver (Ausubel et al., 1989) and digested with restriction enzymes for 3 hr at 37°C. The digested DNA was electrophoresed on 0.8% agarose gels, denatured in 0.5 M NaOH, and vacuum transferred to Hybond-N in 20× SSC. Hybridization with the same ^{32}P-labeled PCR fragment was as described for the Northern blots. Blots were exposed to Fuji RX film (Genetic Research Instrumentation, Dunmow, Essex, England) and developed using Kodak LX24 developer and FX40 fixer.

In Vitro Transcription and Translation

Clone pA1BG was ligated into the pSPORT 1 vector and purified using Qiagen tips (Hybaid, Teddington, England) following the manufacturer's instructions and digested with XbaI. T7 RNA polymerase was used to transcribe 2.5 μg of purified plasmid in a 25 μl reaction mixture using the Riboprobe Gemini II system (Promega). Capped mRNA was obtained by including m^7(G)(5′)ppp(5′)G (Boehringer Mannheim) in the transcription mixture.

Aliquots of the mRNA transcribed in vitro and total RNA from day 15 rat sciatic nerve were used to program a reticulocyte lysate translation system (Promega). A fraction of the total translation products was solubilized by boiling in 2% SDS containing 10 μg/ml leupeptin and 10 μg/ml antipain and was diluted with 4 vol of solution A (50 mM Tris-HCl [pH 7.4], 2.5% (v/v) Triton X-100, 150 mM NaCl, 4 mM EDTA) containing 10 μg/ml leupeptin and 10 μg/ml antipain. Anti-p170 antibody (15 μl) was added, and the immunocomplexes were incubated for 60 min at room temperature, following which protein A agarose (Sigma) was added for an additional 60 min. Immunocomplexes were centrifuged at 13,000 × g for 5 min and washed 6 times with solution A containing 0.1% SDS and finally with solution A without detergents. The samples were solubilized and electrophoresed on 5%–17% gradient polyacrylamide gels (Laemmli, 1970). Gels were stained with 0.2% Coomassie blue (PAGE Blue 83, BDH, Glasgow, Scotland), destained, incubated for 30 min in Amplify (Amersham), and dried. The dried gel was exposed to X-ray film (Fuji RX) at −70°C.

Electron Microscopy

Sciatic nerves from 3- to 4-day-old rats were fixed by immersion in 4% formaldehyde (freshly prepared from paraformaldehyde) in a 0.01 M periodate, 0.075 M lysine, 0.1 M phosphate buffer containing 3% sucrose at pH 7.4 (McLean and Nakane, 1974) for 2 hr at room temperature. The tissue was washed several times with phosphate buffer containing 3.5% sucrose and stained with 0.25% tannic acid in the same buffer for 1 hr at 4°C (subsequent steps were performed at 4°C). After several washes in phosphate sucrose buffer, aldehydes were quenched in 50 mM NH_4Cl in the same buffer. The tissue was then washed 4 times in 0.1 M maleate buffer (pH 6.2) containing 4% sucrose, followed by 2% uranyl acetate in maleate sucrose buffer for 1 hr. The tissue was dehydrated to 90% ethanol (from 70% ethanol onward, all steps were at −20°C), infiltrated with a 1:1 ratio of LR Gold (Agar Scientific Ltd., Stanstead, Essex) and ethanol, followed by a 7:3 ratio of LR Gold and ethanol and two changes of LR Gold for 2–3 hr each. The tissue was infiltrated overnight in LR Gold containing 0.5% benzoin methyl ether and embedded in gelatin capsules. Polymerization was by ultaviolet irradiation at a wavelength of 365 nm for 24 hr at −20°C.

Sections on formvar carbon-coated nickel grids were blocked with 1% bovine serum albumin, 0.5% fish skin gelatin, 0.05% Triton X-100, 0.05% Tween 20 in Tris buffer (10 mM Tris, 500 mM NaCl [pH 7.4]) for 30 min at room temperature and incubated

with anti-P_0, anti-MAG, or anti-170pep1 antibody in the same buffer overnight at 4°C. Grids were washed 4 times with the above buffer and incubated for 1 hr with goat anti-rabbit IgG conjugated to 10 nm gold (1:20; Amersham). The grids were then washed on drops of distilled water, fixed with 2.5% aqueous glutaraldehyde, and rinsed in a stream of distilled water. After postfixing for 15 min with 2% aqueous OsO_4, the grids were stained with lead citrate and examined at 80 kV in a JEOL 100CX electron microscope.

Acknowledgments

We wish to thank L. Taylor for photographic assistance and F. McAllister for technical assistance. B. M. Kelly and D. A. Vouyiouklis are thanked for a critical reading of the manuscript. This work benefitted from the use of the SEQNET service at SERC, Daresbury Laboratory.

This work was supported by the Multiple Sclerosis Society of Great Britain in Scotland.

The costs of publication of this article were defrayed in part by the payment of page charges. This article must therefore be hereby marked "*advertisement*" in accordance with 18 USC Section 1734 solely to indicate this fact.

Received November 29, 1993; revised January 14, 1994.

References

Ausubel, F. M., Brent, R., Kingston, R. E., Moore, D. D., Seidman, J. G., Smith, J. A., and Struhl, K. (1989). Current Protocols in Molecular Biology (New York: Wiley-Interscience).

Aviv, H., and Leder, P. (1972). Purification of biologically active globin messenger RNA by chromatography on oligothymidylic acid cellulose. Proc. Natl. Acad. Sci. USA *69*, 1408–1412.

Brunden, K. R., Windebank, A. J., and Poduslo, J. F. (1990). Role of axons in the regulation of Po synthesis by Schwann cells. J. Neurosci. Res., *26*, 135–143.

Bunge, R. P., Bunge, M. B., and Eldridge, C. F. (1986). Linkage between axonal ensheathment and basal lamina production by Schwann cells. Annu. Rev. Neurosci. *9*, 305–328.

Bunge, R. P., Bunge, M. B., and Eldridge, C. F. (1989). Movements of the Schwann-cell nucleus implicate progression of the inner (axon-related) Schwann cell process during myelination. J. Cell Biol. *109*, 273–284.

Devereaux, J. P., Haeberli, P., and Smithies, O. (1984). A comprehensive set of sequence analysis programs for the VAX. Nucl. Acids Res. *12*, 387–395.

Dieperink, M. E., O'Neill, A., Magnoni, G., Wollmann, R. L., Heinrikson, R. L., Zurcher-Neely, H. A., and Stefansson, K. (1992). SAG: a Schwann cell membrane glycoprotein. J. Neurosci. *12*, 2177–2185.

Doyle, J. P., and Colman, D. R. (1993). Glial-neuron interactions and the regulation of myelin formation. Curr. Opin. Cell Biol. *5*, 779–785.

D'Urso, D., Brophy, P. J., Staugaitis, S. M., Gillespie, C. S., Frey, A. B., Stempak, J. G., and Colman, D. R. (1990). Protein zero of peripheral nerve myelin: biosynthesis, membrane insertion, and evidence for homotypic interaction. Neuron *4*, 449–460.

Feinberg, A. P., and Vogelstein, B. (1983). A technique for radiolabelling DNA restriction endonuclease fragments to high specific activity. Anal. Biochem. *132*, 6–13.

Field, E. J., Hughes, D., and Raine, C. S. (1968). Electron microscopic observations on the development of myelin in cultures of neonatal rat cerebellum. J. Neurol. Sci. *8*, 49–60.

Filbin, M. T., Walsh, F. S., Trapp, B. D., Pizzey, J. A., and Tennekoon, G. I. (1990). Role of myelin P_0 protein as a homophilic adhesion molecule. Nature *344*, 871–872.

Frail, D. E., Webster, H., and Braun, P. E. (1985). Developmental expression of the myelin-associated glycoprotein in the peripheral nervous system is different from that in the central nervous system. J. Neurochem. *45*, 1308–1310.

Frohman, M. A., Dush, M. K., and Martin, G. R. (1988). Rapid production of full-length cDNAs from rare transcripts: amplification using a single gene-specific oligonucleotide primer. Proc. Natl. Acad. Sci. USA *85*, 8998–9002.

Giese, K. P., Martini, R., Lemke, G., Soriano, P., and Schachner, M. (1992). Mouse P_0 gene disruption leads to hypomyelination, abnormal expression of recognition molecules, and degeneration of myelin and axons. Cell *71*, 565–576.

Gillespie, C. S., Wilson, R., Davidson, A., and Brophy, P. J. (1989). Characterization of a cytoskeletal matrix associated with myelin from rat brain. Biochem. J. *260*, 689–696.

Henikoff, S. (1984). Unidirectional digestion with Exonuclease III creates targeted breakpoints for DNA sequencing. Gene *28*, 351–359.

Hunkapiller, M. W., Lujan, E., Ostrander, F., and Hood, L. E. (1984). Isolation of microgram quantities of proteins from polyacrylamide gels for amino acid sequence analysis. Meth. Enzymol. *91*, 227–236.

Jessen, K. R., and Mirsky, R. (1991). Schwann cell precursors and their development. Glia *4*, 18–194.

Kelly, B. M., Gillespie, C. S., Sherman, D. L., and Brophy, P. J. (1992). Schwann cells of the myelin-forming phenotype express neurofilament protein NF-M. J. Cell Biol. *118*, 397–410.

Kozak, M. (1991). An analysis of vertebrate mRNA sequences: intimations of translational control. J. Cell Biol. *115*, 887–903.

Kroczek, R. A., and Siebert, E. (1990). Optimization of northern analysis by vacuum-blotting, RNA-transfer visualization and ultraviolet fixation. Anal. Biochem. *184*, 90–95.

Laemmli, U. K. (1970). Cleavage of structural proteins during the assembly of the head of bacteriophage T_4. Nature *227*, 680–685.

Lemke, G., and Axel, R. (1985). Isolation and sequence of a cDNA encoding the major structural protein of peripheral myelin. Cell *40*, 501–508.

Lemke, G., and Chao, M. (1988). Axons regulate the major myelin and NGF receptor genes. Development *102*, 499–504.

Luna, E. J., and Hitt, A. L. (1992). Cytoskeleton-plasma membrane interactions. Science *258*, 955–964.

Martin, J. R., and Webster, H. D. (1973). Mitotic Schwann cells in developing nerve: their changes in shape, fine structure, and axon relationships. Dev. Biol. *32*, 417–431.

Martini, R., and Schachner, M. (1988). Immunoelectron microscopic localization of neural cell adhesion molecules (L1, N-CAM, and myelin-associated glycoprotein) in regenerating adult mouse sciatic nerve. J. Cell Biol. *106*, 1735–1746.

Matsudaira, P. (1991). Modular organization of actin cross-linking proteins. Trends Biochem. Sci. *16*, 87–92.

McLean, I. W., and Nakane, P. K. (1974). Periodate-lysine paraformaldehyde fixative: a new fixative for immunoelectron microscopy. J. Histochem. Cytochem. *22*, 1077–1083.

Morgan, L., Jessen, K. R., and Mirsky, R. (1991). The effects of cAMP on differentiation of cultured Schwann cells: progression from an early phenotype (04+) to a myelin phenotype (P_0^+, GFAP$^-$, N-CAM$^-$, NGF-receptor$^-$) depends on growth inhibition. J. Cell Biol. *112*, 457–467.

Owens, G. C., and Bunge, R. P. (1989). Evidence for an early role for myelin-associated glycoprotein in the process of myelination. Glia *2*, 119–128.

Owens, G. C., and Bunge, R. P. (1991). Schwann cells infected with a recombinant retrovirus expressing myelin-associated glycoprotein antisense RNA do not form myelin. Neuron *7*, 565–575.

Peters, A., and Muir, A. R. (1959). The relationship between axons and Schwann cells during development of peripheral nerves in the rat. Quart. J. Exp. Physiol. *44*, 117–130.

Poltorak, M., Sadoul, R., Keilhauer, G., Landa, C., Fahrig, T., and Schachner, M. (1987). Myelin-associated glycoprotein, a member of the L2/HNK-1 family of neural cell adhesion molecules, is

fully appreciated as yet. Over recent years, it has become apparent that certain well-studied proteins, that in other cell types are known to be involved in cell or membrane motility and the generation of cell shape and polarity are found within the channel network of the Schwann cell. These include tubulin (Peters et al., 1991), actin, and spectrin (Trapp et al., 1989), ankyrin (Kordeli et al., 1990), connexin 32 (Bergoffen et al., 1993), and certain integrins (Einheber et al., 1993).

The structural integrity of Schwann cells, particularly the paranodal loops, has been shown to be sensitive to calcium (Blank et al., 1974). When cultured sensory ganglia were incubated in low calcium medium, lengthening of the node of Ranvier, swelling of the extracellular space between the paranodal loops, and separation and shrinkage of the axon away from the myelin sheath were observed. Over time, dissociation of the junction between the paranodal loops and the axolemma was noted. These changes were reversible upon return to normal calcium concentrations. These data prompted us to examine whether cadherins might be involved in the formation and maintenance of the nodal architecture.

The cadherins are a superfamily of calcium dependent adhesion proteins that function in cell recognition and segregation, morphogenetic regulation, and tumor suppression (for reviews see Magee and Buxton, 1991; Takeichi, 1991; Geiger and Ayalon, 1992; Grunwald, 1993). The classical cadherins are the most well studied and include N-cadherin (neural cadherin, ACAM), E-cadherin (epithelial cadherin, uvomorulin, arc LCAM), and P-cadherin (placental cadherin). They have a common primary structure that consists of an NH_2-terminal extracellular domain, a short transmembrane domain and a highly conserved COOH-terminal cytoplasmic domain which is responsible for interaction with cytoplasmic proteins (Nagafuchi and Takeichi, 1988) and subsequent stabilization of junctional complexes (Näthke et al., 1994). The extracellular domain can be divided into five regions referred to as extracellular regions 1 (EC1) to EC5 (Grunwald, 1993). EC1 through EC4 are highly homologous to each other and contain putative calcium binding sequences. EC5 is the least homologous region and had been distinguished from the other EC regions as a premembrane domain (Berndorff et al., 1994) or the extracellular anchor domain (Magee and Buxton, 1991).

Using highly specific antibodies that we raised against EC5 of E-cadherin, we now demonstrate by confocal laser and electron immunomicroscopy that E-cadherin is a major adhesive glycoprotein restricted to noncompacted plasma membranes within myelin internodes in peripheral nerve. E-Cadherin is excluded from myelin and therefore does not take an active role in the compaction or adhesion of these membranes. Most importantly, E-cadherin is not detected in the axonal membrane, and thus in the PNS, E-cadherin uniquely mediates adhesion between plasma membranes elaborated by a single cell. E-cadherin is concentrated at the inner and outer loops, and in Schmidt-Lanterman incisures, but is most intensely distributed in plasma membranes associated with electron-dense cytoplasmic plaques that are in register across paranodal loops. We identify these complexes as helically arranged adherens-type junctions that are autotypic; that is, they link plasma membrane wraps of the same Schwann cell. Our findings reveal that cytoplasmic regions in the Schwann cell are actively self-adherent and structurally maintained at least in part by an E-cadherin–mediated adhesion mechanism.

Materials and Methods

Antibodies

For neurofilament immunolabeling, a mixture of two mouse monoclonal antibodies, SMI 32 and RMO108, was used. SMI32 (Sternberger Monoclonals Inc., Baltimore, MD) recognizes a nonphosphorylated epitope in high neurofilament protein, and RMO108 (Lee et al., 1987) recognizes a phosphorylated epitope in rat middle neurofilament protein. MAG antibodies (Mouse anti-MAG clone 513; Boehringer-Mannheim Biochemicals, Indianapolis, IN) were used for double-labeling experiments. β-Catenin antibodies (mouse anti-β-catenin), used for immunocytochemistry, were a gift of Karen Knudsen (Lankenau Medical Research Center, Wynnewood, PA). Phalloidin-rhodamine (0.33 μM; Molecular Probes, Eugene, OR) was used to localize F-actin, and diD (1-1′-dioctadecyl-3,3,3′3,3′-tetramethylindodicarbocyanine, Molecular Probes) was used at 25 μm/ml to label membranes. Commercially available E-cadherin antibodies, DECMA-1 (rat anti-uvomorulin) and ECCD-2 (rat anti-E-cadherin) were purchased from Sigma Chem. Co., St. Louis, MO and Zymed Labs Inc. (S. San Francisco, CA), respectively. N-cadherin antibodies (mouse anti-ACAM, clone GC-4) and mouse anti-vinculin (clone hVIN-1) were purchased from Sigma Chem. Co. Rabbit anti-α- and β-catenin, were a gift of Barry Gumbiner (Memorial Sloan-Kettering Cancer Center, New York, NY).

Preparation of EcadEC5 Antibodies

To produce an E-cadherin specific antibody, E-cadherin cDNA was RT-PCR amplified from total RNA which had been purified from adult mouse brain (strain B6D2 F_1) using RNAzol B (Cinna/Biotecx, Houston, TX). A 300-bp Bam HI fragment (nucleotides 1920-2212, Nagafuchi et al., 1987), which contained most of the fifth extracellular region and a small portion of the transmembrane domain of mouse E cadherin (see Fig. 1 *A*), was purified and subcloned into the glutathione-S-transferase (GST) fusion protein bacterial expression vector, pGEX 3X (Pharmacia, Piscataway, NJ). The fusion protein, GST-EcadEC5, was purified from bacterial lysates by affinity chromatography using glutathione-agarose (Sigma Chem. Co.). GST-EcadEC5 was digested with Factor Xa (Boehringer-Mannheim Biochemicals) to generate an EcadEC5 fragment which was then purified using Pharmacia Mono Q FPLC anion exchange chromatography. Rabbits were immunized with EcadEC5 at Pocono Rabbit Farms (Canadensis, PA). To generate EcadEC5 antibodies, a primary injection (50 μl) of purified EcadEC5 (100 μg) emulsified in Freund's complete adjuvant was injected into the popliteal lymph nodes of rabbits. Boosts, consisting of EcadEC5 (50 μg) emulsified in Freund's incomplete adjuvant were administered by subcutaneous injection on days 7, 14, and 28, and every fourth week thereafter. Serum was collected weekly. High titer antiserum (>1:5,000 dilution on Western blots of fusion protein) was obtained after the third boost. Anti-EcadEC5 was affinity purified (Harlow and Lane, 1988) using GST-EcadEC5–conjugated Sepharose columns.

SDS-PAGE and Western Blotting

Freshly dissected adult mouse (strain B6D2 F_1) or rat (Sprague Dawley) sciatic nerves were homogenized in 5% SDS, 200 mM DTT, aprotinin (1 μg/ml), leupeptin (10 μg/ml), 1 mM pefabloc SC, and pepstatin (10 μg/ml) (Boehringer-Mannheim Biochemicals). The homogenates were briefly centrifuged for 1 min at 14,000 rpm to remove insoluble material, diluted 1:1 with SDS-PAGE sample buffer and boiled for 5 min. Sciatic nerve homogenates were separated by SDS-PAGE using 7.5% polyacrylamide gels and transferred to nitrocellulose. An osmotically shocked membrane fraction was prepared from two week old Wistar rat trigeminal or sciatic nerves as previously described (Gillespie et al., 1994), separated by SDS-PAGE on 5–17% gradient polyacrylamide gels and transferred to nitrocellulose. For immunodetection, the nitrocellulose was blocked with 5% nonfat milk and incubated with primary antibodies. Anti-EcadEC5 was used at 1:1,000 dilution (serum) or at 2.5 μg/ml (affinity purified). Commercial primary antibodies were diluted according to the manufacturers' recommendations. For detection, the blots were incubated with alkaline phosphatase (Sigma Chem. Co.) or peroxidase (Jackson ImmunoResearch Laboratories, Inc., West Grove, PA) conjugated secondary antibodies and developed with nitro

blue tetrazolium and 5-bromo-4-chloro-3-indolyl phosphate (Sigma Chem. Co.) or chemiluminescence (Amersham Corp.). Relative molecular weights for E-cadherin and the catenins were calculated using broad range molecular weight standards (Bio-Rad Laboratories, Cambridge, MA).

Immunoprecipitations

Freshly dissected kidney and sciatic nerve from adult mice (Strain B6D2 F_1), and human brain tissue were homogenized in ice cold 2% SDS, TBS (20 mM Tris, pH 7.5, 150 mM NaCl), aprotinin (1 μg/ml), leupeptin (10 μg/ml), 1 mM pefabloc SC, and pepstatin (10 μg/ml), and boiled for 5 min. Homogenates (200 μl) were mixed with 800 μl ice cold immunoprecipitation buffer (1% NP-40, 1% Triton X-100, 1 mM $CaCl_2$ in TBS) and precleared with protein A–Sepharose (20 μl; Sigma Chem. Co.) or goat anti-rat IgG agarose (50 μl; Sigma Chem. Co.). The homogenates were incubated with rabbit anti-EcadEC5 (2.5 μl), DECMA-1 (1 μl), or ECCD-2 (2.5 μl) for 60 min, followed by protein A–Sepharose (20 μl), or goat anti-rat IgG agarose (50 μl) for an additional 30 min. The resin was collected by centrifugation, washed extensively with immunoprecipitation buffer, resuspended in SDS-PAGE sample buffer, and analyzed by SDS-PAGE and immunoblotting.

Immunohistochemistry

Sciatic nerves, obtained from 4% paraformaldehyde perfused mice and rats were cyroprotected with 20% sucrose and quick frozen in Tissue-Tek OCT compound (Miles Inc., Kankakee, IL) in liquid nitrogen. Cryosections (15 μm) were placed on TESPA (3-aminopropyltriethoxysilane; Sigma Chem. Co.) treated glass slides, stored at −80°C, and immunostained following standard procedures. To TESPA treat slides, slides were dipped in 2% TESPA (diluted in acetone) and then rinsed two times in acetone and one time in water. The slides were dried in a 50°C oven and stored at room temperature. For immunolabeling, sections were placed in 4% paraformaldehyde for 5 min, washed twice (10 min each) with TBS, and treated with blocking solution (5% normal goat serum, 0.1% Triton X-100 in TBS) for 15 min. The sections were then incubated with primary antibodies for 18 h at room temperature. For E-cadherin immunolabeling, affinity purified anti-EcadEC5 (25 μg/ml) was used; commericial antibodies were used according to the manufacturers' recommendations. After washing and blocking as described above, the sections were incubated with species specific fluorochrome-conjugated secondary antibodies (Jackson ImmunoResearch Laboratories, Inc.) for 30 min at room temperature and washed with TBS. Mounting medium (50 mM Tris, pH 8.6, 2.5% DABCO [1,4-diazabicyclo{2.2.2}octane; Sigma Chem. Co.], 90% glycerol) and cover slips were applied.

Because the mouse β-catenin antibodies were sensitive to paraformaldehyde fixation, methanol-fixed teased sciatic nerve fibers were used for double immunolabeling with mouse β-catenin and rabbit EcadEC5 antibodies. To obtain teased nerve fibers sciatic nerves were dissected from adult mice and placed in ice cold tissue culture medium (DME, 7.5% fetal bovine serum; GIBCO BRL, Gaithersburg, MD). After the epineurium was removed, the nerves were gently teased with a stainless steel probe to free individual fibers, fixed in −20°C methanol for 20 min and immunostained as described above.

After immunolabeling, sections and teased fibers were examined with a Leica TCS 4D confocal scanning microscope.

Confocal Microscopy Image Analysis

For each image, a data set from a series of incremental scans through the z axis of a tissue section was collected. Each scan produced a thin optical image of the x, y plane of the tissue section. Thus a complete data set could be used to generate three-dimensional reconstructions of labeled tissue, or a single scan could be used to show low-magnification images with exceptional clarity (see Fig. 4) and details of highly magnified morphological features (see Fig. 5 *B, insets*). However the z axis of single scans were often too thin to view structures in their entirety. Therefore geometric plane projections, which are "compressions" of three-dimensional data sets (i.e., a series of scans) into single flat images, were used to obtain images of nerve structure (see Figs. 5, *A* and *B*, and 7 *D*).

To generate views of labeled images from many different angles, the data from a series of scans was computationally rotated (see Fig. 5 *C*) and presented as geometric plan projections. Stereo images (see Fig. 6) were obtained by rotating geometric plane projections by 5°. Finally, video animation and three dimensional reconstructions, were used to aid in the interpretation of immunofluorescence patterns. All image processing was done using the Scanware software on the Leica TCS 4D confocal scanning microscope and Adobe Photoshop software.

Confocal images resulting from the analysis of tissue sections labeled with only one primary antibody are shown in glow color scale. This color scale shows the most intense labeling in white and the middle range intensities in yellow/orange. The use of the glow color scale seemed to yield superior visibility of the signal in the middle and low intensity ranges as compared to the gray color scale.

For double immunostained sections, data from two channels were collected simultaneously thus providing a precise colocalization, and individually analyzed to show the localization of each antigen. The data from one channel is indicated in green and data from the other channel is indicated in red. To examine the distribution of two antigens, data from both channels were overlayed to produce a single image in which regions of colocalization are indicated in yellow.

To compensate for the many scans required for three dimensional analyses low averaging values were used. This decreased the time required for each scan, and therefore allowed more scans to be performed before the signal quenched. However, one consequence of low averaging values was some statistical noise which produced a certain degree of graininess in the images (see Fig. 7, *C* and *D*).

Immunoelectron Microscopy

Sciatic nerves (8-d old) and intestine (18-d old) from Wistar rats were fixed by immersion in 4% paraforamldehyde, 0.1% glutaraldehyde, 0.5 mM $CaCl_2$, in 0.1 M sodium cacodylate buffer containing 3% sucrose, pH 7.4, for 2 h at room temperature. The tissue was rinsed in cacodylate buffer containing 3% sucrose, washed several times with phosphate buffer containing 3% sucrose, and stained with 0.25% tannic acid in the same buffer for 1 h at 4°C (subsequent steps were performed at 4°C). After several washes in phosphate sucrose buffer, aldehydes were quenched in 50 mM NH_4Cl in the same buffer. The tissue was then washed four times in 0.1 M maleate buffer, pH 6.2, containing 4% sucrose, followed by 2% uranyl acetate in maleate sucrose buffer for 1 h. The tissue was dehydrated to 90% ethanol (from 70% ethanol onward all steps were at −20°C), infiltrated with a 1:1 ratio of LR Gold (Electron Microscopy Sciences, Fort Washington, PA) and ethanol, followed by a 7:3 ratio of LR Gold and ethanol, and two changes of LR Gold for 2–3 h each. The tissue was infiltrated overnight in LR gold containing 0.5% benzoin methyl ether and embedded in gelatin capsules. Polymerization was by UV irradiation at a wavelength of 365 nm for 24 h at −20°C.

Sections on formvar-coated nickel grids were blocked with 1% BSA, 0.5% fish skin gelatin, 0.05% Triton X-100, 0.05% Tween 20 in Tris buffer (10 mM Tris, 500 mM NaCl, pH 7.4) for 30 min at room temperature, and incubated with affinity purified anti-EcadEC5(25 μg/ml) in the same buffer for 3 h at room temperature. Grids were washed four times with the above buffer and incubated for 1 h with goat anti-rabbit IgG conjugated to 10 nm gold (1:20; Amersham Corp., Arlington Heights, IL). The grids were then washed on drops of distilled water, fixed with 2.5% aqueous glutaraldehyde and rinsed in a stream of distilled water. After postfixing for 15 min with 2% aqueous OsO_4 the grids were stained with lead citrate and examined at 80 kV in a JEOL100CX electron microscope.

Results

E-Cadherin and Its Associated Proteins, α- and β-Catenin Are Expressed in Adult Peripheral Nerve

To generate specific polyclonal antibodies against E-cadherin, most of the EC5 domain (Fig. 1 *A*) of mouse E-cadherin (EcadEC5) was bacterially expressed as a GST fusion protein. The fifth extracellular domain was chosen because it is the least homologous region among the cadherins. For example, mouse N-cadherin, a likely candidate for expression in peripheral nerve, has only 34% identity in a 102-amino acid stretch with the EcadEC5 sequence and among the mammalian cadherin sequences in the Genbank database, bovine P-cadherin has the highest degree of identity (43% in a stretch of 85 amino acids). In both sequences the maximum

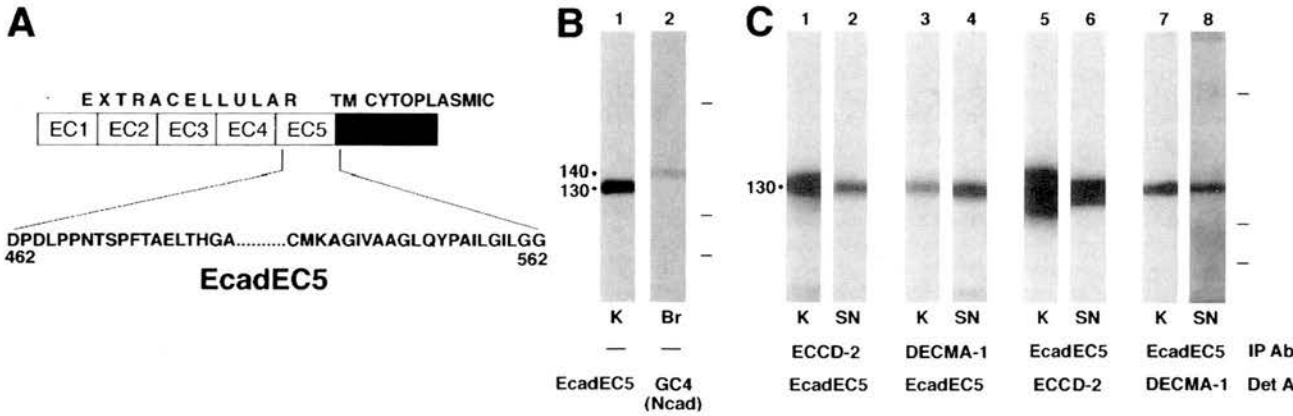

Figure 1. Characterization of EcadEC5 antibodies. (*A*) E-cadherin has a large extracellular domain (*white*) which can be divided into five homologous regions termed extracellular regions 1 through 5 (*EC1-EC5*), a short transmembrane domain (*black*) and a cytoplasmic domain (*gray*). EC5 is the least homologous region and was used to generate specific polyclonal antibodies. The antigenic epitope for EcadEC5 consists of 82 amino acids from EC5 and 19 amino acids from the transmembrane domain. (*B*) Kidney (*K*) and brain homogenates (*Br*) were separated by SDS-PAGE and transferred to nitrocellulose. E-Cadherin was detected in kidney homogenates with anti-EcadEC5 (lane *1*) and N-cadherin was detected in brain homogenates with CG-4 (anti-ACAM, lane *2*). Molecular weight standards (200, 116, and 97 kD) are indicated to the right of the blot. (*C*) E-cadherin was immunoprecipitated from mouse kidney (*K*, lanes *1*, *3*, *5*, and *7*) and sciatic nerve (*SN*, lanes *2*, *4*, *6*, and *8*) homogenates using ECCD-2 (lanes *1* and *2*), DECMA-1 (lanes *3* and *4*) or anti-EcadEC5 (lanes *5–8*), separated by SDS-PAGE, and transferred to nitrocellulose. Immunoprecipitated protein was detected using anti-EcadEC5 (lanes *1–4*), ECCD-2 (lanes *5* and *6*) or DECMA-1 (lanes *7* and *8*). (*IP Ab*) Immunoprecipitation antibody; (*Det Ab*) detection antibody. Molecular weight standards (200, 116, and 97 kD) are indicated to the right of the blot.

number of contiguous identical amino acids is four. Thus, we considered it unlikely that antibodies directed against the EcadEC5 epitope would recognize either P- or N-cadherin.

On immunoblots of kidney homogenates, a well-characterized source of E-cadherin (Gumbiner and Simons, 1987; Behrens et al., 1989), anti-EcadEC5 detected a single band of 130 kD (Fig. 1 *B*, lane *1*). This relative molecular mass was slightly larger than that reported for E-cadherin in other cells (120 kD, Nagafuchi et al., 1987), and was similar to the reported relative molecular mass of N-cadherin (130 kD). To confirm that anti-EcadEC5 detected E-cadherin and not N-cadherin, anti-ACAM (clone GC-4), a commercially available N-cadherin antibody, was used to detect N-cadherin in brain homogenates. Anti-ACAM detected a single band of 140 kD in brain homogenates (Fig. 1 *B*, lane *2*), which migrated more slowly than E-cadherin (Fig. 1 *B*, lane *1*), strongly indicating that anti-EcadEC5 does not recognize N-cadherin.

To verify the specificity of anti-EcadEC5, E-cadherin was immunoprecipitated from adult kidney and sciatic nerve homogenates with ECCD-2 or DECMA-1 and detected by immunoblotting with anti-EcadEC5 (Fig. 1 *C*, lanes *1–4*). The reverse experiment, in which E-cadherin was immunoprecipitated with anti-EcadEC5 and detected with ECCD-2 or DECMA-1, was also performed (Fig. 1 *C*, lanes *5–8*). DECMA-1 is a monoclonal antibody which blocks E-cadherin function and recognizes an epitope in the EC5 region of E-cadherin (Ozawa et al., 1989). ECCD-2 is a monoclonal antibody which recognizes E-cadherin but does not inhibit its function (Shirayosi et al., 1986). In all immunoprecipitation experiments, single bands, having identical molecular masses of 130 kD, were detected in the kidney (Fig. 1 *C*, lanes *1*, *3*, *5*, and *7*) and sciatic nerve (Fig. 1 *C*, lanes *2*, *4*, *6* and *8*) homogenates. Note that when anti-EcadEC5 was used to immunoprecipitate E-cadherin from kidney homogenates, a very intense broad signal was obtained upon detection with ECCD-2 (Fig. 1 *C*, lane *5*). This was likely due to the efficiency of EcadEC5, a polyclonal antibody, as an immunoprecipitating agent, and the high reactivity of ECCD-2 with E-cadherin. The results of the immunoprecipitation experiments demonstrate that anti-EcadEC5 specifically recognizes the same protein as ECCD-2 and DECMA-1, i.e., E-cadherin.

In sciatic nerve homogenates, ECCD-2 (Fig. 2 *A*, lane *1*) and anti-EcadEC5 (Fig. 2 *A*, lane *2*) both detect bands of ~130 kD. This band was not detectable in competition experiments in which anti-EcadEC5 and the fusion protein GST-EcadEC5 were preincubated (Fig. 2 *A*, lane *3*). In epithelial cells, E-cadherin associates with α-, β-, and γ-catenin, a family of cytoplasmic proteins whose interactions with cadherins appear to be required for adhesion (Hirano et al., 1992; Kintner, 1992). Therefore we probed identical immunoblots with α- and β-catenin antibodies and found that bands having molecular masses of ~108 and ~95 kD, which corresponded to the relative molecular masses of α- and β-catenins, respectively (Ozawa et al., 1989; Hinck et al., 1994) were detected in sciatic nerve homogenates (Fig. 2 *A*, lanes *4* and *5*). E-cadherin and α- and β-catenin were also found in osmotically shocked membrane fractions of sciatic and trigeminal nerves (Fig. 2 *B*). Because this membrane fraction is known to consist almost entirely of Schwann cell plasma membranes and myelin, E-cadherin in this fraction was likely to be derived from Schwann cells. The presence of α- and β-catenins in these membranes suggested that they were associated with E-cadherin, and/or perhaps other as yet unidentified cadherins.

EcadEC5 Antibodies Specifically Recognize Adherens Junctions

Previous immuno-electron microscopy studies have established that E-cadherin is a marker of adherens junctions in

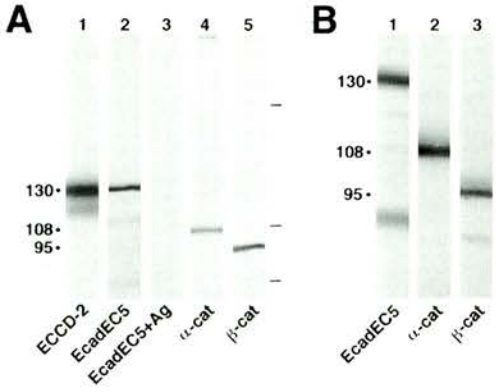

Figure 2. E-cadherin and α- and β-catenins are expressed in peripheral nerve. Adult mouse sciatic nerve homogenates (*A*) and an osmotically shocked membrane fraction from trigeminal nerves (*B*) were separated by SDS-PAGE, transferred to nitrocellulose and immunostained using ECCD-2 (*A*, lane *1*), affinity purified anti-EcadEC5 (*A*, lanes *2* and *3*, *B*, lane *1*), anti-α-catenin (*A*, lane *4*, *B* lane *2*) or anti-β-catenin (*A*, lane *5*, *B*, lane *3*). Ag, GST-EcadEC5. Molecular weight standards (200, 116 and 97 kD) are indicated to the right of the blot in *A*.

rat intestine (Boller et al., 1985). To verify the specificity of EcadEC5 antibodies that we raised for the localization studies, anti-EcadEC5 was tested on thin sections of rat intestinal tissue (Fig. 3). At the lateral boundaries of longitudinally (Fig. 3 *A*) and obliquely (Fig. 3 *B*) sectioned rat intestine, adherens junctions (*arrows*) and desmosomes (*A*, *arrowheads* and *B*, *asterisk*) are evident. EcadEC5 antibodies strongly and specifically labeled adherens junctions (Fig. 3, *arrows*) but did not label desmosomes (*arrowheads*) or any other structures.

E-Cadherin Has a Restricted Distribution within the Cytoplasmic Compartments of Peripheral Nerve Schwann Cells, and is Highly Concentrated in Schmidt-Lanterman Incisures and Paranodes

In tissue sections anti–EcadEC5 intensely labeled trigeminal and sciatic nerves from mice and rats. Confocal microscopy was routinely used to localize E-cadherin distribution in these tissues. In cross sections of E-cadherin immunolabeled peripheral nerve, individual fibers were easily identified by circumferential fluorescence (Fig. 4 *A*), indicating that E-cadherin was present in the outer cytoplasmic loops of Schwann cells. At the outer loop, at least one intense fluorescent spot could be detected (Fig. 4 *A*, *small arrows*), indicat-

Figure 3. EcadEC5 antibodies specifically recognize adherens junctions. Longitudinally (*A*) and obliquely (*B*) sectioned rat intestinal tissue was labeled with EcadEC5 antibodies. The apically located microvilli are at the top of the figure. At the lateral surface, adherens junctions are strongly labeled with EcadEC5 antibodies (*arrows*). Desmosomes (*A*, *arrowheads*), including those with an extensive filamentous network (*B*, *asterisk*), are devoid of label. Bars, 0.1 μm.

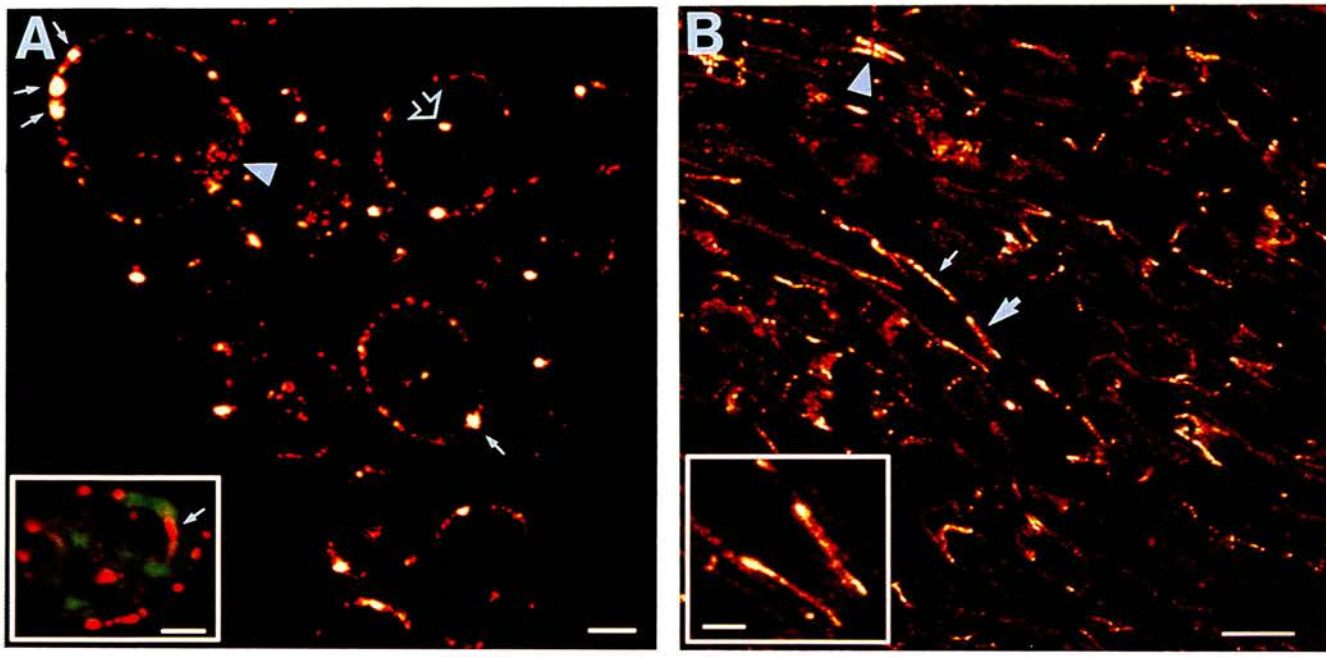

Figure 4. E-cadherin localizes to the cytoplasmic compartments of Schwann cells. Cryosections of adult mouse sciatic nerve were immunolabeled with anti-EcadEC5 and viewed by confocal microscopy. (*A*) In cross section, anti-EcadEC5 localized to numerous puncta in the outer loops (*small arrows*) and a single dot in the inner loops (*open arrow*). Labeling of the Schwann cell cytoplasm (*arrowhead*) was faint. The inset in *A* shows two nerve fibers labeled with EcadEC5 (*red*) and diD (*green*), a lipophilic dye that intensely labels myelin. A cross section of a Schmidt-Lanterman incisure, labeled by anti-EcadEC5, is apparent in this field (*A*, *inset*, *arrow*). (*B*) In longitudinal section, anti-EcadEC5 labeling revealed the classic morphology of Schmidt-Lanterman incisures (large arrow, and see *inset*). Anti-EcadEC5 also labeled the outer loop of nerve fibers (*small arrow*) and the paranodes (*arrowhead*). (See Fig. 5 *A* for the intensity scale.) Bars: (*A* and *B*) 10 μm; (*insets*) 2 μm.

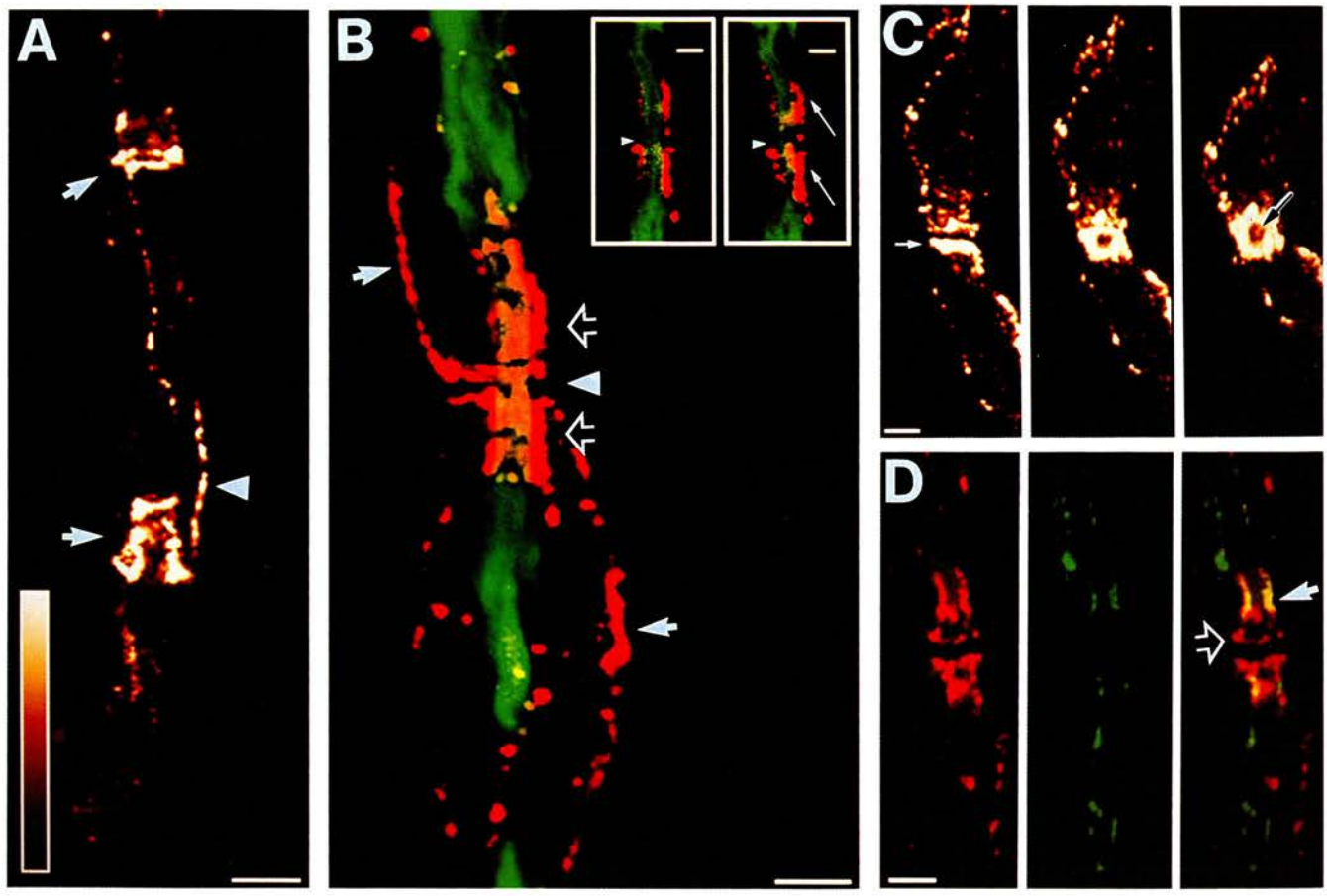

ing that E-cadherin was concentrated in discrete subdomains. Punctate labeling at the inner loop was occasionally noted (Fig. 4 *A*, *open arrow*), but, in contrast to the outer loop, only one E-cadherin site per inner loop was detected. The Schwann cell cytoplasm was also faintly labeled (Fig. 4 *A*, *arrowhead*), consistent with synthesis of this transmembrane protein on rough endoplasmic reticulum and post-translational processing in the Golgi apparatus. Significantly, compact myelin and axons were devoid of E-cadherin immunofluoresence. Fig. 4 *A* (*inset*) shows two myelinated axons labeled with E-cadherin (red) and diD (green), a lipophilic dye which intensely labels myelin. Note the absence of E-cadherin in the myelin and axons, and the punctate E-cadherin labeling surrounding the myelin, which corresponds to the outer loop. The arrow (Fig. 4 *A*, *inset*) indicates a cross section of a Schmidt-Lanterman incisure, which was also intensely labeled by anti-EcadEC5. In longitudinal section, the outer loops were labeled in discontinuous tracts resembling "beads on a string" that were parallel to the axes of the fibers (Fig. 4 *B*, *small arrow*). It is interesting to note that, in contrast to the outer loop, clearly delineated E-cadherin tracts were not found at the inner loops in longitudinal sections. Longitudinal sectioning also revealed that E-cadherin was highly concentrated in Schmidt-Lanterman incisures (Fig. 4 *B*, *large arrow* and *inset*) and paranodes (Fig. 4 *B*, *arrowhead*). Thus in Schwann cells, E-cadherin is found exclusively in the outer and inner loops, paranodes, Schmidt-Lanterman incisures, i.e. in the regions which comprise the continuous cytoplasmic channel network that forms the boundary domain of compact myelin.

At high resolution, E-cadherin immunofluorescence clearly yielded the classical funnel-shaped image of Schmidt-Lanterman incisures (Hall and Williams, 1970; Ghabriel and Allt, 1981) in both trigeminal and sciatic nerves (Fig. 5 *A*, *arrows*). These thin spiral channels interrupt compact myelin within the internode and have been implicated in the metabolic maintenance of the myelin sheath (Ghabriel and Allt, 1981). At both ends of an incisure ring-like structures which completely encircled the axon were detected (Fig. 5 *A*), with slightly more intense labeling at the periphery (see also Fig. 4 *B*, *inset*). Often Schmidt-Lanterman incisures were linked to each other by E-cadherin-positive tracts (Fig. 5 *A*, *arrowhead*).

Most interestingly, anti-EcadEC5 strongly highlighted the paranodal region (Fig. 5, *B–D*). To obtain a highly detailed image of E-cadherin localization, a series of 44 confocal scans through a "paranode-node-paranode" was analyzed using three dimensional reconstructions and video animation, and presented as a geometric plane projection (Fig. 5 *B*). E-Cadherin labeling is indicated in red and the axon, demarcated by anti-neurofilament labeling, is shown in green. The node of Ranvier is indicated by the arrowhead. The high degree of color saturation in the EcadEC5 channel results from an intense immunofluorescent signal and photodetector settings optimized for low signal levels. These conditions were used to ensure detection of all E-cadherin positive structures. E-Cadherin immunofluorescence flanked the narrowed paranodal axon, precisely terminating at the locus where the axonal diameter enlarged (Fig. 5 *B*, *open arrows*). Enlargements of single scans of the nodal region showed that E-cadherin was absent from the node of Ranvier (Fig. 5 *B*, *insets*, *arrowheads*). One feature of E-cadherin localization, which was revealed by three-dimensional imaging, was that E-cadherin helically encircled the narrowed paranodal axon. This helicity is suggested in single optical images (Fig. 5 *B*, *right inset*, *arrows*), and is depicted on the cover of this issue. E-cadherin immunolabeling of the outer loop is also apparent (Fig. 5 *B*, *white arrows*).

Another interesting feature of paranodal E-cadherin distribution was that at the limiting edge of some, but not all, paranodes, E-cadherin completely encircled the axon forming a cylindrical collar. Fig. 5 *C* is a series of rotations around the x axis of an anti-EcadEC5 immunolabeled paranodal region. The left panel (0°) shows the paranodal region in longitudinal section; the right panel (50°) shows the paranodal region in a slightly oblique cross section. As the

Figure 5. E-cadherin is highly concentrated in Schmidt-Lanterman incisures and paranodes in sciatic nerve. (*A*) Confocal image of two Schmidt-Lanterman incisures (*arrows*) labeled with anti-EcadEC5. A thin E-cadherin positive tract (*arrowhead*) appears to connect the incisures. To reconstruct the incisures, two 0.27-μm incremental scans in the z axis were merged into a single image. The scale at the right indicates the glow scale labeling intensity. (*B*) Confocal image of a paranodal region immunolabeled with anti-EcadEC5 (*red*) and anti-neurofilament (*green*). A geometric plane projection of the paranode was created by merging 44 0.1-μm incremental scans in the z axis into a single image. The color saturation in the anti-EcadEC5 channel (*red*) was the result of an intense signal and photodetector settings optimized for low signal levels. These conditions were used to ensure detection of all E-cadherin–positive structures. Signals from each antibody were simultaneously collected as two separate data sets, and overlaid to produce a single image. Neurofilament immunolabeling demarcates the axon. Anti-EcadEC5 labeled paranodal regions (*open arrows*), and outer loops (*white arrows*) but did not label the node of Ranvier (*arrowhead*). Note that yellow does not indicate regions of colocalization (see text). The left inset is an individual scan (z axis, 0.1 μm) taken at the midpoint of the axon and shows that anti-EcadEC5 labeling is situated at the edge of the axon, not in the axon. The right inset is an individual scan (z axis, 0.1 μm) taken in the top quarter of the nerve fiber and indicates that the adaxonal labeling (*arrows*) is helically orientated around the axon. In both insets, the node of Ranvier is indicated by the arrowhead. (*C*) Rotations around the x axis of an EcadEC5-labeled paranode. 29 scans of a longitudinally sectioned paranode, taken at 0.13-μm increments in the z axis, were merged into a single image to create a geometric plane projection of the paranodal region (0° *left*). The geometric plane projection was computationally rotated around the x axis by 30° (*middle*) and by 50° (*right*). The disc indicated by the arrow (*left*) represents anti-EcadEC5 paranodal labeling which completely encircles the axon and forms a paranodal collar. The paranodal collar is clearly evident after rotating the image around the x axis (*middle* and *right*). In the right panel, the axon, which is devoid of E-cadherin labeling, is indicated by the arrow. (See *A* for intensity scale.) (*D*) confocal images of a paranode labeled with rabbit anti-EcadC5 (*left*, *red*) and mouse anti-MAG (*middle*, *green*). The overlay (*right*) shows regions of E-cadherin and MAG colocalization (*yellow*). Two confocal scans of a longitudinally sectioned paranodal region, taken at 0.11-μm increments in the z axis, were merged into a geometric plane projection. The overlay (*right*) indicates that both anti-EcadEC5 (*red*) and anti-MAG (*green*) demonstrate adaxonal labeling (*open arrow*, *yellow*), but only anti-EcadEC5 labels the paranodal collar (*solid arrow*). Bars: (*A*) 5 μm; (*B*) 2 μm; (*insets*, 1 μm; (*C* and *D*) 2 μm.

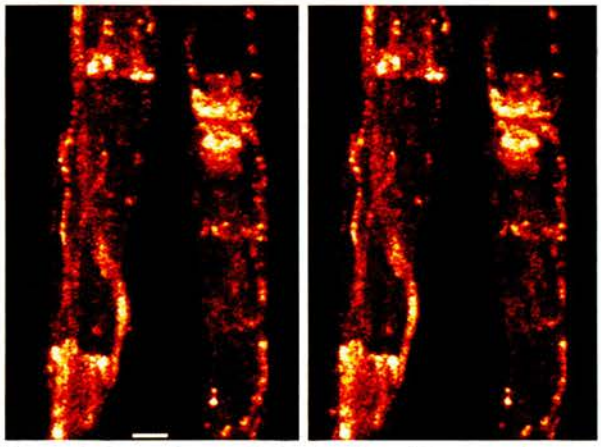

Figure 6. Stereo image of E-cadherin positive tracts in two sciatic nerve fibers. Confocal scans were merged into geometric plane projections which were then computationally rotated around the y axis. The two images, differing by 5°, can be paired to produce a stereo image. Bar, 2 μm.

fiber was rotated, the flattened disc in the left panel (Fig. 5 *C*, *arrow*), became a hollow E-cadherin positive ring encircling the axon (Fig. 5 *C*, *right*, *arrow*; see also Fig. 6, *right fiber*). In most paranodes where collars were found, two collars, one at the limiting edge of each internode were observed.

In Schwann cells, E-cadherin distribution was remarkably similar but not identical, to that of an IgCAM superfamily protein, MAG (myelin-associated glycoprotein). While both proteins were restricted to the cytoplasmic channels of Schwann cells, they did not exhibit an exact colocalization. For example, in the inner loop, MAG was evenly distributed (Trapp et al., 1989) while E-cadherin was restricted to a single punctate site (see Fig. 4 *A*). In addition, in the paranodal region, both E-cadherin and MAG flanked the paranodal axon (Fig. 5 *D*, *solid arrow*, *yellow*), but E-cadherin, alone, formed a paranodal collar (Fig. 5 *D*, *open arrow*, *red*).

Helical E-cadherin Tracts Are in Register Across Adjacent Internodes

A distinguishing feature of E-cadherin distribution in the internode was its organization into discontinuous longitudinal tracts that wound helically along the periphery of the Schwann cell in the outer loops (Fig. 6). Indeed, the punctate fluorescence in the outer loop observed in cross sections (see Fig. 4 *A*) corresponded to labeling of the tracts. As the E-cadherin tracts wove among the outer loop, they crisscrossed and often extended from one Schmidt-Lanterman incisure to the next (see also Fig. 5 *A*), indicating that E-cadherin was part of a highly organized substructure within the entire cytoplasmic channel network of Schwann cells. Video animation revealed that the helical paths delineated by E-cadherin continued in register from internode to

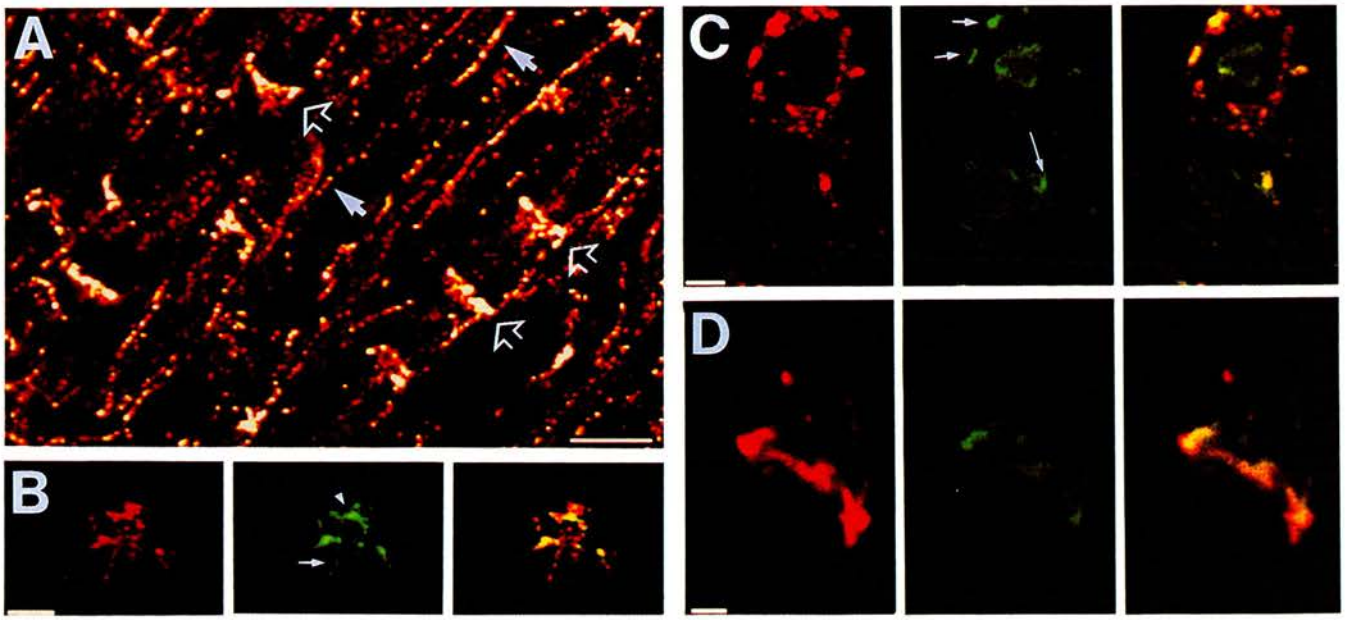

Figure 7. β-catenin and F-actin colocalize in peripheral nerve fibers. (*A*) Peripheral nerve, immunolabeled with anti–β-catenin was analyzed by confocal microscopy. Two scans, taken at 1.7-μm increments in the z axis, were merged into a geometric plane projection. The open arrows demarcate labeling of Schmidt-Lanterman incisures and the solid arrows indicate labeling of the outer loops. (*B*) Confocal image of a paranodal region immunolabeled with anti–EcadEC5 (*left*, *red*) and anti–β-catenin (*middle*, *green*). The regions of colocalization are indicated in yellow in the overlay (*right*). A single confocal scan was taken through the midpoint of an obliquely cut paranode. Both adaxonal labeling (*arrow*) and paranodal collar labeling (*arrowhead*) were apparent with anti–β-catenin (*middle*). The overlay (*right*) shows colocalization of E-cadherin and β-catenin (*yellow*). (*C*) Confocal image of two nerve fibers immunolabeled with anti–EcadEC5 (*left*) and phalloidin (*middle*) which binds to F-actin. Two scans, taken at 1.3-μm increments in the z axis, were merged into a geometric plane projection. The graininess in this set of images is due to low averaging values used during data collection. F-Actin (*middle*) is found in the outer loop (*short arrows*) and inner loop (*long arrow*). These regions colocalize with anti–EcadEC5 (*right*, *yellow*). (*D*) Confocal image of a Schmidt-Lanterman incisure immunolabeled with E-cadherin (*left*) and phalloidin (*middle*). Nine confocal scans, taken at 0.54-μm increments in the z axis, were merged into a geometric plane projection. The overlay (*right*) shows E-cadherin and F-actin colocalization (*yellow*) in Schmidt-Lanterman incisures. Bars: (*A*) 10 μm; (*B* and *C*) 2 μm; (*D*) 1 μm.

internode. This novel observation suggested, surprisingly, that adjacent Schwann cells may be functionally associated with one another. Thus the morphology of the E-cadherin network revealed a previously unsuspected organization of Schwann cells into what might be a globally interactive unit.

β-Catenin and F-Actin Colocalize with E-Cadherin in the Outer and Inner Loops and at Schmidt-Lanterman Incisures and Paranodes

Low magnification confocal images of β-catenin immunolabeled peripheral nerve were similar to those observed for E-cadherin labeled tissue (Fig. 7 *A*). Schmidt-Lanterman incisures (Fig. 7 *A*, *open arrows*) and labeling at the outer loop (Fig. 7 *A*, *white arrows*) were clearly visible. At the paranodes, β-catenin flanked the axon (Fig. 7 *B*, *middle*) and formed a paranodal collar (Fig. 7 *B*, *arrowhead*), thus demonstrating a precise colocalization with E-cadherin (Fig. 7 *B*, *right*, *yellow*).

F-Actin, another protein which associates with E-cadherin, also localizes to E-cadherin positive regions (Fig. 7, *C* and *D*). F-actin, labeled by phalloidin, had a punctate appearance in the outer loop (Fig. 7 *C*, *middle*, *short arrows*) which precisely colocalized with E-cadherin (Fig. 7 *C*, *right*). In the inner loop, a single distinct spot of F-actin was found (Fig. 7 *C*, *long arrow*), which co-distributed with E-cadherin (Fig. 7 *C*, *right*, *yellow*). Finally F-actin (Fig. 7 *D*, *middle*) and E-cadherin (Fig. 7 *D*, *left*) colocalized in Schmidt-Lanterman incisures (Fig. 7 *D*, *right*, *yellow*). The graininess in Fig. 7 (*C* and *D*) is from statistical noise produced when using low averaging values during data collection, and is not due to a weak signal. Sciatic and trigeminal nerves were also examined for the presence of vinculin, another protein which is associated with E-cadherin adhesion complexes (Geiger and Ginsberg, 1991). Preliminary data indicated that vinculin antibodies strongly labeled blood vessels in peripheral nerve but did not colocalize with E-cadherin (data not shown). The co-distributions of E-cadherin with β-catenin and F-actin provide strong evidence that these proteins may organize into an adhesion complex that has characteristics of adherens junctions and is integral to the stability of the inner and outer loops, Schmidt-Lanterman incisures and the paranodes.

E-Cadherin Mediates Adhesion within an Individual Schwann Cell

A striking finding was that by immunoelectron microscopy, E-cadherin strongly labeled Schwann cell membranes associated with cytoplasmic densities in the paranodes (Fig. 8), Schmidt-Lanterman incisures (Fig. 9) and outer mesaxons (Fig. 10, *B–D*). No E-cadherin was observed at the Schwann

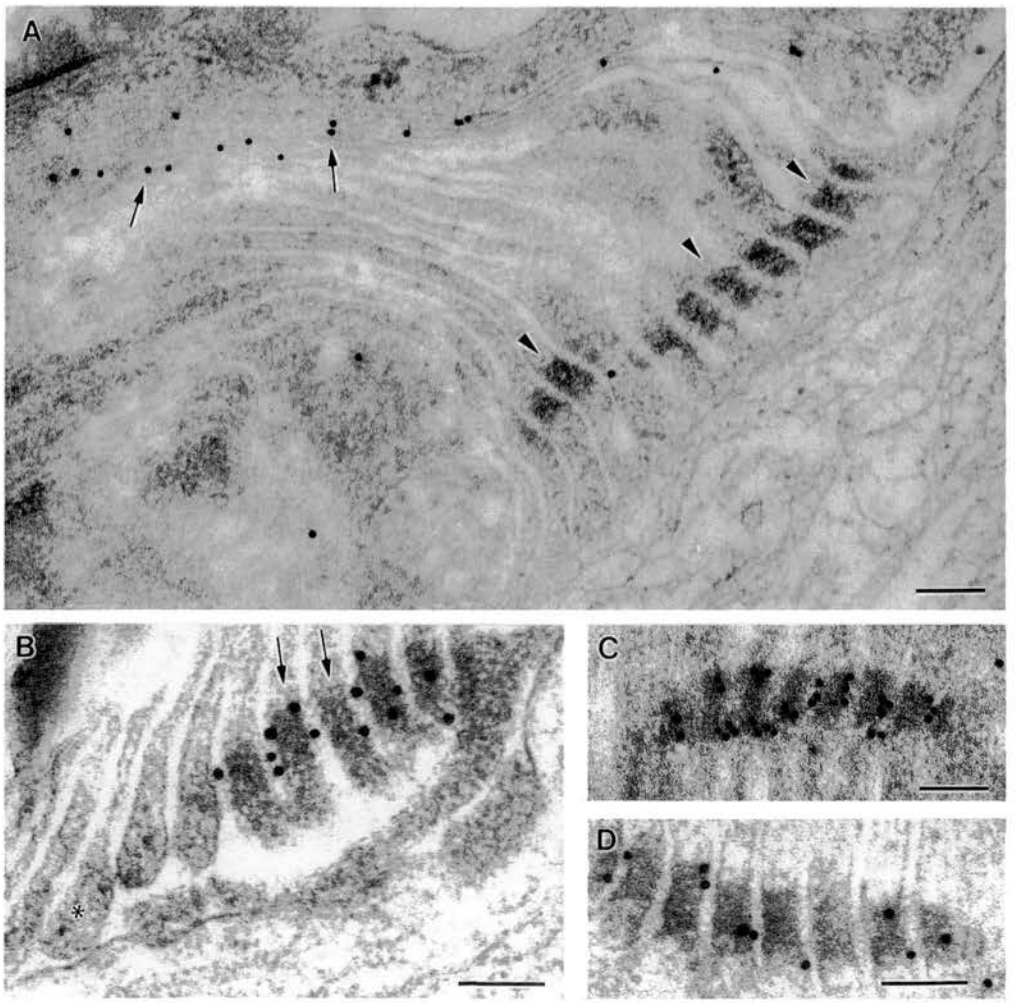

Figure 8. E-cadherin localizes to densities in the paranodal channels. Immunoelectron microscopy of sciatic nerve from 7-d-old mice and rats labeled with anti-P_0 (*A*) or anti-EcadEC5 (*B–D*). Anti-EcadEC5 intensely labels densities in the paranode (*B*, *arrows*). Note the extensive labeling of the densities in *C*. In *D*, the narrowing of the cytoplasm and the widening of the intracellular space is apparent. In a control P_0-labeled paranode (*A*) myelin (*arrows*) is labeled, but the densities (*arrowheads*) remain unlabeled. Bars, 0.1 μm.

cell–axonal interface, nor between the membranes of two Schwann cells. Thus, in the PNS, E-cadherin is unusual in that it mediates adhesion between membranes elaborated by an individual cell.

In longitudinally sectioned paranodes, cytoplasmic densities were strongly labeled with anti-EcadEC5 (Figs. 8, *B–D*). In control sections, P_0, the major glycoprotein of peripheral nerve myelin localized specifically to compact myelin (Fig. 8 *A*, *arrows*), and was absent from the densities (Fig. 8 *A*, *arrowheads*). Loops extending from the innermost myelin lamellae consistently contained the most well developed densities (Fig. 8 *B*, *arrows*), while the outermost turns (Fig. 8 *B*, *asterisk*) were often devoid of densities and E-cadherin labeling. Since the tissue used for the immunoelectron microscopy was obtained from 7-d-old animals, the preferential labeling of the inner turns may have been related to a developmentally transient event. We did not observe immunogold labeling of structures which would correspond to the collars seen in some paranodes by light microscopy (see Figs. 5 *C* and 7). The absence of such labeling may be developmentally related and/or it could be due to the lower sensitivity of immunoelectron microscopy. The arrangement of the plaques across several turns of the paranodal channel produced a large zonula-like junctional complex. Within the junctional array, there was a distinct narrowing of the cytoplasm from 85 to 45 nm (Fig. 8 *D*), accompanied by a local widening of the extracellular space (see also Harkin, 1964). In addition the densities extended across the full length of the cytoplasm, in effect dividing the paranodal channel into two separate compartments.

E-Cadherin is also highly concentrated in densities found in Schmidt-Lanterman incisures. Fig. 9 *A* is a transverse section of a developing myelin sheath showing what is likely to be a forming Schmidt-Lanterman incisure. At the periphery of the sheath, three densities are specifically labeled by anti-EcadEC5 (Fig. 9 *A*, *arrows*). Two well-developed Schmidt-Lanterman incisures and their associated densities (Fig. 9 *B*, *arrows*) are shown in a P_0-labeled control section. As in the paranodal channel, densities in the Schmidt-Lanterman incisures are highly ordered and aligned in contiguous cytoplasmic wraps. E-Cadherin thus may have an important role in the formation of Schmidt-Lanterman incisures.

At the outer loop, E-cadherin was associated with densities that were either macular (Fig. 10 *D*, *arrows*) or reasonably extensive ($\geqslant$350 nm, Fig. 10 *C*). E-cadherin was also present at densities at the outer mesaxon (Fig. 10 *B*). The presence of these profiles directly correlated with the punctate and linear E-cadherin fluorescence patterns we detected along outer loops by confocal microscopy (see Figs. 4, 5 *A*, and 6). The inner mesaxon was the only region that consistently showed E-cadherin localization in the absence of cytoplasmic densities (Fig. 10 *A*, *arrows*). However, densities at some inner mesaxons were noted by Bunge et al. (1989) in sheaths that had only a few compact wraps. The labeled inner mesaxons that we observed were in sheaths with numerous turns of compact myelin. At the inner mesaxon, it is possible that the appearance of these densities may be transiently coordinated with the state of myelin bilayer compaction. The presence of E-cadherin together with the absence of densities suggests that only relatively weak adhesion could be required at the inner mesaxon after compaction has occurred. In contrast, the presence of dense plaques in the paranodes and outer mesaxons is indicative of strong adhesive and mechanical stabilization in these regions.

Discussion

The data presented here reveal E-cadherin to be an important component in the cytoarchitecture of individual Schwann cells. In other cell types, cadherins mediate intercellular adhesion. Even in peripheral nerve, it has been shown that

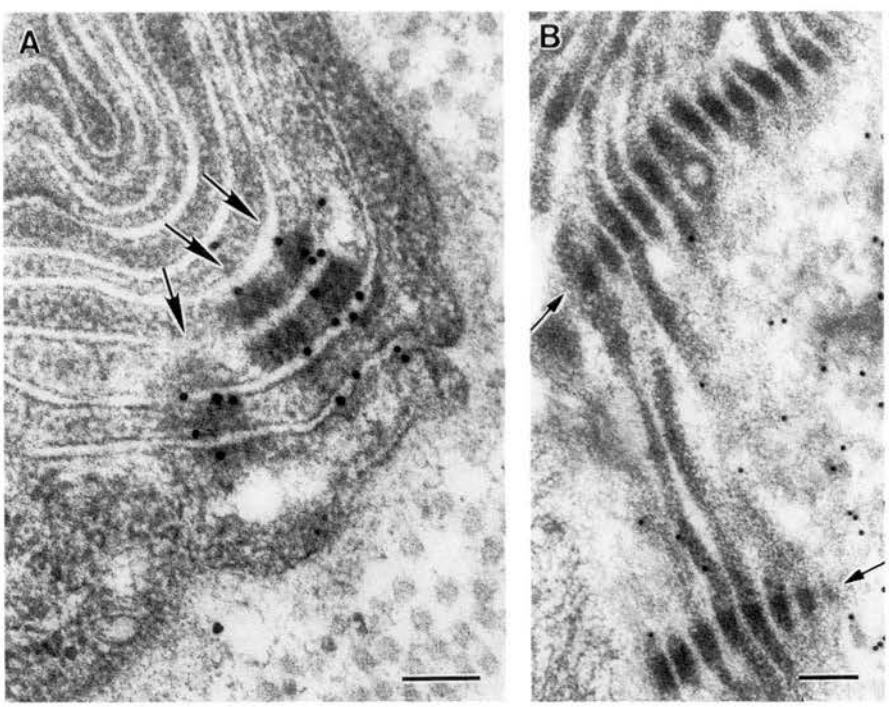

Figure 9. Distribution of cytoplasmic plaques in Schmidt-Lanterman incisures. Immunoelectron microscopy of Schmidt-Lanterman incisures labeled with anti-EcadEC5. In *A*, the arrows indicate three labeled densities in a forming Schmidt-Lanterman incisure. In a control P_0-labeled incisure (*B*), labeling of myelin is apparent, but the densities (*arrows*) remain unlabeled. Bars, 0.1 μm.

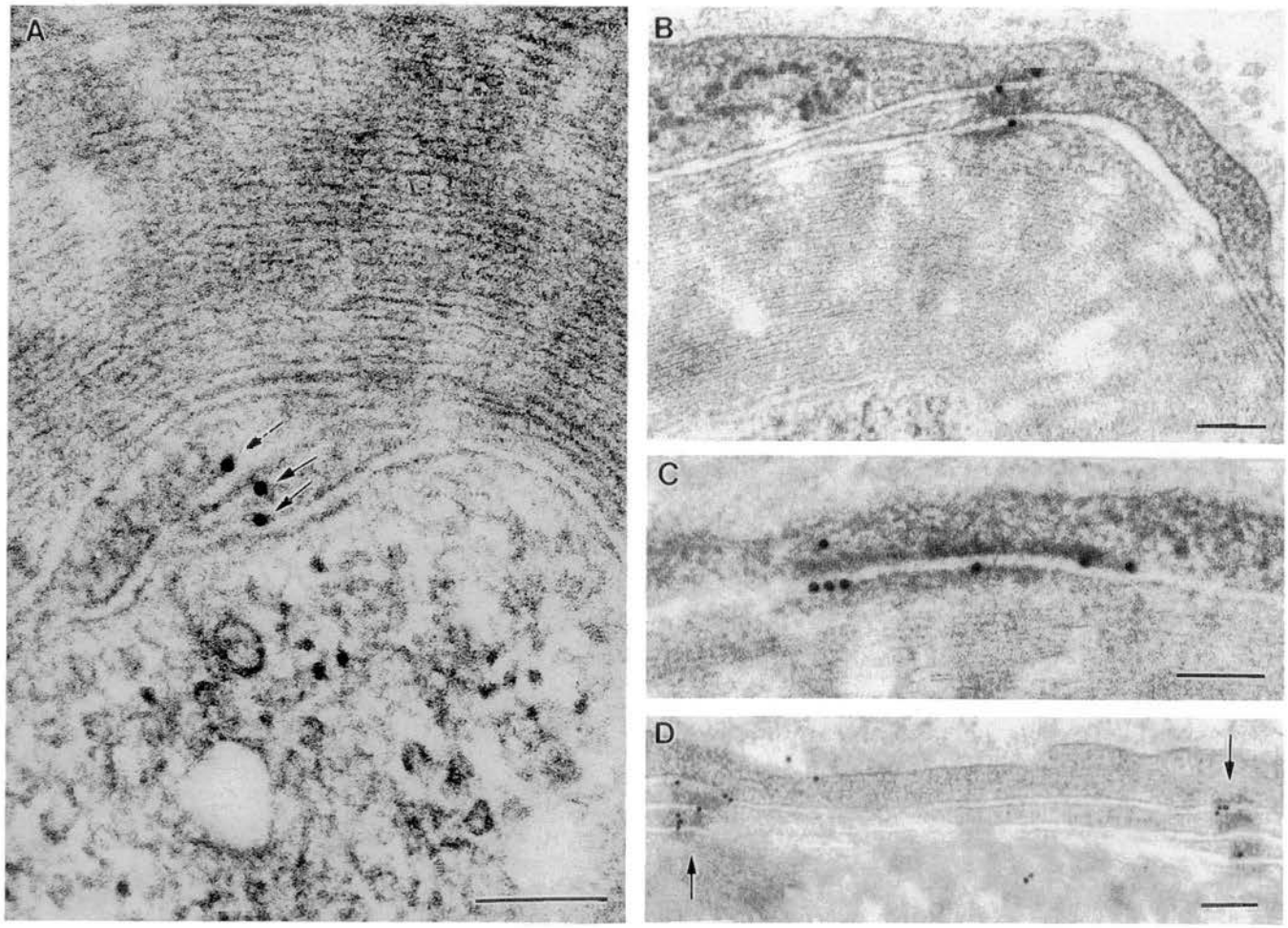

Figure 10. Distribution of E-cadherin in the inner and outer mesaxons and the outer loops of Schwann cells. Immunoelectron microscopy of Schwann cells labeled with anti–EcadEC5. (*A*) E-cadherin is present at the inner mesaxon (*arrows*) in the absence of a well-developed plaque. Conversely, at the outer mesaxon, E-cadherin is associated with well-developed densities (*B*). In the outer loop, anti–EcadEC5 localizes to large, extensive densities (*C*) and to macular densities (*D*, *arrows*). Bars, 0.1 μm.

satellite cells, which surround dorsal root ganglion cells, express E-cadherin at cell to cell contact sites (Shimamura et al., 1992; Uchiyama et al., 1994). However, in the Schwann cell, E-cadherin is unique in that it mediates adhesion between membranes elaborated by a single cell. E-cadherin was not detected between two Schwann cells nor between Schwann cells and the axon. In Schwann cells, E-cadherin localizes to densities which we have designated as autotypic adherens-type junctions, in contrast to homotypic (between two similar cell types) and heterotypic (between two different cell types) junctions. To our knowledge this is the first documentation of functional E-cadherin mediated adhesion within an individual cell.

Densities in the paranodes (Harkin, 1964), mesaxons (Bunge et al., 1989) and Schmidt-Lanterman incisures (Hall and Williams, 1970) have been noted but infrequently discussed. It is now clear that these densities are components of an adherens junctional system that serves to anchor adjacent membranes. The argument that these are adherens-type junctions is based on their ultrastructural morphology as well as the presence of E-cadherin, and likely β-catenin and F-actin, hallmark molecules of adherens junctions found in other tissues (Boller et al., 1985; Volk and Geiger, 1986*a*, *b*; Le Bivic et al., 1990; Geiger and Ginsberg, 1991; Geiger and Ayalon, 1992). Despite the similarities with classical junctions, Schwann cell adherens junctions are unusual in that the subplasmalemmal plaque traverses the cytoplasmic compartment and appears to fuse with the adjacent plaque.

E-Cadherin adhesion loci in the Schwann cell are distributed throughout the cytoplasmic channel network, which is most easily illustrated in an "unrolled" Schwann cell (Fig. 11 *A*). The continuous channel network (light gray) borders the compact myelin domains (dark gray) and consists of the outer loop, paranodal channels, the inner loop and the Schmidt-Lanterman incisures. The data in this study demonstrates that E-cadherin sites (black) have a restricted distribution within the cytoplasmic network. Diagrammed in situ (Fig. 11 *B*, *bottom*), E-cadherin loci become aligned in contiguous cytoplasmic wraps, thus forming extended junctional complexes. This is most evident in the paranodal channel (Fig. 11 *B*, *top*) where two helically oriented junctional complexes (black) are depicted. Note that the orientation of

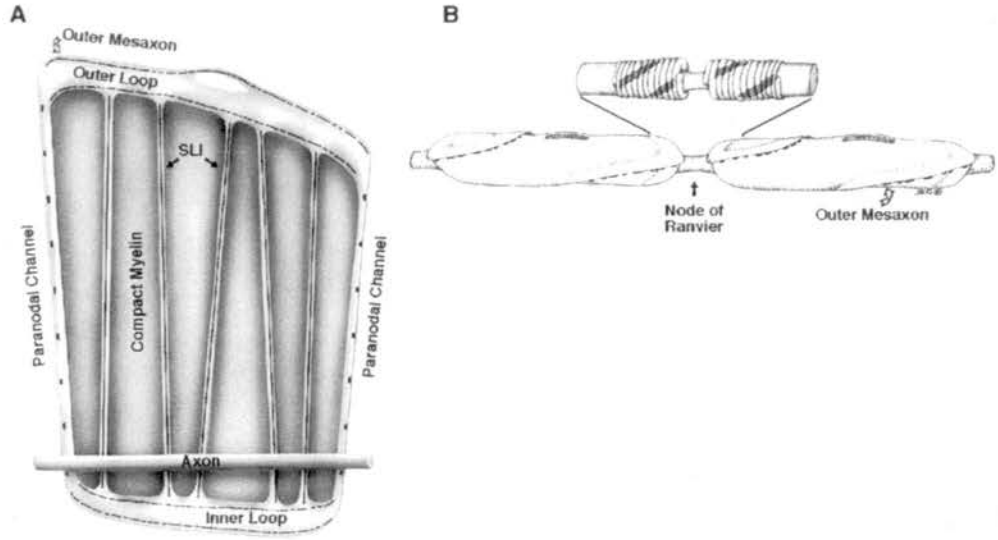

Figure 11. Model for the distribution of E-cadherin adherence sites in an "unrolled" Schwann cell, in the paranodal channels and in a native Schwann cell. (*A*) In an unrolled Schwann cell, E-cadherin adherence sites are found in regions which form the outer boundaries of the cell. These include the outer mesaxon, the outer loop, the inner loop and the paranodal channel. E-cadherin adherence sites are also found in the internal portion of the cell in the Schmidt-Lanterman incisures. Thus, E-cadherin loci are restricted to a cytoplasmic network which sequesters compact myelin into discrete domains. (*B, bottom*). In a Schwann cell in its native ("rolled") conformation, E-cadherin adherence sites become aligned with each other, allowing the formation of an extensive series of transcytoplasmic densities which contribute to the overall stability of the cell. The location of the E-cadherin adherence sites in the outer mesaxon suggests that the outer mesaxon helically wraps around the cell and its orientation continues in register in the adjacent cell. (*B, top*). In paranodal channels stripped of their myelin, E-cadherin containing densities form two helically oriented complexes of transcytoplasmic densities in each paranode.

these complexes is in register across the node of Ranvier. This model for the organization of paranodal junctions is based on confocal and immuno-electron microscopy (this study), and serial electron microscopy (Harkin, 1964). In the outer loop, E-cadherin loci are helically placed, which gives the impression that the outer mesaxon twists along the length of the internode (Fig. 11 *B, lower*) Attachment sites at the outer mesaxon have been previously noted (Bunge et al., 1989), and it is of great interest that freeze–fracture studies reveal extensive linear arrays of particles on the P face at the mesaxonal border (Peters et al., 1991). Some of these particles may, in fact, correspond to E-cadherin loci.

We can speculate that adherens junctions in the Schwann cell may assist in compensatory mechanisms during the stretching and contraction of peripheral nerve. Mechanical stresses on nerve fibers may perhaps be accommodated by changing the degree of coiling of the helical E-cadherin tracts. In this regard, it should be noted that expansion and contraction of Schmidt-Lanterman incisures have been observed in situ (Singer and Bryant, 1969). The alignment of the tracts in the outer loop and mesaxon from one internode to the next suggests that responses may even be coordinated along the entire length of an individual fiber. The adherens junctions in the paranodes may locally supplement the response by maintaining a constant length at the node of Ranvier. This is important since it is generally believed that to ensure efficient saltatory conduction, sodium channels in the nodal axon must be sequestered within relatively non-variant membranous area (Rosenbluth, 1988; Joe and Angelides, 1992).

Autotypic adherens junctions in the Schwann cell may have evolved to mediate rapid intracellular communication which would bypass signaling around the spiral turns. Recent studies have demonstrated that some components of adherens junctions, notably, β-catenin and plakoglobin, are homologues of the Drosophila protein, armadillo, which has been shown to be involved in signal transduction pathways (Nusse and Varmus, 1992). The fact that Schwann cell junctions completely straddle the cytoplasm suits their putative function as efficient signal transducers, and is consistent with the notion that adherens junctions are involved in cellular communication (Gumbiner, 1993; Peifer, 1993).

E-Cadherin may also organize and polarize Schwann cell plasma membrane proteins and other junctional components. Past studies have indicated that adherens junctions and E-cadherin are involved in tissue morphogenesis (Wheelock and Jensen, 1992) and are integral to the maintenance of a polarized epithelium. In addition, E-cadherin seems to act as an organizer of other cell adhesion molecules, and is involved in long-term assembly of the plasma membrane. In the Schwann cell plasma membrane, there is, in effect, a sharply polarized distribution of the two bona fide adhesion molecules characterized in these cells to date: P_0, a member of the Ig superfamily, is restricted to compact myelin, and E-cadherin is restricted to the channel network. The plasma membrane of the Schwann cell actually has four contact sites, three of which have been described as authentic junctions. These include adherens junctions (this paper); tight junctions, (also termed zonula occludens; Mugnaini and Schnapp, 1974; Schnapp and Mugnaini, 1978; Peters et al., 1991); and axoglial junctions, which bridge the paranodal channel and the axonal membrane. The fourth contact site is compact myelin which is a vast planar junction. These junctions are stereotypically organized within the Schwann cell, particularly within the paranodal loops. In fact E-cadherin may play an integral role in establishing Schwann cell polarity in a manner that is analogous to, but certainly distinct from, that in other epithelial cells.

The formation of autotypic junctions must have a crucial role in myelinogenesis. During development of the sheath,

there is both circumferential deposition of myelin lamellae and longitudinal expansion of Schwann cell membrane that proceeds in parallel with the lengthening of the axonal fiber (Webster, 1971). In the establishment of the node of Ranvier, each successive paranodal turn must guide itself around the adjacent channel segment to establish axonal contact. Junctions in the paranodes, Schmidt-Lanterman incisures and outer loops probably stabilize subsequent wraps of myelin as the sheath enlarges. As each turn is completed, newly formed plaques may link with those from previous wraps and, thus, result in contiguously arranged transcytoplasmic junctions. As the myelin sheath forms, E-cadherin mediated adhesive bonds may be continually established, dissociated, and re-established. This activity is likely to depend on interactions between E-cadherin and the actin cytoskeleton, and it is worth noting in this regard that F-actin is localized in peripheral nerve in a labeling pattern that is extraordinarily congruent to E-cadherin distribution (this study; see also Trapp et al., 1989). The adhesive interplay between noncompacted membranes required during myelinogenesis may be analogous to that found in epithelial compaction in which E-cadherin seems to be the major mediator of adhesion (Fleming and Johnson, 1988). During the compaction process, it is thought that E-cadherin induces submembranous, transient changes that are labile and cell contact dependent. Thus, E-cadherin is a good candidate for directing the transient alterations in adhesivity which are likely to be involved in the sequential laying down of the myelin spiral.

In the mature sheath the transcytoplasmic plaques may act as a scaffolding, and perhaps serve to maintain a minimum cytoplasmic width. The absence of a cytoplasmic undercoating at the inner mesaxon may be indicative of more labile membrane–membrane interactions, although there is no direct experimental evidence to support this at present. The relative lability of this interaction would be consistent with one model for myelin membrane deposition that predicts that the myelin sheath enlarges by addition of membrane at the inner loop concurrent with the movement of the inner loop around the axon (Bunge et al., 1989). However, addition of myelin components at the inner loop is not likely to be the only mechanism by which myelin components are deposited in the sheath inasmuch as others have demonstrated that the paranodal and outer loops are also sites of vigorous myelin-related synthetic activity (Gould and Sinatra, 1981; Griffiths et al., 1989), and probable membrane deposition.

In conclusion, E-cadherin is a major adhesion protein in peripheral nerve Schwann cells and is unusual in that it mediates adhesion between membranes synthesized by a single cell. E-cadherin localizes to unique adhesion specializations, now identified as autotypic adherens junctions, that are restricted to subdomains within the noncompacted regions. The junctional complexes may be important stabilization sites in myelination and may mediate rapid signaling across cytoplasmic compartments, which suggests specialized functions in addition to those required for myelinogenesis. Our findings also indicate that the orientations of cytoplasmic networks in Schwann cells are in register across adjacent internodes and this implies that contiguous Schwann cells may have the capacity to act in concert with each other as part of a globally interactive unit. Most importantly, because E-cadherin is fundamentally involved in cellular organization in other cell systems, our data allows us to adduce that E-cadherin may have a similar role in organizing the polarized distributions of Schwann cell proteins, such as P_0 and other components of the myelin sheath. Finally the localization of E-cadherin at the border of each compact myelin domain, taken together with the known susceptibility of this molecule to proteolyze under certain conditions, suggests that failure of E-cadherin mediated adhesion may be one means by which demyelination may proceed in certain pathological states in peripheral nerve.

The authors thank Ms. Jill Gregory for artwork, and Lawrence Shapiro and Drs. Wayne Hendrickson, Harry Webster, Jack Rosenbluth, Barry Gumbiner, and Mary Bunge for helpful discussions. This is manuscript number 172 from the Brookdale Center for Molecular Biology.

This investigation was supported by National Institutes of Health grant NS20147 and by a pilot grant to D. R. Colman and a fellowship to A. M. Fannon (FA 1024-A-1) from the National Multiple Sclerosis Society. Initial support was also provided by a fellowship to A. M. Fannon from the Human Frontier Science Program Organization. V. L. Friedrich was supported by National Institutes of Health grant NS 29056. P. J. Brophy acknowledges support from the Multiple Sclerosis Societies of Great Britain.

Received for publication 13 August 1994 and in revised form 29 December 1994.

References

Behrens, J., M. M. Mareel, R. F. Van, and W. Birchmeier. 1989. Dissecting tumor cell invasion: epithelial cells acquire invasive properties after the loss of uvomorulin-mediated cell–cell adhesion. *J. Cell Biol.* 108:2435–2447.

Bergoffen, J., S. S. Scherer, S. Wang, M. Oronzi Scott, L. J. Bone, D. L. Paul, K. Chen, M. W. Lensch, P. F. Chance, and K. H. Fishbeck. 1993. Connexin mutations in X-linked Charcot-Marie-Tooth disease. *Science (Wash. DC).* 22:2039–2042.

Berndorff, D., R. Gessner, B. Kreft, N. Schnoy A. M. Lajouspetter N. Loch, W. Reutter, M. Hortsch, and R. Tauber. 1994. Liver-intestine cadherin: molecular cloning and characterization of a novel Ca^{2+}-dependent cell adhesion molecule expressed in liver and intestine. *J. Cell Biol.* 123:1353–1369.

Blank, W. F., M. B. Bunge, and R. P. Bunge. 1974 The sensitivity of the myelin sheath particularly the Schwann cell-axolemma junction, to lowered calcium levels in cultured sensory ganglia. *Brain Res.* 67:503–518.

Boller K., D. Vestweber, and R. Kemler. 1985. Cell-adhesion molecule uvomorulin is localized in the intermediate junctions of adult intestinal epithelial cells. *J. Cell Biol.* 100:327–332.

Bunge, R. P., M. B. Bunge, and M. Bates. 1989. Movements of the Schwann cell nucleus implicate progression of the inner (axon-related) Schwann cell process during myelination. *J. Cell Biol.* 109:273–284.

Doyle, J. P., and D. R. Colman. 1993. Glial-neuron interaction and the regulation of myelin formation. *Curr. Opin. Cell Biol.* 5:779–785.

D'Urso D., P. J. Brophy, S. M. Staugaitis, C. S. Gillespie, A. B. Frey, J. G. Stempak, and D. R. Colman. 1990. Protein zero of peripheral nerve myelin: biosynthesis membrane insertion, and evidence for homotypic interaction. *Neuron.* 4:449–460.

Einheber S., T. A. Milner, F. Giancotti and J. L. Salzer. 1993. Axonal regulation of Schwann cell integrin expression suggests a role for alpha 6 beta 4 in myelination. *J. Cell Biol.* 123:1223–1235.

Filbin, M., F. S. Walsh, B. D. Trapp, J. A. Pizzy, and G. I. Tennekoon. 1990. Role of myelin P_0 protein as a homophilic adhesion molecule. *Nature (Lond.).* 34:871–872.

Fleming T. P., and M. H. Johnson. 1988. From egg to epithelium. *Annu. Rev. Cell Biol.* 4:459–485.

Geiger, B., and O. Ayalon. 1992. Cadherins. *Annu. Rev. Cell Biol.* 8:307–332.

Geiger, B., and D. Ginsberg. 1991. The cytoplasmic domain of adherens-type junctions. *Cell Motil. & Cytoskeleton.* 20:1–6.

Ghabriel, M. N., and G. Allt. 1981. Incisures of Schmidt-Lanterman. *Prog. Neurobiol.* 17:25–58.

Gillespie, C. S., D. L. Sherman, G. E. Blair, and P. J. Brophy. 1994. Periaxin, a novel protein of myelinating Schwann cells with a possible role in axonal ensheathment. *Neuron.* 12:497–508.

Gould, R. M., and R. S. Sinatra. 1981. Internodal distribution of phosphatidylcholine biosynthetic activity in teased peripheral nerve fibres: an autoradiographic study. *J. Neurocytol.* 10:161–167.

Griffiths J. R., L. S. Mitchell, K. McPhilemy, S. Morrison, E. Kyriakides, and J. A. Barrie. 1989. Expression of myelin protein genes in Schwann cells. *J. Neurocytol* 18:345–352.

Grunwald, G. B. 1993. The structural and functional analysis of cadherin calcium-dependent cell adhesion molecules. *Curr. Opin. Cell Biol.* 5:797–805.

Gumbiner B., and K. Simons. 1987. The role of uvomorulin in the formation of epithelial occluding junctions. *Ciba Found. Symp.* 125:168–186.

Gumbiner, B. M. 1993. Proteins associated with the cytoplasmic surface of adhesion molecules. *Neuron.* 11:551–564.

Hall, S. M., and P. L. Williams. 1970. Studies on the 'incisures' of Schmidt and Lanterman. *J. Cell Sci.* 6:767–791.

Harkin, J. C. 1964. A series of desmosomal attachments in the Schwann sheath of myelinated mammalian nerves. *Z. Zellforsch. Mikrosk. Anat.* 64:189–195.

Harlow, E., and D. Lane. 1988. Antibodies: A Laboratory Manual. Cold Spring Harbor Laboratory, Cold Spring Harbor, NY. 726 pp.

Hinck, L., I. S. Näthke, J. Papkoff, and W. J. Nelson. 1994. Dynamics of cadherin/catenin complex formation: Novel protein interactions and pathways of complex assembly. *J. Cell Biol.* 125:1327–1340.

Hirano S., N. Kimoto, Y. Shimoyama, S. Hirohashi, and M. Takeichi. 1992. Identification of a neural alpha-catenin as a key regulator of cadherin function and multicellular organization. *Cell.* 70:293–301.

Joe E. H., and K. Angelides. 1992. Clustering of voltage-dependent sodium channels on axons depends on Schwann cell contact. *Nature (Lond.).* 356:333–335.

Kintner, C. 1992. Regulation of embryonic cell adhesion by the cadherin cytoplasmic domain. *Cell.* 69:225–236.

Kordeli, E., J. Davis, B. Trapp, and V. Bennett. 1990. An isoform of ankyrin is localized at Nodes of Ranvier in myelinated axons of central and peripheral nerves. *J. Cell Biol.* 11:1341–1352.

Le Bivic, A., Y. Sambuy, K. Mostov, and E. Rodriguez-Boulan. 1990. Vectorial targeting of an endogenous apical membrane sialoglycoprotein and uvomorulin in MDCK cells. *J. Cell Biol.* 10:1533–1539.

Lee V. M.-Y., M. J. Carden, W. W. Schlaepfer, and J. O. Trojanowski. 1987. Monoclonal antibodies distinguish several differentially phosphorylated states of the two largest rat neurofilament subunits (NF-H and NF-M) and demonstrate their existence in the normal nervous system of the adult rat. *J. Neurosci.* 7:3474–3488.

Magee, A. I., and R. S. Buxton. 1991. Transmembrane molecular assemblies regulated by the greater cadherin family. *Curr. Opin. Cell Biol.* 3:854–861.

Mugnaini, E., and B Schnapp. 1974. Possible role of zonula occludens of the myelin sheath in demyelinating conditions. *Nature (Lond.).* 251:725–727.

Nagafuchi, A., and M. Takeichi. 1988. Cell binding function of E-cadherin is regulated by the cytoplasmic domain. *EMBO (Eur. Mol. Biol. Organ.) J.* 7:3697–3684.

Nagafuchi, A., Y. Shirayoshi, K. Okazari, K. Yasuda, and M. Takeichi. 1987. Transformation of cell adhesion properties by exogenously introduced E cadherin cDNA. *Nature (Lond.).* 329:341–343.

Näthke, I. S., L. Hinck, J. R. Swedlow, J. Papkoff and W. J. Nelson. 1994. Defining interactions and distributions of cadherin and catenin complexes in polarized epithelial cells. *J. Cell Biol.* 125:1341–1352.

Nusse, R., and H. E. Varmus. 1992. Wnt genes. *Cell.* 69:1073–1087.

Ozawa, M., H. Baribault, and R. Kemler. 1989. The cytoplasmic domain of the cell adhesion molecule uvomorulin associates with three independent proteins structurally related in different species. *EMBO (Eur. Mol. Biol. Organ.) J.* 8:1711–1717.

Peifer, M. 1993. The product of the drosophila segment polarity gene armadillo is part of a multi-protein complex resembling the vertebrate adherens junction. *J. Cell Sci.* 105:993–1000.

Peters, A., S. L. Palay, and H. deF. Webster. 1991. The Fine Structure of the Nervous System: Neurons and their Supporting Cells. Oxford University Press, New York. 494 pp.

Rosenbluth J. 1988. Role of glial cells in the differentiation and function of myelinated axons. *Int. J. Dev. Neurosci.* 6:3–24.

Schnapp, B., and E. Mugnaini. 1978. Membrane architecture of myelinated fibers as seen by freeze-fracture. *In* Physiology and Pathobiology of Axons. S. Waxman, editor. Raven Press, New York. 83–123.

Shimamura, K., T. Takahashi, and M. Takeichi. 1992. E-cadherin expression in a particular subset of sensory neurons. *Dev. Biol.* 152:242–254.

Shirayoshi, Y., A. Nose, K. Iwasaki, and M. Takeichi. 1986. N-linked oligosaccharides are not involved in the function of cell-cell binding glycoprotein E-cadherin. *Cell Struct. Func.* 11:245–252.

Singer M., and S. Bryant. 1969. Movements in the myelin Schwann sheath of the vertebrate axon. *Nature (Lond.).* 221:1148–1150.

Takeichi, M. 1991. Cadherin cell adhesion receptors as a morphogenetic regulator. *Science (Wash. DC).* 251:1451–1455.

Trapp, B. D., S. B. Andrews, A. Wong, M. O'Connell, and J. W. Griffin. 1989. Co-localization of the myelin-associated glycoprotein and the microfilament components, F-actin and spectrin, in Schwann cells of myelinated nerve fibres. *J. Neurocytol.* 18:47–60.

Uchiyama N., M. Hasegawa, T. Yamashima, J. Yamashita, K. Shimamura, and M. Takeichi, 1994. Immunoelectron microscopic localization of E-cadherin in dorsal root ganglia, dorsal root and dorsal horn of postnatal mice. *J. Neurocytol.* 23:460–468.

Volk, T., and B. Geiger. 1986*a*. A-CAM: a 135-kD receptor of intercellular junctions. I. Immunoelectron microscopic localization and biochemical studies. *J. Cell Biol.* 103:1441–1450.

Volk, T., and B. Geiger. 1986*b*. A-CAM: a 135-kD receptor of intercellular adherens junctions. II. Antibody-mediated modulation of junctions. *J. Cell Biol.* 103:1451–1464.

Webster H. deF. 1971. The geometry of peripheral myelin sheaths during their formation and growth in rat sciatic nerve. *J. Cell Biol.* 48:348–367.

Wheelock M. J., and P. J. Jensen. 1992. Regulation of keratinocyte intercellular junction organization and epidermal morphogenesis by E-cadherin. *J. Cell Biol.* 117:415–425.

Development 121, 4265-4273 (1995)
Printed in Great Britain © The Company of Biologists Limited 1995
DEV9441

Periaxin expression in myelinating Schwann cells: modulation by axon-glial interactions and polarized localization during development

Steven S. Scherer[1,*], Yi-tian Xu[1], Peter G. C. Bannerman[2], Diane L. Sherman[3] and Peter J. Brophy[3]

[1]Department of Neurology, Room 460 Stemmler Hall, 36th Street and Hamilton Walk, The University of Pennsylvania School of Medicine, Philadelphia, PA 19104-6146, USA (email: scherer@shy.neuro.upenn.edu)
[2]Department of Neurology, Children's Hospital of Philadelphia, Philadelphia, PA 19104, USA
[3]Department of Preclinical Veterinary Sciences, University of Edinburgh, Summerhall, Edinburgh EH9 1QH, Scotland, UK (email: Peter.Brophy@ed.ac.uk)

*Author for correspondence

SUMMARY

Periaxin is a newly described protein that is expressed exclusively by myelinating Schwann cells. In developing nerves, periaxin is first detected as Schwann cells ensheathe axons, prior to the appearance of the proteins that characterize the myelin sheath. Periaxin is initially concentrated in the adaxonal membrane (apposing the axon) but, during development, as myelin sheaths mature, periaxin becomes predominately localized at the abaxonal Schwann cell membrane (apposing the basal lamina). In permanently axotomized adult nerves, periaxin is lost from the abaxonal and adaxonal membranes, becomes associated with degenerating myelin sheaths and is phagocytosed by macrophages. In crushed nerves, in which axons regenerate and are remyelinated, periaxin is first detected in the adaxonal membrane as Schwann cells ensheathe regenerating axons, but again prior to the appearance of other myelin proteins. Periaxin mRNA and protein levels change in parallel with those of other myelin-related genes after permanent axotomy and crush. These data demonstrate that periaxin is expressed by myelinating Schwann cells in a dynamic, developmentally regulated manner. The shift in localization of periaxin in the Schwann cell after completion of the spiralization phase of myelination suggests that periaxin participates in membrane-protein interactions that are required to stabilize the mature myelin sheath.

Key words: Wallerian degeneration, peripheral nerve, axotomy, nerve growth factor receptor, myelin, Schwann cell, rat

INTRODUCTION

Myelin is a multi-lamellar structure that surrounds axons and increases axonal conduction velocity. It is formed by the spiral wrapping of the cell membrane of Schwann cells (in the PNS) and oligodendrocytes (in the CNS). Compact myelin is chiefly composed of lipids, but also contains a unique set of proteins; in the PNS, these are P_0, myelin basic protein (MBP), and peripheral myelin protein-22 kD (PMP-22) (Lemke, 1992; 1993). Other membrane proteins are excluded from compact myelin even though their expression is characteristic of myelinating Schwann cells. Their discrete localization emphasizes that myelinating Schwann cells appear to be polarized epithelial cells, whose plasma membrane contains several distinct domains, each of which has its own distinct repertoire of proteins. Thus, myelin-associated glycoprotein (MAG), the gap junction protein connexin32, oligodendrocyte-myelin glycoprotein and E-cadherin are all found in the perinodal regions and the Schmidt-Lanterman incisures (Trapp and Quarles, 1982; Bergoffen et al., 1993; Apostolski et al., 1994; Fannon et al., 1995; Scherer et al., 1995) In contrast, the integrins $\alpha 6$ and $\beta 4$ are localized to the (abaxonal) surface of myelinating Schwann cells, which apposes their basal laminae (Einheber et al., 1993; Feltri et al., 1994). The adaxonal surface and its associated periaxonal rim of cytoplasm, which appose the axon, are characterized by the expression of MAG, spectrin and F-actin (Trapp et al., 1989). This complex organization of the Schwann cell-axon unit is presumed to contribute to the structural basis required for the formation and stabilization of the myelin sheath.

In addition to myelin-forming Schwann cells, mature peripheral nerve also contains non-myelinating Schwann cells. They ensheathe one or more axons without forming a myelin sheath around any of them (Peters et al., 1991). In addition to these morphological distinctions, non-myelinating and myelinating Schwann cells have different molecular phenotypes. Non-myelinating Schwann cells express glial fibrillary acid protein (GFAP), p75/low-affinity nerve growth factor receptor (NGFR), growth-associated protein 43 kD (GAP-43), neural cell adhesion molecule (N-CAM), and the cell adhesion molecule L1, but not P_0, MBP, PMP-22 and MAG (Mirsky and Jessen, 1990; Snipes et al., 1992; Curtis et al., 1992; Scherer et al., 1994b). Conversely, myelinating Schwann cells do not express GFAP, NGFR, GAP-43, N-CAM and L1. In spite of these differences, the phenotype of Schwann cells depends on their association with axons, and can be experimentally altered,

so that non-myelinating Schwann cells can become myelinating Schwann cells and vice versa. Thus, previously non-myelinating Schwann cells can form myelin sheaths if they are transplanted into a nerve that normally contains many myelinating Schwann cells (Langley and Anderson, 1903; Simpson and Young, 1945; Aguayo et al., 1976b; Weinberg and Spencer, 1976). This finding demonstrates that axons, and not the Schwann cells themselves, determine whether a Schwann cell has a myelinating or a non-myelinating phenotype.

The maintenance of the myelinating phenotype requires continuous axon-Schwann cell interactions, as illustrated by the sequence of events that follow axotomy, which causes axons to degenerate distal to the lesion. Within a few days of axotomy, the axons and myelin sheaths begin to degenerate, but the Schwann cells survive and even proliferate. Myelinating Schwann cells cease expressing high levels of myelin-related proteins and their mRNAs, and begin expressing ones that are more characteristic of non-myelinating Schwann cells, such as the NGFR and GAP-43 (Taniuchi et al., 1988; Curtis et al., 1992; Plantinga et al., 1993; Scherer et al., 1994b). However, if axons regenerate and are remyelinated, the pattern of gene expression reverses: the expression of myelin-related genes increases and the expression of NGFR and GAP-43 falls (Taniuchi et al., 1988; Plantinga et al., 1993; Scherer et al., 1994b). The coordinate increase in myelin-related genes occurs in a manner that appears quite similar to that seen during the onset of myelination in developing nerves. The levels of myelin-related proteins and mRNAs increase, probably because the rate of their transcription increases (Wood and Engel, 1976; Uyemura et al., 1979; Stahl et al., 1990; Wiktorowicz and Roach, 1991). Thus, there is a coordinate program of myelin gene expression, regulated at the level of transcription, which accompanies the synthesis of myelin during both development and regeneration.

In this paper, we have investigated the expression and localization of a newly described protein, periaxin (Gillespie et al., 1994), which is probably the same protein previously identified as P170 and SAG (Shuman et al., 1986; Dieperink et al., 1992). In adult nerve, we find that periaxin is expressed exclusively by myelinating Schwann cells and is predominately localized to their abaxonal surface. In developing and regenerating nerves, however, periaxin is predominately localized to the adaxonal surface of Schwann cells as they begin to form compact myelin. Periaxin immunoreactivity is seen before those of MAG, MBP or P_0, which is consistent with the electron microscopic evidence that it is expressed by ensheathing Schwann cells (Gillespie et al., 1994). Periaxin mRNA levels change in parallel with those of other myelin-related genes in permanently axotomized and regenerating nerves. These data show that periaxin is a myelin-related protein, and the dynamic changes in its localization during ensheathment and myelination suggest that it may play ar important role in these processes.

MATERIALS AND METHODS

Sciatic nerve transection and crush

Using aseptic technique, the sciatic nerves of anesthetized (50 mg/kg pentobarbital i.p.), adult (10-13 week old) Sprague-Dawley rats were exposed at the sciatic notch. Some nerves were doubly ligated, tran-

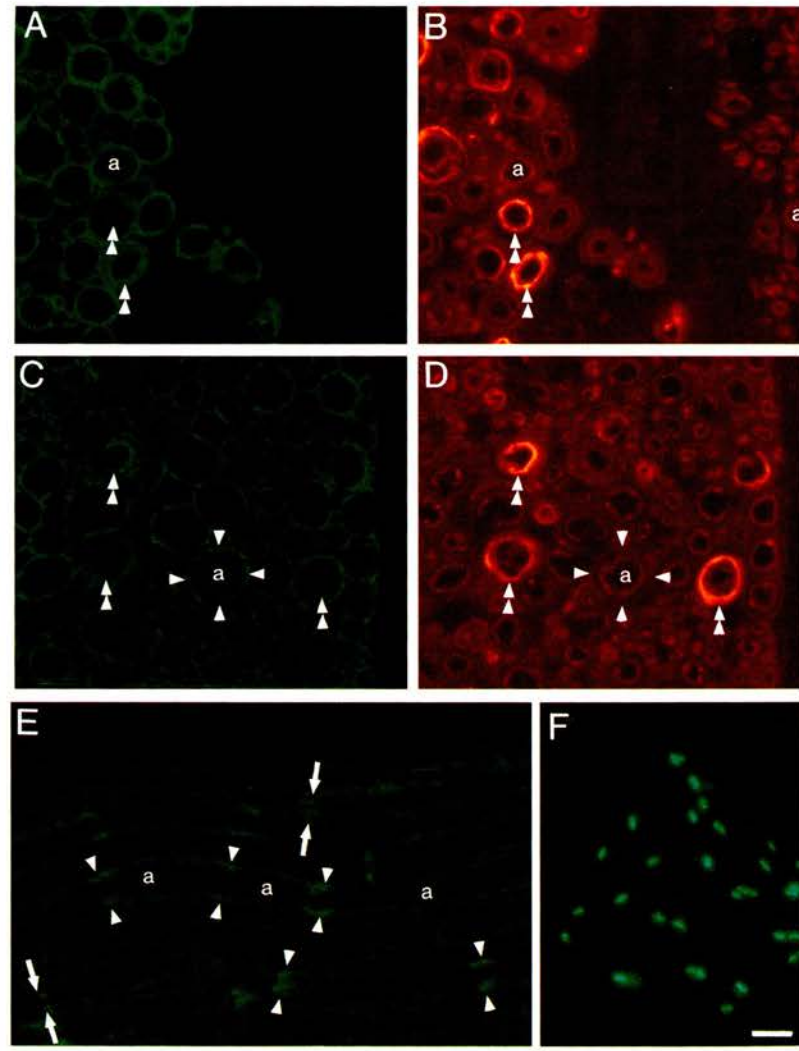

Fig. 1. Immunohistochemical analysis of periaxin in the adult rat PNS. (A-D) Transverse sections of the lumbar dorsal roots, double-labeled for periaxin (fluorescein; A,C) and MAG (rhodamine; B,D). Some incisures are indicated by double-arrowheads and a few axons are labeled (a). At the dorsal root entry zone (A,B), periaxin is expressed by myelinating Schwann cells (left side), but not by oligodendrocytes (right side), whereas MAG is found in a adaxonal distribution in both PNS and CNS myelin sheaths. (C,D) Periaxin immunoreactivity of myelinating Schwann cells is greater on the abaxonal surface (arrowheads) than on the adaxonal surface, in contrast to the adaxonal localization of MAG. (E) Longitudinal section of sciatic nerve that had been treated for 1 hour in 100% Triton-X to better reveal periaxin immunoreactivity in the incisures (arrowheads) and paranodes (arrows) of myelinated axons (a). (F) Transverse section of cervical sympathetic trunk, demonstrating periaxin immunoreactivity is associated with myelinating, but not non-myelinating, Schwann cells. Scale bar: 10 μm.

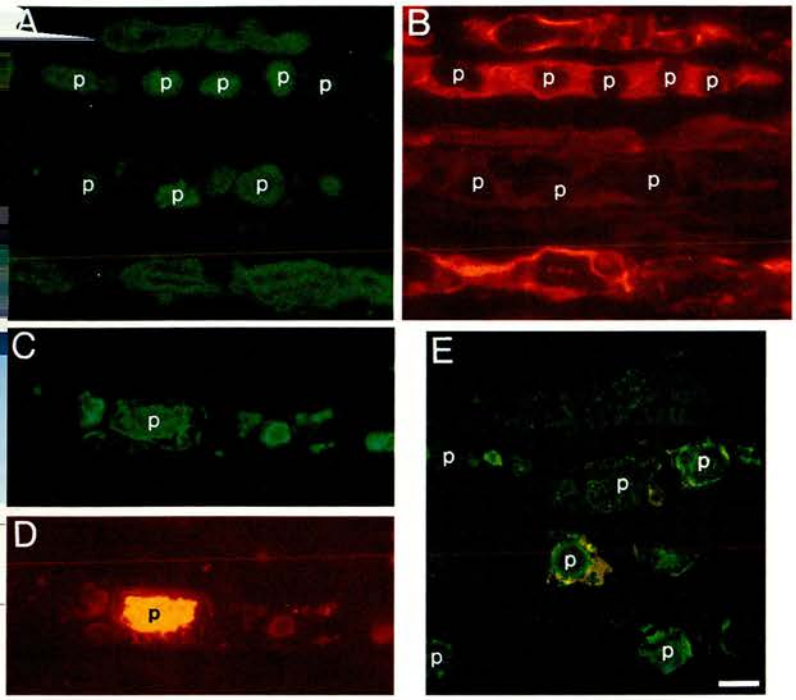

Fig. 2. Immunohistochemical analysis of periaxin expression in Wallerian degeneration. These are longitudinal sections of the distal nerve stump of an adult rat sciatic nerve at 8 (E), 12 (A,B), and 24 (C,D) days post-transection. Periaxin immunoreactivity is green (fluorescein); the rhodamine is either S-100β (B), MBP (D) or ED-1 (E). Pairs of photomicrographs (A,B and C,D) were taken from the same field; (E) is a confocal image. (A,B) Periaxin-immunoreactive material (p) is found in both S-100β-positive (Schwann cells) and S-100β-negative cells (macrophages). (C,D) Periaxin-immunoreactive material (p) is associated with MBP-positive myelin ovoids. (E) Periaxin-immunoreactive material (p) is found within both ED-1-positive (macrophages) and ED-1-negative cells (Schwann cells). Scale bar: 10 μm.

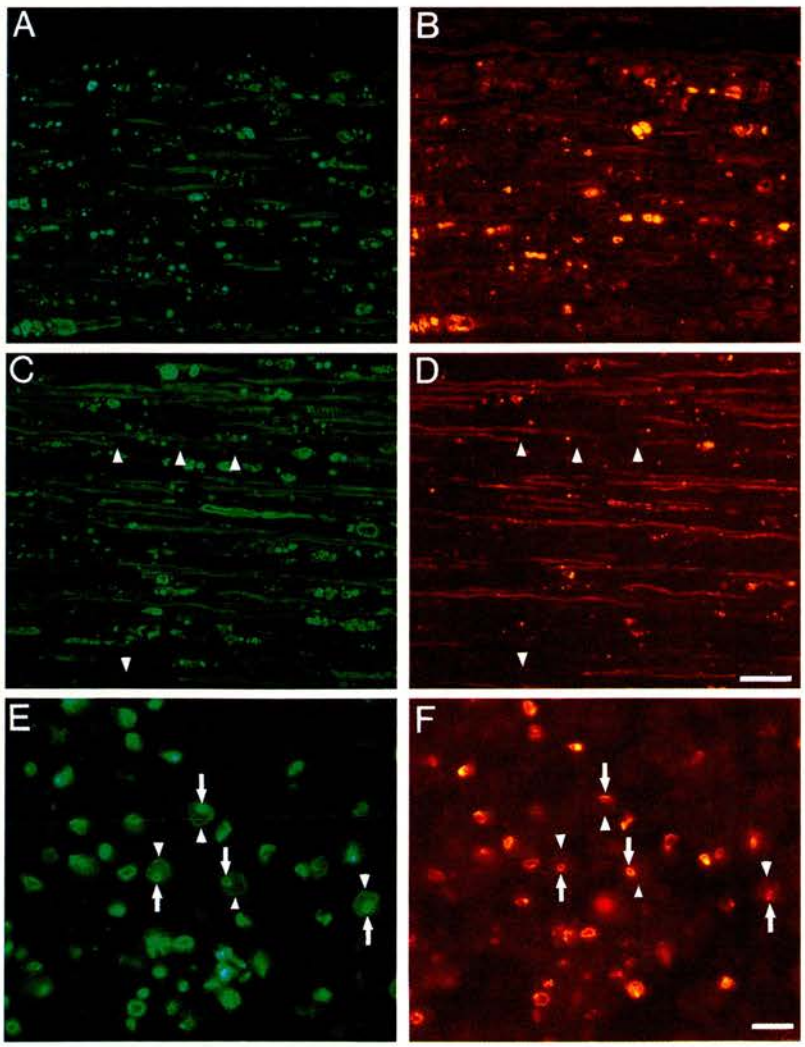

Fig. 3. Immunohistochemical analysis of periaxin in regenerating adult rat sciatic nerve. Longitudinal sections from the distal nerve stump at 12 days (A-D) and transverse sections at 24 days (E,F) postcrush were double-labeled for periaxin (A,C,E; fluorescein) and either P_0 (B) or MAG (D,F). The periaxin-positive Schwann cells that are associated with regenerating axons form long strands that run between clumps of degenerating periaxin-positive debris (A,C). Two periaxin-positive, MAG-negative Schwann cells are indicated by arrowheads (C,D), whereas most of the periaxin-positive cells are P_0-negative (A,B). In transverse sections, many myelinating Schwann cells have a double ring of periaxin labeling: an inner (adaxonal) ring that superimposes with MAG immunoreactivity (arrows), and an outer ring that marks the abaxonal surface (arrowheads). Scale bars: 50 μm (A-D); 10 μm (E,F).

sected with iridectomy scissors, and the two nerve stumps were sutured at least 1 cm apart; this technique prevents axonal regeneration to the distal nerve stump for at least 2 months. Nerve crush was produced by tightly compressing the sciatic nerve at the sciatic notch with flattened forceps twice, each time for 10 seconds; this technique causes all of the axons to degenerate, but allows axonal regeneration. At varying times after nerve injury, the animals were killed by CO_2 inhalation, the distal nerve stumps were removed, and the most proximal 2-3 mm were trimmed off. For transected nerves, the entire distal nerve stump was taken from just below the lesion to the ankle (about 4 cm long). For crushed nerves, the distal nerve stump was divided into two equal segments, termed the proximal and distal segments, each about 2 cm long. The nerves were immediately frozen in liquid nitrogen and stored at −80°C. Unlesioned sciatic nerves were obtained from animals of varying ages, from P1 (the day after birth) to P90. All animal protocols were approved by the Institutional Animal Care and Use Committee of The University of Pennsylvania.

Northern blotting

RNA was isolated from rat sciatic nerves and Schwann cells by $CsCl_2$ gradient centrifugation (Chirgwin et al., 1979). Equal samples (10 μg) of total RNA were electrophoresed in 1% agarose, 2.2 M formaldehyde gels, transferred to nylon membranes (Duralon, Stratagene) in 6× SSC, and u.v. cross-linked (0.12 joules). Blots were prehybridized, hybridized and washed using standard techniques; the final stringency of the wash was 0.2× SSC at 65°C for 30 minutes (Sambrook et al., 1989). The following cDNAs were utilized as probes, a 1.1 kb fragment of rat periaxin (Gillespie et al., 1994), a full-length cDNA of rat P_0 (Lemke and Axel, 1985), a 0.7 kb *Bam*HI fragment of rat NGFR (Radeke et al., 1987) and a full-length cDNA of glyceraldehyde 3-phosphate dehydrogenase (GAPDH; (Fort et al., 1985). Plasmid inserts were isolated after restriction endonuclease digestion, separated by agarose gel electrophoresis and purified by electrolution. ^{32}P-labeled cDNA probes with specific activities of $2\text{-}5\times10^9$ cts/minute/μg were prepared by primer extension with random hexamers using the Prim-a-gene kit (Promega) according to the manufacturer's instructions.

Immunohistochemistry and immunocytochemistry

The distal nerve stumps of transected and crushed rat sciatic nerves, as well as unlesioned nerves and spinal cords, were fixed for 24 hours in Bouins solution or 4% paraformaldehyde, cryoprotected in 20% sucrose and embedded in OCT (Miles). Fixation in Bouins solution gave the best periaxin immunoreactivity, but fixation in paraformaldehyde better preserved the structure of the myelin sheaths. Both transverse and longitudinal sections of the nerves, 6-8 μm thick were obtained and mounted on glass slides. The sections were treated with acetone for 10 minutes at room temperature, blocked for at least 1 hour in 10% fish skin gelatin containing 0.1% Triton-X, and incubated 24-48 hours at 4°C with a various combinations of a primary antibodies. To better visualize periaxin immunoreactivity in the Schmidt-Lanterman incisures, some sections were initially treated with 100% Triton-X for 1 hour. We used a rabbit polyclonal antibody (1:2000 final dilution) against a full-length fusion protein of rat periaxin (Gillespie et al., 1994), as well as guinea pig and rabbit antisera against P170 (Shuman et al., 1986). These antibodies were used in various combinations with a rabbit polyclonal antibody against purified bovine S-100β (East Acres Biologicals), as well as mouse monoclonal antibodies against purified rat GAP-43 (Schreyer and Skene, 1991), bovine myelin basic protein (Serotec clone 2), rat MAG (Boehringer-Manheim), purified bovine S-100β (East Acres Biologicals), rat P_0 (Archelos et al., 1993), or rat macrophages (ED1, Serotec; Dijkstra et al., 1985). After incubating with the primary antibodies, the sections were washed, then incubated with a fluorescein- and rhodamine-conjugated donkey anti-rabbit and anti-mouse secondary antibodies (Jackson ImmunoResearch Laboratories), respectively. Non-immune rabbit serum, diluted to have the same protein concentration as the primary antibodies, was used to control for the specificity of the primary antibodies. Sections were photographed on a Leitz microscope equipped for epifluorescence or scanning laser confocal microscopy.

Electron microscopy

P28 Wistar rats were anaesthetized and perfused with 4% formaldehyde (freshly prepared from paraformaldehyde) in 0.01 M periodate 0.075 M lysine, 0.1 M phosphate buffer at pH 7.4 (McLean and Nakane, 1974). The sciatic and trigeminal nerves were removed and fixed for another 2-3 hours at room temperature. Sciatic nerves were removed and fixed by immersion in the same fixative for 2-3 hours at room temperature. The tissues were processed according to the method of Berryman et al. (1992). Briefly, tissues were washed several times with 0.1 M phosphate buffer containing 3.5% sucrose and stained with 0.2% tannic acid in the same buffer for 1 hour at 4°C (subsequent steps were performed at 4°C). After several washes, aldehydes were quenched in 50 mM NH_4Cl in the same buffer. The tissues were then washed four times in 0.1 M maleate buffer (pH 6.2) containing 4% sucrose, followed by 1% uranyl acetate in maleate-sucrose buffer for 1 hour. The tissues were dehydrated to 90% ethanol (from 70% ethanol onward all steps were at −20°C), absolute ethanol for 15 minutes then infiltrated with a 1:1 ratio of LR Gold (Agar Scientific Ltd., Stanstead, Essex) and ethanol, followed by a 7:3 ratio of LR Gold and ethanol, and two changes of LR Gold for 1 hour and overnight. The tissues were infiltrated in two changes of LR Gold containing 0.5% benzoin methyl ether, for 1 hour and then overnight, and embedded in gelatin capsules. Polymerization was by u.v. irradiation at a wavelength of 365 nm for 48 hours at −20°C.

Sections were collected on nickel grids that were coated with formvar and carbon, blocked (1% BSA, 0.5% fish skin gelatin, 0.05% Triton-X 100, 0.05% Tween 20, 500 mM NaCl, in 10 mM Tris, pH 7.4) for 30 minutes at room temperature and incubated overnight at 4°C with affinity-purified rabbit anti-periaxin antiserum (Gillespie et al., 1994) in the same buffer. Grids were rinsed with the above buffer, incubated for 1 hour with goat anti-rabbit IgG conjugated to 10 nm gold particles (1:20, Amersham), washed on drops of distilled water, fixed with 2.5% aqueous glutaraldehyde and rinsed in a stream of distilled water. After postfixing for 15 minutes with 2% aqueous OsO_4, the grids were stained with lead citrate and examined at 80 kV in a JEOL 100CX electron microscope.

RESULTS

Periaxin is expressed by myelinating Schwann cells

Since periaxin has only been found in myelinating Schwann cells (Gillespie et al., 1994), we compared its localization to those of other Schwann cell markers in the adult rat PNS. As shown in Fig. 1A, periaxin immunoreactivity stopped abruptly at the interface of the PNS and CNS, demonstrating that it is not expressed by oligodendrocytes. P_0 and PMP-22 immunoreactivities were also confined to myelinating Schwann cells (data not shown), whereas MAG (Fig. 1B), MBP (data not shown), and S-100β immunoreactivities (data not shown) were found in both the PNS and the CNS. In both the nerve roots and the sciatic nerve of adult rats, periaxin was predominately localized to the abaxonal surface of myelinating Schwann cells, which apposes their basal laminae (Fig. 1A,C,E). There was also distinct staining of the adaxonal surface, which apposes the axon, as well as of the incisures and paranodes (Fig. 1A,C,E), but compact myelin was not labeled. We compared the localization of periaxin with that of MAG (Fig. 1B,D), which was localized at the adaxonal membrane of

Schwann cells and oligodendrocytes (Sternberger et al., 1979), and even more prominently in the incisures and paranodes (Trapp and Quarles, 1982). To determine whether periaxin was expressed by non-myelinating Schwann cells, we examined the cervical sympathetic trunk, which is mostly composed of unmyelinated axons and their (non-myelinating) Schwann cells (Aguayo et al., 1976a). Periaxin immunoreactivity was found only around the thinly myelinated axons (Fig. 1F), which was confirmed by double-labeling for P_0 and MBP (data not shown). Thus, in the mature PNS, periaxin is exclusively found in myelinating Schwann cells, predominately at the abaxonal surface.

Periaxin has a similar mobility by SDS-polyacrylamide gel electrophoresis to two proteins previously isolated from peripheral nerve myelin, P170 and SAG (Shuman et al., 1986; Dieperink et al., 1992). When sections of adult spinal cord were labeled with two rabbit and three guinea pig antisera against P170 (kindly provided by Dr David Pleasure), all stained myelinating Schwann cells in an identical pattern to that of the periaxin antiserum. As this pattern of staining is essentially the same as described for SAG (Dieperink et al., 1992), periaxin, P170 and SAG are probably the same protein.

Periaxin expression in degenerating and regenerating nerves

It was of interest to learn what happens to periaxin after nerve injury, since most myelin-related proteins disappear after axotomy, as the distal nerve stump undergoes Wallerian degeneration (Mirsky and Jessen, 1990; Scherer and Salzer, 1995). Thus, we examined the distal nerve stumps after both permanent axotomy (transection) and nerve crush, which also causes Wallerian degeneration, but allows axonal regeneration. By 4 days postlesion, the smooth rim of abaxonal periaxin immunoreactivity was largely gone; focal aggregates of periaxin were seen in the Schwann cell cytoplasm, but separate from the degenerating myelin sheaths. After 4 days, most of periaxin immunoreactivity was found in large aggregates, often associated with the degenerating myelin sheaths, the so-called myelin ovoids, which contained the myelin proteins P_0, MBP and MAG (Fig. 2C,D). The amount of periaxin-positive material, as well as myelin debris, fell progressively after 8 days postinjury, but was still found here and there even at 58 days postlesion. The periaxin aggregates were initially found mostly in Schwann cells and not in macrophages, but by 58 days postlesion, most of the periaxin-immunoreactive material was found in macrophages (Fig. 2A,B,E). Thus, even though periaxin is not present in compact myelin, it is degraded along with the components of the myelin sheath by Schwann cells and macrophages (Stoll et al., 1989).

Since regenerating axons are remyelinated after nerve crush (Ramon y Cajal, 1928), we could evaluate further how axon-Schwann cell interactions regulate periaxin expression. In crushed nerves, the periaxin that was previously associated with myelinating Schwann cells appeared to be degraded as in transected nerves but, in addition, periaxin was re-expressed as Schwann cells ensheathed and myelinated regenerating axons (Fig. 3). Schwann cells with periaxin-positive sheaths ensheathing regenerating axons, which were labeled by a rat monoclonal antibody against neurofilaments, were seen in the proximal segment of distal nerve stumps at 8 days. By 12 days, these Schwann cells were much more numerous and extended much further into the distal nerve stump and, by 24 and 58 days postcrush, they were found through the full extent of the distal nerve stump. As the temporal and spatial gradient of periaxin-expressing Schwann cells is consistent with the idea that Schwann cells re-express periaxin as they remyelinate axons, we performed double labeling for periaxin and MAG, P_0 or MBP to determine whether these proteins were co-expressed. At 8 days (data not shown) and 12 days postcrush (Fig. 3C,D), most periaxin-positive cells were also MAG-positive, although a few were MAG-negative. In contrast, at these early stages of regeneration, many periaxin-positive (and MAG-positive) cells were P_0- (Fig. 3A,B) and MBP-negative (not shown). At 24 (Fig. 3E,F) and 58 days (not shown) most of the periaxin-positive Schwann cells also expressed MAG, P_0 and MBP. These data demonstrate that periaxin and MAG are re-expressed by Schwann cells as they ensheathe axons, and prior to the onset of P_0 and MBP expression.

We also noted a change in the distribution of periaxin immunoreactivity during remyelination. Between 12 and 24 days postcrush, it was difficult to determine whether the periaxin immunoreactivity was abaxonal or adaxonal, owing to the thinness of the myelin sheath. At the level of the Schwann cell nucleus, where the nucleus and perinuclear cytoplasm separated the abaxonal and adaxonal surfaces, it was possible to determine that there was both abaxonal and adaxonal periaxin immunoreactivity, and that the latter typically predominated (Fig. 3E,F). By 58 days postcrush, most of the periaxin immunoreactivity was found abaxonally (data not shown), as in normal adult nerve. Thus, the localization of periaxin changes dynamically as Schwann cells ensheathe and remyelinate axons.

To confirm that the amount of periaxin protein changed as predicted by the above immunohistochemistry, we performed western blot analysis using the rabbit polyclonal serum against rat periaxin fusion protein. After transection, the amount of periaxin protein decreased to a low level by 24 days and remained at this level until at least 60 days post-transection (data not shown). In crushed nerves, the amount of periaxin decreased to a nadir at 28 days, then returned to nearly normal levels at 60 days postcrush (data not shown). Thus, the level of periaxin protein changed in parallel with the immunohistochemical changes in periaxin expression in both transected and crushed nerves. These results show that the expression of periaxin, like other myelin-related proteins, depends on axon-Schwann cell interactions (Mirsky and Jessen, 1990; Scherer and Salzer, 1995).

Periaxin expression in developing peripheral nerve

The shift in the subcellular localization of periaxin during remyelination probably reconciles the contrasting immunohistochemical data from adult and neonatal nerves. In adult nerves, periaxin is predominately abaxonally localized (Fig. 1A), whereas we previously reported that periaxin was mostly adaxonal, which was based on our observations of neonatal nerves (Gillespie et al., 1994). To confirm that periaxin is redistributed during development, we analyzed P1, P6 and P15 sciatic nerves, spanning the most active period of myelination (Webster and Favilla, 1984). As expected, the number of periaxin-positive, as well as MAG-, MBP- and P_0-positive Schwann cells increased dramatically during this period (Hahn et al., 1987). While there were numerous Schwann cells that

had robust periaxin staining both adaxonally and abaxonally in P1 and P6 nerves, by P15 abaxonal staining predominated in most myelinating Schwann cells. To determine whether periaxin was expressed prior to MAG, MBP and P_0, we performed double-labeling. At P1, most of the periaxin-positive Schwann cells were also MAG-positive, but there were many periaxin-positive and MBP- or P_0-negative cells (Fig. 4C-F). These data suggest that periaxin expression in developing nerves is similar to that in regenerating nerves: the expression of periaxin immunoreactivity precedes that of MAG, P_0 and MBP, and that the predominant localization of periaxin changes from adaxonal to abaxonal.

This shift in localization during development was confirmed by immunoelectron microscopy. In P3 sciatic nerve, periaxin was found to be localized both adaxonally and abaxonally (Fig. 5A). In P28 trigeminal nerve, however, the amount of adaxonal labeling was considerably diminished, whereas the abaxonal surface remained heavily labeled (Fig. 5B). Although adult trigeminal nerve is illustrated, the localization of periaxin was identical in adult sciatic nerve (data not shown).

Periaxin mRNA levels depend on axon-Schwann cell interactions

The above data, taken together, show that periaxin is expressed in concert with the other myelin-related genes in Schwann cells. Since the mRNA levels of these genes are exquisitely sensitive to the disruption of axon-Schwann cell interactions (Scherer and Salzer, 1995), we analyzed the levels of periaxin mRNA after permanent axotomy (transection) and nerve crush by northern blot analysis. To better illustrate the changes in gene expression in crushed nerves, we divided the distal nerve stumps into a proximal and a distal segment, as axons regenerate in a proximal-to-distal manner.

As shown in Fig. 6A, the steady state level of periaxin mRNA fell dramatically by 4 days post-transection and did not return even by 58 days. After nerve crush, the level of periaxin mRNA also fell over a similar time course, but began to return by 12 days in the proximal segment and by 24 days in the distal nerve segment (Fig. 6B). The level of periaxin mRNA in both segments continued to increase until at least 58 days postcrush. We compared the changes in periaxin mRNA with that of P_0, NGFR and GAPDH, by reprobing the same blots. The changes in the levels of periaxin and P_0 mRNA were strikingly similar in both transected and crushed nerves. The level of NGFR mRNA, in contrast, was reciprocally related to those of periaxin and P_0, both in transected and in crushed nerves. The level of GAPDH mRNA did not change significantly after transection or crush.

These data indicate that axon-Schwann cell interactions are necessary to maintain the high level of periaxin mRNA, and that the increase in the expression of myelin-related genes, including periaxin, in regenerating nerves is mediated by axon-Schwann cell interactions. To demonstrate directly that regenerating axons were required for the return of periaxin mRNA in crushed nerves, we transected regenerating nerves at 24 days postcrush, when periaxin levels had begun to return. As shown in Fig. 6C, 2 days after transection of the regenerating nerve, the level of periaxin mRNA fell in the distal nerve stump. The blot was reprobed for P_0 and NGFR mRNA, thereby demonstrating a fall in the expression of other myelin-related mRNAs, and an increase in the expression of genes expressed by denervated Schwann cells, respectively (Gupta et al., 1993; Scherer et al., 1994a).

DISCUSSION

Periaxin is a protein whose deduced amino acid sequence predicts a cytoplasmic protein (Gillespie et al., 1994). We have shown that periaxin is expressed by myelinating Schwann

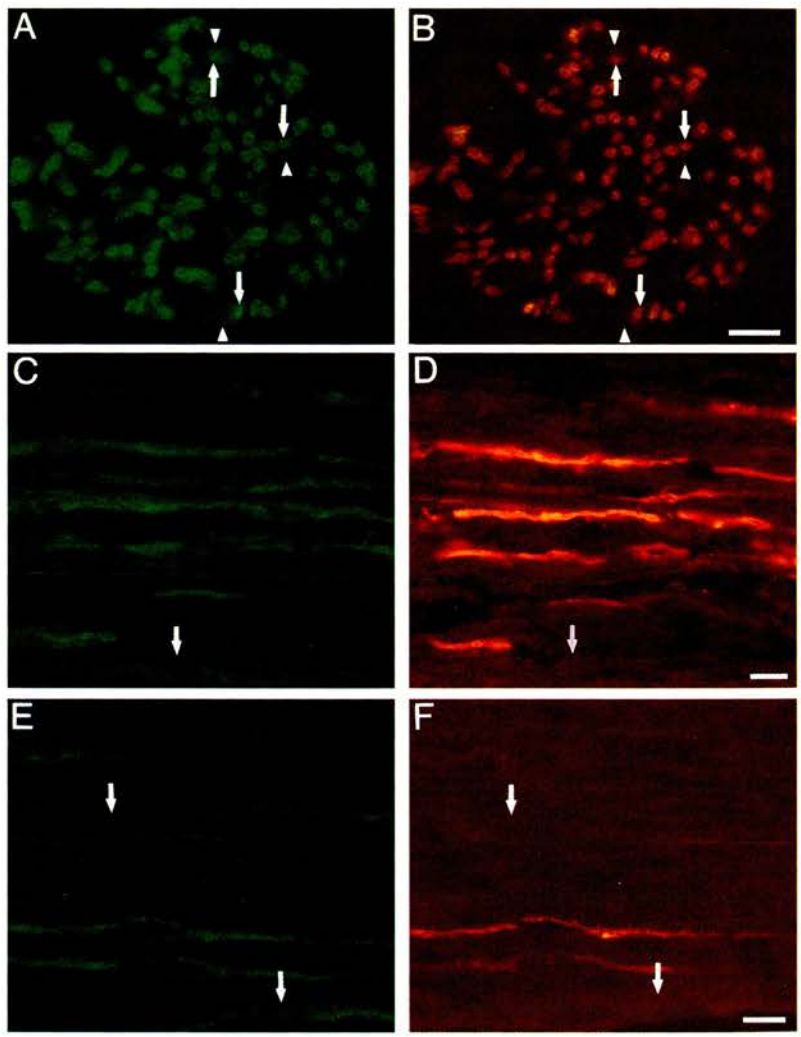

Fig. 4. Immunohistochemical analysis of periaxin in developing rat sciatic nerve. These are photomicrographs of the same field of P6 (A,B; transverse sections) and P1 (C-F; longitudinal sections) sciatic nerves. Periaxin immunoreactivity is green (fluorescein); the rhodamine is either MAG (B), P_0 (D) or MBP (F). (A,B) Note that many myelinating Schwann cells have a double ring of periaxin labeling: an inner (adaxonal) ring that superimposes with MAG immunoreactivity (arrows) and an outer ring that marks the abaxonal surface (arrowheads). (C-F) Note that some periaxin-positive cells are P_0- and MBP-negative (arrows). Scale bars: 10 μm.

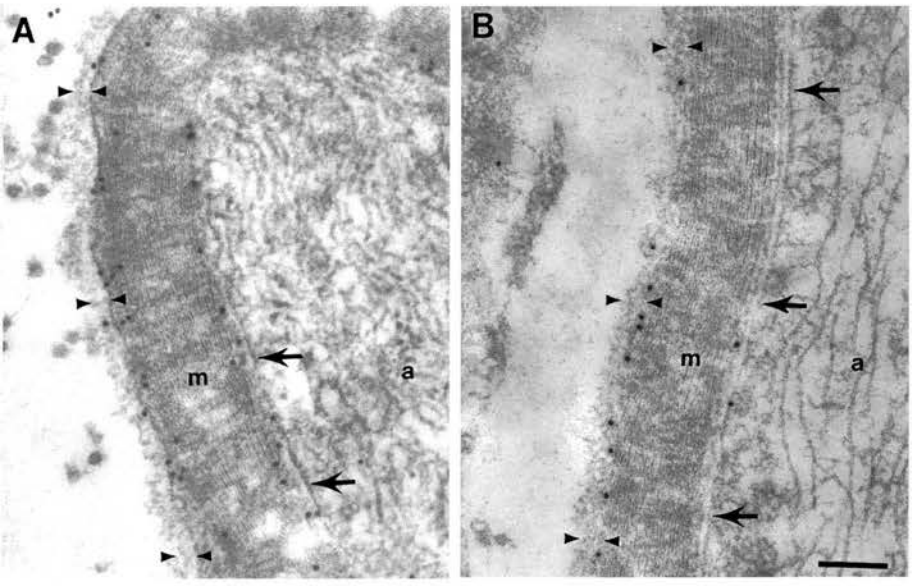

Fig. 5. Comparison of periaxin localization in longitudinal sections of P3 sciatic nerve (A) and P28 (B) rat trigeminal nerve by immunoelectron microscopy. A basal lamina (between arrowheads) surrounds compact myelin (m), which in turn, surrounds the axon (a). The axolemma is indicated by arrows. Gold particles (10 nm) are abundantly detected in at both the adaxonal and abaxonal myelin membranes at P3 (A), whereas by P28 the shift to a predominantly abaxonal localization has become apparent. Scale bar: 200 nm.

cells, and that its localization changes dynamically during ensheathment and myelination. Since P170 and SAG have the same molecular weight and insolubility in Triton-X as periaxin, as well as the same immunohistochemical localization, all three are probably the same protein (Shuman et al., 1986; Dieperink et al., 1992; Gillespie et al., 1994). Furthermore, like other myelin-related proteins, the expression periaxin mRNA and protein is tightly regulated by axon-Schwann cell interactions (Scherer and Salzer, 1995). These data suggest that periaxin has a specific function in myelinating Schwann cells.

Periaxin is expressed in ensheathing Schwann cells

In both developing and regenerating nerves, we found that periaxin is initially found predominately in the adaxonal Schwann cell membrane. At the ultrastructural level, periaxin is expressed as soon as Schwann cells ensheathe axons in a 1:1 relationship, which corresponds to the onset of MAG expression (Gillespie et al., 1994; Martini and Schachner, 1986, 1988). The onset of P_0 expression is slightly later, as it is first expressed after a few lamellae of compact myelin are formed (Hahn et al., 1987; Lamperth et al., 1990; Martini et al., 1988). Although periaxin, MAG, and P_0 all appear to be expressed at roughly the same time, we found a few Schwann cells were periaxin-positive and MAG-negative, and many that were periaxin-positive and P_0- and MBP-negative (see also Owens and Bunge, 1989), indicating that periaxin, MAG and P_0 are expressed in that order in individual, myelinating Schwann cells. The earlier onset of periaxin and MAG immunoreactivities, however, do not necessarily mean that their corresponding mRNAs are expressed earlier than those of P_0 and MBP. In oligodendrocytes, the onset of proteolipid protein (PLP) expression is delayed by as much as 3 days relative to other MBP, whereas the onset of PLP and MBP

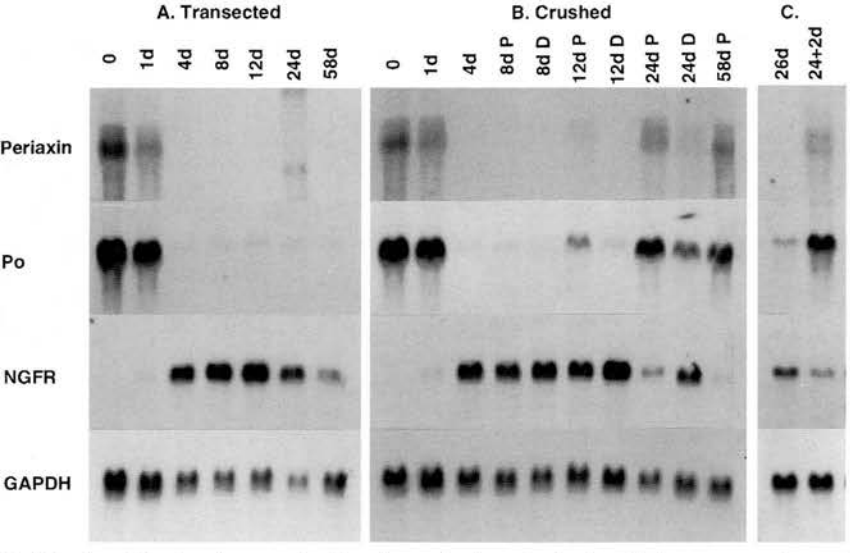

Fig. 6. Northern blot analysis of normal and lesioned adult rat sciatic nerves. Each lane contains an equal amount (10 μg) of total RNA isolated from the distal stumps of sciatic nerves that had been transected (A), crushed (B) or transected 24 days after nerve crush and allowed to degenerate for an additional 2 days (C). The number of days after each of these lesions in indicated; the '0' time point is from unlesioned nerves. In crushed nerves (B), the distal nerve stumps were divided into proximal (P) and distal (D) segments of equal lengths. The blots were successively hybridized with a radiolabeled cDNA probe for periaxin (A), NGFR (C), GAPDH (D) and P_0 (B). The films were exposed for the following times: periaxin, 2 weeks; P_0, 2 hours; NGFR, 1 day; GAPDH, 3 days. The periaxin signal is composed of two transcripts that are similar in size (data not shown); these two bands are difficult to discern on these blots. The identity of the band recognized by the periaxin probe in the 24 day transected sample is not known, but is probably due to cross-hybridization with a plasmid that contaminated this sample of RNA.

mRNA expression is the same (Dubois-Dalcq et al., 1987; Grinspan et al., 1993).

The localization of periaxin is developmentally regulated

We found that periaxin was predominately localized to the adaxonal Schwann membrane during ensheathment and early myelination, then predominately to the abaxonal membrane as myelination continued. These data reconcile previous reports on the localization of periaxin, SAG and P170 in peripheral nerve. Like the ultrastructural study of Gillespie et al. (1994), we find that periaxin is abundant in the adaxonal Schwann cell membrane in early postnatal rat sciatic nerves. SAG was localized to the adaxonal and abaxonal Schwann cell membranes of myelinated axons in human neurofibromas (Dieperink et al., 1992), which agrees with our localization in adult nerves. Finally, although P170 was initially reported to be in compact myelin (Shuman et al., 1986), we have repeated this experiment using the same antibodies and find that it is predominantly localized to the abaxonal membrane in adult nerve.

The developmental regulation of periaxin localization may reflect the reorganization of the Schwann cell membrane during myelination. There is a growing body of evidence that, as Schwann cells ensheathe axons, they become polarized. In axon-Schwann cell co-cultures, Schwann cells need to interact with axons in order to assemble a basal lamina (Clark and Bunge, 1989), and Schwann cells need a basal lamina in order to properly ensheathe and myelinate axons and to express MAG and P_0 (Eldridge et al., 1987, 1989; Fernandez-Valle et al., 1993). The redistribution of periaxin from the adaxonal to the abaxonal Schwann cell membrane may mark the polarization of myelinating Schwann cells. Periaxin is not the only protein to be redistributed, since MAG becomes restricted to the adaxonal surface as Schwann cells ensheathe axons (Martini and Schachner, 1986, 1988). Finally, the integrin subunits $\alpha 6$ and $\beta 4$ are found only on the abaxonal surface (Einheber et al., 1993; Feltri et al., 1994), even as they first appear in the rat sciatic nerve (about P6, Scherer, unpublished observations). Thus, periaxin, MAG and $\alpha_6\beta_4$ integrin are all restricted with respect to the adaxonal and abaxonal Schwann cell membrane. The spatial restriction of these molecules is presumably important for their function in myelinating Schwann cells, although to date this has been shown directly only for MAG (Owens and Bunge, 1989; Li et al., 1994; Montag et al., 1994). Analysis of the molecular basis by which the polarization of periaxin distribution is accomplished during the maturation of the myelin sheath is likely to foster a better understanding of the cell biology of myelination in the peripheral nerve.

This work was supported by NS-01565 and NS-08075 to S. S. S., and by a grant from the Medical Research Council to P. J. B.. We thank Drs D. Pleasure, D. Schreyer, D. Colman, V. M.-Y. Lee, and J. Archelos for their generous gifts of antibodies.

REFERENCES

Aguayo, A. J., Bray, G. M., Terry, L. C. and Sweezey, E. (1976a). Three-dimensional analysis of unmyelinated fibers in normal and pathologic autonomic nerves. *J. Neuropathol. Exp. Neurol.* **35**, 136-151.

Aguayo, A. J., Chavron, L. and Bray, G. M. (1976b). Potential of Schwann cells from unmyelinated nerves to produce myelin: A quantitative ultrastructural and radiographic study. *J. Neurocytol.* **5**, 565-573.

Apostolski, S., Sadiq, S. A., Hays, A., Corbo, M., Suturkova, L., Chaliff, P., Stefansson, K., LeBaron, R. G., Ruoslahti, E., Hays, A. P. and Latov, N. (1994). Identification of Gal(β1-3)GalNAc bearing glycoproteins at the nodes of Ranvier in peripheral nerve. *J. Neurosci. Res.* **38**, 134-141.

Archelos, J. J., Roggenbuck, K., Schneider-Schaulies, J., Linington, C., Toyka, K. V. and Hartung, H. P. (1993). Production and characterization of monoclonal antibodies to the extracellular domain of PO. *J. Neurosci. Res.* **35**, 46-53.

Bergoffen, J., Scherer, S. S., Wang, S., Oronzi-Scott, M., Bone, L., Paul, D. L., Chen, K., Lensch, M. W., Chance, P. and Fischbeck, K. (1993) Connexin mutations in X-linked Charcot-Marie-Tooth disease. *Science* **262**, 2039-2042.

Berryman, M. A., Porter, W. R., Rodewald, R. D. and Hubbard, A. L. (1992). Effects of tannic acid on antigenicity and membrane contrast in ultrastructural immunocytochemistry. *J. Histochem. Cytochem.* **40**, 845-857.

Chirgwin, J. M., Przbyla, A. E., MacDonald, R. J. and Rutter, R. J. (1979) Isolation of biologically active ribonucleic acid from sources enriched in ribonuclease. *Biochem.* **18**, 5294-5299.

Clark, M. B. and Bunge, M. B. (1989). Cultured Schwann cells assemble normal-appearing basal laminae only when they ensheathe axons. *Dev. Biol.* **133**, 393-404.

Curtis, R., Stewart, H. J. S., Hall, S. M., Wilkin, G. P., Mirsky, R. and Jessen, K. R. (1992). GAP-43 is expressed by nonmyelin-forming Schwann cells of the peripheral nervous system. *J. Cell Biol.* **116**, 1455-1464.

Dieperink, M. E., Oneill, A., Magnoni, G., Wollmann, R. L., Heinrikson, R. L., Zurcherneely, H. A. and Stefansson, K. (1992). SAG - a Schwann cell membrane glycoprotein. *J. Neurosci.* **12**, 2177-2185.

Dijkstra, C. D., Doop, E. A., Joling, P. and Kraal, G. (1985). The heterogeneity of mononuclear phogocytes in lymphoid organs: distinct macrophage subpopulations in the reat recognized by monoclonal antibodies ED1, ED2 and ED3. *Immunol.* **54**, 589-600.

Dubois-Dalcq, M., Behar, T. and Lazzarini, R. A. (1987). Emergence of three myelin proteins in oligodendrocytes cultured without neurons. *J. Cell Biol.* **102**, 384-392.

Einheber, S., Milner, T., Giancotti, F. and Salzer, J. (1993). Axonal regulation of Schwann cell integrin expresssion suggests a role for α6β4 in myelination. *J. Cell Biol.* **123**, 625-638.

Eldridge, C. F., Bunge, M. B. and Bunge, R. P. (1989). Differentiation of axon-related Schwann cell *in vitro*: II. Control of myelin formation by basal lamina. *J. Neurosci.* **9**, 625-638.

Eldridge, C. F., Bunge, M. B., Bunge, R. P. and Wood, P. M. (1987) Differentiation of axon-related Schwann cells *in vitro*. I. Ascorbic acid regulates basal laminia assembly and myelin formation. *J. Cell Biol.* **105**, 1023-1034.

Fannon, A. M., Sherman, D. L., Ilyina-Gragerova, G., Brophy, P. J., Friedrich, V. L. and Colman, D. R. (1995). Novel E-cadherin mediates adhesion in peripheral nerve: Schwann cell architecture is stabilized by autotypic adherens junctions. *J. Cell Biol.* **129**, 189-202.

Feltri, M. L., Scherer, S. S., Nemni, R., Kamholz, J., Vogelbacker, H., Oronzi-Scott, M., Canal, N., Quaranta, V. and Wrabetz, L. (1994). β4 integrin expression in myelinating Schwann cells is ab-axonally polarized, developmentally-regulated, and axonally-dependent. *Development* **120**, 1287-1301.

Fernandez-Valle, C., Fregien, N., Wood, P. M. and Bunge, M. B. (1993) Expression of the protein zero myelin gene in axon-related Schwann cells is linked to basal lamina formation. *Development* **119**, 867-880.

Fort, P., Marty, L., Piechaczyk, M., Sabrouty, S. E., Dani, C., Jeanteur, P. and Blanchard, J. M. (1985). Various rat adult tissues express only one major mRNA species from the glyceraldehyde-3-phosphate-dehydrogenase multigenic family. *Nucl. Acids Res.* **13**, 1431-1442.

Gillespie, C. S., Sherman, D. L., Blair, G. E. and Brophy, P. J. (1994) Periaxin, a novel protein of myelinating Schwann cells with a possible role in axonal ensheathment. *Neuron* **12**, 497-508.

Grinspan, J., Wrabetz, L. and Kamholz, J. (1993). Oligodendrocyte maturation and myelin gene expression in PDGF-treated cultures from rat cerebral white matter. *J. Neurocytol.* **22**, 322-333.

Gupta, S. K., Pringle, J., Poduslo, J. F. and Mezei, C. (1993). Induction of myelin genes during peripheral nerve remyelination requires a continuous signal from the ingrowing axon. *J. Neurosci. Res.* **34**, 14-23.

Hahn, A. F., Whitaker, J. N., Kachar, B. and Webster, H. d. (1987). P2, P1

and P0 myelin basic protein expression in developing rat sixth nerve: a quantitative immunocytochemical study. *J. Comp. Neurol.* **260**, 501-512.

Lamperth, L., Manuelidis, L. and Webster, H. d. (1990). P0 glycoprotein: messenger RNA distribution in myelin-forming Schwann cells at the developing rat trigeminal ganglion. *J. Neurocytol.* **19**, 756-769.

Langley, J. N. and Anderson, H. K. (1903). On the union of the fifth cervical nerve with the superior cervical ganglion. *J. Physiol.* **30**, 439-442.

Lemke, G. (1992). Myelin and myelination. In *Molecular Neurobiology*, (ed. Z. W. Hall), pp. 281-312. Sunderland, MA: Sinauer.

Lemke, G. (1993). The molecular genetics of myelination - an update. *Glia* **7**, 263-271.

Lemke, G. and Axel, R. (1985). Isolation and sequence of a cDNA encoding the major structural protein of peripheral myelin. *Cell* **40**, 501-508.

Li, C., Topak, M. B., Gerial, R., Calpoff, S., Abramow-Newerly, W., Trapp, B., Peterson, A. and Roder, J. (1994). Myelination in the absence of myelin-associated glycoprotein. *Nature* **369**, 747750.

Martini, R., Bollensen, E. and Schnachner, M. (1988). Immunocytological localization of the major peripheral nervous system glycoprotein P0 and the L2/HNK-1 and L3 carbohydrate structures in developing and adult mouse sciatic nerve. *Dev. Biol.* **129**, 330-338.

Martini, R. and Schachner, M. (1986). Immunoelectron microscopic localization of neural cell adhesion molecules (L1, N-CAM, and MAG) and their shared carbohydrates epitope and myelin basic protein in developing sciatic nerve. *J. Cell Biol.* **103**, 2434-2448.

Martini, R. and Schachner, M. (1988). Immunoelectron microscopic localization of neural cell adhesion molecules (L1, N-CAM, and myelin-associated glycoprotein) in regenerating adult mouse sciatic nerve. *J. Cell Biol.* **106**, 1735-1746.

McLean, I. W. and Nakane, P. K. (1974). Periodate-lysine paraformaldehyde fixative: A new fixative for immunoelectron microscopy. *J. Histochem. Cytochem.* **22**, 1077-1083.

Mirsky, R. and Jessen, K. R. (1990). Schwann cell development and the regulation of myelination. *Semin. Neurosci.* **2**, 423-435.

Montag, D., Giese, K. P., Bartsch, U., Martini, R., Lang, Y., Bluthmann, H., Karthigasan, J., Kirschner, D. A., Wintergerst, E. S., Nave, K.-A., Zielasek, J., Toyka, K. V., Lipp, H.-P. and Schachner, M. (1994). Mice deficient for the myelin-associated glycoprotein show subtle abnormalities in myelin. *Neuron* **13**, 229-246.

Owens, G. C. and Bunge, R. P. (1989). Evidence for an early role of myelin-associated glycoprotein in the process of myelination. *Glia* **2**, 119-128.

Peters, A., Palay, S. L. and Webster, H. d. (1991). *The Fine Structure of the Nervous System*. 494 p. New York: Oxford University Press.

Plantinga, L. C., Verhaagen, J., Edwards, P. M., Hol, E. M., Bar, P. R. and Gispen, W. H. (1993). The expression of B-50/GAP-43 in Schwann cells is upregulated in degenerating peripheral nerve stumps following nerve injury. *Brain Res.* **602**, 69-76.

Radeke, M. J., Misko, T. P., Hsu, C., Herzenberg, L. A. and Shooter, E. M. (1987). Gene transfer and molecular cloning of the rat nerve growth factor receptor. *Nature* **325**, 593-597.

Ramon y Cajal, S. (1928). Degeneration and Regeneration of the Nervous System. (ed. R. M. May). pp. 769. Oxford: Oxford University Press.

Sambrook, J., Fritsch, E. F. and Maniatis, T. (1989). *Molecular Cloning*. Cold Spring Harbor Press.

Scherer, S. S., Deschenes, S. M., Xu, Y.-t., Grinspan, J. B., Fischbeck, K. H. and Paul, D. L. (1995). Connexin32 is a myelin-related protein in the PNS and CNS. *J. Neurosci.* (in press).

Scherer, S. S. and Salzer, J. L. (1995). Axon-Schwann cell interactions in peripheral nerve regeneration. In *Glial Cell Development*, (ed. K. R. Jessen and W. D. Richardson). Bios Scientific Publishing. (in press).

Scherer, S. S., Wang, D.-y., Kuhn, R., Lemke, G., Wrabetz, L. and Kamholz, J. (1994a). Axons regulate Schwann cell expression of the POU transcription factor SCIP. *J. Neurosci.* **14**, 1930-1942.

Scherer, S. S., Xu, Y.-T., Roling, D., Wrabetz, L., Feltri, M. L. and Kamholz, J. (1994b). Expression of growth-associated protein-43 kD in Schwann cells is regulated by axon-Schwann cell interactions and cAMP. *J. Neurosci. Res.* **38**, 575-589.

Schreyer, D. J. and Skene, J. H. P. (1991). Fate of GAP-43 in ascending spinal axons of DRG neurons after peripheral nerve injury - delayed accumulation and correlation with regenerative potential. *J. Neurosci.* **11**, 3738-3751.

Shuman, S., Hardey, M. and Pleasure, D. (1986). Immunochemical characterization of peripheral nervous system myelin 170,000-M_r glycoprotein. *J. Neurochem.* **47**, 811-818.

Simpson, S. A. and Young, J. Z. (1945). Regeneration of fibre diameter after cross-union of visceral and somatic nerves. *J. Anat.* **79**, 48-65.

Snipes, G. J., Suter, U., Welcher, A. A. and Shooter, E. M. (1992). Characterization of a novel peripheral nervous system myelin protein (PMP-22/SR13). *J. Cell Biol.* **117**, 225-238.

Stahl, N., Harry, J. and Popko, B. (1990). Quantitative analysis of myelin protein gene expression during development in the rat sciatic nerve. *Mol. Brain Res.* **8**, 209-212.

Sternberger, N. H., Quarles, R. H., Itoyama, Y. and Webster, H. d. (1979). Myelin-associated glycoprotein demonstrated immunocytochemically in myelin and myelin-forming cells of developing rat. *Proc. Natl. Acad. Sci. USA* **76**, 1510-1514.

Stoll, G., Griffin, J. W., Li, C. Y. and Trapp, B. D. (1989). Wallerian degeneration in the peripheral nervous system: participation of both Schwann cells and macrophages in myelin degradation. *J. Neurocytol.* **18**, 671-683.

Taniuchi, M., Clark, H. B., Schweitzer, J. B. and Johnson, E. M., Jr. (1988). Expression of nerve growth factor receptors by Schwann cells of axotomized peripheral nerves: Ultrastructural location, suppression by axonal contact, and binding properties. *J. Neurosci.* **8**, 664-681.

Trapp, B. D., Andrews, S. B., Wong, A., O'Connell, M. and Griffin, J. W. (1989). Co-localization of the myelin-associated glycoprotein and the microfilament components, F-actin and spectrin, in Schwann cells of myelinated nerve fibers. *J. Neurocytol.* **18**, 47-60.

Trapp, B. D. and Quarles, R. H. (1982). Presence of the myelin-associated glycoprotein correlates with alterations in the periodicity of peripheral myelin. *J. Cell Biol.* **92**, 877-882.

Uyemura, K., Horie, K., Kitamura, K., Suzuki, M. and Uehara, S. (1979). Developmental changes of myelin protein in the chick peripheral nerve. *J. Neurochem.* **32**, 779-788.

Webster, H. d. and Favilla, J. T. (1984). Development of peripheral nerve fibers. In *Peripheral Neuropathy*, (ed. P. J. Dyck, P. K. Thomas, E. H. Lambert and R. Bunge), pp. 329-359. Philadelphia: W.B. Saunders.

Weinberg, H. J. and Spencer, P. S. (1976). Studies on the control of myelinogenesis. II. Evidence for neuronal regulation of myelin production. *Brain Res.* **113**, 363-378.

Wiktorowicz, M. and Roach, A. (1991). Regulation of myelin basic protein gene transcription in normal and *shiverer* mutant mice. *Dev. Neurosci.* **13**, 143-150.

Wood, J. G. and Engel, E. L. (1976). Peripheral nerve glycoproteins and myelin fine structure during development of rat sciatic nerve. *J. Neurocytol.* **5**, 605-615.

(Accepted 15 September 1995)

THE JOURNAL OF BIOLOGICAL CHEMISTRY
Vol. 273, No. 10, Issue of March 6, pp. 5794–5800, 1998
Printed in U.S.A.

Two PDZ Domain Proteins Encoded by the Murine Periaxin Gene Are the Result of Alternative Intron Retention and Are Differentially Targeted in Schwann Cells*

(Received for publication, July 25, 1997, and in revised form, November 3, 1997)

Lee Dytrych, Diane L. Sherman, C. Stewart Gillespie, and Peter J. Brophy‡

From the Department of Preclinical Veterinary Sciences, University of Edinburgh, Edinburgh EH9 1QH, United Kingdom

Periaxin was first described as a 147-kDa protein that was suggested to have a potential role in the initiation of myelin deposition in peripheral nerves based upon its abundance, cell type specificity, pattern of developmental expression, and localization (Gillespie, C. S., Sherman, D. L., Blair, G. E., and Brophy. P. J. (1994) *Neuron* 12, 497–508). Here we show that the murine periaxin gene spans 20.6 kilobases and encodes two mRNAs of 4.6 and 5.2 kilobases that encode two periaxin isoforms, L-periaxin and S-periaxin of 147 and 16 kDa respectively. The larger mRNA is produced by a retained intron mechanism that introduces a stop codon and results in a truncated protein with an intron-encoded C terminus of 21 amino acids. Both proteins possess a PDZ domain at the N terminus; nevertheless, they are targeted differently in Schwann cells. Like other proteins that contain PDZ domains, L-periaxin is localized to the plasma membrane of myelinating Schwann cells: in contrast, S-periaxin is expressed diffusely in the cytoplasm. This suggests that proteins that contain this protein-binding module may also participate in protein-protein interactions at sites other than the cell cortex.

Periaxin was first identified as a relatively abundant 146-kDa protein of myelinating Schwann cells in a screen for novel cytoskeleton-associated proteins with a role in peripheral nerve myelination (1). Like P_0, the major integral membrane protein of peripheral nervous system myelin, periaxin is detectable at an early stage of peripheral nervous system development (2). However, in contrast to P_0, periaxin is not incorporated into compact myelin (1), but is initially concentrated in the plasma membrane, the abaxonal membrane (apposing the basal lamina), and the adaxonal membrane (apposing the axon). As myelin sheaths mature periaxin becomes concentrated in the abaxonal membrane and plasma membrane (2). This shift in the localization of the protein in the Schwann cell after completion of the spiralization phase of axon ensheathment suggests that periaxin may participate in the membrane-protein interactions that are required to stabilize the mature sheath. To shed light on the protein's function, we were particularly interested to determine if modular protein-binding domains might be represented in the periaxin amino acid sequence. Although no such domains were identified from initial data base comparisons (1), here we report that the periaxin gene does encode one of the most interesting of these protein-binding motifs to emerge over recent years, namely the PDZ domain.

The PDZ domain was named after the three proteins in which it was first identified, namely post-synaptic density protein **P**SD-95, *Drosophila* ***d****iscs large* (*dlg*) tumor suppressor gene, and the tight junction-associated protein **Z**O-1 (3). It consists of an approximately 90-amino acid protein-binding motif found in proteins that interact with the cytoplasmic tail of plasma membrane proteins and with the cortical cytoskeleton (4). Although the binding site for some PDZ domains is the simple peptide sequence (S/T)*X*V found at the C terminus of certain plasma membrane proteins (5), PDZ-containing proteins can recognize somewhat different sequences and can even form homophilic clusters with the PDZ domains of other proteins (6, 7) . So far, two major functions have been ascribed to PDZ domains on the basis of their interactions with plasma membrane proteins and their presence in known signaling molecules such as *dlg* (6). First, they may organize and recruit proteins to the plasma membrane as has been proposed for PSD-95 (3). Secondly, they may link transmembrane proteins with the actin cytoskeleton via actin-binding proteins such as protein 4.1 (8–10).

Here we report the structure of the murine periaxin gene, which reveals that there are two periaxin isoforms, L-periaxin and S-periaxin. The smaller protein, S-periaxin, is generated by a relatively rare retained intron mechanism (11), which is probably favored by the presence of suboptimal 5′- and 3′-splice sites in the final intron together with a downstream putative exonic splicing enhancer (12, 13). Although both are PDZ proteins, L- and S-periaxin are targeted differently in the Schwann cell, indicating that the PDZ domain is not the sole determinant of their subcellular localization. To our knowledge this is the first example of the differential localization of two protein isoforms with the same PDZ domain.

EXPERIMENTAL PROCEDURES

Isolation and Characterization of Genomic Clones—A 129SV murine genomic library (gift from Dr W. Skarnes, Center for Genome Research, Edinburgh University) in the bacteriophage Lambda Dash II (Stratagene, Cambridge, UK) was screened by plaque hybridization (14) with a ^{32}P-labeled probe comprising nucleotides 1–3000 of rat periaxin cDNA (1). Hybridization was at 60 °C in QuikHyb (Stratagene, Cambridge, UK), and the filters were washed in 2 × SSC (300 mM NaCl, 30 mM sodium citrate, pH 7), 0.1% (w/v) SDS at room temperature and finally at 60 °C in 0.2 × SSC, 0.1% SDS. From 1×10^6 clones, twelve positive plaques were identified after three rounds of screening, and *Eco*RI fragments of each insert were subcloned into the pIBI30 plasmid (IBI, Cambridge, UK) for analysis. The ends of each clone were sequenced by the dideoxy chain termination method (15) using a T7 DNA polymerase kit (Pharmacia LKB Biotech, Uppsala, Sweden), which showed that the twelve clones comprised three groups of sequences that overlapped (H1, F2, and I1). Oligonucleotide primers designed from these sequences were used to determine the order of the *Eco*RI fragments within the

* This work was supported by the Biotechnology and Biological Sciences Research Council, the Medical Research Council, and the Wellcome Trust. The costs of publication of this article were defrayed in part by the payment of page charges. This article must therefore be hereby marked "*advertisement*" in accordance with 18 U.S.C. Section 1734 solely to indicate this fact.

‡ To whom correspondence should be addressed: Dept. of Preclinical Veterinary Sciences, University of Edinburgh, Summerhall, Edinburgh EH9 1QH, UK.

gene by PCR[1] using purified bacteriophage DNA (1 μl of 1:500 dilution) as template (first cycle of 94 °C for 5 min, 60 °C for 1 min, and then 72 °C for 1 min; 36 cycles of 94 °C for 1 min, 60 °C for 1 min, and then 72 °C for 1 min, 7 min during the last cycle). The reactions (50 μl) included primers (5 μM) and Dynazyme DNA polymerase (5 units) (Flowgen Ltd., Sittingbourne, UK). Periaxin sequence was mapped to the *Eco*RI fragments by Southern blot with regional periaxin probes. Briefly, *Eco*RI-digested plasmid DNA from each *Eco*RI subclone was electrophoresed on a 1% agarose gel and vacuum blotted to Magma nylon membrane (Micron Separations Inc., Westborough, MA). The membrane was hybridized with ^{32}P-labeled rat periaxin cDNA fragments covering the entire rat cDNA, and the order of the genomic clones was determined. The cDNA and genomic sequences were compared using the University of Wisconsin GCG software package. Analysis of the three clone types from the first screening revealed the absence of sequence corresponding to the first 297 bases of the rat cDNA, which includes the initiation codon and the 5′-untranslated region. Therefore a further 6×10^5 plaques were screened with a probe corresponding to nucleotides 50–297 of the rat sequence (1), which was generated by reverse transcription-PCR of the 5′-end of mouse periaxin mRNA (see below). Two clones were isolated and characterized as described above and were shown to be identical. This sequence (HH1) did not overlap with the 5′-end of H1. However HH1 and H1 were shown to be contiguous by PCR performed on 129SV genomic DNA as template (first cycle of 94 °C for 5 min, 60 °C for 1 min, and then 72 °C for 1 min; 36 cycles of 94 °C for 1 min, 60 °C for 1 min, and then 72 °C for 1 min, 7 min during the last cycle). The reactions (50 μl) contained genomic DNA (200 ng) primers (5 μM) and Dynazyme DNA polymerase (5 units) (Flowgen Ltd.). The PCR product was isolated from an agarose gel with the QIAEX II gel extraction kit (Qiagen Ltd, Crawley, UK) cloned into the pGEM-T vector (Promega Ltd., Southampton, UK) according to the manufacturer's instructions and sequenced using a T7 sequencing kit, with T7 and M13(R) primers (Pharmacia).

Reverse Transcription-PCR—To obtain a probe for the 5′-end of the mouse periaxin mRNA, total RNA was isolated from the sciatic nerves of 15-day-old mice with RNAzol B (Biogenesis, Bournemouth, UK) according to the manufacturer's instructions. Reverse transcriptions (20 μl) contained RNA (2 μg), random hexamers (150 ng), dithiothreitol (10 mM), dNTPs (0.5 mM), and SuperScript reverse transcriptase (400 units) (Life Technologies Inc., Paisley, Scotland) in first strand synthesis buffer and were incubated at 42 °C for 1 h. The reactions were terminated by heating at 80 °C, and 1 μl of this reaction was used as a template for PCR using primers corresponding to nucleotides 50–71 and 631–650 of the published rat periaxin cDNA sequence (1). PCR conditions were: five cycles of 94 °C for 1 min, 55 °C for 1 min, and 72 °C for 1 min followed by 26 cycles of 94 °C for 40 s, 55 °C for 1 min, and 72 °C for 1 min (4 min during last cycle). Reactions (50 μl) contained primers (5 μM) and Dynazyme DNA polymerase (1 unit) (Flowgen Ltd.). The product was subcloned into the pGEM-T (Promega Ltd., Southampton, UK) vector according to the manufacturer's instructions and sequenced with a T7 DNA polymerase kit (Pharmacia).

Determination of Periaxin Transcriptional Initiation Site—An oligonucleotide complementary to nucleotides 50–71 of the rat periaxin cDNA (1) was end-labeled with [γ-^{32}P]ATP and T4 polynucleotide kinase. Total RNA (10 μg) from the trigeminal nerves of 13-day-old mice was hybridized to labeled oligonucleotide (5 pmol) and reverse transcribed for 10 min at 80 °C followed by 18 h at 42 °C. Reverse transcription employed SuperScript reverse transcriptase (Life Technologies Inc.) in a buffer supplied by the manufacturer and included 50 μg/ml actinomycin D. Extended products were resolved on a 6% polyacrylamide DNA sequencing gel adjacent to a dideoxy sequencing ladder comprising the 5′-end of periaxin primed using an oligonucleotide complementary to nucleotides 103–122 of mouse periaxin cDNA.

Isolation of cDNA Clones Encoding Two Periaxin Isoforms—Two periaxin mRNAs of 5.2 and 4.6 kb were detected in mouse and rat sciatic nerve. We had previously cloned the cDNA for the smaller mRNA (1). To identify how the larger mRNA differed from the 4.6-kb mRNA, 3×10^5 clones of a 15-day-old rat sciatic nerve cDNA library constructed in *Eco*RI-digested λgt11 (Promega Ltd., Southampton, UK) according to the manufacturer's instructions were screened with a probe comprising nucleotides 1–597 of the rat periaxin cDNA previously described (1). Screening was carried out essentially as for the genomic library, and 24 positive plaques were purified. DNA from each of these phage clones was digested with *Not*I, and the inserts were subcloned into the pGEM11zf plasmid (Promega Ltd., Southampton, UK) and sequenced. Of 11 clones that included a sequence homologous to exon 6 of the mouse gene, five included a sequence corresponding to the intron between exons 6 and 7. Total RNA from both rat and mouse sciatic nerves was subsequently Northern blotted with a PCR generated probe for this intronic sequence with identical results.

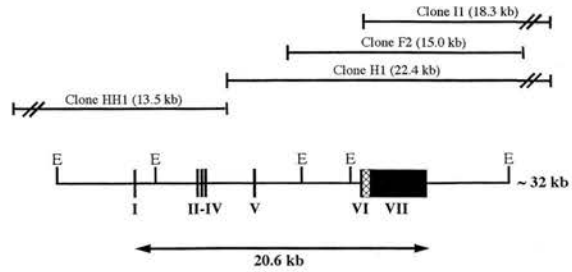

FIG. 1. **Structure of the murine periaxin gene.** Exons are numbered and indicated by *solid rectangles*. Introns are shown as *solid lines* between the exons, except for intron 6, which is depicted as a *hatched box* between exons VI and VII. *Eco*RI (*E*) restriction sites are indicated and were used to subclone the genomic clones F2, H1, and I1 (from the first screen) and HH1 (from the second screen).

Northern Blotting—Total RNA from 15-day-old mouse sciatic nerves was electrophoresed on 0.8% agarose formaldehyde gels and transferred to Magna nylon membrane (Micron Separations Inc., Westborough, MA) by vacuum blotting in 20 × SSC. Filters were probed for 1.5 h in Rapid Hyb buffer (Amersham) at 65 °C with an exon 7-specific probe, a 1.3-kb restriction fragment corresponding to nucleotides 1–1324 of the rat periaxin cDNA sequence, or a PCR product homologous to the intron 6 of the mouse gene labeled with [α-^{32}P]dCTP by random priming (Life Technologies Inc.) and were washed to a final stringency of 0.2 × SSC at 65 °C. The intron probe was prepared using one of the five rat cDNA clones isolated as described above as template with primers that flanked 100 bp of intron sequence. The PCR conditions used for the preparation of this intronic probe were: first cycle of 94 °C for 1 min, 55 °C for 1 min, and then 72 °C for 1 min; 28 cycles of 94 °C for 40 s, 55 °C for 1 min, and then 72 °C for 1 min, 4 min during the last cycle. Reactions (50 μl) contained primers (5 μM) and Dynazyme DNA polymerase (0.5 unit) (Flowgen Ltd.).

Antibody Production—The anti-SPeri and anti-NTerm antibodies were raised in rabbits against the synthetic peptides AKLVRVLSPVPVQDSPSDRVAAAC and EARSRSAEELRRAEC, respectively, which were generous gifts from Prof. N. Groome, Department of Biology, Oxford Brookes University. The former peptide corresponded to the C-terminal 23 amino acids of mouse S-periaxin, and the latter comprised the N-terminal 14 amino acids of mouse periaxin ,which is identical in L-periaxin and S-periaxin. The C-terminal cysteine residue of each peptide was coupled to Keyhole Limpet hemocyanin by standard techniques and used to immunize rabbits. Anti-SPeri antibody was affinity purified by immunoabsorption to a column of peptide coupled to Sepharose (Sigma Chemical Company, Poole, UK).

Immunofluorescence Microscopy—20-day-old mice were perfused intracardially with a 4% solution of paraformaldehyde in 0.1 M sodium phosphate, pH 7.4. Sciatic nerves were then removed and fixed for a further 2 h at room temperature. After washing, nerves were cryoprotected by immersion for 15 min in 5% (w/v) and then 10% (w/v) sucrose in 0.1 M phosphate, pH 7.4, followed by overnight incubation in a 20% (w/v) solution at 4 °C. Cryoprotected nerves were subsequently frozen in OCT embedding compound (Tissue TEK) using isopentane. Transverse sections (7 μm) were collected on 3-aminopropyltriethoxysilane-subbed glass slides. Following removal of OCT by washing in phosphate-buffered saline (PBS) (Sigma), sections were blocked for 3 h at room temperature in a solution of 10% (v/v) goat serum (Scottish Antibody Production Unit, Law Hospital, Carluke, Scotland), 0.2% (w/v) gelatin, and 0.3% (v/v) Triton X-100 in PBS. Blocked sections were incubated overnight with rabbit anti-170pep1 (1) (diluted 1:3000) or affinity-purified anti-SPeri (diluted 1:200) with mouse anti-myelin basic protein (diluted 1:200) (from Prof. N. Groome, Department of Biology, Oxford Brookes University) in 4% (v/v) goat serum, 0.2% (w/v) gelatin and 0.3% (v/v) Triton X-100 (in PBS) under humid conditions at room temperature. Slides were washed in blocking buffer minus goat serum and then incubated with the secondary antibodies fluorescein isothiocyanate-labeled goat anti rabbit (Cappel, Durham, NC) (diluted 1:200) and biotinylated goat anti-mouse (Kirkegaard and Perry) (diluted 1:500). Both antibodies were in 4% (v/v) goat serum, 0.2% (w/v) gelatin, and 0.3% (v/v) Triton X-100 (in PBS) and incubated for 1 h at

[1] The abbreviations used are: PCR, polymerase chain reaction; kb, kilobase pair(s); bp, base pair(s); PBS, phosphate-buffered saline.

TABLE I

Exon/intron position, size, and junction sequence structure of the mouse periaxin gene

The intronic 5′-splice donor GT and 3′-splice acceptor AG are in bold type. The exonic sequences are capitalized. The interruption of codons by introns is indicated by the phase. A phase of 0 indicates no interruption, and insertion of an intron after the first nucleotide of the codon is indicated by phase 1. All numbering is relative to the deduced cDNA sequence of the mouse 4.6-kb periaxin message.

Exon no. (size in bp)	cDNA position	5′-Splice donor	Intron no. (size in bp)	3′-Splice acceptor	Codon phase	Amino acid at splice site
1 (32)	1–32	CCACCG**gt**aaga	1 (4900)	tcct**ag**AGCCCC		
2 (44)	33–76	CCTCAG**gt**gaga	2 (88)	tggc**ag**GCAGCA		
3 (99)	77–175	GAAGCG**gt**gagg	3 (116)	cccc**ag**GCTCAG		
4 (126)	176–301	GCTGAG**gt**gggt	4 (2900)	tcgc**ag**GAGCTG	0	(Glu/Glu)[a]
5 (157)	302–458	AAGAAG**gt**aggc	5 (7500)	ttgc**ag**GGGACC	1	Gly^{62}
6 (197)	459–655	AAGCTG**gt**acgc	6 (592)	cctc**ag**AACATC	0	$(Leu/Asn)^{127}$
7 (4002)	656–4657					

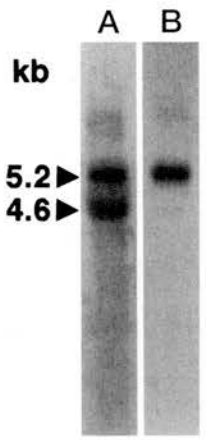

FIG. 2. **Alternative splicing of a retained intron generates two mRNAs.** Sciatic nerve RNA from 15-day-old mice was electrophoresed on a 0.8% agarose formaldehyde gel (2 μg/lane), transferred to nylon membrane and probed in *lane A* with a 1.3-kb restriction fragment of nucleotides 1–1324 of the rat periaxin cDNA and in *lane B* with a PCR product comprising intron 6 of the mouse gene. Both probes were labeled with [α-^{32}P]dCTP by random priming as described under "Experimental Procedures." Autoradiography was for 48 h.

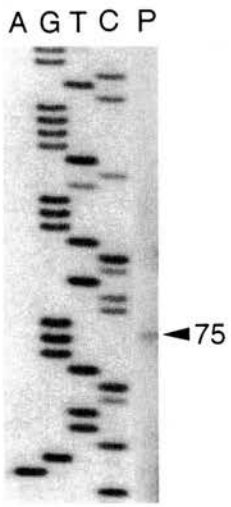

FIG. 3. **Determination of the periaxin transcription initiation site by primer extension.** An oligonucleotide complementary to nucleotides 50–71 of rat periaxin cDNA (1) was end-labeled with [γ-^{32}P]ATP and T4 polynucleotide kinase. Total RNA (10 μg) from the trigeminal nerves of 13-day-old mice was hybridized to labeled oligonucleotide (5 pmol) and reverse transcribed. Extended products were resolved on a 6% polyacrylamide sequencing gel adjacent to a sequencing ladder comprising the 5′ end of periaxin primed using an oligonucleotide complementary to nucleotides 103–122 of mouse periaxin cDNA. (lane *P*).

```
-491  ACAAC CTTCA AGAGG TAAGC ATTCT TACTA CTACT ATTTC AAAGA CAAAG

-441  AACTG AGGGC CCAGT GATGC CCTGT GATTG CTGAA GTTCC CGGAG CCAGG

-391  AATGC CTGAG CTGGG ACTTG AACCC AAATT CTCAA GGAGA CAGTG TAAGA
                                    GCRE
-341  GGTTG TTTTG AGAGT CTCAG GGACT ATGTG GGCTA GGCCT GGGTC CAGGA

-291  GCCCA GAGAT GATGG GGGTG GGGTG CTGAG TATTC GAATG GGGGT GGTAT
      SCIP/Oct-6
-241  GCAAA TTCTT GAACT AAGGC TGGGG TGGAG GTCTG GGCTC TGGCA AGGGA

-191  GAGGT TCATG TTTCC ACATC CCCAC GCCCT TGCAG ATGGA TGTAG TGCAC

-141  AGAAG GGGAT GTTTG TTTCC CCACC ACCCA CCCTT TGGGT GACAT CACAG
            CAAT BOX
 -91  CAGGA CAGCC AATGG CCAGG GTCCC CCTTC TGCCC CCCCC TTCCC ATTCC
                                                        +1
 -41  TTTTC CCTCC CAGCC CAAGG CTAGG ACTAA ACAGA CAGAC CAAGG AGCTC

 +10  TGGAG GTGTC TGGAG GCCCA CCGgt
```

FIG. 4. **Nucleotide sequence of the transcriptional initiation site and consensus sequences of transcription factor-binding elements in the putative core promoter.** Exon 1, which comprises 32 (*positive numbers*) and 491 bp of the putative core promoter (*negative numbers*) are shown relative to the transcriptional intiation site (*+1*) determined by primer extension. The sequences recognized by STAT proteins (29), SCIP/Oct-6 (18–20), SREBP1 (30), and NF-Y (31) together with the consensus glial cAMP response element (*GCRE*) (21) are *underlined*. The CAAT box is *double-underlined*.

room temperature. Further washes in blocking buffer minus serum were followed by a 1-h incubation with streptavidin-Texas red (Vector laboratories) (diluted 1:1500) and several washes in PBS. Sections were subsequently examined with a Leica TCS4D confocal microscope.

Western Blot Analysis—Sciatic nerve homogenates (10 μg) were resolved by SDS-polyacrylamide gel electrophoresis on 4–20% gradient polyacrylamide gels, and Western blotting was performed as described previously (1). Rabbit anti-170pep1 (1) was diluted 1:2000, affinity-purified rabbit anti-SPeri was diluted 1:200, and rabbit anti-NTerm was diluted 1:1000. Goat anti-rabbit IgG-horseradish peroxidase conjugate (Scottish antibody production unit) was used at a dilution of 1:500. The peroxidase reaction was stopped by the addition of SDS to 2% (v/v).

RESULTS

Intron-Exon Structure of Murine Periaxin Gene—Three different clones were isolated from a murine 129SV genomic library using a rat periaxin cDNA as a hybridization probe. A fourth, which included the 5′-end of the gene, was isolated using a murine cDNA probe that had been generated by reverse transcription-PCR. The clones were digested with *Eco*RI and subcloned into pIBI30. These clones were analyzed by PCR and Southern blot and were sequenced, which demonstrated that they encompassed the entire periaxin gene. The gene is divided into seven exons, and the coding region spans were approximately 20.6 kb (Fig. 1). Exons 1–6 range in size from 32 (exon 1) to 197 bp (exon 6). Exon 7 is the largest by far at 4002 bp. The

A

```
MOUSE     1 MEARSRSAEE LRRAELVEII VETEAQTGVS GFNVAGGGKE GIFVRELRED SPAAKSLSLQ EGDQLLSARV FFENFKYEDA LRLLQCAEPY KVSFCLKRTV
RAT       1 ********** ********** ********** ********** ********** ********** ********** ********** ********** **********
                                              ▼
MOUSE   101 PTGDLALRPG TVSGYEMKGP RAKVAKLNIQ SLAPVKKKKM VTGALGTPAD LAPVDVEFSF PKFSRLRRGL KAEAVKGPVP AAPARRRLQL PRLRVREVAE
RAT     101 ********** ********** ********** **S******* *I*T****** ********** ********** **D******* ********** **********

MOUSE   201 EAQVARMAAA APPPRKAKAE AEAATGAGFT APQIELVGPR LPSAEVGVPQ VSVPKGTPST EAASGFALHL PTLGLGAPAA PAVEPPATGI QVPQVELPTL
RAT     201 ********** ***S****S* **V******* ********** *********K ********** ********** ********** ******T*** **********

MOUSE   301 PSLPTLPTLP CLDTQEGAAV VKVPTLDVAA PSMGVDLALP GAEVEAQGEV PEVALKMPRL SFPRFGIRGK EATEAKVVKG SPEAKAKGPR LRMPTFGLSL
RAT     301 ********** ********** ********** **VE****** ********** ********** ******V*** ********** ********** **********

MOUSE   401 LEPRPSGPEA VAESKLKLPT LKMPSFGIGV AGPEVKAPTG PEVKLPKVPE VKLPKVPEAA IPDVQLPEVQ LPKMSDMKLP KIPEMVVPDV RLPEVQLPKV
RAT     401 **S******V A********* ********S* *********K ********** I****A**** ********** ********** *****A***** H****K****

MOUSE   501 PEMKVPEMKL PKWPEMAVPD VHLPDVQLPK VPE-----MK LPKVPEMAVP DVHLPDVQLP KVPEMKLPEM KLPKVPEMAV PDVRLPEVQL PKVSEVKLPK
RAT     501 ********** **I******* *****I**** ***MKLPD** ********** ******I*** ********D* ********** ****I***** **********

MOUSE   596 MPEMAVPDVH LPELQLPKMS EVKLPKMPEM AVPDVRLPEV QLPKVSEMKL PKMPEMTMPD IRLPEVQLPK VPDIKLPEMK LPEIKLPKVP DMAVPDVPLP
RAT     601 I*D******R ********** ******I*D* ********** *******L** **V******* ********** *****----- ********** E*********

MOUSE   696 ELQLPKVSDI RLPEMQVSQV PEVQLPKMPE MKLSKVPEVQ RKSAGAEQAK GTEFSFKLPK MTMPKLGKVG KPGEASIEVP DKLMTLPCLQ PEVGTEASHV
RAT     696 ******---- ------**** ***H***V** ***P****A* *********E K********* **V******T *****G**** ***LI***** ******VAR*

MOUSE   796 GVPSLSLPSV ELDLPGALGL EGQVQEAVPG KVEKPEGPRV AVGVGEVGFR VPSVEIVTPQ LPTVEVEKEQ LEMVEMKVKP SSKFSLPKFG LSGPKAVKGE
RAT     786 ********** ********** ********S* ********** ***T**A*** *******N** ******K*** ********** T********* ********A*

MOUSE   896 VEGPGRATKL KVSKFTISLP KARAGTEAEA KGAGEAGLLP ALDLSIPQLS LDAQLPSGKV EV--ADSKPK SSRFALPKFG VKGRDSEADV LVAGEAELEG
RAT     886 ********** *****A**** R*****D*D* ********** ********** ********** **AG*E**** G********* A********* **********

MOUSE   994 KGWGWDGKVK MPKLKMPSFG LSRGKEAETQ DGRVSPGEKL EAIAGQLKIP AVELVTPGAQ ETEKVTSGVK PSGLQVSTTG QVVAEGQESV QRVSTLGISL
RAT     986 ********** ********** ********I* ********** ********** E********* ********** *********R ********GA ****S*****

MOUSE  1094 PQVELASFGE AGPEIVAPSA EGTAGSRVQV PQVMLELPGT QVAGGDLLVG EGIFKMPTVT VPQLELDVGL GHEAQAGEAA KSEGGIKLKL PTLGTGSRGE
RAT    1086 ********** *****A**** ***V***I** ********** ********** ********** ********** ********T* *****L**** ****A*GK**

MOUSE  1194 GVEPQGPEAQ RTFHLSLPDV ELTSPVSSHA EYQVVEGDGD GGHKLKVRLP LFGLAKAKEG IEVGEKVKSP KLRLPRVGFS QSESVSGEGS PSPEEEEEGS
RAT    1186 *A*A*S**** H***I***** ********** ********** ********** *****R**** **T******* ********** ****A***** **********

MOUSE  1294 GEGASSRRGR VRVRLPRVGL ASPSKVSKGQ EGDATSKSPV GEKSPKFRFP RVSLSPKARS GSRDREEGGF RVRLPSVGFS ETAVPGSTRI EGTQAAAI*
RAT    1286 *****G**** ********** *****G**** ****A***** ********** ********** **K******* ********** ***A***A** *********
```

B

```
MOUSE     1 MEARSRSAEE LRRAELVEII VETEAQTGVS GFNVAGGGKE GIFVRELRED SPAAKSLSLQ EGDQLLSARV FFENFKYEDA LRLLQCAEPY KVSFCLKRTV
RAT       1 ********** ********** ********** ********** ********** ********** ********** ********** ********** **********
                                              ▼
MOUSE   101 PTGDLALRPG TVSGYEMKGP RAKVAKLVRV LSPVPVQDSP SDRVAAAP*
RAT     101 ********** ********** ********** ********** **A***_**
```

FIG. 5. **Comparison of the amino acid sequences of mouse and rat periaxin.** Alignment of the deduced amino acid sequence of mouse and rat L-periaxin (*A*) and S-periaxin (*B*) using the single-letter code. Identity is depicted by an *asterisk*, and *dashes* indicate gaps introduced for optimal alignment. The point at which L- and S-periaxin diverge in sequence is shown by the *arrows* in *A* and *B*.

sizes of the introns were estimated by restriction mapping and PCR and range from 88 (intron 2) to 7500 bp (intron 5). The exon-intron boundaries were sequenced and the splice donor (GT) and acceptor (AG) sites were identified. This information is summarized in Table I.

Two distinct periaxin mRNAs are expressed in the rat peripheral nervous system (1), and the murine gene also encodes two mRNAs of 4.6 and 5.2 kb of approximately equal abundance (Fig. 2*A*). Of eleven cDNA clones isolated from a rat cDNA library, five included intron 6 (Fig. 1). Confirmation that the murine 5.2-kb mRNA differed from the 4.6-kb mRNA by the inclusion of this 592-bp intron was obtained by Northern blotting (Fig. 2).

Identification of Transcriptional Initiation Site and Core Promoter—The transcriptional initiation site was determined by primer extension and was found to be 75 bp upstream of a primer complementary to a region comprising the final nucleotide of exon 2 and the 5′-end of exon 3 in the murine gene (Fig. 3). This site lay in the sequence $YYA_{+1}AGGA$, which has some similarity to the sequence $YYA_{+1}N(A/T)YY$ believed to be the consensus transcriptional initiator for RNA polymerase II transcripts (16). An identical transcriptional initiation site was found for the rat mRNA (data not shown). Approximately 500 bp of the putative core promoter was sequenced (Fig. 4). Although it lacks a TATA box, the promoter does possess a CAAT box, and between this motif and the initiator the sequence is relatively GC-rich (68%), which is commonly the case in TATA-less promoters (17). A sequence motif corresponding to the SCIP/Oct-6 binding site (position −241) is of particular interest owing to the role that Oct-6 is believed to play in Schwann cell maturation (18–20). An element (GCRE) at position −360 has previously been identified as mediating the induction of several myelin protein genes by forskolin (21). The presence of this sequence would help to explain the ability of cAMP to mimic some of the axonal signals that regulate the expression of differentiation-specific genes in Schwann cells (22, 23).

Deduced Amino Acid Sequence of L-Periaxin and S-Periaxin—The deduced amino acid sequence of the protein encoded by the 4.6-kb mRNA is depicted in Fig. 5*A*. This isoform, termed L-periaxin, is 93% identical to rat periaxin and has a size of 147.500 kDa, slightly larger than the rat protein (1). The presence of a retained intron in the larger 5.2-kb mRNA introduces a stop codon preceded by a sequence that encodes a unique 21-amino acid C terminus. This truncated isoform, termed S-periaxin, has a size of 16.2 kDa (Fig. 5*B*). Except for two differences at the extreme C terminus, the rat and murine S-periaxins are identical. Anti-peptide antibodies recognizing the N terminus of L- and S-periaxin (anti-NTerm), the repeat region unique to L-periaxin (anti-170pep1 (1)), or the C terminus unique to S-periaxin (anti-SPeri) confirmed the structural relationship between the two isoforms (Fig. 6).

A PDZ Domain at the N Terminus of L- and S-Periaxin—The similarity between mouse and rat periaxin is particularly striking in the N-terminal 127 amino acids up to the point where the sequences of L- and S-periaxin diverge. Within this region the rat and mouse polypeptides are identical. This prompted us to

examine this sequence very carefully for conserved motifs that might illuminate the function of these proteins, despite the fact that previous searches of the complete L-periaxin polypeptide had not been informative (1). A degree of sequence similarity with a portion of the PDZ domain of the junction-associated protein ZO-1 provided the necessary clue. Comparison of the N terminus sequence from amino acids 13 to 97 with several well characterized PDZ domains in other proteins confirmed that this region comprises a PDZ domain common to both L- and S-periaxin (Fig. 7).

Because proteins that contain PDZ domains are believed to associate with the plasma membrane (3, 6), it was of considerable interest to compare the subcellular locations of L- and S-periaxin in the Schwann cell. In transverse sections of sciatic nerves from 20-day-old mice L-periaxin was detected in a typical annular pattern that reflected its concentration in the periaxonal and abaxonal myelin lamellae (Fig. 8, *A* and *C*). In contrast to myelin basic protein, L-periaxin was also present at the plasma membrane of the Schwann cell, consistent with the possession of a PDZ domain. As found before, L-periaxin is not present in compact myelin where myelin basic protein is abundant (Fig. 8, *B* and *C*) (1, 2). In contrast, S-periaxin was not concentrated at the interface between the plasma membrane and cytoplasm of the Schwann cell or the myelin sheath (Fig. 8, *D–F*). Instead, this protein seemed to be distributed fairly evenly throughout the cytoplasm. There also appeared to be some S-periaxin in the nucleus of the Schwann cell. Apparently, the presence of a PDZ domain may not be sufficient to direct the association of S-periaxin with either the Schwann cell plasma membrane or its product, the myelin sheath.

FIG. 6. **Western blot of mouse periaxin with domain-specific antibodies.** Mouse sciatic nerves from 15-day-old mice were homogenized and immunoblotted using antibodies raised against peptide sequences comprising either the N terminus of L- and S-periaxin (anti-NTerm), the repeat region unique to L-periaxin (anti-170pep1 (1)) or the C terminus unique to S-periaxin (anti-SPeri). The sizes of L- and S-periaxin are indicated in kDa.

DISCUSSION

One of the most interesting aspects of the expression of the periaxin gene is the fact that alternative splicing involves the retention of an intron. There are approximately equal proportions of two mRNAs that either lack or include the last intron. The factors that determine the retention of introns have been studied in detail by Rottman and colleagues, and a key feature is the "weakness" of the splice sites at the 5′- and 3′-ends of the intron, *i.e.* the extent to which they differ from the consensus sequences that are known to promote splicing (12, 24). These weak splice sites would not normally support splicing without an additional sequence in the downstream exon called the exonic splicing enhancer (13). The main distinguishing feature of exonic splicing enhancers is their high content of purines (13). In support of this model, the splice sites in the last intron of the periaxin gene are divergent from the consensus sequences, and there is a domain downstream in exon 7 that is highly purine-rich. The sequences of these 5′- and 3′-splice sites are CTGgtacgc and tcagA, respectively (intron sequences in lowercase), which are significantly different from the corresponding consensus donor and acceptor sequences of CAGgtragt and ncagG (24). Downstream of the acceptor site and 24 bases into exon 7 there is a 14-base sequence GAAGAAGAAGAAGA, which is an excellent candidate for an exonic splicing enhancer (1, 13).

Of those genes that are typically expressed by myelin-forming Schwann cells, the periaxin gene is one of the first to

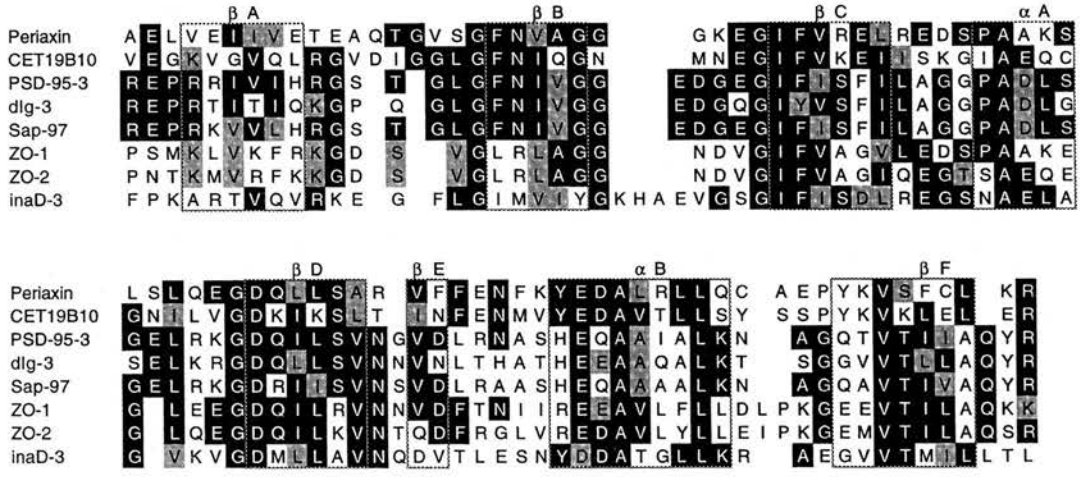

FIG. 7. **Identification of a PDZ domain at the N terminus of L- and S-periaxin.** The sequence of mouse L- and S-periaxin between amino acids 14 and 98 was compared with PDZ domains in the *Caenorhabditis elegans* protein CET19B10 (residues 232–316) (32), PSD-95 (residues 309–393) (33), Discs-Large (dlg) (residues 482–566) (34), SAP97 (residues 461–545) (35), ZO-1 (residues 408–491) (36), ZO-2 (residues 93–176) (37), and inaD (residues 361–447) (38). The eight segments within the domain comprising six β strands and two α-helices are as determined and described by Doyle *et al.* (5). The sequences have been arranged to maximize their similarity. *Solid blocks* show amino acid identity, and *shading* indicates conservative substitutions.

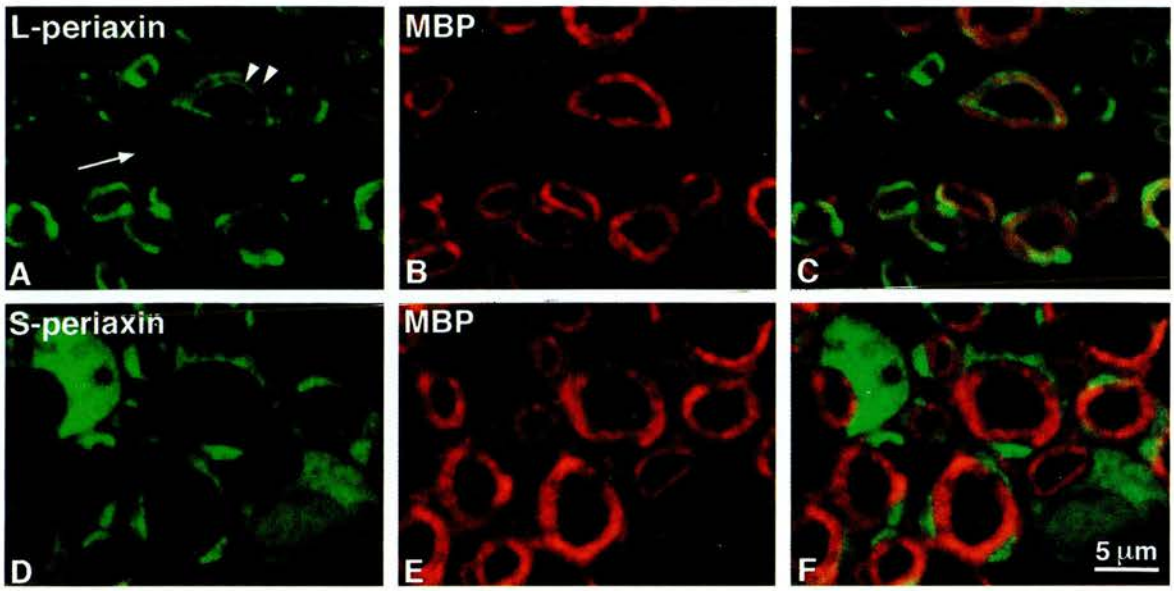

FIG. 8. **Immunofluorescence localization of L- and S-periaxin in mouse Schwann cells.** *A–C*, transverse section of a sciatic nerve from a 20-day-old mouse, double-labeled with anti-170pep1 to detect L-periaxin (fluorescein isothiocyanate, *A*) and antibodies against myelin basic protein (*MBP*) (tetramethyl rhodamine isothiocyanate, *B*). The combined image is shown in *C*. L-periaxin is localized to the plasma membrane (*arrow*) and the abaxonal and adaxonal surfaces (*arrowheads*) of myelinating Schwann cells. Myelin basic protein is restricted to the myelin sheath. *D–F*, transverse section of the same sciatic nerve double labeled with anti-SPeri to detect S-periaxin (fluorescein isothiocyanate, *D*) and anti-myelin basic protein (tetramethyl rhodamine isothiocyanate, *E*). The combined image is shown in *F*. S-periaxin is restricted to the cytoplasm of myelinating Schwann cells. Preincubation of the anti-SPeri with 1 mg/ml of peptide completely abolished staining with this antibody (data not shown).

become transcriptionally active (2). The means by which the gene is regulated is therefore of considerable interest in evaluating how the expression of those genes required for axon ensheathment and myelination is coordinated. The SCIP/Oct-6 transcription factor is known to play a part in Schwann cell maturation, and the presence of a binding site for this protein in the periaxin promoter is intriguing (18–20). However, the timing of expression of periaxin expression in SCIP/Oct-6 null mutants appears to be relatively normal, despite the fact that peripheral myelination is disrupted (20). The presence of a site that bears considerable similarity to the consensus GCRE binding site found in other genes that are characteristically expressed in myelin-forming glia indicates that the the periaxin gene may respond to common signaling mechanisms, in which cAMP can mimic to some extent the inductive interactions of the axon (21). Certainly axonal contact has been shown to be vital to maintain periaxin expression in Schwann cells *in vivo* (2).

So far, two major functions have been ascribed to PDZ domains on the basis of their interactions with plasma membrane proteins and their presence in known signaling molecules such as *dlg* (6). First, they may act as organizers of cortical transduction complexes. In this model the PDZ protein acts as a scaffold on which the macromolecular signaling complex is assembled. These complexes have been termed transducisomes, within which PDZ proteins are key elements (25). Secondly, they may link transmembrane proteins with the actin cytoskeleton via actin-binding proteins such as protein 4.1 (8, 9). Indeed, the insolubilty of periaxin (actually L-periaxin) in Triton X-100 was a key feature in the initial identification of this protein as a potential cytoskeleton-associated protein (1, 3).

The discovery of a PDZ domain in the periaxin proteins is certain to provide exciting new ways of interpreting the function not only of periaxin but also of PDZ domain-containing proteins in general. The PDZ motif in periaxin may either participate in the membrane-protein interactions that are required to promote spiralization or act to recruit proteins to a cortical scaffold important in transmembrane signaling, at least for L-periaxin. The fact that S-periaxin is not concentrated at the membrane-cytoplasm interface but is distributed throughout the cytoplasm of the Schwann cell suggests that this protein has a quite distinct function and that the PDZ domain may not be sufficient to ensure cortical targeting. It is also possible that the unique C terminus of S-periaxin might target the protein away from the plasma membrane. Although most PDZ proteins are localized to the cell cortex, there is an increasing recognition that they do not always function at the plasma membrane (26). The possibility that they play a part in nuclear signaling has been suggested by the fact that the tight junction-associated protein Z0–1 localizes to the nucleus before it is recruited to sites of cell-cell contact (27). Furthermore, a nuclear binding partner for the transcriptional factor SRY is a PDZ protein that is thought to participate in a macromolecular transcription complex (28).

In conclusion, we have shown that two periaxin isoforms, both of which contain the same PDZ domain, are generated in approximately equal amounts by an alternative retained intron mechanism. Furthermore, these PDZ proteins are uniquely targeted to different localizations in myelinating Schwann cells, which suggests that the presence of a PDZ motif may not be the dominant determinant in the selection of binding partners for L- and S-periaxin in myelinating Schwann cells.

REFERENCES

1. Gillespie, C. S., Sherman, D. L., Blair, G. E., and Brophy, P. J. (1994) *Neuron* **12,** 497–508
2. Scherer, S. S., Xu, Y. T., Bannerman, P. G. C., Sherman, D. L., and Brophy, P. J. (1995) *Development* **121,** 4265–4273
3. Kornau, H. C., Schenker, L. T., Kennedy, M. B., and Seeburg, P. H. (1995) *Science* **269,** 1737–1740
4. Sheng, M. (1996) *Neuron* **17,** 575–578
5. Doyle, D. A., Lee, A., Lewis, J., Kim, E., Sheng, M., and MacKinnon, R. (1996) *Cell* **85,** 1067–1076
6. Fanning, A. S., and Anderson, J. M. (1996) *Curr. Biol.* **6,** 1385–1388
7. Songyang, Z., Fanning, A. S., Fu, C., Xu, J., Marfatia, S. M., Chishti, A. H., Crompton, A., Chan, A. C., Anderson, J. M., and Cantley, L. C. (1997) *Science* **275,** 73–77
8. Lue, R., Marfatia, S. M., Branton, D., and Chishti, A. H. (1994) *Proc. Natl. Acad. Sci. U. S. A.* **91,** 9818–9822

9. Marfatia, S. M., Cabral, J. H. M., Lin, L. H., Hough, C., Bryant, P. J., Stolz, L., and Chishti, A. H. (1996) *J. Cell Biol.* **135,** 753–766
10. Marfatia, S. M., Lue, R. A., Branton, D., and Chishti, A. H. (1995) *J. Biol. Chem.* **270,** 715–719
11. Altieri, D. C. (1994) *Biochemistry* **33,** 13848–13855
12. Dirksen, W. P., Sun, Q., and Rottman, F. M. (1995) *J. Biol. Chem.* **270,** 5346–5352
13. Dirksen, W. P., Hampson, R. K., Sun, Q., and Rottman, F. M. (1994) *J. Biol. Chem.* **269,** 6431–6436
14. Maniatis, T., Fritsch, E. F., and Sambrook, J. (1989) *Molecular Cloning: A Laboratory Manual*, 2nd Ed., Cold Spring Harbor Laboratory, Cold Spring Harbor, NY
15. Sanger, F., Nicklen, S., and Coulson, A. R. (1977) *Proc. Natl. Acad. Sci. U. S. A.* **74,** 5463–5467
16. Javahery, R., Khachi, A., Lo, K., Zenzie-Gregory, B., and Smale, S. T. (1994) *Mol. Cell Biol.* **14,** 116–127
17. Beck, T. W., Brennscheidt, U., Sithanandam, G., Cleveland, J., and Rapp, U. R. (1990) *Mol. Cell. Biol.* **10,** 3325–3333
18. Blanchard, A. D., Sinanan, A., Parmantier, E., Zwart, R., Broos, L., Meijer, D., Meier, C., Jessen, K. R., and Mirsky, R. (1996) *J. Neurosci. Res.* **46,** 630–640
19. Jaegle, M., Mandemakers, W., Broos, L., Zwart, R., Karis, A., Visser, P., Grosveld, F., and Meijer, D. (1996) *Science* **273,** 507–510
20. Bermingham, J. R., Scherer, S. S., O' Connell, S., Arroyo, E., Kalla, K. A., Powell, F. L., and Rosenfeld, M. G. (1996) *Genes Dev.* **10,** 1751–1762
21. Li, X., Wrabetz, L., Cheng, Y., and Kamholz, J. (1994) *J. Neurochem.* **63,** 28–40
22. Lemke, G., and Chao, M. (1988) *Development* **102,** 499–504
23. Poduslo, J. F., Walikonis, R. S., Domec, M. C., Berg, C. T., and Holtzheppelmann, C. J. (1995) *J. Neurochem.* **65,** 149–159
24. Green, M. R. (1991) *Annu. Rev. Cell Biol.* **7,** 559–599
25. Tsunoda, S., Sierralta, J., Sun, Y., Bodner, R., Suzuki, E., Becker, A., Socolich, M., and Zuker, C. S. (1997) *Nature* **388,** 243–249
26. Cruikshank, W. W., Center, D. M., Nisar, N., Wu, W., Natke, B., Theodore, A. C., and Kornfeld, H. (1996) *Proc. Natl. Acad. Sci. U. S. A.* **91,** 5109–5113
27. Gottardi, C. J., Arpin, M., Fanning, A. S., and Louvard, D. (1996) *Proc. Natl. Acad. Sci. U. S. A.* **93,** 10779–10784
28. Poulat, F., de Santa Barbara, P., Desclozeaux, M., Soullier, S., Moniot, B., Bonneaud, N., Boizet, B., and Berta, P. (1997) *J. Biol. Chem.* **272,** 7167–7172
29. Horvath, C. M., Wen, Z., and Darnell, J. E. (1995) *Genes Dev.* **9,** 984–994
30. Kim, J. B., Spotts, G. D., Halvorsen, Y.-D., Shih, H.-M., Ellenberger, T., Towle, H. C., and Spiegelman, B. C. (1995) *Mol. Cell. Biol.* **15,** 2582–2588
31. Hooft van Huijsduijnen, R. A. M., Bollekens, J., Dorn, A., Benoist, C., and Mathis, D. (1987) *Nucleic Acids Res.* **15,** 7265–7282
32. Wilson, R., Ainscough, R., Anderson, K., Baynes, C., Berks, M., Bonfield, J., Burton, J., Connell, M., Copsey, T., Cooper, J., Coulson, A., Craxton, M., Dear, S., Du, Z., and Durbin, R. (1994) *Nature* **368,** 32–38
33. Cho, K. O., Hunt, C. A., and Kennedy, M. B. (1992) *Neuron* **9,** 929–942
34. Woods, D. F., and Bryant, P. J. (1991) *Cell* **66,** 451–464
35. Muller, B. M., Kistner, B. M., Veh, R. W., Cases-Langoff, C., Becker, B., Gudelfinger, E. D., and Garner, C. C. (1995) *J. Neurosci.* **15,** 2354–2366
36. Willott, E., Balda, M. S., Fanning, A. S., Jameson, B., Van Itallie, C., and Anderson, J. M. (1993) *Proc. Natl. Acad. Sci. U. S. A.* **90,** 7834–7838
37. Jesaitis, L. A., and Goodenough, D. A. (1994) *J. Cell Biol.* **124,** 946–961
38. Shieh, B.-H., and Zhu, M.-Y. (1996) *Neuron* **16,** 991–998